

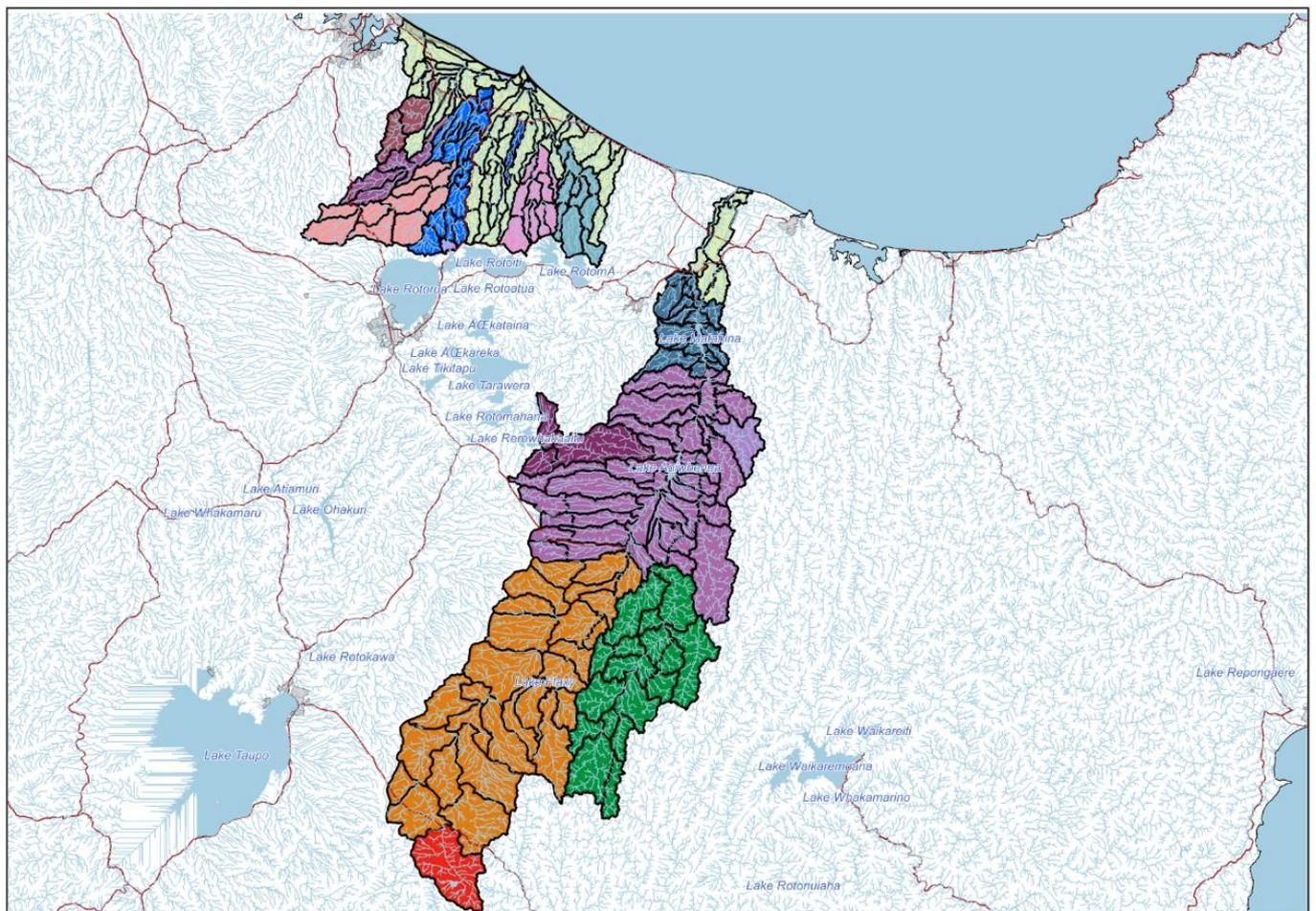
Bay of Plenty Regional Council

Kaituna-Pongakawa-Waitahanui & Rangitāiki Catchment Models

BAY OF PLENTY REGIONAL COUNCIL

WWA0033 | Rev. 12

23 December 2020



Kaituna-Pongakawa-Waitahanui & Rangitāiki Catchment Models

Project no: WWA0033
 Document title: SOURCE Catchment Modelling Analysis
 Revision: 12
 Date: 23 December 2020
 Client name: Bay of Plenty Regional Council
 Project manager: Jon Williamson
 Author(s): WWLA
 File name: G:\Shared drives\Projects\BOPRC\WWA0033_SOURCE Models\Deliverables\SOURCE Report\7. Draft Report_v12\Report_BOPRC_SOURCE_Catchment_Models_Rev12.docx

Williamson Water & Land Advisory

PO Box 314,
 Kumeu 0841,
 Auckland
 T +64 21 654422

Document history and status

Rev	Date	Description	By	Review	Approved
6	3 October 2017	Progress draft for client comment following flow calibration.	Jessie Loft		Jon Williamson
7	6 September 2018	Working DRAFT – work actively being progressed.	Jessie Loft	Jon Williamson	
8	3 October 2018	Initial draft report submitted to BOPRC.	Jessie Loft	Josh Mawer	Jon Williamson
9	23 October 2018	Updated to address client feedback.	Josh Mawer, Jessie Loft	Josh Mawer	Jon Williamson
10	10 May 2019	Updated to address client feedback.	Josh Mawer, Jessie Loft	Josh Mawer	Jon Williamson
11	11 September 2020	Updated following model updates and recalibration.	Elise Legarth	Josh Mawer, Jon Williamson	Jon Williamson
12	23 December 2020	Updated following client review	Elise Legarth	Josh Mawer	Jon Williamson

Distribution of copies

Rev	Date issued	Issued to	Comments
7	6 September 2018	Bay of Plenty Regional Council	Internal review of completed report after initial four scenarios. Review incomplete, hence provided as an update on reporting status.
8	3 October 2018	Bay of Plenty Regional Council	Initial draft full report submitted to BOPRC.
9	23 October 2018	Bay of Plenty Regional Council	Updated to address client feedback.
10	10 May 2019	Bay of Plenty Regional Council	Updated to address client feedback.
11	11 September 2020	Bay of Plenty Regional Council	Updated following model updates and recalibration.
12	23 December 2020	Bay of Plenty Regional Council	Updated following client review

Contents

Executive Summary.....	9
1. Introduction.....	12
1.1 Scope of Works.....	12
1.2 Modelling Tools.....	13
1.3 Project History.....	14
1.4 Project Reporting Structure.....	15
2. Available Data	17
2.1 Catchment Data	17
2.2 Climate Data	18
2.3 River Monitoring Locations	18
2.3.1 Flow Data.....	19
2.3.2 Water Quality Data.....	21
2.4 Takes and Discharges	22
2.4.1 Municipal & Non-Municipal Consented Takes	22
2.4.2 Wastewater Discharges	24
2.4.3 Other Discharge Consents.....	25
2.4.4 Permitted Activities	26
2.4.5 Irrigation Actual Water Usage	26
2.4.6 Assumptions	29
3. Catchment Physical Characteristics	30
3.1 Rainfall Gradient	30
3.2 Elevation and Slope	30
3.3 Geology	32
3.3.1 Kaituna.....	32
3.3.2 Rangitāiki	32
3.3.3 Rock Permeability	33
3.4 Soils	34
3.4.1 Tephra	34
3.4.2 Alluvium and Colluvium.....	34
3.4.3 Peat	34
3.4.4 Wind-Blown Sand	34
3.4.5 Soil Hydraulic Properties.....	35
3.5 Groundwater	36
3.6 Spring Inflows	36
3.7 Land Use	36
4. Catchment Flow Regime.....	39
4.1 Catchment Discharge Coefficient	39
4.2 Catchment Specific Discharge.....	40
4.3 Gauge Catchment Summary	41
5. SOURCE Model.....	47

5.1	SOURCE Model Description.....	47
5.1.1	Time Control	48
5.2	Soil Moisture Water Balance Model Description.....	49
5.3	SOURCE Model Construction.....	53
5.3.1	Sub-Catchment Delineation.....	53
5.3.2	Water Takes and Discharges.....	55
5.3.3	Constructed Models.....	55
5.4	Model Evaluation Criteria.....	56
5.4.1	Statistical Performance Measures	56
5.4.2	The Nash-Sutcliffe Efficiency Coefficient (NSE)	57
5.4.3	Percent Bias (PBIAS).....	59
5.4.4	Percentile Statistics.....	60
5.4.5	Summary of PEC Applied	60
6.	Flow Model Development	62
6.1	Flow Calibration - Kaituna.....	63
6.1.1	Kaituna River at Taheke	63
6.1.2	Paraiti (Mangorewa) River at Saunders.....	64
6.1.3	Kaituna River at Te Matai	66
6.1.4	Waiari River at Muttons.....	69
6.1.5	Raparapahoe River Above Drop Structure	71
6.1.6	Pongakawa River at Old Coach Rd	74
6.1.7	Waitahanui River at Otamarakau Valley Rd	76
6.1.8	Puanene River at State Highway 2 (SH2).....	79
6.1.9	Kaituna Catchment Calibration Summary.....	81
6.2	Flow Calibration - Rangitāiki	83
6.2.1	Rangitāiki River at State Highway 5 (SH5)	83
6.2.2	Rangitāiki River at Murupara	85
6.2.3	Whirinaki River at Galatea	88
6.2.4	Pokairoa River at Railway Culvert	91
6.2.5	Waihua River at Gorge	93
6.2.6	Rangitāiki River at Waiohou Bridge	95
6.2.7	Rangitāiki River at Te Teko.....	98
6.2.8	Rangitāiki Catchment Calibration Summary	100
6.3	Parameter Application to Ungauged Catchments.....	102
6.3.1	ST and Soil Depth.....	104
6.3.2	ZMAX and Soil Permeability	105
6.3.3	FT and Rock Permeability.....	106
6.3.4	DIV and Catchment Average Slope	108
6.3.5	TL and Catchment Area.....	109
6.3.6	Kv and Vertical Hydraulic Conductivity	110
6.3.7	Remaining Parameters	111

6.4	Flow Model Assumptions	111
7.	Constituent Model Development	115
7.1	SOURCE Constituent Configuration	116
7.2	Total Nitrogen	119
7.2.1	APSIM Overview	120
7.2.2	Original APSIM models	120
7.2.3	Drainage comparison between APSIM and SMWBM_Vz	121
7.2.4	Model Improvements	123
7.2.5	TN simulation	124
7.2.6	TN Quick Flow Concentrations	128
7.2.7	TN Inflows	130
7.2.8	TN Calibration Results	131
7.3	Total Phosphorus	143
7.3.1	Generation of TP Components	143
7.3.2	TP Calibration Results	147
7.4	Total Suspended Solids	158
7.4.1	TSS Generation Using Dynamic SedNET	158
7.4.2	dSedNET Parameterisation	161
7.4.3	TSS Calibration Results	167
7.5	Escherichia Coli	178
7.5.1	<i>E. coli</i> Generation	178
7.5.2	<i>E. coli</i> Calibration Results	183
7.6	Constituent Model Assumptions	193
7.6.1	Point Source Contributions	200
7.7	Seasonal Variation of Constituents	200
8.	Summary and Conclusions	201
9.	Recommendations	203
10.	References	204

Table of Figures

Figure 1. The Kaituna River Water Management Area. (Refer to A3 attachment at rear).	12
Figure 2. The Rangitāiki River Water Management Area. (Refer to A3 attachment at rear).	12
Figure 3. Schematic overview of the links between individual modelling systems.	14
Figure 4. VCSN grid data points for the Kaituna Catchment. (Refer A3 attachment at rear).	18
Figure 5. VCSN grid data points for the Rangitāiki Catchment. (Refer A3 attachment at rear).	18
Figure 6. Primary flow monitoring sites in the Kaituna WMA. (Refer A3 attachment at rear).	19
Figure 7. Primary flow monitoring sites in the Rangitāiki WMA. (Refer A3 attachment at rear).	19
Figure 8. Mean monthly metered flow data from municipal supply consent CB11204 (Rangitāiki SC#35).	24
Figure 9. Mean monthly metered flow data from municipal supply consent; CB10921, CB3701, CB1092, CB1000103, CB3702, abstraction take located in Kaituna catchment SC#36.	24
Figure 10. Te Puke wastewater discharge consent metered data.	25
Figure 11. Te Puke interpolated wastewater discharge data.	25
Figure 12. Kaituna WMA rainfall gradient classification zones. (Refer A3 attachment at rear).	30
Figure 13. Rangitāiki WMA rainfall gradient classification zones. (Refer A3 attachment at rear).	30
Figure 14. Kaituna WMA elevation. (Refer A3 attachment at rear).	31
Figure 15. Rangitāiki WMA elevation. (Refer A3 attachment at rear).	31
Figure 16. Kaituna WMA slope. (Refer A3 attachment at rear).	31
Figure 17. Rangitāiki WMA slope. (Refer A3 attachment at rear).	31
Figure 18. Main rock types in the Kaituna WMA. (Refer A3 attachment at rear).	32
Figure 19. Main rock types in the Rangitāiki WMA. (Refer A3 attachment at rear).	33
Figure 20. Sub-catchment vertical hydraulic conductivity in the Kaituna WMA. (Refer A3 attachment at rear).	33
Figure 21. Sub-catchment vertical hydraulic conductivity in the Rangitāiki WMA. (Refer A3 attachment at rear).	33
Figure 22. Soil cover within the Kaituna WMA. (Refer A3 attachment at rear).	35
Figure 23. Soil cover within the Rangitāiki WMA. (Refer A3 attachment at rear).	35
Figure 24. Soil permeability within the Kaituna WMA. (Refer A3 attachment at rear).	35
Figure 25. Soil permeability within the Rangitāiki WMA. (Refer A3 attachment at rear).	35
Figure 26. Soil potential rooting depth within the Kaituna WMA. (Refer A3 attachment at rear).	35
Figure 27. Soil potential rooting depth within the Rangitāiki WMA. (Refer A3 attachment at rear).	35
Figure 28. Depth to Groundwater within the Kaituna WMA. (Refer A3 attachment at rear).	36
Figure 29. Depth to Groundwater within the Rangitāiki WMA. (Refer A3 attachment at rear).	36
Figure 30. Land Use Classifications Across the Kaituna WMA. (Refer A3 attachment at rear).	38
Figure 31. Land Use Classifications Across the Rangitāiki WMA. (Refer A3 attachment at rear).	38
Figure 32. Mean annual precipitation versus specific discharge.	41
Figure 33. Flow diagram of the SMWBM_VZ structure and parameters.	52
Figure 34. Kaituna WMA delineated area. (Refer A3 attachment at rear).	53
Figure 35. Rangitāiki WMA delineated area. (Refer A3 attachment at rear).	53
Figure 36. Kaituna WMA SOURCE model. (Refer A3 attachment at rear).	55
Figure 37. Rangitāiki WMA SOURCE model. (Refer A3 attachment at rear).	55
Figure 38. Sensitivity of NSE to Sample Size.	58
Figure 39. Flow model development process.	62
Figure 40. Hydrograph of the modelled and measured flow of the Paraiti (Mangorewa) River at Saunders.	64
Figure 41. FDC of the modelled and measured flow of the Paraiti (Mangorewa) River at Saunders.	64
Figure 42. Map of changes to the Kaituna Catchment. (Refer A3 attachment at rear).	66
Figure 43. Hydrograph of the modelled and measured flow of the Kaituna River at Te Matai.	66
Figure 44. FDC of the modelled and measured flow of the Kaituna River at Te Matai.	67
Figure 45. Hydrograph of the modelled and measured flow of the Waiari at Muttons.	69
Figure 46. FDC of the modelled and measured flow of the Waiari River at Muttons.	69
Figure 47. Hydrograph of the modelled and measured flow of the Raparapahoe River at Above Drop Structure.	71
Figure 48. FDC of the modelled and measured flow of the Raparapahoe River at Above Drop Structure.	72
Figure 49. Hydrograph of the modelled and measured flow of the Pongakawa River at Old Coach Rd.	74
Figure 50. FDC of the modelled and measured flow of the Pongakawa River at Old Coach Rd.	74
Figure 51. Hydrograph of the modelled and measured flow of the Waitahanui River at Otamarakau Valley Rd.	76

Figure 52. FDC of the modelled and measured flow of the Waitahanui River at Otamarakau Valley Rd.	77
Figure 53. Hydrograph of the modelled and measured flow of the Puanene River at SH2.	79
Figure 54. FDC of the non – irrigation period modelled and measured flow of the Puanene River at SH2.	79
Figure 55. Hydrograph of the modelled and measured flow of the Rangitāiki River at SH5.	83
Figure 56. Hydrograph of the modelled and measured flow of the Rangitāiki River at Murupara.	85
Figure 57. FDC of the modelled and measured flow of the Rangitāiki River at Murupara.	85
Figure 58. Hydrograph of the modelled and measured flow of the Whirinaki River at Galatea.	88
Figure 59. FDC of the modelled and measured flow of the Whirinaki River at Galatea.	88
Figure 60. Hydrograph of the modelled and measured flow of the Pokairoa River at Railway Culvert.	91
Figure 61. FDC of the modelled and measured flow of the Pokairoa River at Railway Culvert.	91
Figure 62. Hydrograph of the modelled and measured flow of the Waihua River at Gorge.	93
Figure 63. FDC of modelled and measured flow of the Waihua River at Gorge.	94
Figure 64. Hydrograph of the modelled and measured flow of the Rangitāiki River at Waiohou Bridge.	96
Figure 65. Hydrograph of the modelled and measured flow of the Rangitāiki River at Te Teko.	98
Figure 66. FDC of the modelled and measured flow of the Rangitāiki River at Te Teko.	99
Figure 67. Kaituna relationship between maximum soil water content (ST) and potential rooting depth.	104
Figure 68. Rangitāiki relationship between maximum soil water content (ST) and plant rooting depth.	104
Figure 69. Kaituna relationship between maximum infiltration rate (ZMAX) and soil permeability class.	105
Figure 70. Rangitāiki relationship between maximum infiltration rate (ZMAX) and soil permeability class.	105
Figure 71. Kaituna relationship between sub-soil drainage rate (FT) and rock permeability.	106
Figure 72. Rangitāiki relationship between sub-soil drainage rate (FT) and rock permeability.	107
Figure 73. Kaituna relationship between surface water ponding (DIV) and catchment slope.	108
Figure 74. Rangitāiki relationship between surface water ponding (DIV) and catchment slope.	108
Figure 75. Kaituna relationship between surface routing coefficient (TL) and catchment area.	109
Figure 76. Rangitāiki relationship between surface routing coefficient (TL) and catchment area.	109
Figure 77. Kaituna relationship between vadose zone travel time (kv) and hydraulic conductivity.	110
Figure 78. Rangitāiki relationship between vadose zone travel time (kv) and hydraulic conductivity.	110
Figure 79. Constituent model development process.	116
Figure 80. Summary of the process for TN reaching waterways considered in the SOURCE Modelling project.	119
Figure 81. Drainage comparison for Kaituna Taupo Matahina dairy.	122
Figure 82. Distribution of the Soil Types from the Fundamental Soils Layer for APSIM. (Refer A3 attachment at rear).	123
Figure 83. Extrapolated Soil Types for each sub – catchment for APSIM. (Refer A3 attachment at rear).	123
Figure 84. Transformation of TN mass in the vadose zone.	125
Figure 85. Example Catchment Attenuation Factor (CAF) evaporation correlation relationship.	127
Figure 86. Kaituna lowland, western and eastern area. (Refer A3 attachment at rear).	129
Figure 87. Rangitāiki lowland, highland and middle area. (Refer A3 attachment at rear).	129
Figure 88. Kaituna TN Index Generation Relationship.	130
Figure 89. Rangitāiki TN Index Generation Relationship.	130
Figure 90. Kaituna Catchment Attenuation Factor applied. (Refer A3 attachment at rear).	131
Figure 91. Constituent Hydrograph Comparing Measured and Modelled TN data for the Kaituna at Te Matai gauge.	132
Figure 92. Constituent Hydrograph Comparing Measured and Modelled TN data for the Pongakawa at Old Coach Rd gauge.	133
Figure 93. Constituent Hydrograph Comparing Measured and Modelled TN data for the SCID114 site.	134
Figure 94. Box plot comparison of measured and modelled TN concentration for all primary calibration sites in the Kaituna WMA.	135
Figure 95. Rangitāiki Catchment Attenuation Factor applied. (Refer A3 attachment at rear).	137
Figure 96. Constituent Hydrograph Comparing Measured and Modelled TN data for the Rangitāiki at Murupara gauge.	137
Figure 97. Constituent Hydrograph Comparing Measured and Modelled TN data for the Whirinaki at Galatea gauge.	139
Figure 98. Constituent Hydrograph Comparing Measured and Modelled TN data for the SCID34 site.	140
Figure 99. Box plot comparison of measured and modelled N concentration for all primary calibration sites in the Rangitāiki WMA.	141
Figure 100. Schematic showing the three components incorporated in the TP constituent model.	144

Figure 101. Schematic view of surface load TP generation from land use.	145
Figure 102. Kaituna PLSC Risk Map (Refer A3 attachment at rear).	145
Figure 103. Rangitāiki PLSC Risk Map (Refer A3 attachment at rear).	145
Figure 104 Relationship between PLSC index and TP concentration	146
Figure 105. Acid Soluble Phosphorus combined with spring inflow for the Kaituna WMA. (Refer A3 attachment at rear).	147
Figure 106. Acid Soluble Phosphorus combined with spring inflow for the Rangitāiki WMA. (Refer A3 attachment at rear).	147
Figure 107. Constituent Hydrograph Comparing Measured and Modelled TP data for the Kaituna at Te Matai gauge.	148
Figure 108. Constituent Hydrograph Comparing Measured and Modelled TP data for the Pongakawa at Old Coach Rd.	149
Figure 109. Constituent Hydrograph Comparing Measured and Modelled TP data for the SCID114 site.	150
Figure 110. Box plot comparison of measured and modelled TP concentration for all primary calibration sites in the Kaituna WMA.	151
Figure 111. Constituent Hydrograph Comparing Measured and Modelled TP data for the Rangitāiki at Murupara gauge.	153
Figure 112. Constituent Hydrograph Comparing Measured and Modelled TP data for the Whirinaki at Galatea gauge.	154
Figure 113. Constituent Hydrograph Comparing Measured and Modelled TP data for the SCID34 site.	155
Figure 114. Box plot comparison of measured and modelled TP concentration for all primary calibration sites in the Rangitāiki WMA.	156
Figure 115. KLSC value with the sub-catchments of the Kaituna WMA. (Refer A3 attachment at rear).	161
Figure 116. KLSC value with the sub-catchments of the Rangitāiki WMA. (Refer A3 attachment at rear).	161
Figure 117. The relationships established between canopy (C) Factor and rainfall (R) Factor.	162
Figure 118. Spatial extent of the four KLSC and DWC relationships developed for the Kaituna WMA. (See A3 attachment at rear).	162
Figure 119. Relationship between KLSC and DWC assigned to the Kaituna WMA.	163
Figure 120. Relationship between KLSC and DWC assigned to the Rangitāiki WMA.	163
Figure 121. The relationships established between the slope and the HSDR value assigned to the Kaituna WMA.	164
Figure 122. The relationships established between the slope and the HSDR value assigned in the Rangitāiki WMA.	164
Figure 123. Time series comparison of measured and modelled TSS data for the Kaituna at Te Matai gauge.	167
Figure 124. Constituent Hydrograph Comparing Measured and Modelled TSS data for the Pongakawa at Old Coach Rd gauge.	169
Figure 125. Constituent Hydrograph Comparing Measured and Modelled TSS data for the SCID114 site.	170
Figure 126. Box plot comparison of measured and modelled TSS concentration for all primary calibration sites in the Kaituna WMA.	171
Figure 127. Constituent Hydrograph Comparing Measured and Modelled TSS data for the Rangitāiki at Murupara gauge.	173
Figure 128. Constituent Hydrograph Comparing Measured and Modelled TSS data for the Whirinaki at Galatea gauge.	174
Figure 129. Constituent Hydrograph Comparing Measured and Modelled TSS data for the SCID34 site.	175
Figure 130. Box Plots Comparing Measured and Modelled TSS data for all Main Sites in Rangitāiki Catchment.	176
Figure 131. Kaituna EMC <i>E. coli</i> generation relationship.	179
Figure 132. Kaituna DWC <i>E. coli</i> generation relationship.	179
Figure 133. Rangitāiki EMC <i>E. coli</i> generation relationship.	180
Figure 134. Rangitāiki DWC <i>E. coli</i> generation relationship.	180
Figure 135. Kaituna decay model relationship with catchment elevation.	182
Figure 136. Rangitāiki decay model relationship with catchment elevation.	182
Figure 137. Constituent Hydrograph Comparing Measured and Modelled <i>E. coli</i> concentrations for the Kaituna at Te Matai gauge.	184
Figure 138. Constituent Hydrograph Comparing Measured and Modelled <i>E. coli</i> concentrations for the Pongakawa at Old Coach Rd gauge.	185

Figure 139. Constituent Hydrograph Comparing Measured and Modelled <i>E. coli</i> concentrations for the SCID114 site.....	186
Figure 140. Box Plots Comparing Measured and Modelled <i>E. coli</i> data for all Main Sites in the Kaituna Catchment.	187
Figure 141. Kaituna NOF bands based on the 95%ile. (Refer A3 attachment at rear).	187
Figure 142. Constituent Hydrograph Comparing Measured and Modelled <i>E. coli</i> data for the Rangitāiki at Murupara gauge.	189
Figure 143. Constituent Hydrograph Comparing Measured and Modelled <i>E. coli</i> data for the Whirinaki at Galatea gauge.	190
Figure 144. Constituent Hydrograph Comparing Measured and Modelled <i>E. coli</i> data for SCID34.	191
Figure 145. Box Plots Comparing Measured and Modelled <i>E. coli</i> data for all Main Sites in Rangitāiki Catchment.	192
Figure 146. Rangitāiki NOF bands based on the 95%ile. (Refer A3 attachment at rear).	192

Executive Summary

Introduction

Williamson Water & Land Advisory (WWLA) was commissioned by the Bay of Plenty Regional Council (BOPRC) in 2017 to develop a hydrological model to simulate the water quantity and quality of the rivers and streams that comprise the Kaituna-Pongakawa-Waitahanui (henceforth Kaituna) and Rangitāiki Water Management Areas (WMAs) using the SOURCE catchment modelling framework.

The project goal was to develop functioning integrated surface catchment models for the Kaituna and Rangitāiki WMAs, that will support policy development under the National Policy Statement for Freshwater Management (NPS-FM).

The work undertaken was a collaboration between WWLA and BOPRC, with WWLA undertaking the data analysis, APSIM¹ and flow and constituent model development, and scenarios assessments and BOPRC:

- supplying the required data for this project, including surface water flow and water quality monitoring data, climate data, and actual use irrigation time series;
- providing technical guidance and experience on local hydrological features; and
- providing shapefiles for naturalised, current and development land use scenarios.

Modelling Platforms

The SOURCE framework is a hydrological modelled platform designed to simulate all aspects of the water resource systems and support the planning and management of catchment to river scale freshwater resources. SOURCE integrates flow and constituent generation processes in each sub-catchment and simulates these variables through the defined downstream network.

A multitude of rainfall-runoff and constituent generation methods can be defined within SOURCE or applied via external methods, such as through the use of plugins and data import tools. Both internal and external generation features were used in this project.

Flow Generation and Calibration

The Soil Moisture Water Balance (Vadose Zone) Model (SMWBM_VZ) developed by WWLA was implemented in SOURCE as a plugin and utilised as the rainfall-runoff generation model for this project. The SMWBM_VZ utilised daily rainfall and potential evapotranspiration data to calculate the soil moisture content and subsequently the hydrological simulation of water through a catchment.

The SMWBM_VZ is parameterised by twelve variables that control features such as the soil infiltration rate, evaporation losses, the surface runoff, and stream base flows. The current version incorporates vadose zone functionality, which provides an improved representation of the timing of sub-soil drainage reaching the groundwater system (groundwater recharge) and ultimately reaching surface waters. The parameters configured for this project were based on an understanding of the sub-catchment physical characteristics. For example, the values assigned to the parameters controlling the sub-soil drainage rate were selected based on the soil permeability and drainage profile defined by the S-map and fundamental soils spatial layers.

The models were calibrated for flow at fifteen primary flow gauging sites, and a range of spot gauge sites were used to provide a secondary level of calibration. The calibration process was carried out working systematically downstream. The calibration process involved assigning realistic values to each parameter, based on known catchment characteristics, running the model and assessing the simulated flow versus the measured flow. The parameters were adjusted, and the process was repeated until either an appropriate level or the best possible match (within the timeframe and/or budget available) between simulated and observed data was achieved.

¹ APSIM is the Agricultural Production SIMulation, developed in Australia by Queensland DPI, CSIRO and University of Queensland

Using an understanding of the catchment characteristics and the calibrated model parameters assigned to gauged catchments, relationships were established to determine appropriate parameter values to assign to the ungauged sub-catchments. Relationships were established between catchment characteristics and the key SMWBM_VZ parameters across the two models. The remaining parameters were assigned fixed values across the model domain.

The flow models in both WMAs were calibrated against available gauge data, with eight primary calibration sites in the Kaituna WMA and seven in the Rangitāiki WMA. Model performance evaluation measures were calculated for the primary gauge locations and ranged from Not Satisfactory to Very Good in the Kaituna WMA and Not Satisfactory to Good in the Rangitāiki WMA based on the Nash-Sutcliffe Efficiency Coefficient (NSE). Model performance based on the Percentage Bias (PBIAS) model evaluation criteria ranged from Good to Very Good in the Kaituna WMA and Not Satisfactory to Very Good in the Rangitāiki WMA.

Overall, based on the PBIAS and NSE performance metrics, and qualitative classification based on visual observation of flow hydrographs and flow duration curves, the model is considered well calibrated, and appropriate for the purpose of catchment scale scenario modelling.

Constituent Generation and Calibration

The model was developed to simulate the following constituents: total nitrogen (TN), total phosphorus (TP), total suspended solids (TSS), and *E. coli*. Individual constituent generation models were developed using a combination of third-party modelling tools, SOURCE plugins, and derived catchment specific constituent generation relationships.

Two TN generation pathways were represented in the model. The baseflow TN component, which represented the sub-soil drainage and leaching of TN into the groundwater, was simulated using the Agricultural Production Systems Simulator (APSIM) model to produce a daily load of TN leaching from each individual land use type within a sub-catchment. The daily TN load was then converted to a concentration and assigned to the groundwater flow component of the SMWBM. The quick flow (overland flow) TN component was simulated through the development of a TN generation index which related catchment slope, vegetation cover and stocking rate to instream TN concentrations. A Catchment Attenuation Factor (CAF) was developed using evaporation as a proxy for climatic conditions, to represent biological uptake and the natural transformation and reduction processes of TN and applied to the baseflow TN component.

Three TP generation pathways were included in the model, representing the surface TP load², the event surface TP load³, and the natural load⁴. The surface TP load was calculated as a percentage of the TN leaching load, as simulated by APSIM, and was applied to the quick flow component of the flow regime. The event surface TP load was simulated through the development of a TP generation index which related the natural TP load, catchment length, slope, and vegetation cover to an event surface TP concentration, and was applied to the quick flow component of the flow regime. The natural TP load was calculated based on each sub-catchment's underlying soil acid soluble phosphorus content (as provided by BOPRC). The natural TP load was applied to the baseflow component of the flow regime. The spring inflow TP load was applied as a constant inflow concentration, and combined with the natural TP load.

The dSedNET SOURCE plugin was used to simulate TSS generation from hillslope erosion processes. dSedNET was configured using a combination of calculated and literature reported values, and a relationship derived relating the Hill Slope Delivery Ratio (HSDR) to average catchment slope. In both the Kaituna and Rangitāiki WMAs multiple relationships were developed to reflect the differing soil type, geology and land uses between catchments. Due to the absence of measured TSS data collected during large event-flow conditions, during which

² Surface Load – Represents the quick flow of fine sediment and particulate P under normal wet weather conditions and is dependent on land uses within each sub-catchment (e.g. agricultural and horticultural land uses). This represents the anthropogenic derived load of TP (e.g. from fertiliser applications).

³ Event Surface Load – An additional supply of TP delivered via surface processes during storm events, where additional parent soil material is mobilised during increased runoff, providing an additional source of naturally occurring TP in the river.

⁴ Natural Load – Represents the natural background levels of TP found leaching from the parent soil (under standard climatic conditions), which moves through the sub-soil system and is then delivered instream. The natural load also included spring inflow TP.

TSS concentrations are typically highest, the TSS generation model was developed with the aim of over-predicting against available measured TSS concentration data to provide a conservative estimate of peak TSS concentrations.

The generation of *E. coli* during dry weather and wet (event) weather conditions was simulated through the development of two relationships which related stocking rate, slope and vegetation cover to dry weather and event *E. coli* generation concentrations. Separate relationships were developed for both the Kaituna and Rangitāiki WMAs. To account for the natural decay (die-off) of *E. coli* as it is transported through river and stream networks, a first order decay function was applied, which assigned a variable decay rate using sub-catchment elevation as a proxy for environmental conditions such as temperature, and solar radiation which are known to influence *E. coli* decay.

The constituent generation models were calibrated against eight primary monitoring sites in the Kaituna WMA and six in the Rangitāiki WMA, and against a range of additional secondary monitoring locations where sufficient data (>5 data points) were available. Model performance, based on the PBIAS criteria across all primary monitoring sites was considered:

- Satisfactory (two primary sites) to Very Good (ten primary sites) for TN;
- Not Satisfactory (three) to Very Good (six) for TP;
- Not Satisfactory (eight) to Very Good (one) for TSS; and
- Not Satisfactory (twelve) to Satisfactory (one) for *E. coli*.

The performance of the model to predict TN, TP and TSS concentrations at most monitoring locations was satisfactory or better in terms of statistics and / or visual observation of time series plots. However, the performance in terms of *E. coli* concentrations was generally Not Satisfactory and caution should be used in interpreting output for this constituent when considering absolute concentrations. However, as the generation of constituent concentrations for *E. coli* (and TN, TP and TSS) were linked to physical catchment characteristics, the model is considered suitable and appropriate for undertaking relative change (i.e. percentage change) analysis resulting from land use change or mitigation-based scenarios across the two WMAs, including sites where classification was considered Not Satisfactory according to the PBIAS classification.

Conclusion

Overall, the model is considered a powerful and effective tool that can be used to aid in the planning and management of water allocation and water quality assessments at the catchment scale through potential land use change and mitigation scenario simulations. The current model calibration is considered appropriate for the analysis of relative change for land use change and mitigation scenarios across the Kaituna and Rangitāiki WMAs, for flow and all four constituents (TN, TP, TSS and *E. coli*). Analysis of finer scale effects such as discharges at an individual property level cannot be undertaken with the model.

1. Introduction

In January 2017, Bay of Plenty Regional Council (BOPRC) commissioned Williamson Water Advisory (WWA), Hydrology and Risk Consulting (HARC), and Eco Logical Australia (ELA) to develop two fully functioning, integrated catchment models for the Kaituna-Pongakawa-Waitahanui (Kaituna) and Rangitāiki Water Management Areas (WMAs).

Integrated catchment models are important decision support tools as they provide a coherent representation of catchment hydrology and water quality. The development of the two models is intended to support community discussions and policy development under the National Policy Statement (NPS) for Freshwater Management, including the establishment of water quantity and water quality limits. This work is further supported by national targets to make all of New Zealand's rivers and lakes swimmable by 2040, and standards in the NPS that provide a framework for managing ecosystem and human health in freshwater.

The surface water quantity and quality of the Kaituna and Rangitāiki WMA areas (**Figure 1** and **Figure 2**) were analysed using the SOURCE hydrological modelling platform developed by eWater Limited.

WWLA's specific engagement comprised technical work to build the SOURCE model, calibrate the model to the measured flow and water quality constituents, and simulate various historical and future land management scenarios. BOPRC staff were heavily involved in data provision, assistance and support roles, particularly with regard to monitoring data collected by BOPRC and the development of analysis scenarios.

Figure 1. The Kaituna River Water Management Area. (Refer to A3 attachment at rear).

Figure 2. The Rangitāiki River Water Management Area. (Refer to A3 attachment at rear).

1.1 Scope of Works

WWLA's scope of work was developed through a two stage ROI and RFP process and was further refined by pre-contract negotiations and during the course of the project. This process resulted in a change in WWLA's original scope to incorporate APSIM as the tool for TN generation and its original consultant provider (ELA) into the WWLA project team, and as mentioned above eventually becoming the APSIM provider for the catchment calibrations.

At a high level, the RFP sought a model framework that is capable of operating at varying spatial and temporal scales depending on the requirements of each catchment. Specific requirements for model design included incorporation of appropriate functionality to enable:

- Use of gridded catchment climate data;
- Rainfall runoff modelling;
- Contaminant generation modelling (including Total Nitrogen and Total Phosphorus, Sediment and *E. coli*);
- Incorporation of water allocation rules and consents (including irrigation demand and use);
- Characterisation of surface water and groundwater interactions;
- Modelling of flow and constituent conservation and attenuation; and
- A reporting tool that accounts for summer and winter variation, lag times within land use, and groundwater attenuation.

At the time of preparing our RFP response, the state of separate MODFLOW groundwater modelling projects for both the Kaituna and Rangitāiki Catchments was unclear, hence any integration with MODFLOW was excluded from the scope, and informed assumptions on groundwater interactions were to be made instead where required. The groundwater modelling projects for the Kaituna and Rangitāiki WMAs are being undertaken by Jacobs Consultancy Limited. Integration between the surface water and groundwater models is something that BOPRC will consider in the future.

The scope of works as agreed in the contract were as follows:

- **Task 1** – SOURCE Model Sub-Catchment and Drainage Pathway Preparation;
- **Task 2** – SOURCE Model Input Data Preparation;
- **Task 3** – Conceptual Model Workshop;
- **Task 4** – SOURCE Model Build;
- **Task 5** – SOURCE Model Flow Calibration;
- **Task 6** – SOURCE Model Constituent Calibration;
- **Task 7** – SOURCE Model Scenario Simulation and Analysis;
- **Task 8** – Reporting;
- **Task 9** – On-Going Support; and
- **Task 10** – Project Management.

During the project, various additional tasks were added to WWLA's scope. These are summarised as follows:

- Actual use irrigation water demand modelling;
- APSIM drainage review;
- Model calibration enhancements, and
- Various additional workshops, presentations and questions raised by the BOPRC's project team.

1.2 Modelling Tools

To provide context on the tools and methodologies that will be discussed in this report, a summary overview of the modelling tools is provided here.

As indicated above, the modelling component of this project was undertaken using the SOURCE catchment model developed in Australia by eWater Ltd. This organisation was initiated as a collaborative venture between several industry and research organisations which, since 2012 has operated as a not-for-profit company owned by the Australian government.

SOURCE provides a framework for simulation and accounting of flows and constituents on a catchment-by-catchment basis. Source is not a single hydrological model. It comprises a range of models and tools that have been incorporated into a single flexible adaptable environment that recognises the practical and technical issues in developing water policy and the need for transparency and sustainability. It was designed to be customisable by users to address specific local problems or can be pre-configured for typical integrated water resource management (IWRM) situations. SOURCE version 4.1.1 was used for this project.

The Soil Moisture Water Balance Model (SMWBM_VZ), developed by WWLA, was used to simulate catchment flow. The SMWBM_VZ is a daily model and functions as a plugin to SOURCE. More details on this plugin are provided in **Section 5.2**

Dynamic SedNet (dSedNet) developed by the CSIRO in Australia was used to generate sediment runoff, and functions as a plugin to SOURCE. Full details of this plugin are provided in **Section 7.4.1**.

To enable assessment of water quality effects associated with land use the Agricultural Production System Simulator (APSIM) was used to generate Total Nitrogen leaching loss from the sub-soil. APSIM comprises several separate modules that simulate biophysical processes in agricultural systems including water balance, N and P transformations, soil pH, erosion and a full range of management controls. APSIM was run independently of the

SOURCE model with outputs imported into the SOURCE model to enable simulation of the effects of nutrient losses associated with agricultural land use on the quality of receiving waters.

A schematic overview of the key datasets and links between the individual modelling components is presented in **Figure 3**.

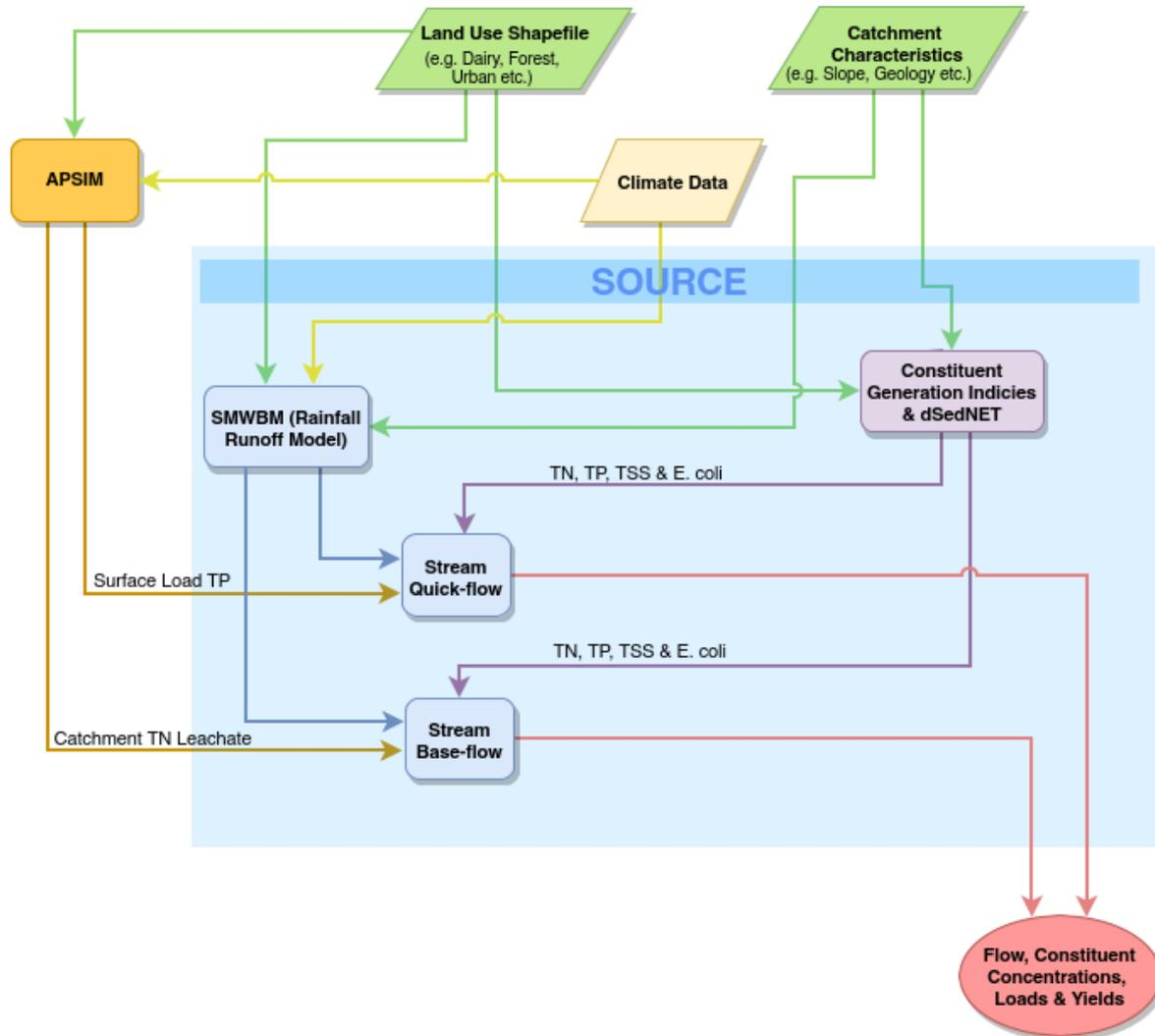


Figure 3. Schematic overview of the links between individual modelling systems.

1.3 Project History

As alluded to in the introduction, HARC assisted with the initial calibration of the model to measured flow, particularly with the development of the lake model aspects. ELA developed the initial APSIM models used for generation of TN. WWLA subsequently refined these APSIM models in the process of calibrating the catchments for TN concentration. Following the initial support on development of the flow model from HARC and initial development of APSIM models by ELA, WWLA subsequently undertook all further technical work.

Revision 10 of this report was issued to BOPRC in May 2019, and subsequently released for review and comment to wider council staff and key stakeholders. Community stakeholder meetings were held in both the Kaituna and

Rangitāiki WMAs in late May 2019 to discuss assessment outcomes and receive further feedback from stakeholders.

This report (Revision 11) presents the updated SOURCE model development and calibration based on new information received since May 2019, and incorporates comments and feedback received from BOPRC staff and community stakeholders.

Key updates and changes of note to the APSIM models included:

- Distinction of highland (2.5 cows/ha) and lowland (3.2 cows/ha) dairy stocking rates;
- Inclusion of stock wintering off in the Lowland catchments of Kaituna and Rangitāiki WMAs;
- Updated representation of fertiliser application rates and amounts in the Dairy and Sheep and Beef models;
- Improved parameterisation of Galatea soils physical characteristics; and
- Benchmarking of the Kiwifruit leaching models to the recently released (July 2019) Plant & Food Research study on nitrate balances under Kiwifruit in the Bay of Plenty Region.

Additional local information on the representation of plantation forestry was provided by Timberlands Ltd, and included:

- Updated information on typical tree age class composition; and
- Aerial photographs for forestry blocks of differing age class, used to inform parameterisation of model vegetation density cover.

Model refinements of TN and TSS were based on industry information and stakeholder feedback provided prior to December 2019. Data or information received after that time has not been incorporated due to practical reasons.

1.4 Project Reporting Structure

The modelling and analysis undertaken for this for project is detailed across a suite of three technical reports, which are:

- **WWLA, 2020a. *Kaituna-Pongakawa-Waitahanui & Rangitāiki Catchment Models*** (this report) – details the development of the water quantity and quality catchment models;
- **WWLA, 2020b. *Kaituna-Pongakawa-Waitahanui & Rangitāiki APSIM Modelling Report*** – details the development of the APSIM Models.
- **WWLA, 2020c. *Kaituna-Pongakawa-Waitahanui & Rangitāiki Scenarios Modelling Report*** – presents the development and analysis of land use change and mitigation scenarios.

This report provides a technical description of the operation, development and application of the SOURCE modelling platform to simulate the quantity and quality of the surface and groundwater in the Kaituna and Rangitāiki WMAs. The report is structured around the following sections:

- **Section 1** - introduction and project overview;
- **Section 2** - review of the available data;
- **Section 3** - the sub-catchments and catchment characteristics for the Kaituna and Rangitāiki WMAs;

- **Section 4** - description of the catchment flow regime
- **Section 5** - overview of the SOURCE modelling framework and model evaluation criteria;
- **Section 6** - flow calibration and simulation results for the Kaituna and Rangitāiki WMAs;
- **Section 7** - constituent model development, calibration, and simulation results; and
- **Section 8** - summary and conclusions from the work undertaken.

2. Available Data

The following section details the range of data utilised to construct and calibrate the SOURCE model.

2.1 Catchment Data

Table 1 summarised data used to delineate sub-catchments in the Kaituna and Rangitāiki WMAs for this study. The catchment characteristics are described in **Section 3**. Data was provided by the BOPRC or obtained from external providers i.e. Land Information NZ (LINZ). The data provided in **Table 1** enabled an enhanced understanding of the differing physical characteristics at a sub-catchment scale and was therefore able to be used in delineating the main catchment properties found within each sub-catchment.

Table 1. Data used in delineation of the Kaituna and Rangitāiki sub-catchments.

Data	Description	Data Origin
Water Management Area (WMA) Shapefiles	Shapefile of the WMA's in the Bay of Plenty Region. These were used to define the outer boundary of the Kaituna and Rangitāiki WMAs	BOPRC
Surface Drainage Catchments Shapefile	Shapefile of the surface water drainage catchments in the Bay of Plenty Region. These were used in conjunction with the above (WMA shapefiles) to delineate larger scale sub-catchments in the Kaituna and Rangitāiki WMAs	BOPRC
Digital Elevation Model (DEM) – 15 m resolution	Raster file of the digital elevation of the Bay of Plenty Region. This raster was used to generate slope and hill-shade raster files. The generated files were used in the delineation process (slope), dSedNET development (see Section 7.2) and reporting.	Land Information New Zealand (LINZ)
River Environment Classification: River Network	The 2010 River Environment Classification, (REC2) stream order 2 coverage was used to determine the drainage network of high-resolution sub-catchments	Ministry for the Environment (MfE) Data Service
River Environment Classification: Catchment orders 1 – 6	The 2010 River Environment Classification (REC) orders 3 and 4 were used to determine sub-catchments of an appropriate scale within the WMA's.	MfE Data Service
Land use raster	A high-resolution coverage of the land use in the BOP region was provided by BOPRC. The Land use raster was used to calculate the areas of different land use within model sub-catchments for base-case and predictive future scenarios. It was used further to define the locality of the different land use for development of the APSIM TN models (see Section 7.2.1).	BOPRC
Land cover database	The Land cover data base is a temporal thematic classification of New Zealand land cover created by Landcare Research, which provides a spatial coverage at five yearly intervals describing changes in land use. In conjunction with the Land use raster the Land cover database was used to calculate the area proportions of differing land use within each sub-catchment.	Land Care Research from the Land Resource Information System (LRIS) portal
New Zealand Fundamental Soil Layer shape file	Spatial information of sixteen key soil attributes, derived from data from the National Soils Database (NSD) and the New Zealand Land Resource Inventory (NZLRI).	Landcare Research, from the LRIS Portal
New Zealand Geological Map (QMap)	1:250 000 geological shape file with accompanying text, describing surface geology, geomorphology, stratigraphy, structural geology, tectonic history, geological resources and hazards, and engineering geology.	GNS Science
Flow Monitoring Sites	Point shapefile of the flow monitoring locations in the Kaituna and Rangitāiki WMAs. The data from these locations was used in flow calibration.	BOPRC
Quality Monitoring Sites	Point shapefile of the locations in the Kaituna and Rangitāiki WMAs where surface water quality variables are measured. The data from these locations was used in constituent calibrations.	BOPRC

2.2 Climate Data

Evaporation and rainfall data were used from the National Institute of Water and Atmospheric Research (NIWA) virtual climate station network (VCSN). The VCSN data includes estimates of daily rainfall and potential evapotranspiration from a regular, 5 km grid that covers New Zealand. Estimates of climate parameters are produced for each VCSN point on a daily time-step based on spatial interpolation of recorded observation data.

The VCSN data points in and adjacent to the two WMAs are shown on **Figure 4** and **Figure 5**, for Kaituna and Rangitāiki, respectively. The following data was requested and downloaded for each point:

- Potential Evaporation;
- Rainfall;
- Minimum and maximum air temperature; and
- Solar radiation.

The data was provided as a series of daily ASCII grid files⁵, from 1 July 1976 to 31 June 2016. All data types supplied were utilised in the APSIM modelling (**Section 7.2.1**), while only the evaporation and rainfall data were utilised in the SOURCE model (**Section 5**).

Figure 4. VCSN grid data points for the Kaituna Catchment. (Refer A3 attachment at rear).

Figure 5. VCSN grid data points for the Rangitāiki Catchment. (Refer A3 attachment at rear).

2.3 River Monitoring Locations

BOPRC and their sub-contractors (e.g. NIWA) maintain a network of flow monitoring stations in the Kaituna and Rangitāiki WMAs which are detailed in **Appendix A**. The primary flow monitoring locations are shown in **Figure 6** and **Figure 7**, and a summary of these sites is provided in **Table 2** and **Table 3**. The differentiation between a primary and other monitoring sites was made based on the data population size and/or the quality of data.

In the Kaituna WMA eight locations were selected as primary flow monitoring sites (**Figure 6**). These sites include:

- Kaituna River at Taaheke;
- Paraiti (Mangorewa) River at Saunders;
- Kaituna River at Te Matai;
- Waiari Stream at Muttons;
- Pongakawa River at Old Coach Rd;
- Waitahanui River at Otamarakau Valley Rd;
- Raparapahoe Stream at Above Drop Structure; and
- Puanene Stream at SH5.

In the Rangitāiki WMA seven locations were selected as primary flow monitoring sites (**Figure 7**):

- Rangitāiki River at SH5;
- Rangitāiki River at Murupara;
- Whirinaki River at Galatea;
- Pokairoa River at Railway Culvert;

⁵ An ASCII grid file defines geographic space as an array of equally sized square grid points arranged in rows and columns, and this type of file is typically used as an export/import format due to its simplicity and editability.

- Waihua River at Gorge;
- Rangitāiki River at Waiohou Bridge; and
- Rangitāiki River at Te Teko

Figure 6. Primary flow monitoring sites in the Kaituna WMA. (Refer A3 attachment at rear).

Figure 7. Primary flow monitoring sites in the Rangitāiki WMA. (Refer A3 attachment at rear).

2.3.1 Flow Data

Flow data for the Kaituna and Rangitāiki WMAs was provided by BOPRC. This data included continuous flow data derived from stage/discharge relationships measured at rated flow monitoring sites, and non-continuous (discrete) gaugings.

Sites with a continuous flow record (exceeding 50 observed data points) were used for the initial flow calibration of the SOURCE model. Flow data from 20 discrete flow (secondary) monitoring locations (13 in the Kaituna WMA and 7 in the Rangitāiki WMA) were also provided by BOPRC, and are outlined in **Appendix A**. These sites included locations with infrequent or periodic flow gaugings or with a short continuous monitoring record.

At several sites measured flow data was supplemented by synthetic flow estimates to infill short duration gaps (days not months) in the monitoring record and derive a continuous flow record for the entire duration of site operation. The longest period of synthesised data was approximately 37 days. Full details on the development of synthetic flow estimates are presented in **Appendix A**.

Table 2. Summary of the Kaituna primary flow sites data provided by BOPRC

River	Site Name	Source Catchment	Record Type ⁶	Data Range
Kaituna River	Kaituna at Taaheke	SC 015	Rated	21/10/1981 to 16/08/2016
Paraiti River	Paraiti (Mangorewa) at Saunders	SC 010	Rated & Synthetic	18/07/1967 to 10/02/2017
Kaituna River	Kaituna at Te Matai	SC 026	Rated & Synthetic ⁷	02/05/1955 to 10/02/2017
Waiari River	Waiari at Muttons	SC 036	Rated & Synthetic	10/11/1966 to 15/07/1995
Pongakawa River	Pongakawa at Old Coach Road	SC 096	Rated	25/06/1997 to 14/08/2013
Waitahanui River	Waitahanui at Otamarakau	SC 113	Rated	04/09/2012 to 11/02/2017
Raparapahoe River	Raparapahoe at Above Drop Structure	SC 044	Rated & Synthetic	24/09/1991 to 11/02/2017
Puanene River	Puanene at SH2	SC 077	Rated	21/07/2013 to 10/03/2017

⁶ Rated data refers to data from stage discharge rating curves, excluding Waihua River which is an index – velocity rating. Synthetic data refers to data that has been calculated to fill in gaps in the time series. Synthetic data has been calculated using correlations with nearby sites, based on the behaviour of the water level during the data gap, or interpolated using the volume of precipitation that fell during the data gap.

⁷ Due to changes in the downstream channel conditions and the tidal influence at the Te Matai recording site from 6 August 1986 onwards, the flow data series is derived from synthesised water levels.

Table 3. Summary of the Rangitāiki primary flow sites data provided by BOPRC

River	Site Name	Source Catchment	Record Type	Data Range
Rangitāiki River	Rangitāiki at SH5	SC 01	Rated	09/06/2004 to 05/12/2016
Rangitāiki River	Rangitāiki at Murupara	SC 026	Rated & Synthetic	01/01/1967 to 05/12/2016
Whirinaki River	Whirinaki at Galatea	SC 047	Rated & Synthetic	03/12/1952 to 02/06/2016
Pokairoa River	Pokairoa at Railway Culvert	SC 073	Rated & Synthetic	23/09/1993 to 07/03/2002
Waihua River	Waihua at Gorge	SC 090	Rated	20/12/1979 to 08/03/2017
Rangitāiki River	Rangitāiki at Waiohou Bridge	SC 032	Rated	30/07/2015 to 10/02/2017
Rangitāiki River	Rangitāiki at Te Teko	SC 037	Rated	02/06/1948 to 02/06/2016

As summarised in **Table 4**, hydrological data were also supplied by BOPRC for the three hydro-schemes in the Rangitāiki Catchment (Wheao River and Flaxy Creek Lake, Lake Aniwanuiwa and Lake Matahina) and Lake Rotoiti in the Kaituna Catchment. In addition, the following contextual information was also provided for the hydro-schemes, where available:

- Dam elevation and storage capacity;
- Bathymetric reports;
- Lake level requirements;
- Lake control provisions (spillway levels, operating range, maximum turbine discharge rates, etc.);
- Flow limits; and
- Consent conditions.

Table 4. Summary of the lake and dam data provided by BOPRC.

Lake or Dam	Catchment	Data Types and Comments	Data Range
Lake Rotoiti	Kaituna, flows into SC#15	Daly time series of flow data from the control gates	03/11/1905 to 31/12/1981
Aniwhenua Dam	Rangitāiki, located in SC#30	Daily discharge data summary including: <ul style="list-style-type: none"> • Minimum and maximum lake level; • Inflow rate; • Minimum and maximum downstream flow; and • Duration period of minimum and maximum flow and lake level. 	29/12/2007 to 17/03/2017 (for all data variables)
Matahina Dam	Rangitāiki, located in SC#34	The Annual Trustpower Report (2016) which outlines: <ul style="list-style-type: none"> • Lake level; • Lake discharge; • Cooling water flow; • Downstream flow (Te Teko); and • Lake Inflow. 	01/09/3015 to 31/08/2016 (in 15-minute intervals)
		Cooling water discharge time series	15/04/2014 to 13/02/2017 (in 15-minute intervals)
		Dam discharge time series	15/04/2014 to 13/02/2017 (in 15-minute intervals)

Lake or Dam	Catchment	Data Types and Comments	Data Range
Wheao River and the Flaxy Creek Lake	Rangitāiki, located in SC#14	Daily Flaxy Creek lake levels, including; <ul style="list-style-type: none"> • Minimum and maximum levels; • Spillways levels. 	01/01/2001 to 31/01/2017
		Wheao River Discharge	01/01/2001 to 31/01/2017

2.3.2 Water Quality Data

Observed water quality data was provided for the four constituents (TN, TP, TSS and *E. coli*). Primary water quality sites were defined as sites that best represented a watershed boundary and had more than 30 sample points available during the model calibration period (June 2011 – June 2016). Sites with less than 30 sample points during the calibration period were considered secondary water quality sites. Full details of all primary and secondary water quality sites are presented in **Appendix B**.

Table 5 and **Table 6** summarise the water quality data available for primary sites in the Kaituna and Rangitāiki WMAs respectively.

Table 5. Summary of the Kaituna primary site constituent data provided by BOPRC

Site Name	SC#	TN Data Range		TSS Data Range		<i>E. coli</i> Data Range		TP Data Range	
Kaituna at Maungarangi Rd	SCID22	19/11/1990	12/01/2017	28/08/1990	13/03/2017	28/08/1990	01/03/2017	28/08/1990	12/01/2017
Kaituna at Te Matai	SCID26	28/08/1990	12/01/2017	28/08/1990	13/03/2017	28/08/1990	13/03/2017	28/08/1990	12/01/2017
Kaituna at Clarkes	SCID53	22/02/1996	12/01/2017	09/04/1991	13/03/2017	25/03/1992	13/03/2017	09/04/1991	12/01/2017
Kaituna at Te Tumu	SCID57	16/09/1993	12/01/2017	17/12/1985	13/03/2017	27/03/1996	13/03/2017	12/09/1985	12/01/2017
Pongakawa at Pumphouse Forest	SCID96	07/10/1999	12/01/2017			28/08/1990	13/03/2017	07/10/1999	12/01/2017
Pongakawa at SH2	SCID96	11/07/1989	12/01/2017	11/07/1989	13/03/2017	07/10/1999	27/02/2017	11/07/1989	12/01/2017
Pongakawa at Old Coach Rd	SCID98	14/07/1999	12/01/2017	14/07/1999	13/03/2017	28/08/1990	20/03/2017	14/07/1999	12/01/2017
Waitahanui at Otamarakau Marae	SCD11 4	02/10/1995	12/01/2017	02/10/1995	13/03/2017	14/07/1999	13/03/2017	02/10/1995	12/01/2017

Table 6. Summary of the Rangitāiki primary site constituent data provided by BOPRC

Site Name	SC#	TN Data Range		TSS Data Range		<i>E. coli</i> Data Range		TP Data Range	
Rangitāiki at SH5	SCID1	26/03/1999	17/01/2017	07/07/1999	02/03/2017	07/07/1999	02/03/2017	26/03/1999	17/01/2017
Rangitāiki at Murupara	SCID26	15/02/1989	08/12/2015	10/04/2001	14/03/2017	10/04/2001	14/03/2017	15/02/1989	08/12/2015
Whirinaki River at Galatea Bridge	SCID47	15/02/1989	08/12/2015	30/07/1990	14/03/2017	30/07/1990	14/03/2017	15/02/1989	08/12/2015
Rangitāiki at Inlet to Aniwenua Canal	SCID30	30/07/1990	17/01/2017	30/07/1990	02/03/2017	14/01/2016	24/02/2016	30/07/1990	17/01/2017
Rangitāiki at Matahina Dam	SCID34	22/08/1995	17/01/2017	22/08/1995	02/03/2017	22/08/1995	02/03/2017	22/08/1995	17/01/2017
Rangitāiki at Te Teko	SCID37			30/07/1990	15/03/2017	30/07/1990	15/03/2017		

Table 7 summarises the lake water quality data provided by BOPRC.

Table 7. Summary of lake and dam data provided by BOPRC.

Lake or Dam	Catchment	Data Types and Comments	Data Range
Lake Rotoiti	Kaituna, flows into SC#15	Spot sampling of constituent data from the control gates	03/11/1905 to 31/12/1981
Aniwhenua Dam	Rangitāiki, located in SC#30	Spot sampling of constituent data taken within the lake	29/12/2007 to 17/03/2017 (for all data variables)
Matahina Dam	Rangitāiki, located in SC#34	Sampling of constituent data taken within the lake	01/09/2015 to 31/08/2016

Preliminary spring water quality data from investigations currently being undertaken by the BOPRC was also provided. No groundwater quality data were provided for the assessment.

2.4 Takes and Discharges

The following data were provided by BOPRC:

- **Consented takes** - A list of the consented groundwater and surface water takes for purposes other than irrigation was provided by BOPRC, including the total annual consent volume, the consented time period (start and finish date), the location of the consents and the purpose of these abstractions e.g. industrial, domestic, commercial, other, or municipal. Metered actual use data were provided for large takes where available.
- **Large wastewater discharges** - Wastewater discharge consent information was provided for the Te Puke wastewater treatment plant, the Fonterra Factory (at Edgecumbe), and the AFFCO Factory (at Rangiora). This included volumetric discharge limits, load/concentration limits for individual water quality parameters as well as volumetric discharge data (where available).
- **Permitted activities** - Spreadsheets and shapefiles of estimated unconsented and permitted water use across the Bay of Plenty Region compiled by Aqualinc (2015).
- **Other discharge consents** - A list of the consented surface water discharges, including the total annual consent volume, discharge location and the purpose of the discharge e.g. industrial, storm water, wastewater, municipal or other.

Prior to the calibration process, the flow model was configured to account for instream gains and losses due to the abstraction of surface and groundwater for irrigation use. The following sections document data available and methodology adopted to estimate the cumulative volume of authorised permitted activity and consented water abstraction and discharge activities across both WMAs.

2.4.1 Municipal & Non-Municipal Consented Takes

Consented groundwater and surface water takes for purposes other than irrigation (covered in **Section 2.4.5**) were divided into two categories - municipal supply and non-municipal - based on water use recorded in the BOPRC consent database. Takes classified as non-municipal supply include abstractions for industrial, domestic, commercial and 'other' purposes.

Non-municipal supply consents were incorporated into both catchment models based on a daily rate of abstraction for the consented time period. The daily abstraction rate was calculated assuming a constant abstraction rate for

every day for the consented period (i.e. equivalent to the annual allocation/365 days). This method was adopted due to limited information available from BOPRC regarding likely seasonal variation in abstraction rates and the short timeframe available to WWLA. While it is recognised this approach is sub-optimal given potential temporal variation in water demand, due to the small volumes of cumulative abstraction across the WMAs (a groundwater average of 0.003 m³/s and a surface water average of 0.03 m³/s), it is considered unlikely that the assumed constant abstraction rate would have a noticeable impact on the simulated flow.

Time series records of recorded abstraction rate/volume of varying data quality and frequency were provided for each of the municipal supply consents, as summarised in **Table 8**. Given the metered data did not cover the whole consent time period for any of the municipal abstractions, the available data were utilised to develop a synthetic time series demand for each of the municipal consents.

The procedure developed for municipal takes involved assessing the metered data for any seasonal trends, as shown in **Figure 8**. If no trend was observed, as occurs in **Figure 9**, non-metered days were assigned a constant daily rate of abstraction, calculated from the consented yearly maximum abstraction volume. If an obvious seasonal trend was identified, this was replicated across the non-metered days by applying a monthly “shape-factor”. The shape-factor was used to distribute the annual consented volume by a ratio for each month, replicating the metered data trend across the period of available data, without exceeding the maximum annual consented volume.

Table 8. Summary of municipal consents and associated metered data. Consent names were not available.

Consent number	BOP Ref	Consent period	Metered Data period	Metered data frequency
CB10921	61574.0.04-WT	12/07/2002 - 30/06/2037	01/07/2013 - 31/08/2014	Daily
CB3701	61574.0.05-WT	12/07/2002 - 30/06/2037	01/07/2013 - 31/08/2014	Daily
CB10920	61574.0.03-WT	12/07/2002 - 30/06/2037	01/07/2013 - 31/08/2014	Daily
CB1000103	61574.0.02-WT	12/07/2002 - 30/06/2037	01/07/2013 - 21/08/2014	Daily
CB3702	61574.0.06-WT	12/07/2002 - 30/06/2037	18/07/2013 - 05/06/2014	Daily
CB11204	64943.0.02-WT	21/09/2007 - 31/07/2022	01/07/2013 - 30/06/2016	Daily
CB3305	65622.0.02-WT	09/03/2009 - 28/02/2019	01/05/2012 - 30/06/2012	Daily
CB3706	61573.0.02-WT	03/07/2002 - 30/06/2037	01/07/2013 - 31/12/2014	Daily
CS1450	20114.0.02-WT	06/09/1973 - 01/10/2026	01/07/2016 - 25/09/2017	Daily

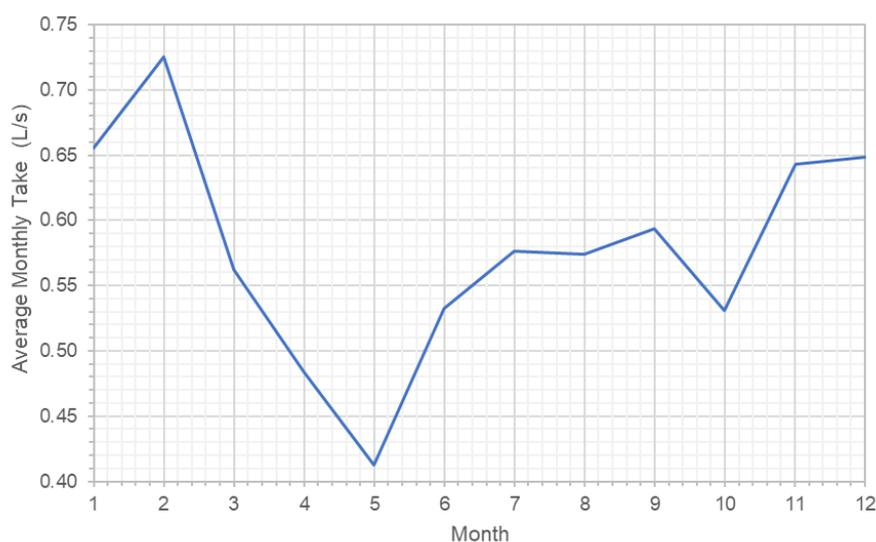


Figure 8. Mean monthly metered flow data from municipal supply consent CB11204 (Rangitāiki SC#35).

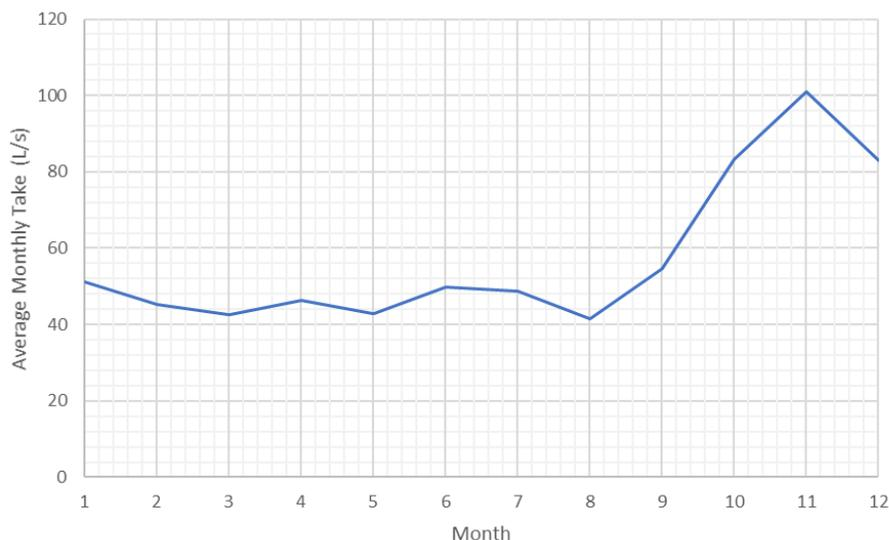


Figure 9. Mean monthly metered flow data from municipal supply consent; CB10921, CB3701, CB1092, CB1000103, CB3702, abstraction take located in Kaituna catchment SC#36

2.4.2 Wastewater Discharges

Wastewater discharge consent information for Te Puke WWTP, AFFCO and Fonterra were provided in conjunction with volumetric discharge data (typically daily volumes), as summarised in **Table 9**.

Table 9. Summary of wastewater discharge consents.

Consent number	Consent period	Metered Data period	Metered data timestep
24211 (Fonterra)	11/04/1997 - 30/06/2010	01/01/1995 - 30/04/2017	Daily
24891 (Te Puke WWTP)	01/01/2012 - 30/11/2016	01/01/2012 - 01/09/2017	Monthly
24932 (AFFCO)	03/11/1997 - 31/05/2016	03/11/1997 - 31/05/2016	Daily

Figure 10 provides data for the Te Puke (municipal) wastewater discharge consent and illustrates the nature of the metered data provided, which in this instance was in the form of an average monthly discharge rate. Linear interpolation was undertaken on the metered data to generate a continuous daily time series for use in the SOURCE model, as shown in and **Figure 11**. This approach was applied to every wastewater consent.

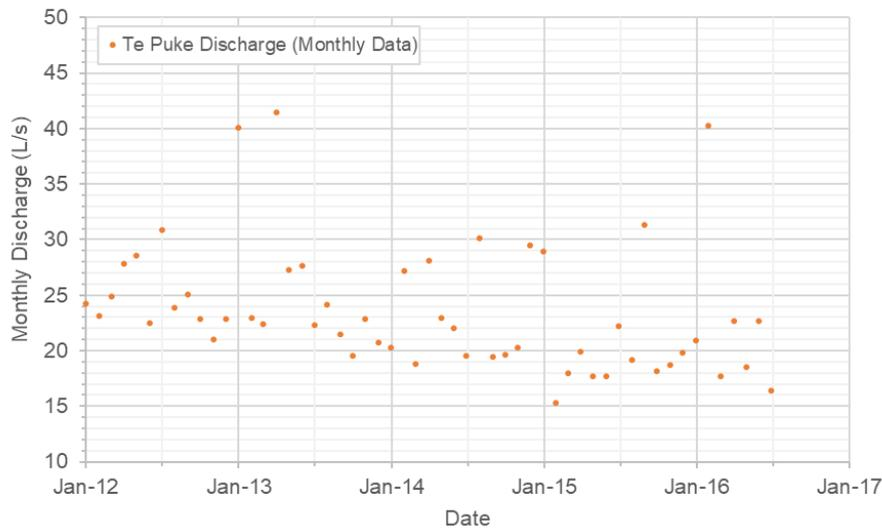


Figure 10. Te Puke wastewater discharge consent metered data.

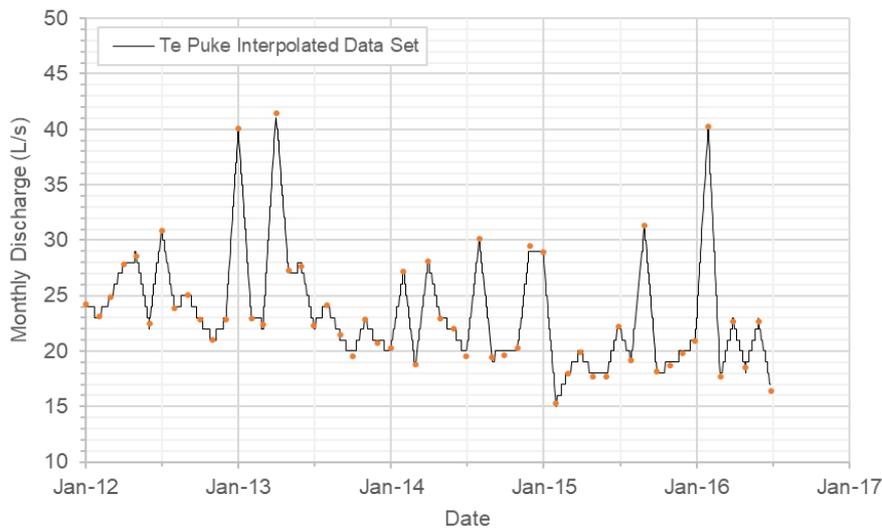


Figure 11. Te Puke interpolated wastewater discharge data.

2.4.3 Other Discharge Consents

Information was provided from BOPRC consent database that included a range of other discharges including stormwater and small on-site wastewater. It was decided that this information provided would not be included in the SOURCE models for the following reasons:

- **Majority of the discharge consents are for stormwater** – SOURCE already simulates and accounts for stormwater discharges in urban area catchments, therefore including these consents would result in double accounting. However, as SOURCE simulates flow at a sub-catchment scale, it was not possible to cross-check point source stormwater discharge flow against available consented data.
- **Lack of information** – A sub-set of the discharge consents in the BOPRC database were unexpectedly large (e.g. 4,200 L/s for a stormwater discharge and 2,420 L/s for onsite wastewater). From a review of the

consent information provided it was established that a majority of such discharges were associated with short-term activities (e.g. earthworks or construction) or based on peak stormwater discharge rates at relatively low recurrence intervals. On this basis it was assumed such discharge rates were unlikely to be representative of average discharge rates associated with these activities and that their inclusion may unrealistically influence sub-catchment water balances in the SOURCE model.

- Other water takes and discharges (excluding irrigation, municipal and hydro takes, and discharges) comprise a relatively minor component of the overall water balance.
- Given the points noted above and the tight timeline associated with the delivery of the updated flow simulation data it was decided that all discharge consents (other than surface water municipal wastewater discharges) would be excluded from the model at the current time.

2.4.4 Permitted Activities

The calculated average daily demand (ADD) of water used for permitted activities (RMA s4(3)(b) water) were provided for each surface water catchment across the whole BOP region within the Aqualinc (2015) report commissioned by BOPRC. The surface water catchments in this report differed from the sub-catchments defined in the Kaituna and Rangitāiki SOURCE models, hence the ADD was interpolated to each SOURCE sub-catchment using a geospatial intersection tool.

While the assessment included permitted takes (e.g. domestic and stock water supply), it was decided that the corresponding discharges (e.g. leaks in troughs etc.) should be excluded. The impact of this is that permitted activities would represent a consumptive take in this model, while in practice the net consumptive take is likely to be small.

2.4.5 Irrigation Actual Water Usage

The modelled actual water use irrigation data, described in WWLA (2017), was aggregated for surface and groundwater takes in the Kaituna and Rangitāiki WMAs and applied at the sub-catchment level in both SOURCE models.

Flow adjustment to account for irrigation water use was based on the extent of the irrigated area in each sub-catchment. The extent of the irrigated area in each WMA sub-catchment over time was determined by generating a time series of irrigated area based on the date consents were granted and expired. Consented irrigated areas for all surface water and groundwater consents were cumulated to estimate the total irrigated area in each SOURCE sub-catchment over time (WWLA, 2017).

Information on the irrigated area was absent for several consents and was estimated using linear relationships established between consented total annual irrigation volume and irrigated area, as outlined in **Appendix C**. It was assumed only 80% of the total consented irrigated area was in practice irrigated, and therefore 20% was deducted from the cumulative irrigated area calculated in each sub-catchment.

A cap was applied to the total water use in each sub-catchment so as to not exceed the consented annual volumes.

Estimates of irrigation water use assumed consent holders irrigate efficiently in terms of application rate and frequency. Details of the modelling assumptions and the calibration of the modelled water use data against the measured data are provided in WWLA (2017). Key assumptions include:

- Irrigation begins when soil moisture content reaches a user defined critical deficit (e.g. typically 40% of plant available water (PAW)).

- Daily irrigation applications cease when either the peak application rate has been applied or the soil moisture content reaches user defined allowable deficits (e.g. typically 80% of PAW).
- Peak application rates vary from 10 mm/day for kiwifruit irrigation to 3.5 to 4.5 mm/day for pasture irrigation.
- Return periods vary according to evaporative demands, soil drainage rates, and the peak application rate.
- An application efficiency of 80% was assumed, which is typical for modern sprinkler and centre pivot irrigation equipment for both horticultural and pasture irrigation. Therefore, the actual water take is 20% greater than the soil demand to account for inefficiency in application.

Table 10 and **Table 11** provide an overview of the consented groundwater and surface abstraction assumed in the Kaituna and Rangitāiki WWLA models, respectively. The consents were applied using Supply and Water User nodes (**Section 5.1**). The nodes represent the cumulative allocation per sub-catchment, which was calculated by aggregating the consents based on the property location e.g. if three irrigators were in SCID5 then these irrigation time series were aggregated together.

Table 10. Summary of the actual groundwater usage in the Kaituna and Rangitāiki Model

Monitoring Code (WUDMS)	Rangitāiki SCID#	Kaituna SCID#	Issue Date	Expiry Date	Type of Take	Max Total Water (m ³ /yr.)
CB204	27		01/04/1982	01/10/2026	Commercial/Industrial	54,750
CB3338	78		07/04/2006	31/03/2026	Commercial/Industrial	273,750
CB12230		3	01/04/2014	31/05/2024	Commercial/Industrial	22,285
CB11391		25	24/01/2008	31/01/2018	Commercial/Industrial	16,607
CB4017		26	02/10/1975	01/10/2026	Commercial/Industrial	597,140
CB1048		32	16/07/2006	31/03/2021	Commercial/Industrial	55,845
CB1001030		48	21/03/2012	31/12/2027	Commercial/Industrial	127,750
CP1021		55	20/09/2006	30/06/2021	Commercial/Industrial	315,360
CB4188		89	02/10/1986	01/10/2026	Commercial/Industrial	13,505
CB4260		89	02/10/1986	01/10/2026	Commercial/Industrial	13,505
CB11191		102	16/04/2009	31/03/2019	Commercial/Industrial	67,525
CP1006		120	07/07/2014	30/06/2024	Commercial/Industrial	91,250
CB4904	2		02/02/1989	01/10/2026	Community/Domestic	1,460
CB1000036	43		29/03/2011	30/06/2031	Community/Domestic	80,520
CB11194	43		29/03/2011	30/06/2031	Community/Domestic	80,520
GB1001298		52	18/09/1985	01/10/2026	Community/Domestic	66,430
CB10651		109	30/06/2008	31/05/2018	Community/Domestic	47,450
CB1298	23		06/03/2009	30/10/2013	Other	54,750
CB11863	44		19/11/2008	31/10/2013	Other	34,310
CB2728	52		01/08/2011	30/06/2016	Other	94,500
CB11878	52		21/10/2011	30/09/2018	Other	237,600
CP1007	56		08/11/2006	30/09/2016	Other	85,750
CB3034	58		04/12/1986	01/10/2026	Other	39,785
CP1018	120		08/02/2011	31/01/2021	Other	91,250
CP1005	120		09/12/2013	30/11/2023	Other	91,250

Table 11. Summary of the actual surface water usage in the Kaituna and Rangitāiki Model.

Monitoring Code (WUDMS)	Rangitāiki SCID#	Kaituna SCID#	Issue Date	Expiry Date	Type of Take	Max Total Water (m ³ /yr.)
CS1006	42		16/06/1977	01/10/2026	Community/Domestic	1,649
CS1459	15		01/07/2013	31/12/2018	Commercial/Industrial	1,204,500
CS1357	17		29/05/2015	31/05/2025	Commercial/Industrial	6,022,500
CS1019	26		02/10/1975	01/10/2026	Commercial/Industrial	597,140
CS1141	30		03/04/1980	01/10/2026	Commercial/Industrial	7,300
CS1299	41		28/06/2007	31/05/2017	Commercial/Industrial	109,500
CS1478	41		28/06/2007	31/05/2017	Commercial/Industrial	36,500
CS1456	41		21/11/2014	01/12/2019	Commercial/Industrial	20,075
CS1010	48		18/06/1976	01/10/2026	Commercial/Industrial	1,078,575
CS11175	66		30/04/2013	31/03/2023	Commercial/Industrial	19,892
CS1451	98		03/02/1983	01/10/2026	Commercial/Industrial	9,125
CS1425	112		25/01/2013	31/12/2022	Commercial/Industrial	571,000
CS1290	120		12/10/2006	30/09/2021	Commercial/Industrial	182,500
CS1339	120		11/01/2010	31/10/2024	Commercial/Industrial	88,300
CS1377	120		08/02/2011	31/01/2021	Commercial/Industrial	54,750
CS1016		27	05/12/1974	01/10/2026	Commercial/Industrial	36,500
CS1490		19	13/03/1978	01/10/2026	Commercial/Industrial	378,432,000
CS1491		21	13/03/1978	01/10/2026	Commercial/Industrial	378,432,000
CS1492		21	13/03/1978	01/10/2026	Commercial/Industrial	66,211,000
CS1182		92	21/12/2000	31/12/2020	Commercial/Industrial	2,300,400
CS1218		38	16/09/2003	30/06/2023	Commercial/Industrial	10,950,000
CS1462	18		19/10/2012	31/10/2047	Other	13,140
CS1316	52		09/07/2008	31/07/2043	Other	94,608,000
CS1301	52		09/07/2008	31/07/2043	Other	6,307,200
CS1474	52		10/06/2013	30/09/2023	Other	9,000
CS1324	53		25/02/2009	31/12/2026	Other	547,500
CS1303	57		07/02/2008	31/05/2013	Other	14,600

2.4.6 Assumptions

Assumptions made with respect to takes and discharges are summarised in **Table 12**.

Table 12. Summary of assumptions related to consented takes and discharges (industrial, commercial, municipal) and permitted activity (stock and domestic) development.

Type of Assumption	Description	Significance
Consent period	Consents were assumed to be exercised for the full consented period (i.e. from the consent start date, until the consent expiry).	Minor - majority of consents (takes and discharges) are small and therefore have little to no influence on simulated flows. A variation in the seasons or periods the consents are exercised is likely to be unnoticeable at this level.
Consented annual maximum abstraction volumes	Where metered actual use data were not available, for a consented abstraction the maximum annual water allocation was divided by the days in a year and applied as an average daily take.	Minor - majority of abstraction consents are small and therefore have little to no influence on simulated flows. A variation in the seasons or periods the consents are exercised is likely to be unnoticeable at this level.
Permitted activities	The calculated ADD per sub-catchment was applied for every day of the model run period.	Minor – the ADD is extremely small in comparison to the flow simulated in majority of sub-catchments. Although it is likely the ADD will have changed since 1976, there is no other data to estimate the ADD prior to 2015.
Exclusion of consents	Not all consents were included. In addition to excluding small discharge consents (other than surface water municipal wastewater discharges), any consents that were provided without appropriate data to determine location, consented period, or a maximum daily or annual abstraction / discharge volume were excluded. Consents supplied with an abstraction rate greater than the flow available in a sub-catchment were also excluded on the basis that the consented value was either a short-term consent or an erroneous value. Such consents were not feasible to include. Appendix C outlines irrigation and horticultural data that were supplied.	Minor – The significance of excluding these consents is low, and likely has less impact than the assumptions that would be required to include consents without requisite information (i.e. location of discharge, consent period, or annual maximum abstraction rates).

3. Catchment Physical Characteristics

Catchment physical characteristics are important to recognise and understand as they play a key role in governing the hydrological functioning of a WMA. In this section, the catchment physical characteristics for both the Kaituna and Rangitāiki WMAs are summarised. **Appendix D** provides additional detail on soil properties on a sub-catchment by sub-catchment scale, while **Section 5.3.1** further describes the delineation of the WMA into SOURCE sub-catchments.

3.1 Rainfall Gradient

NIWA's Virtual Climate Station Network (VCSN) was used to define the rainfall regime in each catchment. A mean annual rainfall map was generated using the kriging spatial interpolation method from the 5 km VCSN grid points. This was overlain on the model domain to enable estimation of the annual rainfall range and gradient for each catchment. Each sub-catchment was applied a rainfall zone classification by grouping the sub-catchments into low, medium and high mean annual rainfall zones as summarised in **Table 13**.

Table 13. Rainfall zones in the Kaituna and Rangitāiki WMAs.

	Rainfall (mm)		
	Low	Medium	High
Kaituna WMA	1,300 – 1,700	1,700 – 2,050	2,050 – 2,400
Rangitāiki WMA	1,150 – 1,400	1,400 – 1,600	1,600 – 1,825

As shown on **Figure 12**, mean annual rainfall in the Kaituna WMA shows a clear correlation with ground surface elevation with highest mean annual rainfall in the upland areas and lowest rainfall on the coastal plains. While rainfall in the Rangitāiki WMA also exhibits orographic influence on higher elevation areas, a clear rain shadow effect is evident across the central portion of the catchment (**Figure 13**).

Figure 12. Kaituna WMA rainfall gradient classification zones. (Refer A3 attachment at rear).

Figure 13. Rangitāiki WMA rainfall gradient classification zones. (Refer A3 attachment at rear).

3.2 Elevation and Slope

Elevation and slope GIS raster files for the Kaituna and Rangitāiki WMAs were generated in Quantum GIS (QGIS) using the Land Information New Zealand (LINZ) Napier and Tauranga 15 m digital elevation model (15 m DEM) published in August 2011 (**Figure 14 - Figure 15** and **Figure 16 - Figure 17**, respectively). These layers were used to help delineate and characterise the hydrological response throughout each WMA (assuming that higher elevation catchments would have a different hydrological response compared to lowland coastal areas in terms of evaporation and rainfall).

Figure 14. Kaituna WMA elevation. (Refer A3 attachment at rear).

Figure 15. Rangitāiki WMA elevation. (Refer A3 attachment at rear).

Figure 16. Kaituna WMA slope. (Refer A3 attachment at rear).

Figure 17. Rangitāiki WMA slope. (Refer A3 attachment at rear).

Elevation and slope statistics calculated for each gauge catchments are summarised for the Kaituna and Rangitāiki WMAs respectively in **Table 14** and **Table 15**.

Table 14. Kaituna elevation and slope and elevation statistics.

Calibration Sites	Area (km ²)	Elevation Mean (m AMSL)	Elevation Minimum (m AMSL)	Elevation Maximum (m AMSL)	Slope Mean (degrees)	Slope Minimum (degrees)	Slope Maximum (degrees)
Kaituna at Taheke	4.6	521.91	358.61	578.43	6.34	0.00	47.41
Paraiti (Mangorewa) at Saunders	192	374.58	38.03	578.43	9.16	0.00	52.02
Kaituna at Te Matai	345	276.58	7.00	578.43	9.11	0.00	52.01
Waiari at Muttons	70	351.78	14.77	644.13	10.28	0.00	53.68
Pongakawa at Old Coach Road	101	193.54	13.50	453.17	9.75	0.00	46.60
Waitahanui at Otamarakau Valley Road	103	199.36	14.36	422.93	13.54	0.00	50.35
Raparapahoe at Drop Structure	51	225.00	8.81	563.92	13.53	0.00	51.02
Puanene at State Highway 2 (SH2)	13	75.96	11.87	186.55	4.52	0.00	37.50

Table 15. Rangitāiki WMA slope and elevation analysis.

Rangitāiki Gauge Catchments	Area (km ²)	Elevation Mean (m AMSL)	Elevation Minimum (m AMSL)	Elevation Maximum (m AMSL)	Slope Mean (degrees)	Slope Minimum (degrees)	Slope Maximum (degrees)
Rangitāiki at State Highway 5 (SH5)	101	767.39	712.80	1,023.60	5.47	0.00	41.52
Rangitāiki at Murupara	1,148	623.03	186.92	1,023.60	3.86	0.00	58.69
Whirinaki at Galatea	507	591.22	208.94	1,240.88	20.24	0.00	61.06
Pokairoa at Railway Culvert	118	430.06	202.57	950.58	8.95	0.00	52.06
Waihua at Gorge	46	470.96	99.27	787.46	28.87	0.01	59.61
Rangitāiki at Waiohou Bridge	2,689	528.59	73.55	1,240.88	10.64	0.00	61.72
Rangitāiki at Te Teko	2,846	510.36	11.68	1,240.88	10.65	0.00	68.64

In the Kaituna WMA, slopes in the lowland plains area are typically less than 5 degrees (classified as flat). In the middle reaches of the catchment the land is generally more rolling with slopes varying between 5 and 16.5 degrees, increasing up to 40 degrees on the sides of river valleys. In the higher elevation or highland areas (as colloquially known) of the Kaituna WMA the topography tends to become flatter and less rolling, except for the incised river valleys, which again can have side slopes commonly exceeding 25 degrees and up to 30 degrees in places.

In the Rangitāiki WMA three distinct areas of differing land surface gradient are apparent:

- A western (highland) domain in the upper reaches of the Rangitāiki River characterised by gentle slopes (4.7° average);
- The eastern domain comprising the Urewera area (Whirinaki River and eastern side sub-catchments) catchment characterised by steep slopes (20° average); and
- A central domain downstream of the Whirinaki River confluence and the Lower Rangitāiki Plains area characterised by predominately flat gradients of 8 degrees.

3.3 Geology

The surficial geology in the western areas of both the Kaituna and Rangitāiki WMAs is dominated by volcanic and volcanoclastic lithologies of the Taupo Volcanic Zone (TVZ), which typically comprise pumice and ignimbrite deposits. Coastal plains and river valleys typically comprise recent alluvial sediments derived from the TVZ mixed with marginal marine and coastal sediments (marine sand and peat) along the coastal margin (GNS QMAP, 2018). The main rock types are discussed below, based on QMAP (GNS, 2018).

3.3.1 Kaituna

The main geology of the Kaituna WMA can be broadly classified into two distinct zones for the purposes of this study (**Figure 18**):

- Upland areas are predominantly mantled by ignimbrite of the Rotoiti Pyroclastic⁸, with Matahina Ignimbrite in the south-east. The ignimbrite is characteristically unwelded and eroded, but becomes progressively harder with depth. Flow within the unwelded ignimbrites behaves in a similar way to the mantle of pyroclastic materials with reasonably moderate to high permeability. However, flow within the harder ignimbrites is governed by fracture propensity and is typically low to moderate permeability overall.
- The low-lying coastal plain generally comprises recent unwelded ignimbrites, gravel, silt, peat, alluvial and aeolian sands, and interbedded pumaceous tuff deposits of the Tauranga Group. The permeability of these materials is typically moderate, but low where silt, peat and clay predominate.

In addition, there are a series of andesite and rhyolite (volcanic hard rock) intrusions that form the Papamoa Ranges in the northwest of the Kaituna WMA and three greywacke basement highs (exposures) inland from Matata in the east of the area.

Figure 18. Main rock types in the Kaituna WMA. (Refer A3 attachment at rear).

3.3.2 Rangitāiki

Figure 19 shows the distribution of main rock types within the Rangitāiki WMA. As in the Kaituna WMA, the predominant geological type in the west are volcanic sediments (ignimbrites) of the TVZ and much of the alluvium sediment found further to east in the valley floors is derived from the TVZ.

The ignimbrites that cover much of the western and northern areas of the WMA are likely to be Whakamaru Ignimbrites, which comprises a number of individual welded ignimbrites. The Rangitāiki ignimbrite, which erupted from the Whakamaru Calder approximately 340-350 ka and is up to 300 m thick, is interpreted to cover much of

⁸ Pyroclastic rocks are the products of volcanic explosions; that is, they are fragmental pieces of rock, whether they be minerals, crystals or glass, ejected from the vent (source: Wikipedia).

the area. The Rangitāiki ignimbrite is considered moderately welded and hence groundwater flow within this unit is governed by fracture propensity, which is variable. However, overall the various ignimbrites in the WMA are typically considered to have only moderate permeability.

Greywacke basement rocks of the Waipapa Terrane form the mountain ranges in the eastern side of the Rangitāiki WMA. Permeability within greywacke rocks is typically controlled by fractures, but due to the age of these deposits (Jurassic to Early Cretaceous 200 to 145 Ma), fractures are typically clay infilled due to extensive weathering. Overall, the permeability of greywacke rocks is typically considered to be very low. Recent alluvial deposits downstream of the greywacke ranges in the south-eastern part of the WMA are generally dominated by greywacke derived gravels.

The Galatea Basin is positioned in the middle of the Rangitāiki WMA between the ignimbrites to the north and west and the greywacke to the south. This structure is infilled with recent alluvium of the Tauranga Group, which composes a mix of alluvial deposits derived from pumice (TVZ) and greywacke sources.

The geology of the Rangitāiki Plains includes river transported pumice and silts interspersed with wetland materials (peats) and old beach and sand dune deposits. The plains are flanked on the east by the greywacke basement rocks of the Raungaehe Range and in the west by the volcanic/sedimentary sediments of the Kaharoa Plateau and Manawahe Hills.

Figure 19. Main rock types in the Rangitāiki WMA. (Refer A3 attachment at rear).

3.3.3 Rock Permeability

As alluded to above, the primary rock types provide a strong control on the sub-soil drainage rate and rate of movement of water through unsaturated zone between the soil and the groundwater table. The SMWBM accounts for this movement of water and requires an estimate of the rock vertical hydraulic conductivity (K_v), which was made on the assumption of rock type horizontal hydraulic conductivity (**Section 6.3.6**).

The distribution of unsaturated zone vertical hydraulic conductivity for the Kaituna and Rangitāiki WMAs, are shown in **Figure 20** and **Figure 21**, respectively based on rock types as described QMAP. Noticeable patterns from these figures are as follows:

- With eastward movement from the highlands to the coast within the Kaituna WMA, K_v values increase, which is reflective of the main geology type changing from a predominately ignimbrite (moderate K_v) to a gravel in the lowland areas.
- Within the Rangitāiki Galatea plains area (central domain downstream of the Whirinaki River confluence and the Lower Rangitāiki Plains) and lowland area there are large K_v values due to the underlying main rock of gravel and pumice respectively; and
- Throughout the rest of the Rangitāiki catchment the prominent rock type is ignimbrite with some sandstone in the eastern domain comprising the Urewera Mountain area (Whirinaki River and eastern side sub-catchments), which has slightly more impermeable K_v values reflective of this sandstone.

Figure 20. Sub-catchment vertical hydraulic conductivity in the Kaituna WMA. (Refer A3 attachment at rear).

Figure 21. Sub-catchment vertical hydraulic conductivity in the Rangitāiki WMA. (Refer A3 attachment at rear).

3.4 Soils

Proximity to the TVZ and the type of parent rocks in the Kaituna and Rangitāiki WMAs have a strong bearing on the type and physical characteristics of the soils in the area. Of primary importance to this study are the hydraulic characteristics and erosivity of the soils. Soil hydraulic characteristics typically reflect soil texture and significantly influence surface infiltration and sub-soil drainage rates which in-turn have a strong bearing on the generation of surface runoff and groundwater recharge. Erosivity of soils exerts a strong influence on sediment generation with more highly erodible soils generating greater volumes of sediment in surface runoff.

There are four primary soil-forming parent materials in the Kaituna and Rangitāiki WMAs (BOPRC, 2010) which are shown in **Figure 22** and **Figure 23**, respectively and further described in the following sub-sections:

- Tephra;
- Alluvium and colluvium;
- Peat; and
- Wind-blown sand.

3.4.1 Tephra

As described in the previous section, in western parts of both WMAs ignimbrite rocks from the TVZ dominate the surficial geology. Generally, these rocks are mantled by tephra⁹ deposits in the form of pumice and ash which are the primary control on soil type and characteristics in this area. The tephra mantle is typically sandy, with coarser grain size in the west closer to the TVZ source becoming progressively finer to the east. However, on steep slopes where the pumice and ash mantle has been removed, basement rock (typically mudstone) determines the nature, magnitude and severity of erosion.

3.4.2 Alluvium and Colluvium

Alluvium is widespread in areas such as the Rangitāiki Plains, and on flood plains deposited along the margins of the main rivers. Colluvium refers to unconsolidated sediments accumulated along the base of hillslopes as fans or valley fill materials as a result of erosion from adjacent hill country. Colluvial deposits are extensive in the eastern part of the Galatea Basin and occur on small fans throughout both WMAs.

3.4.3 Peat

Peat is an accumulation of partially decayed vegetation or organic matter that has been deposited in a damp or wet, mainly anoxic sedimentary environment. In the Kaituna and Rangitāiki WMAs peat deposits occur on the low-lying coastal plains, such as the many areas of the Rangitāiki Plains and on the Te Puke flats. In some small areas, thin to very thin layers of diatomaceous earth occur in the subsoil, which limit sub-soil drainage.

3.4.4 Wind-Blown Sand

Wind-blown sand occurs in a belt along the east coast and in local areas further inland. The dunes along the Rangitāiki Plains coast are covered or mixed with tephra.

⁹ General term for all unconsolidated clastic volcanic material.

Figure 22. Soil cover within the Kaituna WMA. (Refer A3 attachment at rear).

Figure 23. Soil cover within the Rangitāiki WMA. (Refer A3 attachment at rear).

3.4.5 Soil Hydraulic Properties

Appendix D provides a description of the various soil hydraulic properties available in the SMap coverage developed by Landcare Research, which were used to help characterise the soil properties found within the Kaituna and Rangitāiki WMA. The key properties of relevance to this study include the following:

- **Soil Permeability** – the rate that water moves through a saturated soil material. Permeability defines the ability of a soil to drain and therefore the partitioning of heavy rainfall into surface runoff or soil infiltration and ultimately percolation to groundwater. Soil permeability is primarily controlled by the texture, structure and density of the soil materials. Unconsolidated, coarse-textured soils typically exhibit high permeability enabling rapid vertical drainage through the soil profile. In contrast, fine-textured or consolidated soils typically exhibit low permeability increasing the potential for ponding and/or runoff in response to rainfall events. Soil permeability from the SMap coverage was used as a guide to set the soil infiltration capacity value in the rainfall runoff model component of SOURCE (the SMWBM).
- **Potential Rooting Depth** – describes the depths (in metres) to a layer that may impede root extension and hence the depth of soil that a plant can exploit water from. Rooting depth was used as a guide to the relative depths of soil in setting the soil moisture storage value in the rainfall runoff model (the SMWBM).
- **Plant Available Water** – is the amount of water potentially available for plant growth. The capacity to store this water depends on the soil physical characteristics. PAW accounts for variations in soil horizons and is expressed in units of millimetres of water.
- **Depth to Slow Permeable Horizon** – indicates the depth at which the soil becomes less permeable through the soil zone. This helps to describe how well drained a soil zone is, for example if the depth to slow permeable horizon is near the surface then the soil zone is likely to have ponding in high rainfall events (SMap, 2018).
- **Drainage Class** – describes how well drained the soil is (throughout the year). Poorly drained soils indicate areas that limit the amount of flow through the soil zone, while well drained soils indicate highly permeable areas.

The spatial variability in soil permeability and rooting depth in the Kaituna and Rangitāiki WMAs is shown in **Figure 24** to **Figure 27** respectively, while **Table 16** summarises the overall spatial variability of these parameters. From comparison of the mean statistics in **Table 16**, it can be seen the soils are generally deeper and more permeable in Rangitāiki compared to the Kaituna WMA. Therefore, it can be hypothesised that there would be larger baseflow in the Rangitāiki compared to that of the Kaituna (especially in the areas which have flatter areas).

Figure 24. Soil permeability within the Kaituna WMA. (Refer A3 attachment at rear).

Figure 25. Soil permeability within the Rangitāiki WMA. (Refer A3 attachment at rear).

Figure 26. Soil potential rooting depth within the Kaituna WMA. (Refer A3 attachment at rear).

Figure 27. Soil potential rooting depth within the Rangitāiki WMA. (Refer A3 attachment at rear).

Table 16. Summary of the spatial variability in key soil hydraulic properties.

Hydraulic property	Kaituna WMA		Rangitāiki WMA	
	Soil permeability (mm/hr)	Soil potential rooting depth (m)	Soil permeability (mm/hr)	Soil potential rooting depth (m)
Min	<4	0.15	<4	0.15
Mean	33.77	0.37	62.8	0.57
Max	>75	1.5	>75	1.5

3.5 Groundwater

An approximation of the depth to groundwater was required as groundwater table levels were not presently available from the groundwater model currently being developed by Jacobs. The estimated values represent the thickness of the unsaturated zone, which is taken from the base of the soil to the permanent groundwater table. Depth to groundwater was calculated from an estimated mean groundwater elevation in each sub-catchment subtracted from the mean ground surface elevation.

As shown in **Figure 28** the prominent pattern in the Kaituna WMA is that the high elevation areas have a larger depth to groundwater (a longer time period for water from the surface to drain to groundwater) compared to the lowland areas. However, in the Rangitāiki WMA the pattern generated was not so clear, with large values (150 to 250 m) in the mountainous Urewera area (Whirinaki River and eastern side sub-catchments), yet only moderate values in the highland area north of SH5 with values of <30 m (**Figure 29**).

The depth to groundwater data presented in this report should not be considered detailed enough to be used in a groundwater study and is used here as an approximation for parameterisation of the SMWBM.

Figure 28. Depth to Groundwater within the Kaituna WMA. (Refer A3 attachment at rear).

Figure 29. Depth to Groundwater within the Rangitāiki WMA. (Refer A3 attachment at rear).

3.6 Spring Inflows

Freshwater and geothermal springs occur throughout the Kaituna and Rangitāiki WMAs. Spring discharge, particularly from geothermal sources, also may have a significant impact on downstream water quality in terms of selected parameters (e.g. redox, dissolved oxygen, metal ions, sulphate, heavy metals).

At the current time, although there is an investigation being undertaken by the BOPRC, considerable uncertainty remains regarding water quality influences associated with spring discharges in these catchments. In terms of overall catchment water balance, springs typically represent a small component, which is accounted for by the groundwater flow generated by the model. However, the constituent load from springs was not accounted by the model and needed to be estimated and incorporated into the models. This is described for individual constituents in **Section 7**.

3.7 Land Use

The land use and vegetation cover of an area is one of the controlling drivers of hydrological responses. The density of vegetation, the level of disturbance (anthropogenic or natural i.e. storm erosion) and the type of vegetation cover will contribute to how water is moved through a catchment on both a temporal and spatial scale.

Land use practices can also exert a significant influence on the water quality of a catchment, for example higher levels of *E. coli* are typically found in areas of more developed and intensive land use (Collins and Rutherford, 2004.).

BOPRC provided a geospatial land use layer describing either the land use practice (e.g. sheep and beef farming) or the land cover present (e.g. native forest). Land use is used throughout this report to refer to both land use and land cover collectively.

The BOPRC land use layer did not cover the full extent of the catchments¹⁰ and was used in conjunction with the land cover data base (LCDB) geospatial layer to assess the land use types present in the Kaituna and Rangitāiki WMAs.

Both geospatial layers provided a high-resolution interpretation of the differing land use practices and vegetation cover present, with a total of twenty-two and thirty classes present in the Kaituna and Rangitāiki WMAs, respectively. To simplify these layers, land use practices and vegetation types that would likely result in similar hydrological and constituent generation responses were grouped into eleven classes, as summarised in **Table 17**.

Table 17. Grouped land use classifications in the Kaituna and Rangitāiki WMAs.

Land Use Classification	Land Uses Grouped to Form Condensed Classification	Original Data Source
Arable	Arable	BOPRC
Dairy	Dairy, high intensity grazing, and high producing exotic grasslands	BOPRC and LCDB
Forest	Forest native, matagouri, gorse, broom, fern land, Manuka trees, Kanuka trees, indigenous forest, and broadleaf indigenous hardwood	BOPRC and LCDB
Plantation Forest	exotic forest ¹¹ , and harvested forest	BOPRC and LCDB
Hydro	Hydro, rivers, and lakes.	BOPRC and LCDB
Kiwifruit and Orchards	Kiwifruit, orchards, vineyard, and perennial crop	BOPRC and LCDB
Lifestyle	Lifestyle	BOPRC and LCDB
Parks and Reserves	Parks and reservations, and urban parklands	BOPRC and LCDB
Scrub	scrub, mixed exotic scrub, grey scrub	
Sheep and Beef	Deer, sheep and beef, and low producing grasslands	BOPRC and LCDB
Urban, road, rail and unknown	Other, urban/rail/road, unknown, built up area (settlement), transport infrastructure and bare ground	BOPRC and LCDB
Vegetables	Vegetables and short rotation crops	BOPRC and LCDB
Wetlands	wetlands, herbaceous freshwater vegetation, mangrove, and herbaceous saline vegetation	BOPRC and LCDB

The breakdown of area as a percentage of total area for the land use classes in each WMA is outlined in **Table 18**. The largest single land use in the Kaituna WMA is dairy (28%), which is distributed throughout the entire catchment. Also prevalent is plantation forest (22%), native forest (19%), sheep and beef (14%) and horticulture (7%) (**Figure 30**). Whereas, the Rangitāiki WMA is primarily plantation forest (53%) and native forest (28%).

The Rangitāiki WMA also has a high concentration of dairy (9%) and sheep and beef (7%) in the well-developed areas of the Galatea plains and lowland coastal Plains (**Figure 31**).

¹⁰ In the Rangitāiki WMA small areas were missing on the northern side, and in the Kaituna WMA pockets were missing along the north, south and western boundaries.

¹¹ Exotic forest is mentioned under the land use class 'forest' and 'plantation forest' in the LCDB layer, which classifies exotic forest as exotic trees that are not felled or planted for economic profit. BOPRC classifies exotic forest as any plantation forest that undergoes a felling cycle, which will have a different impact on the hydrological and constituent responses. Therefore, the LCDB exotic forest is treated as 'forest', whereas BOPRC exotic forest is classified as plantation forest.

Table 18. Area proportions of the different land use classifications in the Kaituna and Rangitāiki catchment models.

Land Use Classification	Kaituna (% of area)	Rangitāiki (% of area)
Arable	1.4%	1.0%
Dairy	27.5%	9.0%
Forest	19.1%	28.0%
Plantation Forest	22.1%	53.0%
Hydro	0.9%	1.0%
Kiwifruit and Other Horticulture	7.3%	<0.1%
Lifestyle	2.7%	<0.1%
Parks and Reserves	0.2%	<0.1%
Scrub	0.5%	<0.1%
Sheep and Beef	14.4%	7.0%
Urban, Road, Rail or Unknown	3.9%	1.0%
Vegetables	<0.0%	<0.1%

Figure 30. Land Use Classifications Across the Kaituna WMA. (Refer A3 attachment at rear).

Figure 31. Land Use Classifications Across the Rangitāiki WMA. (Refer A3 attachment at rear).

4. Catchment Flow Regime

4.1 Catchment Discharge Coefficient

To provide an understanding of the integrity of gauge data to be used in the flow calibration process and to gain a conceptual understanding of the catchment's flow regime characteristics, catchment water budgets were calculated using the measured flow data provided by BOPRC (**Table 2** and **Table 3**).

For the main flow monitoring locations, mean annual flow and mean annual precipitation were calculated and the ratio of flow to rainfall on an average annual basis (catchment discharge coefficient) are summarised for the Kaituna and Rangitāiki (**Table 19** and **Table 20**).

Depending on the climate and the catchment characteristics, the general expectation based on our experience is that catchment evaporative process in most typical New Zealand catchments will account for approximately 35 – 45% of total rainfall, thus catchment discharge (surface water and groundwater flows collectively) should account for approximately 55 – 65%. This range may vary however, for example, in highland areas this value may increase due to colder climates, which serves to reduce evaporation. It is also important to note that flow in the river (i.e. gauged flow) may not account for all catchment discharge. For example, catchment discharge may not be fully represented by river flow if there are significant surface water losses to groundwater, or groundwater discharging directly to the coast.

In the Kaituna WMA (**Table 19**) it is evident that discharge coefficients vary significantly, with Waiari River at Muttons gauge, Pongakawa at Old Coach Rd gauge and Waitahanui River at Otamarakau Valley Rd gauges on the higher side of that expected (>65%). The Kaituna River at Taheke gauge, Paraiti (Mangorewa) River at Saunders gauge, Puanene Stream at SH2 gauge, were on the lower side of that expected.

In the Rangitāiki WMA (**Table 20**) catchment discharge coefficients were more consistent, with only the Whirinaki River at Galatea and Waihua Gauge at Gorge higher than expected.

Table 19. Kaituna catchment mean annual flow.

Kaituna Gauge Catchments	Area (km ²)	Mean Annual Flow (m ³ /s)	Mean Annual Rainfall (m ³ /s)	Flow as a % of rainfall (%)
Kaituna River at Taheke	4.6	0.14 ¹	0.29	49%
Paraiti (Mangorewa) River at Saunders	173.2	5.99	12.61	48%
Kaituna River at Te Matai	326.1	14.13 ²	20.84	68%
Waiari River at Muttons	70.0	3.83	4.90	78%
Pongakawa River at Old Coach Road	101.1	4.72	6.24	76%
Waitahanui River at Otamarakau Valley Road	152.1	5.80	7.89	74%
Raparapahoe Stream at Drop Structure	51.2	2.00	3.30	60%
Puanene Stream at State Highway 2 (SH2)	12.7	0.10	0.58	17%

Notes:

1. Mean flow excludes the flow from the Rotorua lakes, therefore is effectively the discrete flow generated in the sub-catchment between the outlet of Lake Rototiti. The mean flow including discharge from Rotorua lakes is 21.5 m³/s.
2. The mean flow including discharge from Rotorua lakes is 35.29 m³/s.

Table 20. Rangitāiki catchment mean annual flow.

Rangitāiki Gauge Catchments	Area (km ²)	Mean Annual Flow (m ³ /s)	Mean Annual Rainfall (m ³ /s)	Flow as a percentage of rainfall (%)
Rangitāiki River at SH5	101.1	2.46	4.54	54%
Rangitāiki River at Murupara	1,148.2	32.00	49.67	64%
Whirinaki River at Galatea	507.1	14.13	21.93	64%
Pokairoa River at Railway Culvert	118.1	3.95	6.10	65%
Waihua River at Gorge	45.5	1.48	2.27	65%
Rangitāiki River at Waiohou Bridge	2,689.3	54.69	100.92	54%
Rangitāiki River at Te Teko	2,845.7	65.92	130.28	51%

4.2 Catchment Specific Discharge

The calculated rate of flow per unit area or catchment specific discharge is summarised in **Table 21**. Comparison of specific discharge across the monitoring locations provides an indication of the average flow variability between catchments due to either climatic or catchment characteristics¹². Plotting the specific discharge against mean annual precipitation for each gauged catchment provides a sense of the flow regime variability and readily highlights any outliers (**Figure 32**).

Table 21. Catchment specific discharge.

Gauge Catchments	WMA	Area (km ²)	Mean Q (m ³ /s)	Mean Specific Q (m ³ /s/km ²)
Kaituna River at Taaheke	Kaituna	4.6	0.14	0.031
Paraiti (Mangorewa) River at Saunders	Kaituna	173.2	5.99	0.035
Kaituna River at Te Matai	Kaituna	326.1	14.13	0.043
Waiari River at Muttons	Kaituna	70.0	3.83	0.055
Pongakawa River at Old Coach Road	Kaituna	101.1	4.72	0.047
Waitahanui River at Otamarakau Valley Road	Kaituna	152.1	5.80	0.038
Raparapahoe Stream at Drop Structure	Kaituna	51.2	2.00	0.039
Puanene Stream at State Highway 2 (SH2)	Kaituna	12.7	0.10	0.008
Rangitāiki at SH5	Rangitāiki	101.13	2.46	0.024
Rangitāiki at Murupara	Rangitāiki	1,148.17	32.00	0.028
Whirinaki at Galatea	Rangitāiki	507.18	14.13	0.028
Pokairoa at Railway Culvert	Rangitāiki	118.08	3.95	0.033
Rangitāiki at Waiohou Bridge	Rangitāiki	2,689.26	54.69	0.020
Waihua at Gorge	Rangitāiki	45.51	1.48	0.033
Rangitāiki at Te Teko	Rangitāiki	2,845.65	65.92	0.023

¹² Note – in the calculations the influence of discharges from the Rotorua lakes has been removed.

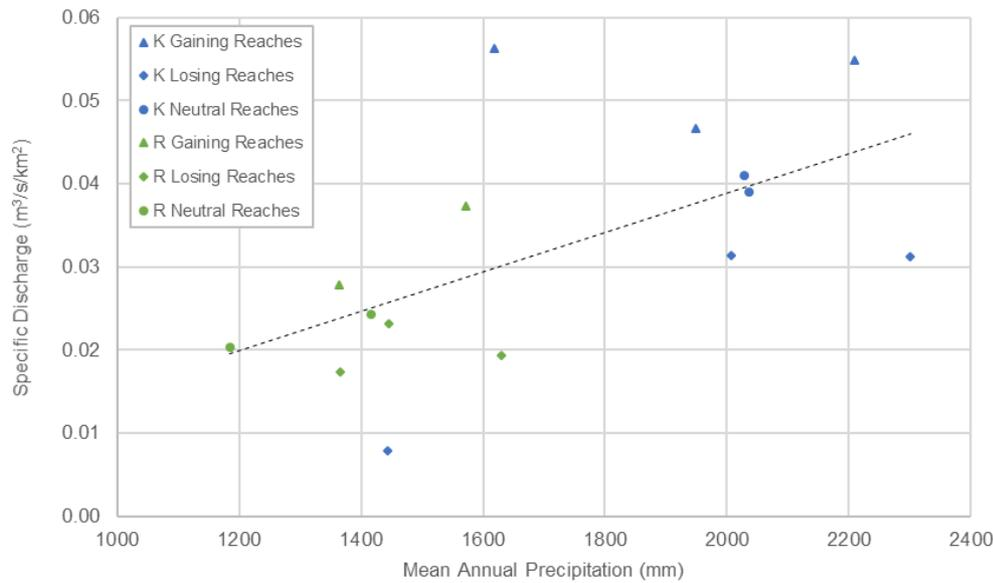


Figure 32. Mean annual precipitation versus specific discharge.

The range in specific discharge is 0.008 to 0.055 m³/s/km², with a median value in the project area of 0.03 m³/s/km². Catchments with specific discharges that are considered close to the median are regarded as “typical” catchments which include Raparapahoe Stream at Drop Structure gauge, Paraiti (Mangorewa) River at Saunders gauge, Waihua at Gorge gauge and Pokairoa at Railway Culvert gauge

4.3 Gauge Catchment Summary

Information on catchment characteristics provided in **Section 3** was used in conjunction with the flow regime analysis in **Sections 4.1** and **4.2** to compare, contrast and explain the overall catchment flow regime within each of the gauged catchments for both WMAs (**Table 22**).

Table 22. Summary of flow regime and predominant relevant catchment physical characteristics.

Gauge Catchments	WMA	MAP (mm) ¹	Soil	Geology	K _v [range and average] (m/s) ²	DTG (mBGL) ³	Summary
Kaituna River at Taaheke (SC15)	Kaituna	2,121	Sandy shallow hill soils cover majority of the catchment derived from the Central Plateau pumice.	This catchment is underlain by sub rock of pumice, lapilli and ash with a main rock of Ignimbrite.	1.65 x10 ⁻⁶	114 m	This catchment is controlled by the inflow from Lake Rotoiti, as the size of this catchment (4.6 km ²) is small in comparison to the drainage network of Lake Rotoiti and Lake Rotorua (Figure 34). Infiltration characteristics are high given the geological aspect of this catchment, which displays high rock permeability allowing enhanced percolation to groundwater. This combined with the high soil permeability of this catchment indicates that the catchment is controlled by baseflow properties. The calculated specific discharge is 0.031 m ³ /s/km ² and discharge as a percentage of rainfall is 49% (Table 19). The influence of the lake inflow has been removed for the catchment analysis calculation. This catchment is comparable to the sub-catchments surrounding, although it does indicate slightly less discharge as a percentage of rainfall, which indicates there are larger losses.
Paraiti (Mangorewa) River at Saunders (SC10)	Kaituna	2,297	Parent material of tephra, associated with Central Plateau pumice	This catchment is underlain by sub rock of pumice, lapilli and ash with a main rock of Ignimbrite.	9.00x10 ⁻⁷ to 6.81x10 ⁻⁶ ; 1.97x10 ⁻⁶	45 to 136 m	Infiltration rates are high due to the sandy soil and permeable geological properties. The flat pumice geology exhibited in the back catchments can influence the direction of sub soil drainage and be different to “apparent” or mapped surface water path. Analysis of this catchment found the specific discharge was 0.035 m ³ /s/km ² and discharge as a percentage of rainfall is 48% (Table 19). This is comparable to the Kaituna river at Taaheke gauge, which stated before shows discharge percentage of rainfall is on the lower side of that expected (<55%).
Kaituna River at Te Matai (SC26)	Kaituna	2,302	The soil characteristics are associated with the Central Plateau pumice with the influence of coastal sands closer to the coast.	This catchment is underlain by sub rock of pumice, lapilli and ash with a main rock of Ignimbrite.	9.00x10 ⁻⁷ to 2.00x10 ⁻⁵ ; 7.45x10 ⁻⁶	8 to 140 m	Soil characteristics are highly permeable throughout the catchment, as is the sub-soil permeability with varied permeability in the lowland area near the coast, which is characteristic of a pumice residual alluvial material. The K _v ranges also indicate that rock permeability increases towards the coast. The slope for the catchment is steep in the headwaters and gradually descending and becomes flatter before the gauge. This will influence the potential overland flow rate for the catchment. Specific discharge was 0.043 m ³ /s/km ² and discharge as a percentage of rainfall is 68% (Table 19). This analysis indicates that the measured flow at this gauge is within a ‘typical’ range for catchments in the Kaituna WMA.

Gauge Catchments	WMA	MAP (mm) ¹	Soil	Geology	K _v [range and average] (m/s) ²	DTG (mBGL) ³	Summary
Waiari River at Muttons (SC36)	Kaituna	2,304	Parent material of tephra, associated with Central Plateau pumice	This catchment is underlain by sub rock of pumice, lapilli and ash with a main rock of Ignimbrite.	8.40x10 ⁻⁷ to 9.04x10 ⁻⁷ ; 8.85x10 ⁻⁷	62 to 110 m	Similar to the above catchments the soil permeability of this catchment indicates that the catchment is controlled by baseflow properties. The geology of this catchment is permeable, however, the average K _v value for this catchment indicates that the rock permeability is less permeable compared to the above catchments. Although this catchment does display large sub surface flow, slope is steeper than the catchments above and will influence the surface runoff potential down the catchment allowing for flashy overland flow. Analysis of this catchment found the specific discharge was 0.055 m ³ /s/km ² and discharge as a percentage of rainfall is 78% (Table 19), which is higher than the above catchments and attributed to cooler climate and lower evaporation (Table 14).
Pongakawa River at Old Coach Road (SC96)	Kaituna	1,882	Parent material of tephra, associated with Central Plateau pumice, with an influence of gravel through the incised river valleys.	This catchment is underlain by sub rock of pumice, lapilli and ash with a main rock of Ignimbrite. Sub rock of gravel influences the highland western area.	9.37x10 ⁻⁷ to 5.84x10 ⁻⁶ ; 3.21x10 ⁻⁶	25 to 87 m	Shallow sandy hill soils cover the majority of the catchment, which is characteristic of well-drained soil combined with permeable geological areas. Combined they result in significant sub-surface flow. The western side of the catchment has a larger slope degree compared to the eastern side, which will generate flashier overland flow for this area. Specific discharge was 0.047 m ³ /s/km ² and discharge as a percentage of rainfall is 76% (Table 19). This catchment is noticeably different to the other catchments in the WMA due to the higher percentage of rainfall, which on average is higher than the expected 55-65 %. However, in highland areas discharge as a percentage of rainfall may increase due to the cooler climate, which is the case here with a mean elevation of 193.5 m AMSL (Table 14).
Waitahanui River at Otamarakau Valley Road (SC112)	Kaituna	1,832	Similar to Pongakawa at Old Coach Road with parent material of tephra with gravels through the incised river valleys.	The main geological parent material in the catchment is ignimbrite, with minor pumice lapilli ash. Gravel influences the highland western area.	9.07x10 ⁻⁷ to 6.68x10 ⁻⁶ ; 3.03x10 ⁻⁶	40 to 89 m	The catchments physical characteristics is similar to the Pongakawa River at Old Coach Rd gauge. Shallow sandy hill soils cover the majority of the catchment, which is characteristic of well-drained soil combined with permeable geological areas. K _v range for this catchment is also similar to the above gauge. There is a steeper gradient compared to Pongakawa, which will influence surface runoff i.e. flashier overland flow. Specific discharge is 0.038 m ³ /s/km ² and discharge as a percentage of rainfall is 74% (Table 19).
Raparapahoe Stream at Drop Structure (SC44)	Kaituna	2,242	Parent Material of tephra associated with Central Plateau pumice.	This catchment is underlain by two types of rock; andesite and ignimbrite. The lower end of the catchment that comprises the flow gauge has alluvial sub-surface materials comprised of gravel, sand and silt.	5.79x10 ⁻⁷ to 1.38x10 ⁻⁵ ; 5.09x10 ⁻⁶	7 to 117 m	Shallow sandy hill soils cover majority of the catchment, which is characterised by well-drained soil. Ignimbrite is generally more porous when compared to andesite, due to the softness of the rock (less indurated). Where andesite prevails, the catchment slope is typically greater and subsurface drainage and unsaturated zone flow rates are at the lower end, which means the soils will become saturated easier and direct rainfall proportionally into surface runoff during wet periods. Depth to groundwaters is greater in the highland areas compared to the lowland area and consequently percolation times are longer in highlands compared to the lowland areas. Analysis of this catchment found the specific discharge was 0.039 m ³ /s/km ² and discharge as a percentage of rainfall of was only 60% (Table 19). This specific discharge and catchment discharge coefficient in the typical range compared to the other gauge catchments in the Kaituna WMA.

Gauge Catchments	WMA	MAP (mm) ¹	Soil	Geology	K _v [range and average] (m/s) ²	DTG (mBGL) ³	Summary
Puanene Stream at State Highway 2 (SH2) (SC77)	Kaituna	1,576	Coastal sandy soil. The parent material being tephra.	The main sub-surface geology is ignimbrite, with gravel near the gauge end of the catchment.	1.10x10 ⁻⁶ to 6.78x10 ⁻⁶ ; 3.94x10 ⁻⁶	25 to 60 m	<p>The well-drained soil and lowland coastal gravel infers moderate to high sub soil drainage. There are only two sub-catchments within this reach, and as indicated from the depth to groundwater, the time for sub-soil drainage to reach the groundwater table is significantly greater in the higher elevation (back) catchment.</p> <p>Analysis of this catchment found the specific discharge was 0.008 m³/s/km² and discharge as a percentage of rainfall of was only 17% (Table 19). This catchment is noticeably different compared to the other catchments in the WMA due to the apparent lack of measured flow at the gauge. A possible reason for this is flow from the higher land areas is either i) recharging a deeper aquifer with flow significantly under the gauge, or ii) dispersing into the alluvial aquifer as it reaches the low gradient section of the reach.</p>
Rangitāiki at SH5 (SC1)	Rangitāiki	1,422	Sandy shallow high-country soils cover majority of the catchment from a parent material of tephra, associated with the Central Plateau pumice.	This catchment is underlain by rhyolitic ignimbrite and includes sub rocks of pumice, ash, gravel, sand, silt beds.	8.76x10 ⁻⁶	75 m	<p>The catchment displays high soil permeability and high rock permeability facilitating reasonably rapid rates of percolation to groundwater. The high permeability combined with relatively flat nature of the catchment results in ponding during heavy rainfall (rather than running off directly), with the ponded water infiltrating into the soils after the rain passes. Analysis of this catchment found the specific discharge was 0.024 m³/s/km² and discharge as a percentage of rainfall is 54% (Table 20). This catchment is within the head of this WMA and indicates a larger flow for its area compared to that of the downstream gauge Rangitāiki at Murupara.</p>
Rangitāiki at Murupara (SC26)	Rangitāiki	1351	Sandy shallow high-country soils cover majority of the catchment from a parent material of tephra, associated with the Central Plateau pumice.	This catchment is underlain by materials from rhyolite and ignimbrite, and includes pumice and breccia beds.	7.91x10 ⁻⁷ to 2.96x10 ⁻⁶ ; 1.09x10 ⁻⁶	29 to 110 m	<p>The combination of the sandy soils and pumice sub rock and a gentle gradient (average 4.7 degrees) (Table 15) indicates that this reach is highly permeable and flow will be directed into sub-surface flow (refer to Section 3.3 and Section 3.4). There is a large range in the depth to groundwater values, reflective of the changing elevations through the catchment (given similar geology). Analysis of this catchment found the specific discharge was 0.028 m³/s/km² and discharge as a percentage of rainfall is 64% (Table 20). This catchment is noticeably different compared to the other catchments in the WMA due to the apparent lack of measured flow at the gauge compared to the surrounding catchments (Rangitāiki at SH5, Whirinaki at Galatea). A possible reason for this is the permeable nature of this catchment and significant depth to groundwater suggests flow to be directed towards a deeper aquifer system that is not captured by the gauge.</p>

Gauge Catchments	WMA	MAP (mm) ¹	Soil	Geology	K _v [range and average] (m/s) ²	DTG (mBGL) ³	Summary
Whirinaki at Galatea (SC47)	Rangitāiki	1,373	Majority of this reach is comprised of steep gradients, with a thin mantle of sandy soils overlaying indurated greywacke basement rocks.	The parent rock is largely greywacke (indurated fine sandstone and mudstone) in the east, with volcanic derived materials in the north and on the Central Plateau further to the west.	2.34x10 ⁻⁷ to 2.26x10 ⁻⁶ ; 7.06x10 ⁻⁷	55 to 194 m	While the soils tend towards highly permeable nature, the greywacke (sandstone and mudstone) are typically of much lower permeability than the volcanic materials of the Central Plateau. This indicates that rates of sub-soil drainage and percolation in this catchment are expected to be lower than other parts of the WMA. This reach is expected to be flashy (highly influenced by surface runoff) due to the typically lower permeability of the soils and sub-soils, and the steep gradient of this catchment (20 degrees). Groundwater recharge rates will be low and travel times long (slow) due to the very deep groundwater and low rock permeability. A specific discharge of 0.028 m ³ /s/km ² and a discharge coefficient of 64% indicates that the catchment has higher rates of discharge compared to its adjacent catchment Rangitāiki at Murupara (Table 20). This is not surprising as most rainfall which falls on this reach will be directed to overland flow (rather than being captured in the soil zone).
Pokairoa at Railway Culvert (SC73)	Rangitāiki	1,563	Soils within this catchment comprise gravel derived from tephra rock.	This catchment is underlain by rocks formed from rhyolite ignimbrite and includes pumice and breccia beds.	2.82x10 ⁻⁷ to 1.48x10 ⁻⁶ ; 9.82x10 ⁻⁷	16 to 89 m	This catchment is well-drained due to the gravelly soils derived from tephra rock. It is assumed that there will be a large sub soil drainage within this catchment. Two sub-catchments are situated on a plateau and have significant groundwater depth. These flat plateaus will result in a propensity for ponding as opposed to direct surface runoff during high intensity rainfall events, and subsequent percolation to groundwater. The third sub-catchment is steep, which will result in flashier overland flow responses during storms. Specific discharge was 0.019 m ³ /s/km ² and discharge as a percentage of rainfall is 37% (Table 20). This catchment is noticeably different compared to the other catchments in the WMA due to the apparent lack of measured flow at the gauge. It has the lowest percentage of rainfall within the Rangitāiki catchment. A possible reason for this is flow from the higher land areas (Plateau) is percolating to the deeper aquifer and not being captured by the gauge.
Waihua at Gorge (SC90)	Rangitāiki	1,571	The majority of soils within this catchment comprise highland sandy soils derived from volcanic activity.	The main rock type on the eastern side of Rangitāiki is greywacke (sedimentary fine sandstone with mudstone sub rock).	2.09x10 ⁻⁷ to 1.55x10 ⁻⁶ ; 8.80x10 ⁻⁷	96 to 209 m	This catchment is similar to Whirinaki at Galatea which has less permeable soil and geology which partitions more rainfall into overland flow compared to infiltrating and draining through the soils (Section 3.3 and Section 3.4). There is also a steep gradient within these sub-catchments which reinforces surface runoff directly to water courses. The specific discharge was 0.033 m ³ /s/km ² and discharge as a percentage of rainfall is 65% (Table 20). This catchment is noticeably different compared to the other catchments in the WMA due to the large measured flow at the gauge compared to the surrounding catchments.

Gauge Catchments	WMA	MAP (mm) ¹	Soil	Geology	K _v [range and average] (m/s) ²	DTG (mBGL) ³	Summary
Rangitāiki at Waiohou Bridge (SC32)	Rangitāiki	1,398	The catchment has three domains (eastern, western and central) with essentially the same sandy shallow soils derived from tephra. However, the eastern domain is significantly steeper and soils shallower.	The parent rock is largely greywacke (indurated fine sandstone and mudstone) in the east, with volcanic derived ignimbrite materials in the west and central domains.	2.13x10 ⁻⁷ to 7.49x10 ⁻⁶ ; 1.92x10 ⁻⁶	81 to 241 m	Rangitāiki at Waiohou bridge is located at the convergence of three sub-catchments discharging from different parts of the catchment (eastern, western and central domain), with the eastern catchments displaying significantly steep land surface gradients than the other two domains. The flow regime is a culmination of many different upstream catchment characteristics, along with the influence of Lake Aniwanuiwa. The sandy soil throughout this catchment exhibits a permeable reach. The main rock in the central domain area (gravel) and the rock exhibited in the western area (ignimbrite) exhibits highly permeable geology. While the eastern side exhibits lower permeability due to the sandstone rock. Groundwater is typically deep to extremely deep in the higher land areas. The central and western domain will be predominately baseflow dominated, while the steeper eastern side will have a greater proportion of surface runoff (quick flow). The discharge coefficient is equivalent to 54%, with a specific discharge of 0.020 m ³ /s/km ² across the whole reach (Table 20). This specific discharge and catchment discharge coefficient in the acceptable range in comparison to the other gauge catchments in the Rangitāiki WMA
Rangitāiki at Te Teko (SC37)	Rangitāiki	1,354	Alluvial soils of sandy loam and loamy sand comprise the main soils in the coastal area of this catchment.	The predominant rock is ignimbrite, with sub rocks of pumice, lapilli and ash.	7.62x10 ⁻⁷ to 5.88x10 ⁻⁶ ; 2.09x10 ⁻⁶	3 to 119 m	The area between the gauge at Rangitāiki and Waiohou Bridge is characteristic of the Western side of the Rangitāiki WMA. The permeable nature of the soils and the geological characteristics infer that the flow infiltration to sub surface flow is high. There is still an influence of the eastern, western and central plateau area within this reach (without the influence of the upstream reaches) however, it is less pronounced. Due to the size of the upstream catchment, a large amount of water funnels through this location, with a mean discharge of 65.9 m ³ /s (Table 20). Analysis of this catchment found the specific discharge was 0.023 m ³ /s/km ² and discharge as a percentage of rainfall is 51% (which is similar to the upstream gauge – Rangitāiki at Waiohou Bridge) (Table 20).

Notes:

1. MAP (mm) is mean annual precipitation in mm.
2. K_v is estimated average maximum vertical unsaturated hydraulic conductivity in m/s.
3. DTW (mBGL) is estimated average depth to groundwater in metres below ground level.

5. SOURCE Model

To simulate flow in the Kaituna and Rangitāiki WMAs, the eWater SOURCE model was used, with the soil moisture water balance model with vadose zone module (SMWBM_VZ) embedded as the rainfall runoff package. The following section will describe:

- the SOURCE model (**Section 5.1**);
- the SMWBM (**Section 5.2**); and,
- how the SOURCE model was used to simulate flow (**Section 5.3**).

5.1 SOURCE Model Description

SOURCE is a hydrological modelling platform developed by eWater in Australia. The platform is comprised of a range of models and tools designed to simulate all aspects of water resource systems at a range of spatial and temporal scales. The models and tools include:

- Rainfall-runoff models;
- Water demand models; and
- Constituent generation, retention, transport and decay models.

The fundamental architecture of a SOURCE model comprises a series of connected sub-catchments and drainage networks. SOURCE uses nodes with connecting links that enable the user to control the route of flow and (hydrological and constituent) processes that occur along the flow path. The following is a description of the features in SOURCE that were used to calibrate the Kaituna and Rangitāiki Model (SOURCE, 2012):

- **Confluence Node:** Confluence nodes represent a natural join in a river system. Confluence nodes were used in both catchment models as they are able to combine the upstream flow from two sub-catchments before they flow into a downstream sub-catchment.
- **Loss Node:** Loss nodes can be used to represent losses from the stream network, such as large abstractions or losses to deeper groundwater. Loss nodes utilise a relationship with river flow to vary the rate of flow loss i.e. a head or water level dependent flow equation. Loss nodes were applied in both WMAs to represent natural seepage losses from the river channel into deeper groundwater systems.
- **Inflow Node:** Inflow nodes allow the addition of extra flow into the stream network that is not generated by rainfall runoff processes. Inflows can include flow being received from outside of the model domain, such as lakes or catchments that have not been captured in the model, point source discharges of water directly into the river network (i.e. industrial plants), or water being received through the river bed from a deeper aquifer system. Inflow nodes have been used in the Kaituna WMA to represent Lake Rotoiti and the inflow of deeper groundwater back into the stream network. Inflow nodes in the Rangitāiki WMA are used to return surface water lost to deeper groundwater back into the river network in lowland areas.
- **Storage Node:** Storage nodes are used to represent locations where water is stored along the river, such as dams, reservoirs, weirs and ponds. In SOURCE, the storage node calculates the water balance over each time step and is governed and constrained by inflows, physical limits on discharges, downstream demands and gain and loss relationships. Storage nodes were used to represent Lake Rotoehu in the Kaituna WMA and Lake Aniwanuiwa and Lake Matahina in the Rangitāiki WMA. Although Lake Rotoehu is outside of the Kaituna WMA, it was included in the model as during the calibration phase it was found to provide a sub-surface source of flow to the Waitahanui River.
- **Minimum Flow Requirement Node:** Minimum Flow Requirement nodes were used to ensure that there is a minimum flow rate at a given/nominated point in a river system to meet various demands (stock,

domestic or environmental needs). They were also used to generate transfers between an upstream and downstream storage, and impose a constraint that must be met at that point in the river model. A minimum flow requirement was configured in the Rangitāiki WMA, downstream of the Matahina Lake to represent the dam releases, and based on available observed flow released data.

- **Gauge Node:** Gauge nodes represent a location in a river network where there is measured data available for comparison to the simulated data. Gauge nodes are used in both models at primary flow monitoring sites in the Kaituna and Rangitāiki WMAs, as outlined in **Section 2.3.1**.
- **Supply Point Node:** A supply point node identifies the location in a river where water can be extracted to meet a demand. The demand can be for regulated surface water, unregulated surface water or groundwater. Supply point nodes are utilised in both the Kaituna and Rangitāiki WMA to represent water permits authorising abstraction of ground or surface water.
- **Water User Node:** The water user node represents a point in the stream network where a demand is modelled, for example a consent for irrigation. A water user node can generate orders, manage extractions and provide drainage return flows (return flows were not configured in this model). A water user node can only be configured if it is connected to a supply point. Therefore, the supply points configured in both WMAs implement water user nodes, specifying the volume of water being extracted for irrigation use based on demand modelling outlined in **Section 2.4**.

SOURCE includes useful pre-processor tools that expedite model construction. Pre-processor tools utilised for this project are described include:

- **Climate Data Import Tool:** This tool provides a mechanism for rapidly importing gridded daily rainfall or potential evapotranspiration (PET) data (e.g. from the NIWA VCSN network) and interpolating the gridded data to corresponding SOURCE sub-catchments as a mean value for each model timestep (day).
- **Data Import Editor:** The data import editor allows the user to import time series of data, such as irrigation demand or flow monitoring data, that can be utilised and assigned to various features of the model.

5.1.1 Time Control

SOURCE models simulate on a daily time step. The full simulation period of the model is governed by the date range of input data used, primarily climate data.

Initially the climate data will determine the simulation period of a model, based on the number of consecutive days where there is both rainfall and potential evapotranspiration data. The model simulation period is then decreased if any other data set used has a shorter period¹³ than the climate data, i.e. an irrigation demand time series.

The initial simulation period for both WMA models was 01 July 1976 to 30 June 2016, the same period as the utilised climate data (**Section 2.2**). This simulation period is retained in the Kaituna Model but was reduced in the Rangitāiki model as measured data from the Te Teko gauge used for the minimum flow requirement node downstream of the Matahina Dam only extends from 01 July 1976 to 02 June 2016.

Analysis of model results was undertaken on the period from 1980 onwards, and therefore, first three and half years of the model simulation were considered a warmup period.

¹³ If any additional data sets have a longer time period than the climate data, the model simulation period will not be extended.

5.2 Soil Moisture Water Balance Model Description

The Soil Moisture Water Balance Model (SMWBM) is a semi-deterministic model based on the algorithms of Pitman (1967), who originally developed the model to simulate river flows in South Africa. Model functionality has been extended by WWLA recently to incorporate a surface ponding function, evaporation functions for differing land cover, vadose zone unsaturated flow and travel time, and an irrigation demand module. The version of the model utilised for this project is denoted as SMWBM_VZ, to reflect the vadose zone processes.

The SMWBM_VZ was developed into a plugin specific for use as the rainfall runoff model within the SOURCE framework. Within SOURCE, the SMWBM_VZ plugin allows catchment parameters to be set for each of the sub-catchments, transforming the SMWBM_VZ from a semi-deterministic lumped parameter model into a powerful conceptual distributed model.

The model utilises daily rainfall and monthly evaporation input data to calculate the soil moisture conditions under natural rainfall conditions, and under different irrigation schemes. The model operates on a daily time step during dry days, however when rain days occur, a finer hourly calculation step is implemented to enable peak flows to be assessed more accurately than a daily time step model.

As outlined in **Table 23**, the SMWBM_VZ plugin version utilised in this project incorporates parameters characterising the catchment in relation to:

- Interception storage;
- Evaporation losses;
- Soil moisture storage;
- Surface runoff;
- Soil infiltration;
- Sub-soil drainage;
- Flow in the unsaturated zone;
- Stream base flows; and
- The recession and/or attenuation of ground and surface water flow components.

Within the SMWBM, the timing of groundwater flow oscillation is simulated on a discrete sub-catchment basis, via two key processes; vadose zone flow, and deeper saturated groundwater flow.

Vadose zone flow represents flow in the unsaturated zone from the bottom of the soil profile, to the groundwater table below. The rate of vadose zone flow is controlled by the depth to groundwater (D), and the vertical hydraulic conductivity (Kv). Larger depth to groundwater and lower vertical hydraulic conductivity increases vadose zone travel times (lag), and vice versa.

The time lag associated with groundwater entering groundwater storage, and re-emerging at the downstream extent of the sub-catchment is represented via the groundwater lag (GL) parameter. The GL parameter is set as a calibration parameter during model development.

The attenuation of water quality constituents associated with groundwater flow is simulated via a catchment attenuation factor. Full details on the development of the catchment attenuation factor and how it was configured within SOURCE for this project are provided in **Section 7.2.5**.

Table 23. SMWBM_VZ parameters.

Parameter	Name	Description
ST (mm)	Maximum soil water content	ST defines the size of the soil moisture store in terms of a depth of water
SL (mm)	Soil moisture content where drainage ceases.	Soil moisture storage capacity below which sub-soil drainage ceases due to soil moisture retention.
FT (mm/day)	Sub-soil drainage rate from soil moisture storage at full capacity	Together with POW, FT (mm/day) controls the rate of percolation to the underlying aquifer system from the soil moisture storage zone. FT is the maximum rate of percolation through the soil zone.
ZMAX (mm/hr)	Maximum infiltration rate	ZMAX and ZMIN are nominal maximum and minimum infiltration rates in mm/hr used by the model to calculate the actual infiltration rate ZACT. ZMAX and ZMIN regulate the volume of water entering soil moisture storage and the resulting surface runoff. ZACT may be greater than ZMAX at the start of a rainfall event. ZACT is usually nearest to ZMAX when soil moisture is nearing maximum capacity.
ZMIN (mm/hr)	Minimum infiltration rate	
POW (>0)	Power of the soil moisture-percolation equation	POW determines the rate at which sub-soil drainage diminishes as the soil moisture content is decreased. POW therefore has significant effect on the seasonal distribution and reliability of drainage and hence baseflow, as well as the total yield from a catchment.
PI (mm)	Interception storage capacity	PI defines the storage capacity of rainfall that that is intercepted by the overhead canopy or vegetation and does not reach the soil zone.
AI (-)	Impervious portion of catchment	AI represents the proportion of the catchment that is impervious and directly linked to drainage pathways.
R (0,1)	Evaporation – soil moisture relationship	Together with the soil moisture storage parameters ST and SL, R governs the evaporative process within the model. Two different relationships are available. The rate of evapotranspiration is estimated using either a linear (0) or power-curve (1) relationship relating evaporation to the soil moisture status of the soil. As the soil moisture capacity approaches, full, evaporation occurs at a near maximum rate based on the mean monthly pan evaporation rate, and as the soil moisture capacity decreases, evaporation decreases according to the predefined function.
DIV (-)	Fraction of excess rainfall allocated directly to pond storage	DIV has values between 0 and 1 and defines the proportion of excess rainfall ponded at the surface due to saturation of the soil zone or rainfall exceeding the soils infiltration capacity to eventually infiltrate the soil, with the remainder (and typically majority) as direct runoff.
TL (days)	Routing coefficient for surface runoff	TL defines the lag of surface water runoff.
GL (days)	Groundwater recession parameter	GL governs the lag in groundwater discharge or baseflow from a catchment.
QOBS (m ³ /s)	Initial observed streamflow	QOBS defines the initial volume of water in the stream at the model start period and is used to precondition the soil moisture status.
K _v (m/s)	Vertical hydraulic conductivity at full saturation	K _v defines the vertical hydraulic conductivity of the parent geology type when at full saturation. The K _v value sets the upper limit on the rate of flow in the vadose zone.
VGn (-)	van Genuchten constant soil type	VGn is a text book value used to define the relationship between soil moisture status and hydraulic conductivity of soil. It is used to determine the actual vertical hydraulic conductivity, which reduces as the soil dries.
n _s (-)	Soil zone porosity	n _s defines the porosity of the soil zone.
n _{vz} (-)	Vadose zone porosity	n _{vz} defines the porosity of the vadose zone and is therefore determined from an understanding of the parent geology material.

D (m)	Thickness of vadose zone (depth to water table)	D defines the thickness or the depth of the vadose zone.
GW_OnOff (True/False)	Groundwater on or off Selection	This feature of the SMWBM allows you to turn off the groundwater component of a sub-catchment so it does not report back to the river. This feature is useful when integrating with groundwater models.
AA, BB	Coefficients for rainfall disaggregation.	Used to determine the rainfall event duration and pattern. Default values usually suffice.

A conceptual diagram of the key components of SMWBM_VZ model structure and functionality is shown in **Figure 33**.

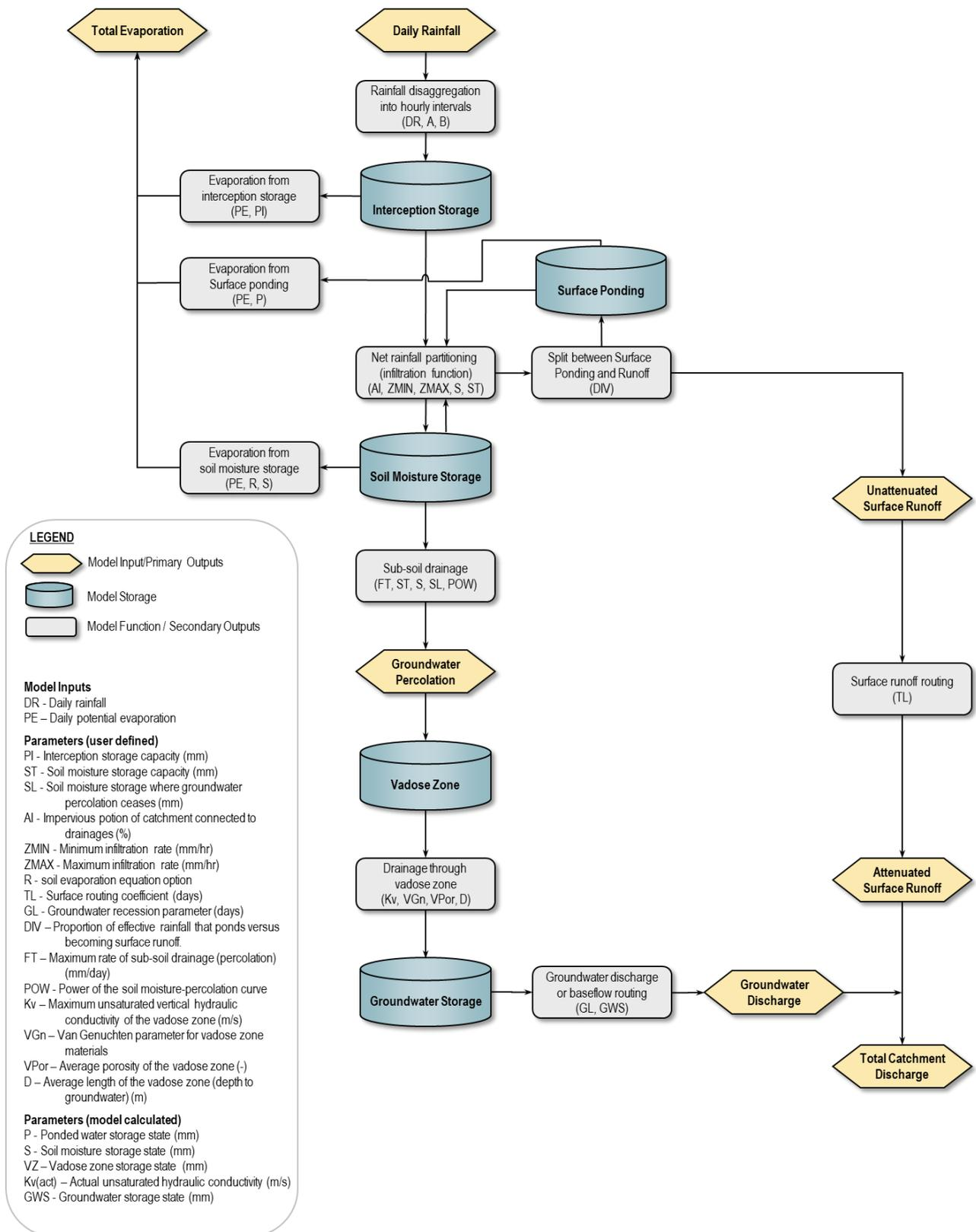


Figure 33. Flow diagram of the SMWBM_VZ structure and parameters.

5.3 SOURCE Model Construction

As indicated in **Section 5.1**, SOURCE is discretised into numerous sub-catchments and drainage networks. These can be developed outside of SOURCE in GIS and directly imported into SOURCE using SOURCE's Geographic Wizard. The climate import tool (described in **Section 4.1**) is used to read and interpolate the NIWA VCSN climate data, automatically assigning a rainfall and evaporation time series to each sub-catchment.

Parameterisation of the SMWBM rainfall/runoff model is a key task in the model calibration process and is described in the following section (**Section 6**).

Each sub-catchment is configured with known gains or losses to the stream, as described in **Section 2.4**.

5.3.1 Sub-Catchment Delineation

A SOURCE catchment model comprises a series of interconnected sub-catchments that are discretised to reflect the localised physical characteristics of each catchment. This is achieved through identifying areas with similar catchment characteristics, as described in **Section 3**, including geology, slope, land use, rainfall, and logical drainage pathways.

Catchment delineation is undertaken with the aim of enabling the application of monogamous catchment parameters in the rainfall-runoff model, i.e. as catchment scale increases, catchment parameters become a blend of area weighted values, whereas as catchment resolution decreases, the parameters applied better reflect local-scale variation.

During the catchment delineation process, consideration must also be given to the number and size of the sub-catchments in the model. Large numbers of small sub-catchments can add to the model complexity and run times, which can make accurate calibration of flow and constituents impractical.

The definition of SOURCE catchments is an iterative process involving a number of steps, each of which considers an important physical characteristic that governs/influences the overall hydrological response and behaviour of the catchment.

The following sub-section discusses the steps involved in delineation of sub-catchments for the Kaituna and Rangitāiki WMA SOURCE models, while **Figure 34** and **Figure 35** show the finalised catchment delineations adopted for this study.

Figure 34. Kaituna WMA delineated area. (Refer A3 attachment at rear).

Figure 35. Rangitāiki WMA delineated area. (Refer A3 attachment at rear).

5.3.1.1 Watershed Boundaries

The first step in defining the SOURCE sub-catchments was to consider catchment watershed boundaries. This was undertaken using catchment order 3 and 4 of the 2010 New Zealand River Environmental Classification (REC2) system for the BOP region.

Each SOURCE sub-catchment is assigned a unique identification number (ID). Numbering of sub-catchments typically starts in the upper headwaters (e.g. SC#1) and increases sequentially with progression down the catchment in a logical manner. In places, adjacent catchments in the Rangitāiki WMA appear to have juxtaposed IDs. This is due to the shape of catchments and complexity introduced with tributaries and confluences. However, this has no consequence for the modelling of the catchment, as it is just an identification number.

5.3.1.2 Slope

Rapid change in topographical elevation or steep slopes can have a significant bearing on the rainfall-runoff generation process and hence the characteristics of flow. As discussed in **Section 3.2** the land surface gradient (slope) within the WMAs were derived from a raster file with a 15 m pixel size. From this raster file the mean, maximum and minimum slope were calculated for each sub-catchment in the model domain, as summarised in **Appendix D**. This calculation was analysed to identify sub-catchments that demonstrated a large slope range and such sub-catchments visually inspected (as a desktop exercise) to determine whether the large slope range represented a gradual slope variation across the sub-catchment or escarpment or gully type feature.

For the Kaituna WMA it was concluded that no sub-catchments demonstrated enough variation in slope to be of significance for hydrological modelling. Based on this assumption no further sub-catchment delineation was required based on slope.

However, in the Rangitāiki WMA the sub-catchments were classified into three distinct slope boundaries. These boundaries were identified upstream of the Rangitāiki River at Waiohou Bridge flow monitoring site, as outlined in **Section 5.3.1**. Delineation changes were made to the Rangitāiki sub-catchment boundaries to reflect these three distinct slope characteristics (**Figure 17**).

5.3.1.3 Geology and Soil

The geology and soil in each WMA were discussed in **Section 3.3** and **3.4**, respectively. A visual analysis of the geology and soil type across each catchment was carried out to determine if any sub-catchments could be further delineated into sub-catchments of similar geology or soil characteristics.

While a number of areas within both WMAs displayed differing geology or soil types as discussed in **Section 3.3** and **3.4**, the differences were not significant on a sub-catchment scale. Therefore, no further delineation was applied to sub-catchments.

5.3.1.4 Monitoring Locations

The final step in the sub-catchment delineation process was to ensure key monitoring locations were positioned in close proximity to a sub-catchment drainage point. The ability to accurately calibrate the model at available flow monitoring sites is enhanced by positioning the drainage point of a sub-catchment at or near a monitoring location.

5.3.1.5 Statistics

The final delineations comprised 119 and 117 sub-catchments for the Kaituna and Rangitāiki models, respectively. Note, five of the sub-catchments (SC119, 115, 116, 117 & 118) neighbour the Kaituna WMA, are not part of the WMA. Sub-catchment 119 was included as it flows into the WMA, and the remaining four were included to cover the small streams within these sub-catchments to allow for future analysis if required.

Statistics were calculated for each sub-catchment for each of the key catchment characteristics to provide preliminary understanding on the likely:

- water balance of each sub-catchment;
- hydrological functionality or behaviour of each sub-catchment; and
- relative differences in hydrological behaviour between catchments.

The statistics outputs are presented in summary tables in **Appendix D** and include the following:

- Area (km²);
- Elevation range (m);
- Slope (°);
- Weighted average soil drainage class;
- Weighted average soil potential rooting depth (PRD) class;
- Weighted average profile available water (PAW) class;
- Weighted average soil permeability class;
- Main soil classes;
- Weighted average depth to low K horizon class;
- The percentage of main rock type; and
- Geological permeability.

The sub-catchment statistics were subsequently used to make informed decisions regarding the initial parameter value assignments in the rainfall-runoff model (SMWBM) (**Table 23**) and during the refinement of model parameters during the calibration process. Additional details on this process are provided in **Section 6.3**.

5.3.2 Water Takes and Discharges

Section 2.4 and **Appendix C** describe the data available and preparation of this data for modelling of water abstraction in the WMAs. As indicated in **Section 5.1**, supply point nodes were utilised to manage abstractions within the model.

Using the data described in **Section 2.4**, which was processed externally to the models, water take and discharges for permitted and consented activities were incorporated into the Kaituna and Rangitāiki SOURCE models, as either constants or time variables, as follows:

- All municipal, non-municipal and Irrigation consents were applied in SOURCE as a time series of demands for the duration of the individual consented period.
- All the wastewater discharge time series were configured in SOURCE as inflow nodes at points representing the physical discharge location.
- Permitted water use as a fixed average daily rate was applied to each sub-catchment within the Kaituna and Rangitāiki models.

A summary of the water takes and discharges in each sub-catchment in the Kaituna and Rangitāiki WMAs are presented in **Appendix C**.

5.3.3 Constructed Models

The constructed SOURCE models for the Kaituna and Rangitāiki WMAs are shown in **Figure 36** and **Figure 37**, respectively.

Figure 36. Kaituna WMA SOURCE model. (Refer A3 attachment at rear).

Figure 37. Rangitāiki WMA SOURCE model. (Refer A3 attachment at rear).

5.4 Model Evaluation Criteria

This section describes the range of approaches used to calibrate the flow and constituent models. These include:

- Flow hydrograph and constituent concentration time series plots;
- Flow duration curves, summary statistics and scatter plots; and
- Statistical performance measures (Nash Sutcliffe Efficiency & Percentage Bias).

Flow hydrographs, constituent time series, and flow duration curves provide a visual means of assessing model calibration, while model performance metrics such as the Nash-Sutcliffe Efficiency Coefficient (NSE) and Percent Bias (PBIAS) allow model performance to be quantified numerically.

Each of the approaches have different strengths and weakness. For example, time series plots provide a useful method to qualitatively assess a model's ability to simulate temporal variations and cycles, which are not evident from statistical measures such as NSE and PBIAS. In contrast, statistical measures (e.g. NSE and PBIAS) provide a quantitative assessment of model performance and allow direct comparison of model performance to be made between sites.

Each of the above calibration techniques were utilised during the model calibration phase, with the aim of producing good agreement to each of them recognising that different model performance measures can have differing ranges of conditions for which they are best suited. For calibration of the flow model, the NSE and flow duration curve were the primary optimisation targets. However, for constituent calibration, time series plots, summary statistics and PBIAS were considered.

5.4.1 Statistical Performance Measures

Statistical performance measures (PMs) and model performance evaluation criteria (PEC) can be used across different spatial and temporal scales to assess the ability of a model to accurately predict nominated variables. A large range of PMs and PEC methods are described in the literature (e.g. Krause (2005); Moriasi (2007); and Moriasi (2015)), with the applicability of specific methods to a specific model dependant on a range of factors including but not limited to the following:

- Spatial resolution of the dataset(s);
- Temporal scale of the datasets;
- The physical characteristics of the variable being simulated; and
- The statistical distribution of the data (i.e. are outliers present, or are the data skewed).

When performing model performance evaluations, it is assumed that the observation dataset is error free and all error variance is contained in the simulation results (Moriasi *et al.*, 2007). Thus, to strictly adhere to this assumption, high-quality data sets should be given more weighting when carrying out model performance evaluations.

For observed data sets where the resolution of the data is coarse (i.e. monitoring frequency is low), the data set is incomplete, or the measured data set is small (i.e. total number of samples is limited), frequency distribution plots and percentile statistics can be more appropriate measures of model performance (Moriasi *et al.*, 2007).

The following sections will outline the performance measures and performance evaluation criteria selected for use in this project.

5.4.2 The Nash-Sutcliffe Efficiency Coefficient (NSE)

The NSE is a single value index that can range from $-\infty$ to 1, with a value of 1 indicating a perfect match between the modelled and measured data. This is a widely used PM and is calculated using **Equation 1**.

Equation 1. Nash-Sutcliffe Efficiency coefficient equation.

$$E = 1 - \frac{\sum_{i=1}^n (O_i - P_i)^2}{\sum_{i=1}^n (O_i - \bar{O})^2}$$

Where:

O_i and P_i are the observation and modelled data points for i th time, respectively.

The NSE is affected by a number of factors including:

- Sample size;
- Outliers; and
- Bias (McCuen *et al.*, 2006).

Research indicates that outliers can significantly influence sample values of NSE, and the time step at which the data is recorded tends to be a significant factor for the NSE when the sample size is small relative to the modelled data set (McCuen *et al.*, 2006). Detailed hydrologic models often have parameters that control the release of water, which can contribute time-offset bias in the model, also having adverse effects on the NSE calculations.

To overcome NSE sensitivity to extreme values a logarithmic transformation of the values can be used to reduce the magnitude of peak values, while the low values remain more or less at the same level (Krause *et al.*, 2005) (**Equation 2**).

Equation 2. Nash-Sutcliffe Efficiency coefficient log transformed equation.

$$E = 1 - \frac{\sum_{i=1}^n (\ln O_i - \ln P_i)^2}{\sum_{i=1}^n (\ln O_i - \ln \bar{O})^2}$$

However, the log transformed version of NSE does not remove the influence of sample size.

WWLA tested the impact of sample size on NSE values using the Rangitāiki River flow at Te Teko. The flow model described in **Section 6.2.7** was calibrated to the full Te Teko flow dataset that comprised approximately 40 years of daily data (14,536 data points).

The analysis used a stochastic approach to test the impact of sample size on NSE (with a model of known performance i.e. NSE of 0.37), whereby 1,000 sample populations of the same number of data points were selected randomly between the start and end date, and each data point was unique (i.e. no duplicates). NSE was performed on each sample realisation. This stochastic procedure was repeated for incrementally increasing sample sizes, as described in the following:

- Randomly select a sample of dates size (n) between the start and the end of the record;
- Perform NSE analysis on sample (size n) and record the NSE value;

- Repeat the above two steps 1,000 times;
- Assess the mean, standard deviation, standard error and relative standard error of the 1,000 NSE outputs.
- Repeat the entire process for the different sample sizes (n = 10; 15; 20; 30; 40; 50; 100; 200; 500; 1,000; 5,000; 10,000).

The results are as shown in **Figure 38**, which provides the following conclusions:

- With increasing sample size, the standard deviation (or variability) and the relative standard error of the NSE outputs decrease (i.e. the randomness of the dates selected is overcome by population size);
- At approximately 500 samples, there is no significant change in all statistical measures, indicating that increasing the population size will not necessarily improve the statistical results (all other external variables remaining equal);
- Where the sample population is <30 the variation in the NSE results exceed the mean NSE value (Std Dev > mean).

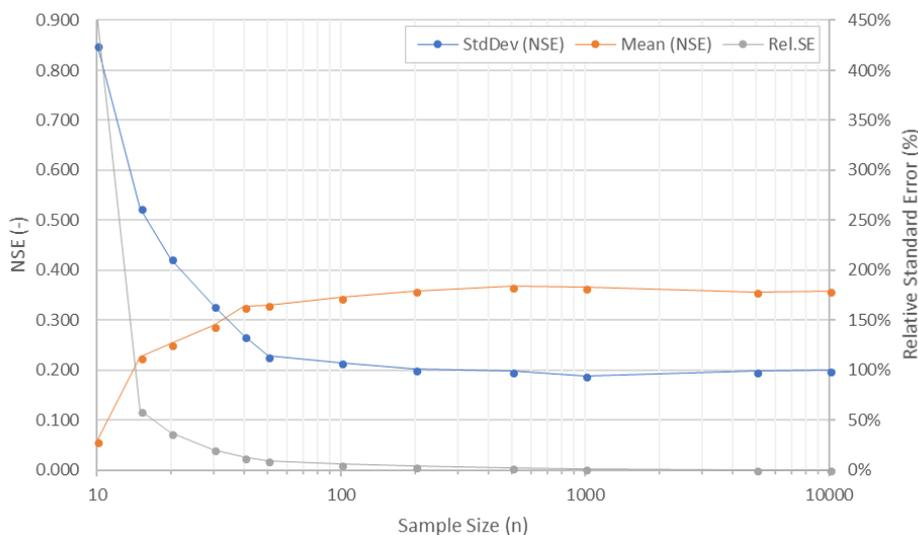


Figure 38. Sensitivity of NSE to Sample Size.

The key outcome of this work was to recommend variable PEC depending on the PM and sample population size.

The NSE can be calculated on a daily, monthly or annual time step. For the purpose of this project, based on the recommendations in Moriasi *et al.* (2007), the log-transformed NSE was selected as the most appropriate statistical PM for flow predictions on a daily time step, where the population size is greater than 500. The log transformed NSE is calculated using the same equation as the standard NSE, but the observed and flow data are log transformed first. The NSE values presented throughout this report represent the log-transformed NSE.

The PEC for NSE coefficients for flow on a daily time step are outlined in **Table 24**. If variables other than flow or samples sizes (temporal scales) are being analysed, the PEC may need to be reassessed.

Table 24. Performance evaluation criteria for flow on a daily basis using the Nash-Sutcliffe coefficient of efficiency (NSE).

Sample Size	Very good	Good	Satisfactory	Not Satisfactory
<30	Inappropriate to apply			
<100	NSE ≥ 0.07		0.05 < NSE ≤ 0.07	NSE ≤ 0.05
<500	0.19	0.14 < NSE ≤ 0.17	0.12 < NSE ≤ 0.14	NSE ≤ 0.12
>500	NSE > 0.75	0.50 < NSE ≤ 0.75	0.30 < NSE ≤ 0.50	NSE ≤ 0.30

5.4.3 Percent Bias (PBIAS)

Percent bias (PBIAS) measures the tendency of a model to predict larger or smaller values compared to the counterpart measured data points. PBIAS is reported as a percentage and values can range from $-\infty$ to ∞ , with the optimal value being zero. Values greater than zero (positive values) indicate the model has a bias towards under estimating the modelled variable. Values less than zero (negative value) indicate the model is bias towards over estimating the modelled variable. PBIAS is calculated using the formula outlined in **Equation 3**.

Equation 3. Percent Bias statistical performance measure equation.

$$PBIAS = \frac{\sum_{i=1}^n (Y_i^{obs} - Y_i^{sim}) * (100)}{\sum_{i=1}^n (Y_i^{obs})}$$

PBIAS has the ability to clearly indicate poor model performance and is therefore often a popular PM. PBIAS has been used in this project as a PM for flow on a daily timestep, and for total nitrogen (TN), total phosphorus (TP), Total suspended solids (TSS) and *E. coli* on a monthly timestep.

Use of PBIAS on a monthly time-step for the water quality variables is due to the coarse resolution of the measured data, which is primarily sampled at an equivalent interval. The NSE PM was not applied for analysis of water quality variables due to its sensitivity to small datasets and outliers.

The PBIAS PEC for flow, TN TP, TSS and *E. coli* are outlined below. Similar to NSE, if the variable being reviewed or the temporal scale of the assessment changes, the PEC may need to be assessed (Moriassi *et al.*, 2015).

Table 25. Performance evaluation criteria for Percent Bias (PBIAS [%]) (Moriassi *et al.* 2015).

Measured	Temporal Scale	Very good	Good	Satisfactory	Not Satisfactory
Flow	Daily/ Monthly/ Annual	PBIAS < ±5	±5 ≤ PBIAS < ±10	±10 ≤ PBIAS < ±15	PBIAS ≥ ±15
Total Nitrogen / Phosphorus	Daily/ Monthly/ Annual	PBIAS < ±15	±15 ≤ PBIAS < ±20	±20 ≤ PBIAS < ±30	PBIAS ≥ ±30
Total Suspended Solids / <i>E. coli</i>	Daily/ Monthly/ Annual	PBIAS < ± 10%	± 10% ≤ PBIAS < ± 15	± 15% ≤ PBIAS < ± 20%	PBIAS ≥ ± 20%

5.4.4 Percentile Statistics

As indicated above, for observed data sets that are small, infrequent, or incomplete, frequency distribution plots and comparative percentile statistics have also been calculated in this study at each calibration location for flow, TN and TP, TSS and *E. coli*.

Flow duration curves (FDC)¹⁴ provide a comparison of measured and simulated flow as a percentage of time (probability) over which flow of a certain magnitude is likely to be equalled or exceeded.

5.4.5 Summary of PEC Applied

As indicated above, evaluation of model performance for the Kaituna and Rangitāiki WMA SOURCE models was undertaken on a case-by-case basis depending on the constituent being evaluated (e.g. flow, nutrient, sediment etc.) and the nature of the “what if tests” anticipated for each variable. The process for determining the appropriate PEC for a specific variable utilised the following steps:

1. A high-level literature review was undertaken with the aim of summarising the PMs used in evaluating model calibration performance from other New Zealand water quality modelling studies.
2. Outliers in the measured data which significantly influence the PM result were removed.
3. The suitability of individual PM to the specific variable being simulated was assessed on the basis of:

Modelled Flow

As noted in the previous section, the flow modelling component was assessed using a range of PEC:

1. **Hydrographs** - Comparison of measured and modelled hydrographs to evaluate the magnitude and timing of flows on an instantaneous basis;
2. **Flow duration curve analyses (FDC)** – FDC analysis shows the percentage of time flow of a certain magnitude is likely to be equalled or exceeded on a long-term basis allowing any differences in the frequency distribution of modelled and measured flows to be readily identified.
3. **Nash Sutcliffe Model Efficiency Measure (NSE)** - calculated for both the daily flow data and on the FDC results.

Constituent Modelling

Due to the limited measured data set available to assess performance of water quality outputs from the models, an evaluation of the applicability of different PMs to the available water quality data was undertaken. The findings and recommendations from this assessment indicate:

1. The removal of outliers is required for sample populations where the relative standard error (RSE) is greater than 10%;
2. It is appropriate to vary the PM (and PEC) depending on the sample size of the data;
3. A combination of PM may be required in circumstances where sample populations are low and data variance is high e.g. PBIAS + RSE – overcomes potential weakness in PBIAS (i.e. overs and under combining to provide acceptable PBIAS statistic);

¹⁴ All FDCs presented in this report present flow (y-axis) on a log scale

4. Estimated PM for sample populations less than 30 are only suited to basic statistics (mean annual averages, RMSE);
5. NSE is not an appropriate PM for sample populations less than 100 and is more suited for populations greater than 500.

6. Flow Model Development

The SOURCE flow model development process is summarised in **Figure 39**. The figure depicts a linear development process with an iterative loop representing the SMWBM calibration process. It is noted that the calibration process is the largest component of flow model development.

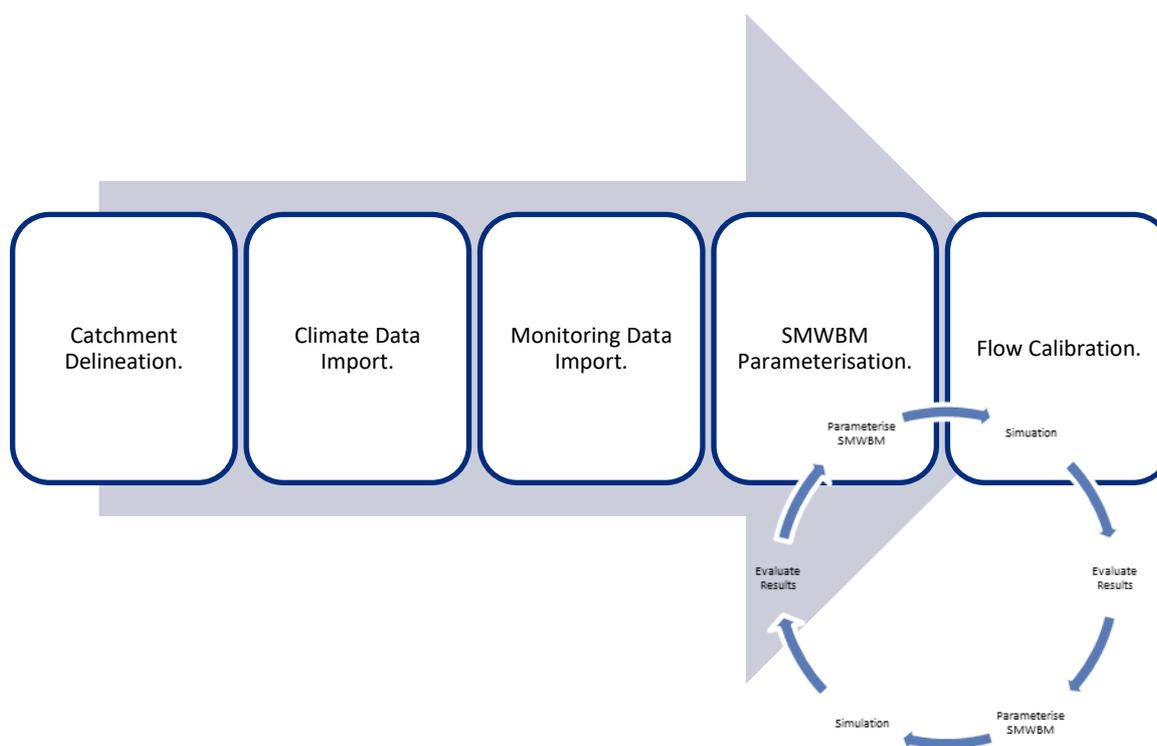


Figure 39. Flow model development process.

Following the configuration of the SOURCE sub-catchments (described in **Section 5.3**) rainfall-runoff models were set up for each SOURCE catchment using the SMWBM plugin. The SMWBM parameters values were initially selected based on the individual sub-catchment characteristics (**Appendix D** and as detailed in **Section 4**), with subsequent refinement during the calibration process, which is described in the sections below.

The model was calibrated to the measured flow at primary flow monitoring sites (defined in **Section 2.3**). The calibration process was carried out systematically working downstream in each WMA. Using the available flow data (**Table 2**), knowledge of the sub-catchment characteristics (**Section 3**), and the hydrological inferences from these characteristics (**Section 4**), SMWBM parameters were first assigned to the SOURCE catchment.

Calibration simulations were repeated multiple times, with SMWBM parameter values manually adjusted in each subsequent run until the highest level of flow calibration that could practically be achieved (as defined by application of PEC described in **Section 5.4**) was produced. The parameter adjustment process maintained a consistent relationship between the model parameters and the physical characteristics of the sub-catchment, which ensured that parameter changes were made in a physically realistic and logical way.

The calibration focussed initially on primary flow monitoring sites that had substantial long-term records. Following this initial calibration step, effort focussed on calibration to discrete monitoring flow sites.

The aim of the initial calibration of flow was to slightly over simulate, so when abstraction takes were subsequently considered, the simulated flow would be brought even closer to the measured flow. After the initial flow model calibration, all consented and permitted takes and discharges were incorporated into the models.

The following **Sections 6.1** and **6.2** detail the flow calibration procedure and results for each of the primary flow sites within the Kaituna and Rangitāiki WMAs, respectively.

6.1 Flow Calibration - Kaituna

6.1.1 Kaituna River at Taheke

Flow in the Kaituna River at Taheke Road is heavily influenced by outflow from Lake Rotorua, which on average discharges 18 m³/s through the Ohau Channel into Lake Rotoiti (Donald, 1997), and subsequently into the river. Lake Rotoiti only has one outlet being the Kaituna River.

The Taheke gauge site was used as an inflow node representing the discharge from Lake Rotoiti (**Section 4.1**). The discharge time series for the Taheke gauge site was synthesised by combining the five years of the discharge data from Lake Rotoiti (1 January 1976 to 20 October 1981) with the 37 years of flow data at the Taheke gauge data (21 October 1981 to 30 May 2016). Combining data from two nearby sites was considered appropriate on the basis that their flow regimes are heavily dominated by Lake Rotorua outflow and therefore very similar. Any gaps in either data set were filled using the calculated daily average flow per month.

Calibration at the Taheke gauge was therefore not a significant task given the flow was largely prescribed, although parameters were set for the small catchment area between the lake and the gauge on the basis of the physical characteristics of the catchment (**Appendix D**).

Table 26 shows the parameters selected for the catchment (SC#15), which being in porous pumice country of the Central Plateau highlands has high infiltration rates and a larger soil moisture zone than is typical for lowland areas, which will sustain more baseflow compared to surface runoff.

Table 26. Calibrated SMWBM parameters used for SC#15 (Kaituna River at Taheke).

SC ID	ST (mm)	ZMAX (mm/hr)	FT (mm/d)	K _v (m/s)	D (m)
SC#15	552	12	7	1.65E-06	114

No comparative statistics are provided for this gauge since the flow is prescribed from outflow from Lake Rotoiti and/or the measured flow at the gauge itself.

6.1.2 Paraiti (Mangorewa) River at Saunders

The flow calibration for the Paraiti (Mangorewa) River at Saunders is shown in the hydrograph and FDC presented in **Figure 40** and **Figure 41**, respectively, while **Table 27** provides comparative statistics between the measured and modelled flow. **Table 28** summarises the calibrated SMWBM model parameters.

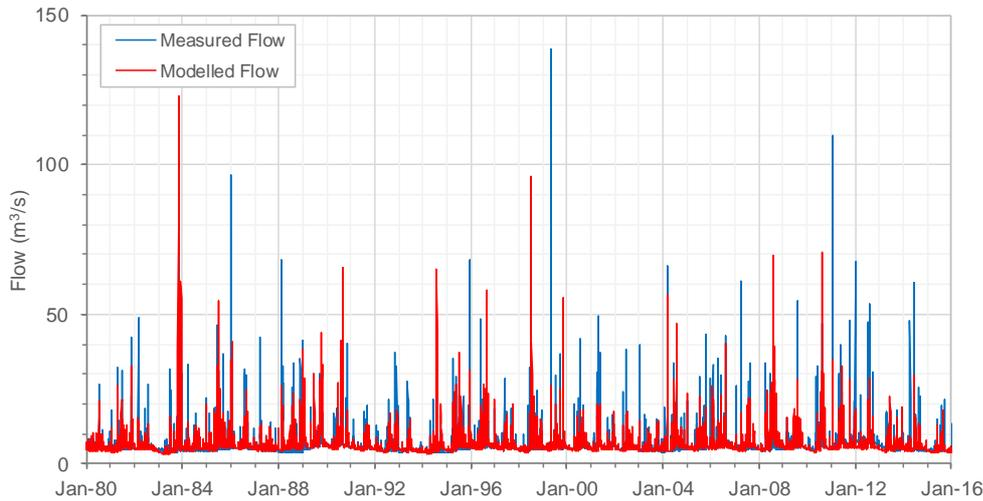


Figure 40. Hydrograph of the modelled and measured flow of the Paraiti (Mangorewa) River at Saunders.

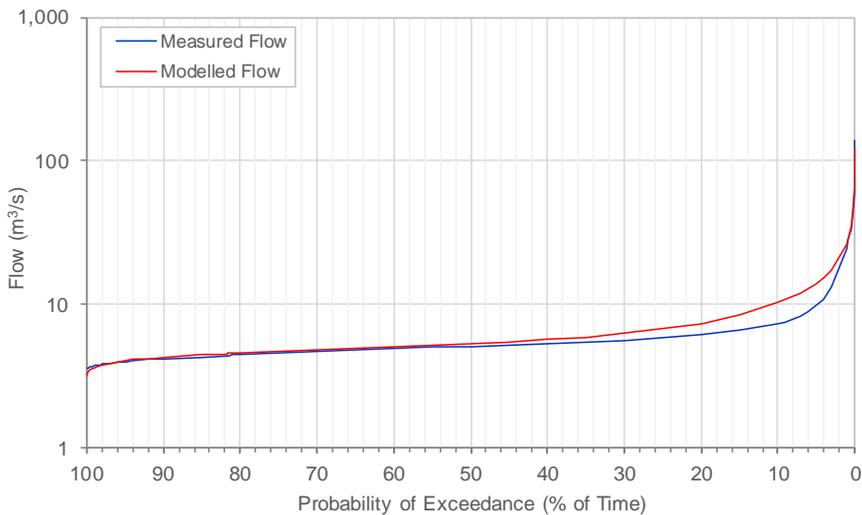


Figure 41. FDC of the modelled and measured flow of the Paraiti (Mangorewa) River at Saunders.

Table 27. Summary of measured versus model flow statistics at Paraiti (Mangorewa) River at Saunders.

Statistic	Measured Flow	Modelled Flow
Min	3.6	3.2
MALF	4.5	4.2
Median	5.1	5.3
Mean	5.9	6.7
Max	138.6	123.1
95%ile	9.6	14.2
99%ile	33.6	30.2
NSE (-)	0.22	
PBIAS (%)	-3.17	

The accuracy of the model calibration at Paraiti (Mangorewa) River at Saunders gauge is summarised as follows:

- **PEC** – based on the PEC outlined in **Table 24**, the model’s ability to predict flow at this monitoring location is considered Not Satisfactory with NSE of 0.22.
- **PBIAS** – based on the PEC outlined in **Table 25**, the model’s ability to predict flow at this monitoring location is considered Very Good with PBIAS of -3.17%, with some tendency to over predict flow at this location.
- **FDC** – FDC indicates low flow are simulated extremely well. Medium to high flows are over simulated, while extremely high flows are under simulated (albeit there is not much confidence in the gauge rating curve at higher flows).

Overall, calibration at this gauge is considered very good, and appropriate for the purposes of this assessment.

Table 28. Calibrated SMWBM parameters for catchments draining to Paraiti (Mangorewa) River at Saunders.

SC ID	ST (mm)	ZMAX (mm/hr)	FT (mm/d)	K _v (m/s)	D (m)
SC#1	547	11.0	1.7	9.00E-07	136
SC#2	502	14.0	4.8	9.00E-07	103
SC#3	635	12.0	6.0	9.00E-07	122
SC#5	626	12.0	6.3	1.08E-06	108
SC#6	594	12.0	7.9	3.28E-06	67
SC#7	585	13.0	6.0	9.41E-07	87
SC#8	623	11.0	8.0	2.93E-06	82
SC#9	498	14.0	6.0	9.00E-07	54
SC#10	513	13.0	9.6	6.81E-06	45
SC#11	619	12.0	6.3	1.04E-06	91

The calibrated model parameter values assigned (**Table 28**) are reflective of the following catchment characteristics:

- **ST** – soil moisture storage values range from approximately 500 to 635 mm, which are reflective of the highly porous soils and relatively large potential rooting depth of each sub-catchment.
- **ZMAX** – infiltration rates are all consistently high ranging from 11 to 14 mm/hr, which means rainfall from storms except the most severe thunderstorms will be infiltrated into the soil.
- **FT** – sub-soil drainage rates are consistently high ranging from 4.8 to 9.6 mm/day (with the exception of SC#1 at 1.7 mm/day), reflecting excellent soil drainability.
- **Kv** - vertical hydraulic conductivity values ranging from 9×10^{-7} m/s to 7×10^{-6} m/s indicated moderate rates of vertical groundwater movement within the unsaturated zone.
- **D** - depth to groundwater is moderate varying from 45 m to 136 m. The larger depth to groundwater it indicates that sub-soil drainage will take longer to percolate to the groundwater table, which implies groundwater discharges will be attenuated and more stable with time.

During the calibration process the catchment area was changed to align more closely with the expected specific discharge. The resulting catchment area is shown in **Figure 42**. However, this did not fully address the model oversupply of water and a loss node was configured to represent groundwater discharging through the deep aquifer under the gauge. The losses were returned to the river just prior to the gauge in the Kaituna River at Te Matai, as discussed in the following section. **Appendix E** provides more detail on both adjustments made to the model during the process of calibration.

Figure 42. Map of changes to the Kaituna Catchment. (Refer A3 attachment at rear).

6.1.3 Kaituna River at Te Matai

The flow calibration for the Kaituna River at Te Matai are shown in the hydrograph and FDC presented in **Figure 43** and **Figure 44**, respectively, while **Table 29** provides comparative statistics between the measured and modelled flow. **Table 30** summarises the calibrated SMWBM model parameters.

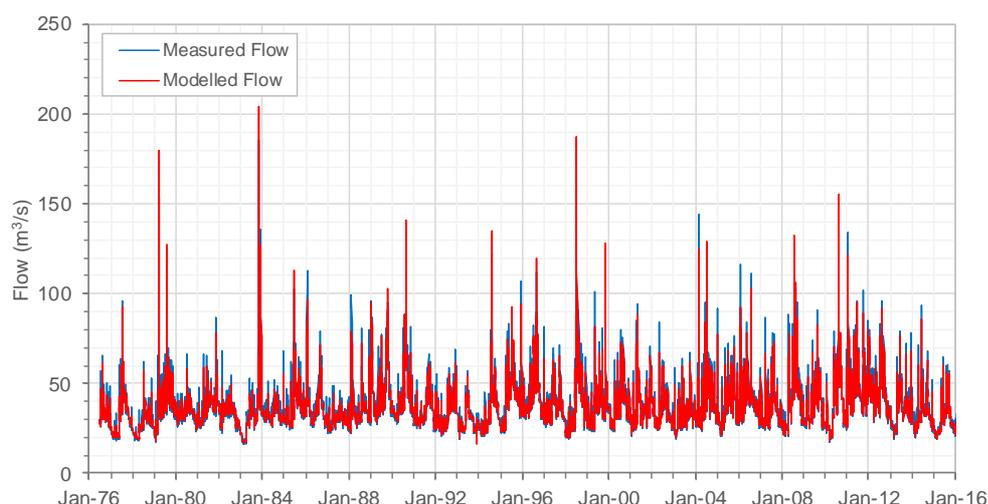


Figure 43. Hydrograph of the modelled and measured flow of the Kaituna River at Te Matai.

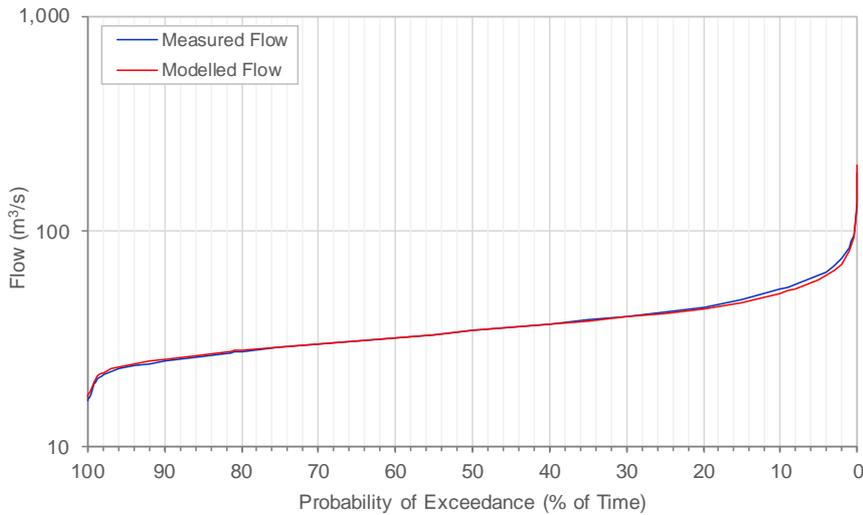


Figure 44. FDC of the modelled and measured flow of the Kaituna River at Te Matai.

Table 29. Summary of measured versus model flow statistics for Kaituna River at Te Matai.

Statistic	Measured Flow	Modelled Flow
Min	16.2	16.8
MALF	22.5	23.3
Median	34.3	34.3
Mean	37.3	36.9
Max	185.8	205.1
95%ile	61.9	59.2
99%ile	83.8	79.8
NSE (-)	0.97	
PBIAS (%)	0.86	

The accuracy of the model calibration at Kaituna River at Te Matai gauge is summarised as follows:

- **PEC** – based on the PEC outlined in **Table 24**, the model’s ability to predict flow at this monitoring location is considered Very Good with NSE of 0.97.
- **PBIAS** – based on the PEC outlined in **Table 25**, the model’s ability to predict flow at this monitoring location is considered Very Good with PBIAS of 0.86%, with some tendency to over predict flow at this location.
- **FDC** – indicates low flow are simulated extremely well throughout the flow regime range.

Based on both the good visual agreement between modelled and measured flow hydrographs and flow duration curve and NSE and PBIAS classification, model calibration is considered very good at this gauge and there is a high level of confidence in the simulated flows.

Table 30. Calibrated SMWBM parameters for catchments draining to Kaituna River at Te Matai.

SC ID	ST (mm)	ZMAX (mm/hr)	FT (mm/d)	K _v (m/s)	D (m)
SC#12	599	11.0	11.0	7.30E-06	60
SC#013	567	10.0	8.0	9.03E-07	118
SC#014	539	11.0	7.0	9.00E-07	90
SC#16	624	11.0	8.0	2.28E-06	75
SC#17	467	15.0	8.0	1.56E-06	56
SC#18	547	12.0	7.0	9.00E-07	36
SC#19	538	11.0	10.0	4.55E-06	30
SC#20	541	11.0	9.0	3.62E-06	55
SC#21	570	15.0	7.0	2.27E-06	26
SC#22	533	11.0	12.0	7.81E-06	19
SC#23	551	11.0	21.0	2.00E-05	18
SC#24	609	14.0	20.0	1.91E-05	19
SC#25	671	16.0	21.0	1.98E-05	12
SC#26	374	14.0	21.0	2.00E-05	8
SC#27	636	11.0	7.0	9.00E-07	113
SC#28	697	10.0	7.0	1.51E-06	74
SC#29	560	13.0	11.0	6.72E-06	44
SC#30	588	12.0	16.0	1.40E-05	32

The calibrated model parameter values assigned (**Table 34**) are reflective of the following catchment characteristics:

- **ST** – soil moisture storage values are in a similar albeit slightly wider range to the Paraiti (Mangorewa) at Saunders catchments, ranging from approximately 375 to 700 mm, which are reflective of the highly porous soils and relatively large potential rooting depth of each sub-catchment.
- **ZMAX** – infiltration rates are all consistently high (similar to Paraiti (Mangorewa) at Saunders) ranging from 10 to 16 mm/hr, which means rainfall from storms except the most severe thunderstorms will be infiltrated into the soil.
- **FT** – sub-soil drainage rates are consistently extremely high ranging from 7 to 21 mm/day, reflecting all the soils in this catchment have excellent drainability.
- **K_v** – vertical hydraulic conductivity values are slightly higher than Paraiti (Mangorewa) Sanders ranging from 9×10^{-7} m/s to 2×10^{-5} m/s indicating moderate rate of vertical groundwater movement within the unsaturated zone.
- **D** – depth to groundwater is quite variable from 8 m to 118 m, dependent on the sub-catchment positioning within the catchment. Similar, to the Saunders catchments, depth to groundwater > 25 m indicate the groundwater flows will typically be attenuated and stable.

Losses to groundwater in the upstream Paraiti (Mangorewa) River catchments were returned within the Kaituna River at Te Matai reach using a gain node.

The adjustments to the respective catchment areas (**Appendix E**) also reduced the measured specific discharge for the Kaituna at Te Matai site from 0.1 m³/s/km² to 0.031 m³/s/km² (and the corresponding discharge from 159% to 49% of mean annual rainfall) (**Table 41**).

6.1.4 Waiari River at Muttons

A comparison of modelled and measured flows along with FDCs generated from the calibration process for the Waiari River at the Muttons site are shown in **Figure 45** and **Figure 46**, respectively, while comparative statistics are summarised in **Table 31**. **Table 32** summarises the calibrated SMWBM parameters.

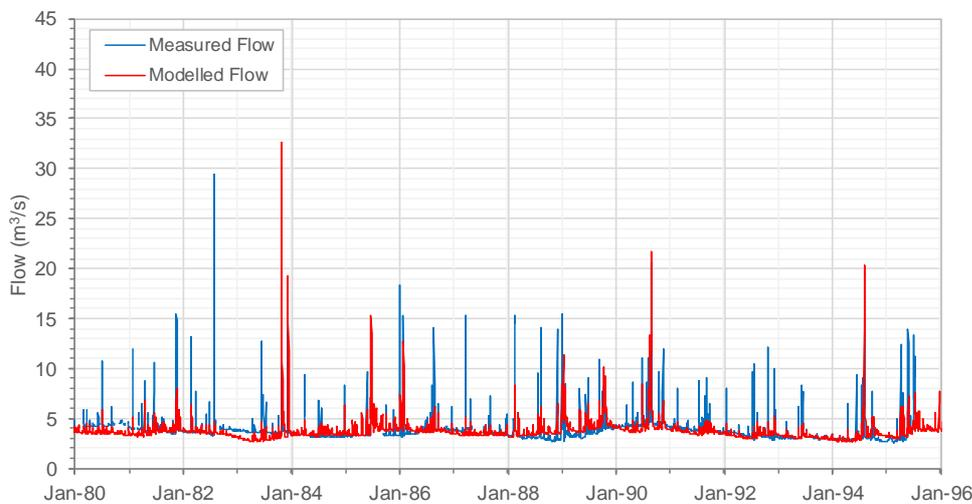


Figure 45. Hydrograph of the modelled and measured flow of the Waiari at Muttons.

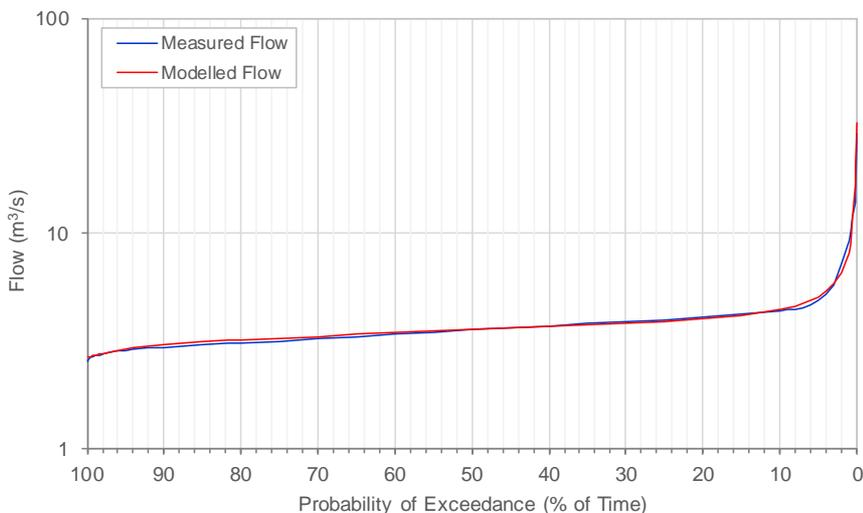


Figure 46. FDC of the modelled and measured flow of the Waiari River at Muttons.

Table 31. Summary of measured versus model flow statistics for Waiari River at Muttons.

Statistic	Measured Flow	Modelled Flow
Min	2.6	2.6
MALF	3.1	3.1
Median	3.6	3.5
Mean	3.8	3.8
Max	29.4	32.6
95%ile	4.9	5
99%ile	9.3	7.6
NSE (-)	0.10	
PBIAS (%)	7.15	

The accuracy of the model calibration at Waiari River at Muttons gauge is summarised as follows:

- **PEC** – based on the PEC outlined in **Table 24**, the model’s ability to predict flow at this monitoring location is considered Not Satisfactory with NSE of 0.10.
- **PBIAS** – based on the PEC outlined in and **Table 25**, the model’s ability to predict flow at this monitoring location is considered Good with PBIAS of 7.15%, evaluation indicates that the model over predicts high flows at this gauge.
- **FDC** – FDC indicates low flow are simulated extremely well throughout the flow regime range.

As seen in the hydrograph and flow duration curve for the Waiari River at Muttons gauge, the model simulated good agreement to observed flow during baseflow conditions, however, tended to under-predict the infrequent peak flow events. As this site is largely baseflow dominated, there is good confidence in the model simulation with the exception of during infrequent high flow events.

Table 32. Calibrated SMWBM parameters for catchments draining to Waiari River at Muttons.

SC ID	ST (mm)	ZMAX (mm/hr)	FT (mm/d)	K _v (m/s)	D (m)
SC#32	564	12.2	8.9	9.00E-07	110
SC#33	570	12.4	9.2	8.82E-07	116
SC#34	617	12.2	9.2	8.40E-07	136
SC#35	596	13.2	8.9	9.00E-07	107
SC#36	607	13.2	8.9	9.04E-07	62

The calibrated model parameter values assigned (**Table 32**) are reflective of the following catchment characteristics:

- **ST** – soil moisture storage values are in a similar range to the Paraiti (Mangorewa) at Saunders catchments, ranging from approximately 565 to 620 mm, which are reflective of the highly porous soils and relatively large potential rooting depth of the sub-catchments.
- **ZMAX** – infiltration rates are all consistently high (similar to Paraiti (Mangorewa) at Saunders) ranging from 12 to 13 mm/hr, which means rainfall from storms except the most severe thunderstorms will be infiltrated into the soil.
- **FT** – sub-soil drainage rates are consistently moderately high ranging from 8 to 9 mm/day, reflecting all the soils in this catchment have excellent drainability.
- **Kv** – vertical hydraulic conductivity values are similar to Paraiti (Mangorewa) at Sanders ranging from 8 to 9×10^{-7} m/s indicating moderate rate of vertical groundwater movement within the unsaturated zone.
- **D** – depth to groundwater is deep ranging from 62 m to 136 m. Similar, to the Paraiti (Mangorewa) at Saunders catchments, depth to groundwater > 25 m indicate the groundwater flows will typically be attenuated and stable.

6.1.5 Raparapahoe River Above Drop Structure

A comparison of modelled and measured flows along with FDCs generated from the calibration process for Raparapahoe River above Drop Structure is shown in **Figure 47** and **Figure 48** respectively. Comparative statistics are summarised in **Table 33**, and the SMWBM input parameters from the final model calibration listed in **Table 34**.

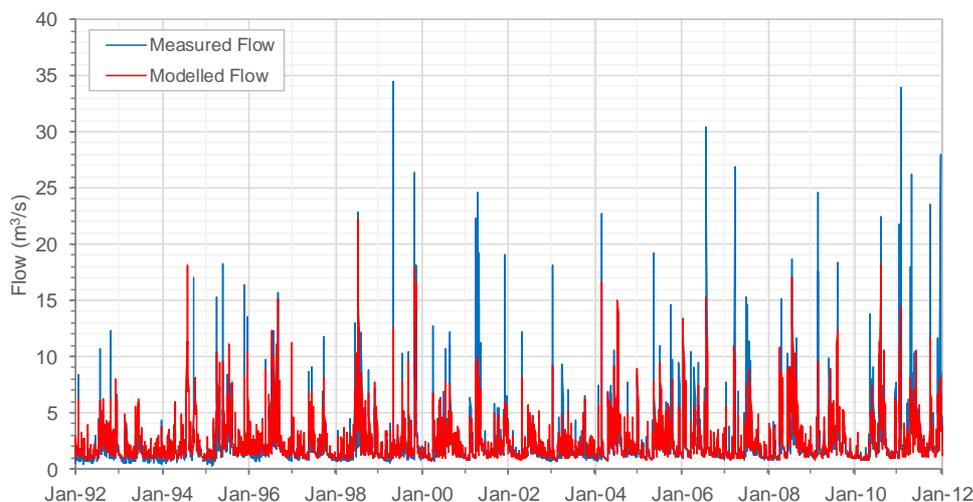


Figure 47. Hydrograph of the modelled and measured flow of the Raparapahoe River at Above Drop Structure.

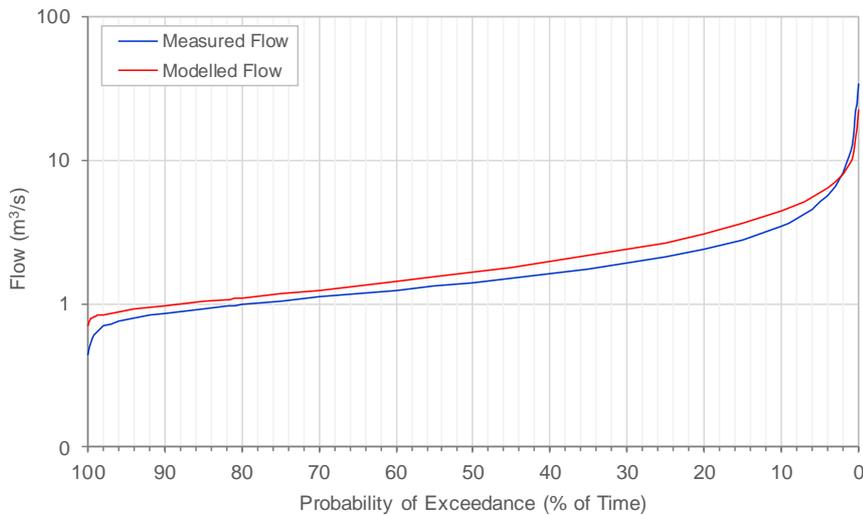


Figure 48. FDC of the modelled and measured flow of the Raparapahoe River at Above Drop Structure.

Table 33. Summary of measured versus model flow statistics for Raparapahoe River above Drop Structure.

Statistic	Measured Flow	Modelled Flow
Min	0.3	0.6
MALF	0.7	0.7
Median	1.4	1.6
Mean	2.0	2.3
Max	34.4	23.3
95%ile	5.0	5.0
99%ile	11.5	11.5
NSE (-)	0.38	
PBIAS (%)	-9.10	

The accuracy of the model calibration at Raparapahoe River at Above Drop Structure is summarised as follows:

- **PEC** – Based on the PEC outlined in **Table 24**, the model’s ability to predict flow at this monitoring location is considered Satisfactory with NSE of 0.38.
- **PBIAS** – Based on the PEC outlined in and **Table 25**, the model’s ability to predict flow at this monitoring location is considered Good with a PBIAS of -9.10%, evaluation indicates that this model under predicts the high flows and over predicts through the rest of the time series.
- **FDC** – Indicates the majority of flows are slightly over simulated throughout the flow regime range, with the exception of extremely high flows.

Based on visual observation of the flow hydrograph the model successfully predicts the general magnitude and timing of flows at the Raparapahoe River at Above Drop Structure gauge. However, the flow duration curve shows the model tended to slightly over-predict all flows, with the exception of extremely high flows. Overall, the level of calibration is considered appropriate, with modelled flows on average within 10% of observed flow.

Table 34. Calibrated SMWBM parameters for catchments draining to Raparapahoe River above Drop Structure.

SC ID	ST (mm)	ZMAX (mm/hr)	FT (mm/d)	K _v (m/s)	D (m)
SC#42	530	5.0	3.0	5.79E-07	117
SC#43	550	5.0	2.0	9.17E-07	96
SC#44	470	18.0	14.0	1.38E-05	7

The calibrated model parameter values assigned (**Table 34**) are reflective of the following catchment characteristics:

- **ST** – soil moisture storage values range from approximately 470 to 550 mm, which are reflective of the highly porous soils and relatively large potential rooting depth of the sub-catchments and are similar to other catchments in this area.
- **ZMAX** – infiltration rates are variable, with moderate values of 5 mm/hr in SC#42 and SC#43 and a high value of 18 mm/hr in SC#44, which is characterised by highly drainable sand and gravel alluvium, whereas the subsurface geology in upper sub-catchments (SC#42 and SC#43) typically comprises relatively lower permeability andesite and ignimbrite.
- **FT** – similar to ZMAX, the pattern of FT is for relatively lower values from 2-3 mm/day in the two upper sub-catchments and a relatively high value of 14 mm/day in SC#44.
- **K_v** – the pattern of vertical hydraulic conductivity values also reflects the geology described above, with relatively lower values in the upper sub-catchments (5 to 9x10⁻⁷ m/s) and a more moderate value of 1x10⁻⁵ m/s in the lower sub-catchment reflecting more rapid rates of vertical groundwater movement within the unsaturated zone in the low land area.
- **D** – depth to groundwater is deep ranging from significant depths in the highland sub-catchments to shallow groundwater of < 10 m in the lowland catchment.

6.1.6 Pongakawa River at Old Coach Rd

A comparison of modelled and measured flows along with FDCs generated from the calibration process for Pongakawa River at Old Coach Rd are shown in **Figure 49** and **Figure 50** respectively. Comparative statistics are summarised in **Table 35**, and the SMWBM input parameters from the final model calibration listed in **Table 36**.

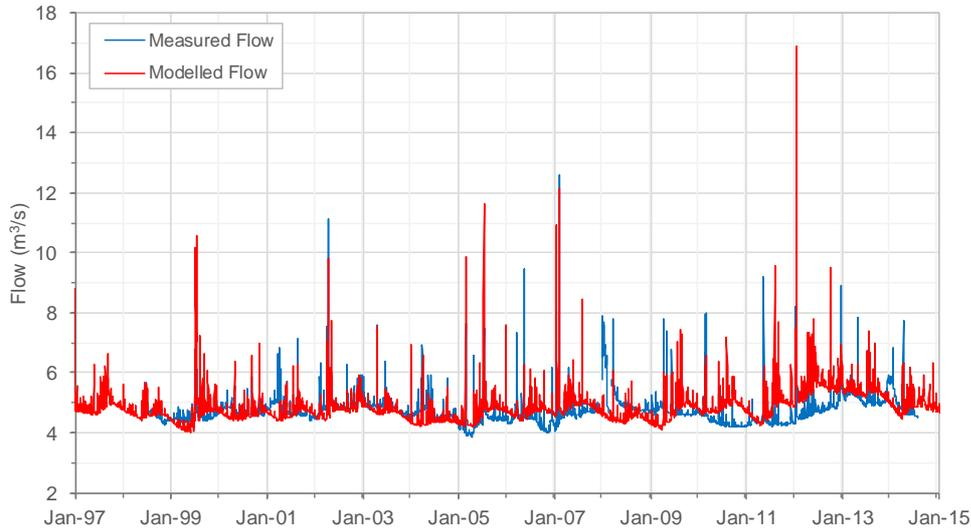


Figure 49. Hydrograph of the modelled and measured flow of the Pongakawa River at Old Coach Rd.

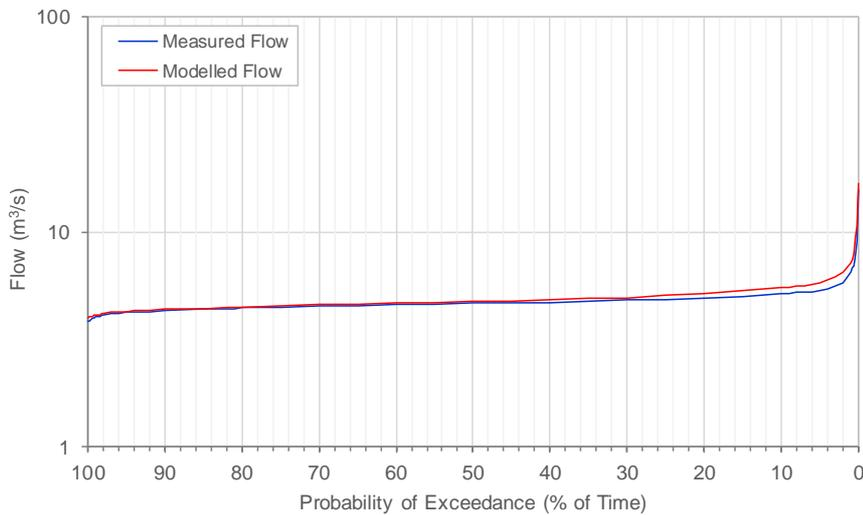


Figure 50. FDC of the modelled and measured flow of the Pongakawa River at Old Coach Rd.

Table 35. Summary of measured versus model flow statistics for Pongakawa River at Old Coach Rd

Statistic	Measured Flow	Modelled Flow
Min	3.8	4.0
MALF	4.4	4.4
Median	4.7	4.8
Mean	4.7	4.9
Max	15.7	17.4
95%ile	5.4	5.8
99%ile	6.5	7.2
NSE (-)	-0.12	
PBIAS (%)	-0.01	

The accuracy of the model calibration at Pongakawa at Old Coach Road gauge is summarised as follows:

- **PEC** – Based on the PEC outlined in **Table 24**, the model’s ability to predict flow at this monitoring location is considered Not Satisfactory with NSE of -0.12.
- **PBIAS** – Based on the PEC outlined in and **Table 25**, the model’s ability to predict flow at this monitoring location is considered Very Good with a PBIAS of -0.01%, evaluation indicates that the model over predicts at the high flow and low flow times.
- **FDC** – Indicates a good match of the frequency of flow for the majority flow regime.

Based on visual observation of the flow hydrograph, the model predicts the general seasonal variation of baseflow, and magnitude of peak flow events with some under and over-predictions. Overall, model calibration is considered good at this location.

Table 36. Calibrated SMWBM parameters for catchments draining to Pongakawa River at Old Coach Rd.

SC ID	ST (mm)	ZMAX (mm/hr)	FT (mm/d)	K _v (m/s)	D (m)
SC#86	725	14.0	11.6	5.04E-06	87
SC#87	725	17.0	10.4	3.59E-06	56
SC#88	725	12.0	9.8	2.89E-06	59
SC#89	725	12.0	8.5	1.44E-06	67
SC#90	725	17.0	8.8	1.81E-06	56
SC#91	725	12.0	9.6	2.67E-06	68
SC#92	725	12.0	9.5	2.54E-06	79
SC#93	703	13.0	11.0	4.41E-06	65
SC#94	714	12.0	10.9	4.18E-06	69
SC#95	725	22.0	8.1	9.37E-07	59
SC#96	546	21.0	12.3	5.84E-06	24

The calibrated model parameter values assigned (**Table 36**) are reflective of the following catchment characteristics:

- **ST** – soil moisture storage values range from approximately 546 to 725 mm, which are marginally deeper than other sub-catchments discussed to-date. These are also reflective of deep highly porous soils and relatively large potential rooting depth of the sub-catchments and are similar to other catchments in this area.
- **ZMAX** – infiltration rates are high ranging from 12 to 22 mm/hr variable, with the higher rates occurring in SC#95 and SC#96, which are located on the threshold between highland and lowland areas where a higher proportion of gravels occurs.
- **FT** – similar to ZMAX, the pattern of FT is for consistently moderate to high values ranging from 8-12 mm/day. The uniformly high ZMAX and FT values used for calibration are consistent with hydraulic properties of the well-drained highly permeably sandy soils found throughout the catchment.
- **Kv** – the pattern of vertical hydraulic conductivity is fairly uniform across the catchment in the range of 1 to 5×10^{-6} m/s, which reflects moderate rates of vertical groundwater movement.
- **D** – depth to groundwater is typically relatively deep in the 50-90 m range for the majority of sub-catchments with the exception of SC#96.

6.1.7 Waitahanui River at Otamarakau Valley Rd

A comparison of modelled and measured flows along with FDCs generated from the calibration process for Waitahanui River at Otamarakau Valley Rd are shown in **Figure 51** and **Figure 52** respectively. Comparative statistics are summarised in **Table 37**, and the SMWBM input parameters from the final model calibration listed in **Table 38**.

The steady decline in both measured and modelled flow over the period 2012 to 2016 is due to a decrease in rainfall during this period. Similar decreases were observed in neighbouring catchments, albeit to a lesser extent.

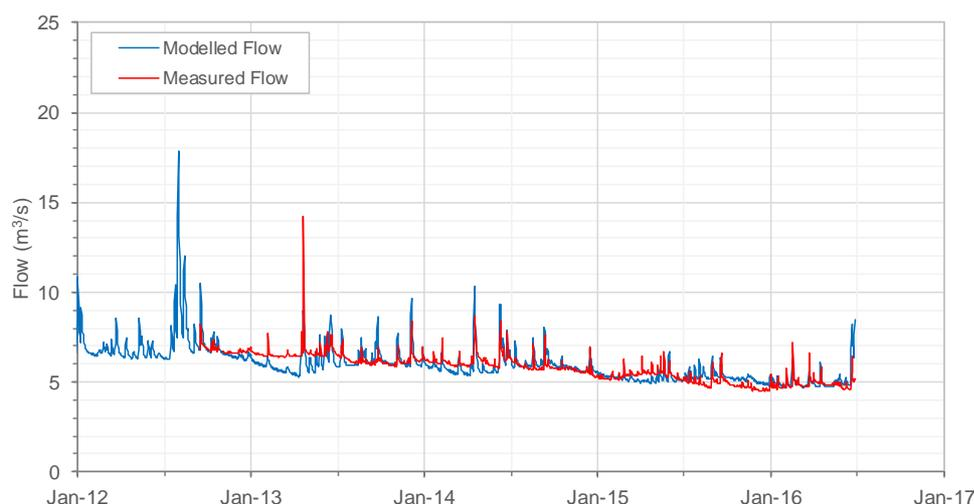


Figure 51. Hydrograph of the modelled and measured flow of the Waitahanui River at Otamarakau Valley Rd.

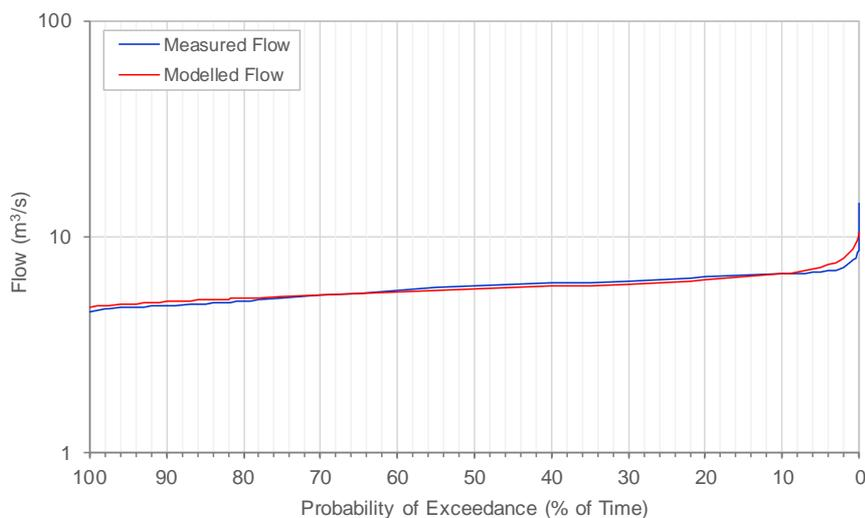


Figure 52. FDC of the modelled and measured flow of the Waitahanui River at Otamarakau Valley Rd.

Table 37. Summary of measured versus model flow statistics for Waitahanui River at Otamarakau Valley Rd.

Statistic	Measured Flow	Modelled Flow
Min	4.5	4.6
MALF	5.3	5.2
Median	5.9	5.7
Mean	5.8	5.8
Max	14.2	10.5
95%ile	6.9	7.2
99%ile	7.7	8.6
NSE (-)	0.52	
PBIAS (%)	-0.04	

The accuracy of the model calibration at Waitahanui at Otamarakau Valley Road gauge is summarised as follows:

- **PEC** – Based on the PEC outlined in **Table 24**, the model’s ability to predict flow at this monitoring location is considered Good with NSE of 0.52.
- **PBIAS** – Based on the PEC outlined in and **Table 25**, the model’s ability to predict flow at this monitoring location is considered Very Good with a PBIAS of -0.04%, evaluation indicates that the model under predicts the high flows.
- **FDC** – Indicates a good match of the frequency of flow for the majority flow regime, albeit a slight over prediction at low flow and under prediction at moderate to higher flows.

Based on visual observation of the hydrograph the model successfully simulates the general timing and magnitude of both baseflow and high flow events. This is supported by the Good and Very Good NSE and PBIAS classifications respectively. Therefore, there is high confidence in the model’s ability to predict flow at the Waitahanui at Otamarakau Valley Road gauge.

Table 38. Calibrated SMWBM parameters for catchments draining to Waitahanui River at Otamarakau Valley Rd

SC ID	ST (mm)	ZMAX (mm/hr)	FT (mm/d)	K _v (m/s)	D (m)
SC#104	650	14.0	6.3	1.86E-06	87
SC#105	650	14.0	6.0	9.13E-07	54
SC#106	650	10.0	6.0	9.07E-07	89
SC#107	650	13.0	6.3	1.99E-06	86
SC#108	593	11.0	8.8	5.28E-06	52
SC#109	650	18.0	7.2	2.80E-06	78
SC#110	650	14.0	7.1	2.30E-06	55
SC#111	650	10.0	8.0	3.83E-06	44
SC#112	590	10.0	9.5	6.68E-06	40
SC#113	546	11.0	7.6	3.77E-06	53

The calibrated model parameter values assigned (**Table 38**) are reflective of the following catchment characteristics:

- **ST** – soil moisture storage values are very consistent and range from approximately 550 to 650 mm. These are also reflective of deep highly porous soils and relatively large potential rooting depth of the sub-catchments and are similar to other catchments in this area.
- **ZMAX** – infiltration rates are high ranging from 11 to 18 mm/hr, with the higher rates occurring in SC#109, which is located in the highlands to the northeast of Lake Rotoma. The high ZMAX values reflect a mantle of highly porous pumice soils.
- **FT** – FT is for consistently moderately high ranging from 6 to 9.5 mm/day, which are consistent with hydraulic properties of the well-drained highly permeably sandy soils found throughout the catchment.
- **K_v** – the pattern of vertical hydraulic conductivity is fairly uniform across the catchment in the range of 1 to 6x10⁻⁶ m/s, which reflects moderate rates of vertical groundwater movement.
- **D** – depth to groundwater is typically relatively deep in the 40-90 m range for the majority of sub-catchments.

Additional commentary on the model calibration, with respect to the requirement for an inflow node to raise flows to measured levels, and the impact these had on specific discharge is provided in **Appendix E**.

6.1.8 Puanene River at State Highway 2 (SH2)

A comparison of modelled and measured flows along with FDCs generated from the calibration process for Puanene River at SH2 are shown in **Figure 53** and **Figure 54** respectively. Comparative statistics are summarised in **Table 39**, and the SMWBM input parameters from the final model calibration listed in **Table 40**.

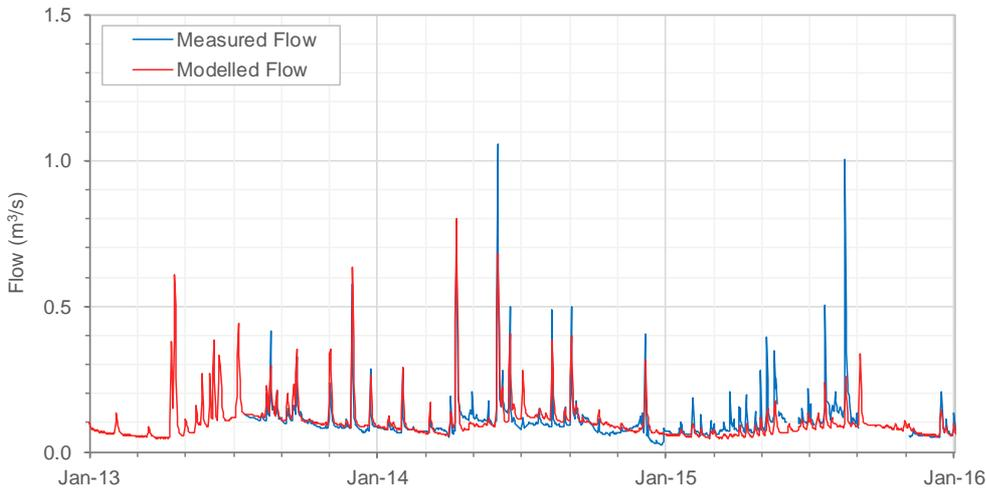


Figure 53. Hydrograph of the modelled and measured flow of the Puanene River at SH2.

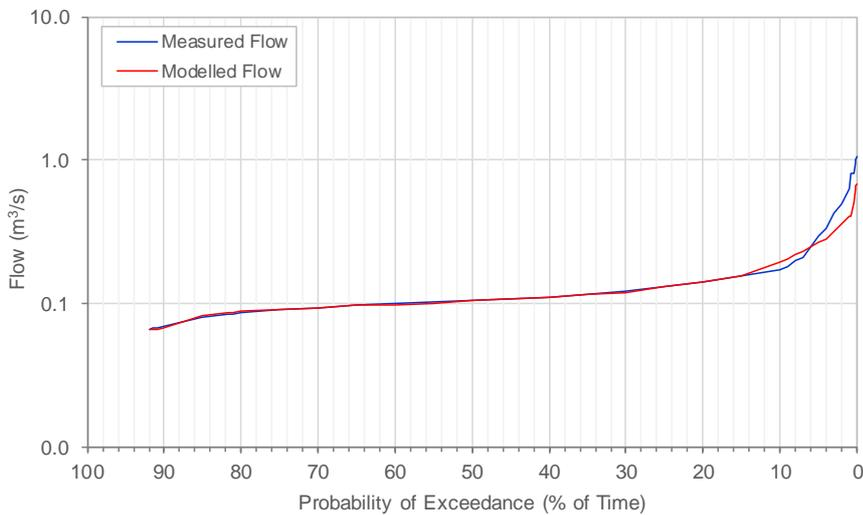


Figure 54. FDC of the non – irrigation period modelled and measured flow of the Puanene River at SH2.

Table 39. Summary of measured versus model flow statistics for Puanene River at SH2.

Statistic	Measured Flow	Modelled Flow
Min	0.05	0.05
MALF	0.04	0.05
Median	0.11	0.10
Mean	0.13	0.12
Max	1.06	0.68
95%ile	0.21	0.29
99%ile	0.51	0.50
NSE (-)	0.55	
PBIAS (%)	5.09	

The accuracy of the model calibration at Puanene River at SH2 gauge is summarised as follows:

- **PEC** – Based on the PEC outlined in **Table 24**, the model’s ability to predict flow at this monitoring location is considered Good with NSE of 0.55.
- **PBIAS** - Based on the PEC outlined in and **Table 25**, the model’s ability to predict flow at this monitoring location is considered Good with a PBIAS of 5.09, evaluation indicates the model is under-predicting.
- **FDC** - Indicates a good match of the frequency of flow for the majority flow regime, with the exception of higher flows that occur on average less than 15% of the time.

Based visual observation of the hydrograph the model successfully simulates the general timing and magnitude of both baseflow and high flow events. This is supported by the Good NSE and PBIAS classifications. Therefore, there is high confidence in the model’s ability to predict flow at the Puanene River at SH2 gauge.

Table 40. Calibrated SMWBM parameters for catchments draining to Puanene River at SH2.

SC ID	ST (mm)	ZMAX (mm/hr)	FT (mm/d)	K _v (m/s)	D (m)
SC#76	608	16.0	8.0	1.10E-06	60
SC#77	572	17.0	11.0	6.78E-06	25

The calibrated model parameter values assigned (**Table 40**) are reflective of the following catchment characteristics:

- **ST** – soil moisture storage values range from 570 to 610 mm. These are also reflective of deep highly porous soils and relatively large potential rooting depth of the sub-catchments and are similar to other catchments in this area.
- **ZMAX** – infiltration rates are high ranging from 16 to 17 mm/hr. The high ZMAX values reflect a mantle of highly porous pumice soils.
- **FT** – FT is for consistently high ranging from 8 to 11 mm/day, which are consistent with hydraulic properties of the well-drained highly permeably sandy soils found throughout the catchment.

- **K_v** – vertical hydraulic conductivity is fairly uniform across the catchment in the range of 1 to 7x10⁻⁶ m/s, which reflects moderate rates of vertical groundwater movement.
- **D** – depth to groundwater is strongly controlled by the elevation of these catchments with ranging from 25 to 60 m, with the shallow groundwater located in the lower elevation catchment (SC#77).

Additional commentary on the model calibration, with respect to the requirement for a loss node to decrease flows to measured levels, and the impact these had on specific discharge, is provided in **Appendix E**.

6.1.9 Kaituna Catchment Calibration Summary

6.1.9.1 Discharge Characteristics

Table 41 provides a collated summary of key flow regime statistics from the calibration to the gauged sites. The data is provided for comparison between different parts of the model domain. It should be noted, while these are the same statistics as presented in **Section 4**, the values presented in **Table 41** were calculated based on the modelled flow outputs, and therefore may differ slightly to those presented in **Section 4**, which were calculated from available measured flow data.

Table 41. Kaituna – Calibrated model catchment discharge characteristics.

Calibration Sites	Area (km ²)	Mean Flow (m ³ /s)	Specific Q (m ³ /s/km ²)	Q Coefficient (% MAP)
Kaituna at Taaheke ¹	4.6	0.1	0.031	49%
Paraiti (Mangorewa) at Saunders	173	7.2	0.041	57%
Kaituna at Te Matai ¹	326	15.4	0.047	74%
Waiari at Muttons	70	3.6	0.051	73%
Pongakawa at Old Coach Rd	101	4.1	0.041	67%
Puanene at SH2	13	0.1	0.009	17%
Raparapahoe at Drop Structure	51	2.4	0.046	71%
Waitahanui at Otamarakau Valley Rd	152	6.2	0.041	67%

¹ Calculation includes the catchment area of Lake Rotorua.

The range in catchment specific discharge from **Table 41** is from 0.009 m³/s/km² in the Puanene catchment to 0.051 m³/s/km² in the Waiari catchment, with typical values around 0.031 to 0.041 m³/s/km². The discharge coefficient for the Puanene catchment is on 17% of rainfall, reflecting the water loss from the system within the catchment are not recorded by the gauge. In comparison, the discharge coefficient for the remaining catchments range from 49% to 74% of the rainfall within each catchment.

6.1.9.2 Water Balance Summary

The discharge coefficient discussed in the previous section is the end-product of the catchment hydrological processes of partitioning rainfall. An understanding of the various other components of the catchment water balance is also useful in comparing the hydrological functioning of different catchments, and provide visibility on the dominant processes

Table 42 summarises the partitioning of rainfall within each catchment or catchment water balance. It is evident that percolation to groundwater is the largest component of the catchment water balance, ranging from 38% to 72% of MAP. This is reflective of the highly permeable soils and sub-soil geological profile within the WMA.

Soil evaporation is typically the second largest component ranging from 11% to 21% of the water balance. The exception to this would be the Raparapahoe catchment where surface runoff accounts for 30% of the water balance, which is a function of the generally steeper catchment and slightly lower permeability soils.

Table 42. Kaituna WMA calibrated model water balance summary (% of MAP).

Catchment	Interception Loss	Pondage Evaporation	Soil Evaporation	Percolation to Groundwater	Surface Runoff
Kaituna at Paraiti (Mangorewa)	12%	0%	15%	59%	15%
Kaituna at Te Matai	12%	0%	16%	61%	11%
Waiari at Muttons	11%	0%	14%	66%	8%
Raparapahoe at Drop Structure	13%	0%	19%	38%	30%
Puanene at SH2	13%	0%	21%	56%	10%
Pongakawa at Old Coach Rd	13%	0%	11%	72%	3%
Waitahanui at Otamarakau Valley Rd	14%	0%	19%	57%	10%

6.2 Flow Calibration - Rangitāiki

6.2.1 Rangitāiki River at State Highway 5 (SH5)

A comparison of modelled and measured flows generated from the calibration process for Rangitāiki River at SH5 are shown in **Figure 55**. No FDC was produced for this gauge due to the short record length, as described below. **Table 43** provides comparative statistics between the measured and modelled flow. **Table 44** summarises the calibrated SMWBM model parameters.

Flow measurements of the Rangitāiki River at SH5 began in Jun 2004 and were taken every 1 to 2 months until November 2005. Subsequently there was a nine-year gap in the monitoring regime, until flow measurements began again in January 2015. From March 2015 flow recording was occurring on a daily basis.

Due to the low count of measured data in comparison to other monitoring sites (less than two years of continuous data, and a temporal gap in the sampling regime) FDC analysis and analysis of model performance statistics were not carried out at this location. However, given the sampling intensity since early 2015, the monitoring location was used largely as a spot location.

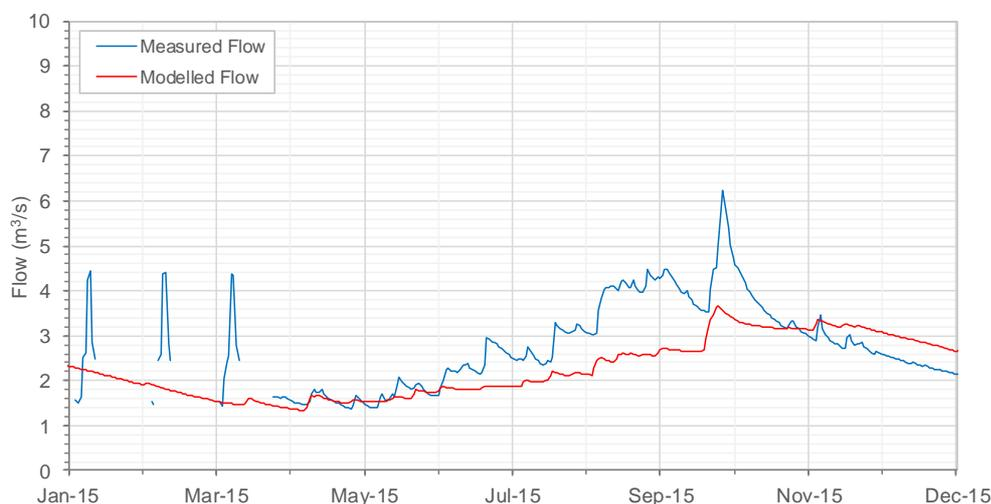


Figure 55. Hydrograph of the modelled and measured flow of the Rangitāiki River at SH5.

Table 43. Summary of measured versus model flow statistics at Rangitāiki River at SH5.

Statistic	Measured Flow	Modelled Flow
Min	1.4	1.3
MALF	2.1	2.0
Median	2.2	3.2
Mean	2.5	3.3
Max	6.2	8.2
95%ile	4.3	5.4
99%ile	5.0	5.9

Based on visual observation of the measured and modelled flow hydrograph, the model was shown to predict the general magnitude of baseflow conditions, however, did not predict peak flows well. Given this, and the limited measured flow data at this location, a level of uncertainty exists in the model's ability to predict flow at this location.

Table 44. Calibrated SMWBM parameters for catchments draining to Rangitāiki River at SH5.

SC ID	ST (mm)	ZMAX (mm/hr)	FT (mm/d)	K _v (m/s)	D (m)
SC#1	1,200	6	25	8.7x10 ⁻⁶	75

The calibrated model parameter values assigned (**Table 44**) are reflective of the following catchment characteristics:

- **ST** – soil moisture storage probably reflecting a combination of very high soil storage and deeper sub-soil storage.
- **ZMAX** – a moderate value of 6 mm/hr, which signals some impedence to infiltration in comparison to some of the very high rates in other catchments;
- **FT** – a very high FT value signals rapid drainage out of the sub-soil. It is assumed because of the low gradient and influence of the pumice (high permeability) in this area a large portion of the runoff generated in SC#1 will be lost to deeper groundwater flow.
- **K_v** – is moderately high at 9x10⁻⁶ m/s, reflecting the rapid rates of percolation to the groundwater table from the sub-soil consistent with the high permeability and well drained nature of materials (soils and sub-soils) derived from tephra and pumice.
- **D** – the depth to groundwater is relatively deep at 75 m.

6.2.2 Rangitāiki River at Murupara

The flow calibration for the Rangitāiki River at the Murupara Rd gauge is shown in the hydrograph and FDC presented in **Figure 56** and **Figure 57**, respectively, while **Table 45** provides comparative statistics between the measured and modelled flow. **Table 46** summarises the calibrated SMWBM model parameters.

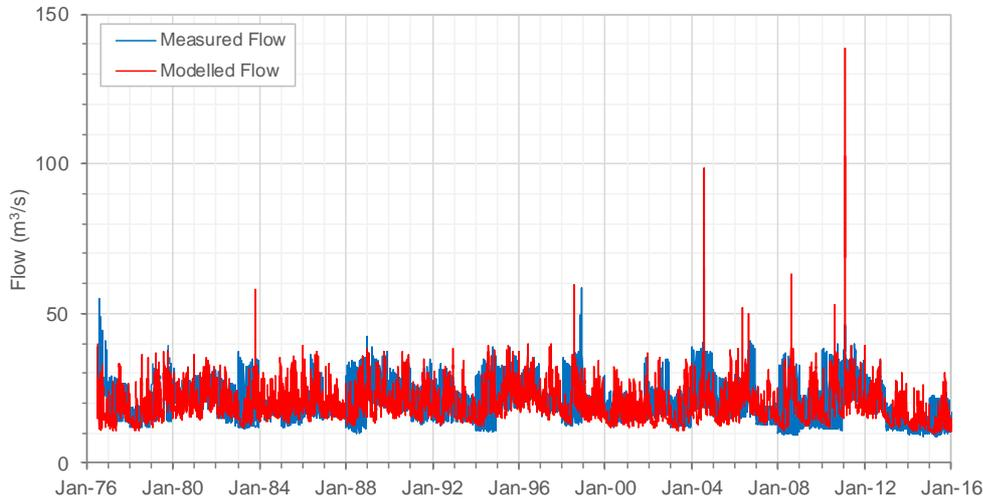


Figure 56. Hydrograph of the modelled and measured flow of the Rangitāiki River at Murupara.

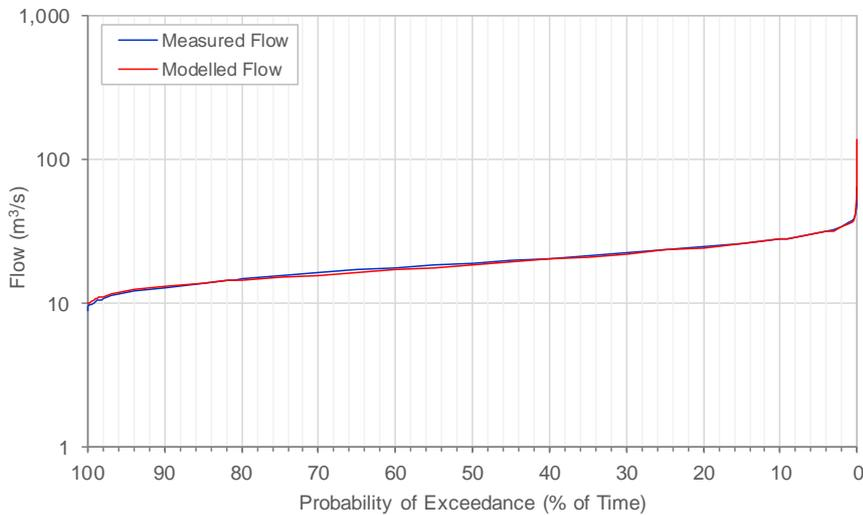


Figure 57. FDC of the modelled and measured flow of the Rangitāiki River at Murupara.

Table 45. Summary of measured versus model flow statistics for Rangitāiki River at Murupara

Statistic	Measured Flow	Modelled Flow
Min	9.0	9.2
MALF	13.8	14.2
Median	19.0	18.7
Mean	19.9	19.7
Max	65.4	138.6
95%ile	30.9	30.9
99%ile	36.4	36.1
NSE (-)	0.46	
PBIAS (%)	0.61	

The accuracy of the model calibration at Rangitāiki River at the Murupara Rd gauge is summarised as follows:

- **PEC** – based on the PEC outlined in **Table 24**, the model’s ability to predict flow at this monitoring location is considered Satisfactory with NSE of 0.46.
- **PBIAS** – based on the PEC outlined in **Table 25**, the model’s ability to predict flow at this monitoring location is considered Very Good with PBIAS of 0.61%, with some tendency to over predict flow at the high flow for this location.
- **FDC** – FDC indicates good simulated flow across the entire flow regime with the exception of extreme floods are simulated extremely well.

Based visual observation of the hydrograph the model successfully simulates the general timing and magnitude of both baseflow and high flow events. This is supported by the Satisfactory and Very Good NSE and PBIAS classifications respectively. Therefore, there is confidence in the model’s ability to predict flow at the Rangitāiki River at Murupara Rd Gauge.

Table 46. Calibrated SMWBM parameters for catchments draining to Rangitāiki River at Murupara.

SC ID	ST (mm)	ZMAX (mm/hr)	FT (mm/d)	K _v (m/s)	D (m)
SC #002	309	5	2.9	8.86E-07	36
SC #003	199	5	3.0	9.00E-07	32
SC #004	232	5	3.0	8.99E-07	53
SC #005	364	5	3.0	9.50E-07	42
SC #006	264	5	3.0	9.45E-07	63
SC #007	341	5	3.2	1.11E-06	71
SC #008	385	5	3.0	9.27E-07	35
SC #009	323	5	3.0	9.06E-07	43
SC #010	630	5	3.0	1.12E-06	29
SC #011	407	5	3.0	9.00E-07	52
SC #012	362	5	3.0	9.00E-07	50
SC #013	364	5	3.0	1.05E-06	38
SC #014	403	5	3.0	9.51E-07	34

SC ID	ST (mm)	ZMAX (mm/hr)	FT (mm/d)	K _v (m/s)	D (m)
SC #015	330	5	3.0	1.22E-06	35
SC #019	716	4	2.8	8.64E-07	110
SC #020	735	5	3.0	8.95E-07	82
SC #021	448	5	3.0	9.33E-07	73
SC #022	488	5	3.2	1.08E-06	73
SC #023	550	4	2.5	7.91E-07	97
SC #024	392	4	3.6	1.79E-06	40
SC #025	544	4	3.0	1.05E-06	76
SC #026	554	5	4.8	2.96E-06	84
SC #055	367	5	3.0	9.00E-07	40
SC #056	322	5	3.0	9.00E-07	36
SC #057	561	4	3.0	9.27E-07	83
SC #058	438	4	3.0	9.00E-07	38
SC #059	683	4	3.7	1.70E-06	65

The calibrated model parameter values assigned (**Table 46**) are reflective of the following catchment characteristics:

- **ST** – soil moisture storage values range from approximately 320 to 735 mm, which is reflective of the highly porous soils and relatively large potential rooting depth of each sub-catchment.
- **ZMAX** – infiltration rates are all consistently in the moderate range at 4-5 mm/hr, which is likely to provide a balance between partitioning the smaller rainfall events into soil infiltration and larger events predominantly into surface runoff.
- **FT** – sub-soil drainage rates are consistently only moderate ranging from 2.5 to 4.8 mm/day, reflecting all the soils in this catchment have moderate drainability.
- **K_v** – vertical hydraulic conductivity values range from 9×10^{-7} m/s to 3×10^{-6} m/s indicating moderate rate of vertical groundwater movement within the unsaturated zone.
- **D** – depth to groundwater is quite variable from 30 m to 110 m, dependent on the sub-catchment positioning within the catchment, but overall groundwater is moderate to deep, which means sub-soil drainage will take longer to reach the groundwater table and the level of groundwater connection to rivers could be lower than catchments with more shallow groundwater.

During the model calibration, initially the simulated flow was over-predicted in comparison to the measured flow. Similar to the upstream site, SH5 (**Section 6.2.1**), it was assumed that sub-surface flow was occurring as a direct result of the highly permeable catchment characteristics.

These characteristics suggest that the gauge is not measuring all the flow in the catchment and a portion of water is lost to the deeper aquifer groundwater. To simulate this groundwater loss, a head dependent loss relationship was created, which facilitated an acceptable calibration between simulated and measured flow. The mechanics of the loss node are described in **Appendix E**.

6.2.3 Whirinaki River at Galatea

The flow calibration for the Whirinaki River at the Galatea gauge is shown in the hydrograph and FDC presented in **Figure 58** and **Figure 59**, respectively, while **Table 47** provides comparative statistics between the measured and modelled flow. **Table 48** summarises the calibrated SMWBM parameters.

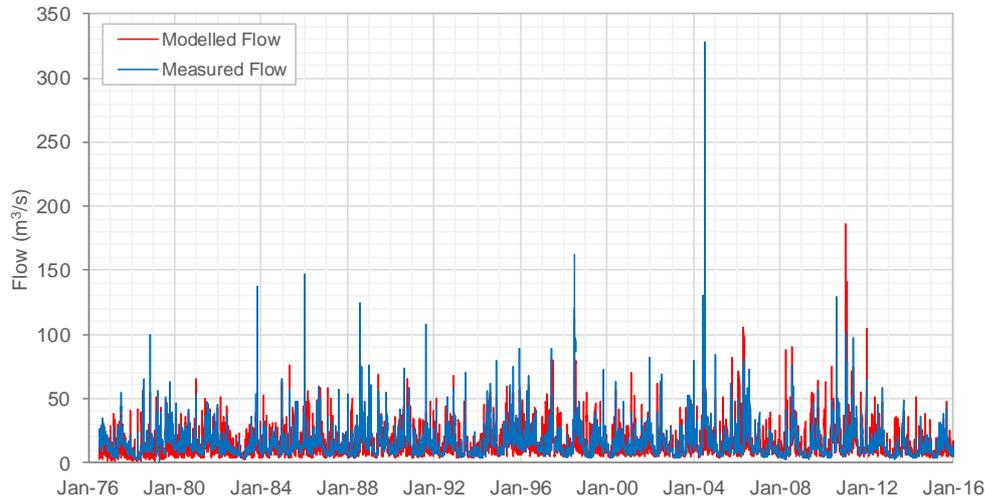


Figure 58. Hydrograph of the modelled and measured flow of the Whirinaki River at Galatea.

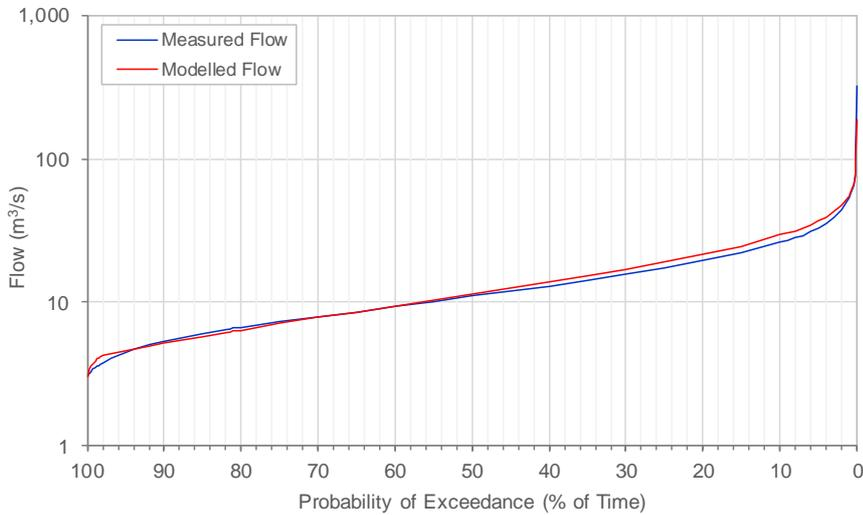


Figure 59. FDC of the modelled and measured flow of the Whirinaki River at Galatea.

Table 47. Summary of measured versus model flow statistics for Whirinaki River at Galatea.

Statistic	Measured Flow	Modelled Flow
Min	2.9	3.0
MALF	4.6	3.9
Median	11.1	11.5
Mean	14.1	15.0
Max	327.4	186.3
95%ile	32.9	37.1
99%ile	53.9	54.8
NSE (-)	0.60	
PBIAS (%)	-5.72	

The accuracy of the model calibration at Rangitāiki River at the Galatea gauge is summarised as follows:

- **PEC** – based on the PEC outlined in **Table 24**, the model’s ability to predict flow at this monitoring location is considered Good with NSE of 0.60.
- **PBIAS** – based on the PEC outlined in **Table 25**, the model’s ability to predict flow at this monitoring location is considered Good with PBIAS of -5.72%, with some tendency to over predict flow at the high flows and low flows, while under-predicting at the middle flow.
- **FDC** – the FDC indicates a good match for the majority of time. However, low flows are slightly over simulated during drought, with the exception of the most severe drought, and flow greater than the median (wet periods) are slightly over simulated.

Based visual observation of the hydrograph the model successfully simulates the general timing and magnitude of both baseflow and high flow events. This is supported by the Good NSE and PBIAS classifications. Therefore, there is high confidence in the model’s ability to predict flow at the Rangitāiki River at Galatea gauge.

Table 48. Calibrated SMWBM parameters for catchments draining to Whirinaki River at Galatea.

SC ID	ST (mm)	ZMAX (mm/hr)	FT (mm/d)	K _v (m/s)	D (m)
SC #016	207	2	1.4	2.34E-07	179
SC #017	600	1	1.8	4.77E-07	140
SC #018	656	1	2.0	3.2E-07	119
SC #039	338	2	1.4	2.34E-07	179
SC #040	743	1	1.9	6.68E-07	92
SC #041	657	1	1.8	6.18E-07	107
SC #042	439	2	2.6	1.2E-06	127
SC #043	678	1	3.5	2.02E-06	69
SC #044	567	1	3.5	2.26E-06	55

SC ID	ST (mm)	ZMAX (mm/hr)	FT (mm/d)	K _v (m/s)	D (m)
SC #045	243	2	2.0	3.18E-07	104
SC #046	587	2	1.9	6.27E-07	105
SC #047	278	3	2.5	6.38E-07	191
SC #048	262	2	2.1	2.49E-07	149
SC #049	345	2	2.1	2.85E-07	139
SC #050	213	3	2.0	2.45E-07	194
SC #053	631	1	2.5	8.64E-07	68
SC #054	435	2	2.1	7.49E-07	84

The calibrated model parameter values assigned (**Table 48**) are reflective of the following catchment characteristics:

- **ST** – soil moisture storage values have a wide range in this catchment range from approximately 210 to 740 mm. The value at the lower end of the spectrum relate to sub-catchment with predominantly shallow soils on hard rock (greywacke) parent materials in the east of the catchment (e.g. SC#16, SC#50). The higher values are reflective of the typical volcanic soils, being highly porous and with a relatively large potential rooting depth.
- **ZMAX** – infiltration rates are all consistently in the low to moderate range (1-3 mm/hr), which is reflective of the lower permeability sub-soils to the east and the influence weathering by-products from these may have in soils as you move progressively down the catchment. Consequently, the flow regime of these catchments will be dominated by surface runoff rather than groundwater processes.
- **FT** – sub-soil drainage rates are consistently only low to moderate ranging from 1.4 to 3.5 mm/day, and slightly lower compared to the Murupara catchment, which is consistent with the explanation provided for ZMAX.
- **K_v** – vertical hydraulic conductivity values range from 2×10^{-7} m/s to 2×10^{-6} m/s indicating low to moderate rate of vertical groundwater movement within the unsaturated zone, again consistent with the lower range of FT values compared to Murupara.
- **D** – depth to groundwater is quite variable but overall deep from approximately 50 m to 200 m, depending on the sub-catchment positioning within the catchment. The significant depth coupled with the low to moderate vertical hydraulic conductivity mean significant time is required for sub-soil drainage to exit the system as groundwater.

6.2.4 Pokairoa River at Railway Culvert

The flow calibration for the Pokairoa River at Railway Culvert gauge is shown in the hydrograph and FDC presented in **Figure 60** and **Figure 61**, respectively, while **Table 49** provides comparative statistics between the measured and modelled flow. **Table 50** summarises the calibrated SMWBM model parameters.

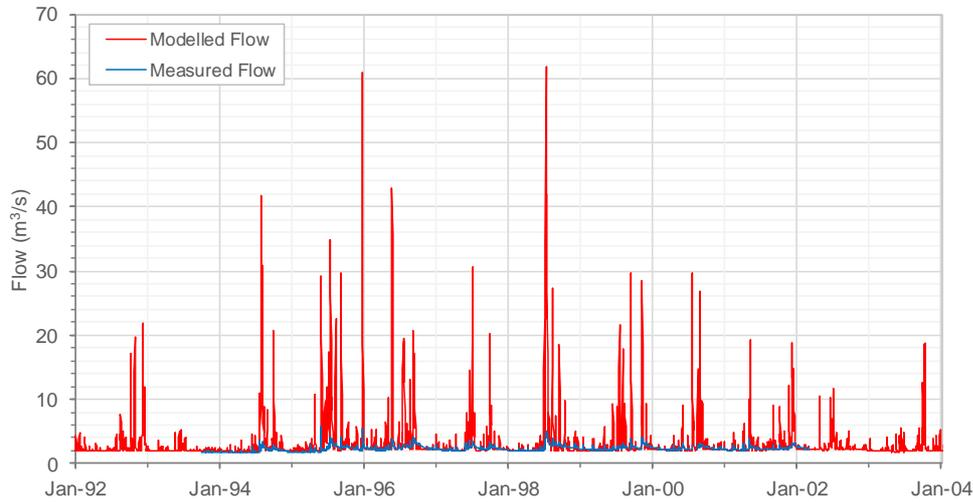


Figure 60. Hydrograph of the modelled and measured flow of the Pokairoa River at Railway Culvert.

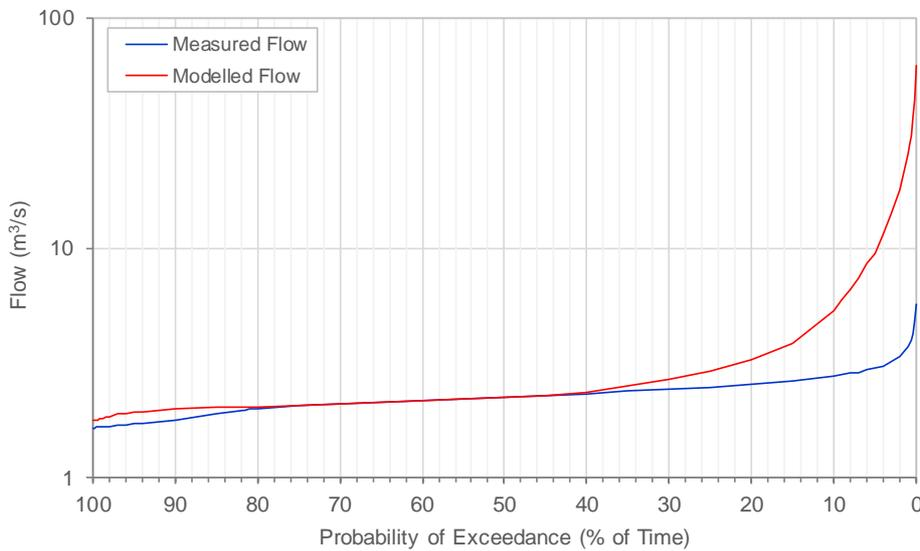


Figure 61. FDC of the modelled and measured flow of the Pokairoa River at Railway Culvert.

Table 49. Summary of measured versus model flow statistics the Pokairoa River at Railway Culvert.

Statistic	Measured Flow	Modelled Flow
Min	1.6	1.8
MALF	1.9	2.0
Median	2.2	2.2
Mean	2.3	3.5
Max	5.7	61.8
95%ile	3	9.5
99%ile	3.7	26.2
NSE (-)	-45.20	
PBIAS (%)	-54.04	

The accuracy of the model calibration at Pokairoa River at the Railway Culvert gauge is summarised as follows:

- **PEC** – based on the PEC outlined in **Table 24**, the model’s ability to predict flow at this monitoring location is considered Not Satisfactory with NSE of -45.20. The match to low flows is good, but the model is currently over predicting high flows. We recommend revisiting the calibration on this gauge to attempt to reduce simulated surface runoff to better align with the gauge by increasing discharge to groundwater and introducing a groundwater loss node (deep aquifer flow);
- **PBIAS** – based on the PEC outlined in **Table 25**, the model’s ability to predict flow at this monitoring location is considered Not Satisfactory with PBIAS of -54.04, with over prediction of flow at this location.
- **FDC** – the FDC indicates a good match for low flow, but extremely poor match from the 40%ile high flows due to over prediction of high flows.

Based visual observation of the hydrograph the model successfully simulates the magnitude of baseflow conditions, however, significantly over-predicts high flow events. Given the large over-simulation of high flow events caution is recommended when interpreting results during high flow events at this gauge. The implication of this is that is likely constituent loads will be over-simulated at this location.

Table 50. Table of parameters used for Pokairoa River at Railway Culvert.

SC ID	ST (mm)	ZMAX (mm/hr)	FT (mm/d)	K _v (m/s)	D (m)
SC #071	741	15	1.4	2.82E-07	16
SC #072	673	15	2.2	1.48E-06	58
SC #073	742	15	1.8	1.19E-06	89

The calibrated model parameter values assigned (**Table 50**) are reflective of the following catchment characteristics:

- **ST** – soil moisture storage values are high in this catchment ranging from 670 to 740 mm, which is reflective of the highly porous pumice soils.
- **ZMAX** – infiltration rates are consistently high (15 mm/hr), again due to the high porosity pumice soils.

- **FT** – sub-soil drainage rates are currently set at reasonable low values ranging from 1.4 to 2.2 mm/day. This was done to provide a match on the baseflow, but as a consequence, soils fill rapidly due to the high infiltration rates and result in surface runoff due to soil moisture excess. Trials were undertaken with higher FT values and while this reduced high flows significantly, baseflows were significantly over predicted. It is conceptualised that groundwater recharge in the highland area is draining to deep groundwater and not reporting to the gauge, hence the gauge is not a true reflection of the catchment water balance. It is recommended that FT is increased to a realistic value for these highly drainable catchments and to compensate for the resulting increase in river baseflows, a loss node be assigned proportionally by area to the three sub-catchments;
- **K_v** – vertical hydraulic conductivity values range from approximately 3×10^{-7} m/s to 1×10^{-6} m/s indicating low to moderate rates of vertical groundwater movement within the unsaturated zone.
- **D** – depth to groundwater is quite variable from approximately 16 m to 90 m, reflecting the topographic elevation of the sub-catchment.

6.2.5 Waihua River at Gorge

The flow calibration for the Waihua River at Gorge gauge is shown in the hydrograph and FDC presented in **Figure 62** and **Figure 63**, respectively, while **Table 51** provides comparative statistics between the measured and modelled flow. **Table 52** summarises the calibrated SMWBM model parameters.

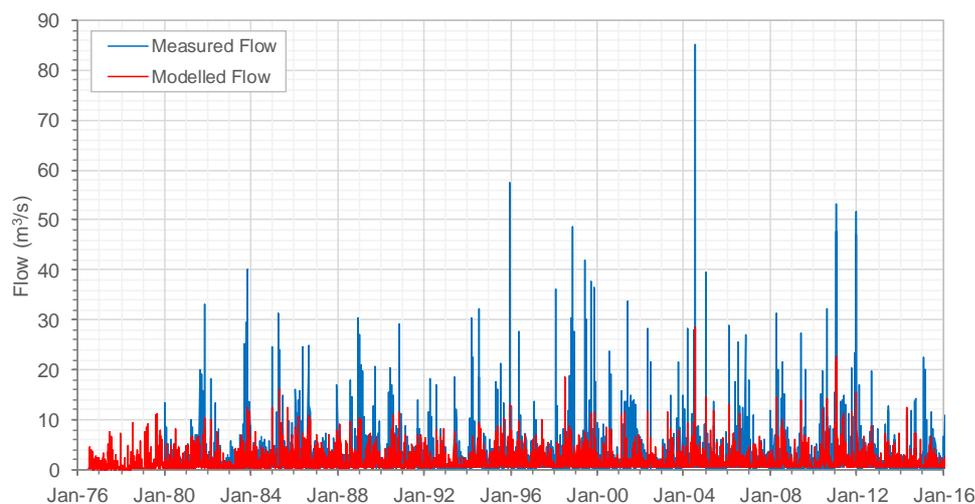


Figure 62. Hydrograph of the modelled and measured flow of the Waihua River at Gorge.

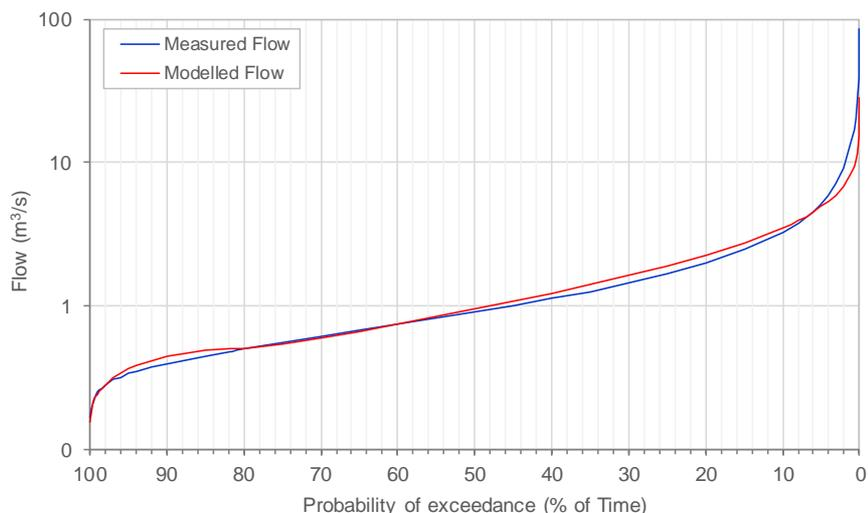


Figure 63. FDC of modelled and measured flow of the Waihua River at Gorge.

Table 51. Summary of measured versus model flow statistics for the Waihua River at Gorge.

Statistic	Measured Flow	Modelled Flow
Min	0.2	0.2
MALF	0.3	0.4
Median	0.9	0.9
Mean	1.7	1.6
Max	85.2	28.5
95%ile	5.1	4.9
99%ile	14.1	8.3
NSE (-)	0.63	
PBIAS (%)	6.69	

The accuracy of the model calibration at Waihua River at Gorge gauge is summarised as follows:

- **PEC** – based on the PEC outlined in **Table 24**, the model's ability to predict flow at this monitoring location is considered Good with NSE of 0.63.
- **PBIAS** - based on the PEC outlined in **Table 25**, the model's ability to predict flow at this monitoring location is considered Good with PBIAS of 6.69, with some tendency to over predict low flow and under predict high flows at this location.
- **FDC** – the FDC indicates a good match for low to medium flows, but the model is currently over predicting flows medium flow in the 1 to 5 m³/s range, and under-predicting high flows >5 m³/s.

Based visual observation of the hydrograph and flow duration curve the model successfully simulates the magnitude of baseflow conditions, however, under-predicts the infrequent high flow events. The model simulates good agreement to measured flow data the majority (>95%) of the time, and overall model calibration performance is considered good at this site.

Table 52. Table of parameters used for Waihua River at Gorge.

SC ID	ST (mm)	ZMAX (mm/hr)	FT (mm/d)	K _v (m/s)	D (m)
SC#89	224	2	2.4	2.09E-07	209
SC#90	726	2	2.2	1.55E-06	96

The calibrated model parameter values assigned (**Table 52**) are reflective of the following catchment characteristics:

- **ST** – soil moisture storage values are moderately shallow in SC#89 and deep in SC#90, which is due to the catchments parent geology, with SC#89 being located on bedrock, which SC#90 is located downstream on more porous alluvium.
- **ZMAX** – infiltration rates are moderately low at 2 mm/hr due to the influence of rock weathering and associated weathering by-products lowering soil infiltration rates.
- **FT** – sub-soil drainage rates are reasonably low ranging from 2.2 to 2.4 mm/day.
- **K_v** – vertical hydraulic conductivity values are quite different in these two catchments, with SC#89 being predominantly hard rock having a much lower K_v value of 2×10^{-7} m/s compared to the higher permeability alluvial catchment SC#90 with a K_v value of 1.5×10^{-6} m/s.
- **D** – depth to groundwater is also variable from approximately 100 to 209 m, reflecting the low to high topographic elevations of each catchment.

6.2.6 Rangitāiki River at Waiohou Bridge

The flow calibration for the Rangitāiki River at Waiohou Bridge gauge is shown in the hydrograph presented in **Figure 64**. This monitoring station captures all the sub-catchments downstream of the Murupara, Galatea, and Railway culvert flow sites, along with two discharges for Lake Aniwanuiwa and Flaxy Dam.

While the site has less than two years of data available for comparison purposes, the do occur at a high frequency, hence it was considered a primary site for calibration. A FDC was not produced due to the short period of data. **Table 53** provides comparative statistics between the measured and modelled flow, while **Table 54** summarises the calibrated SMWBM model parameters.

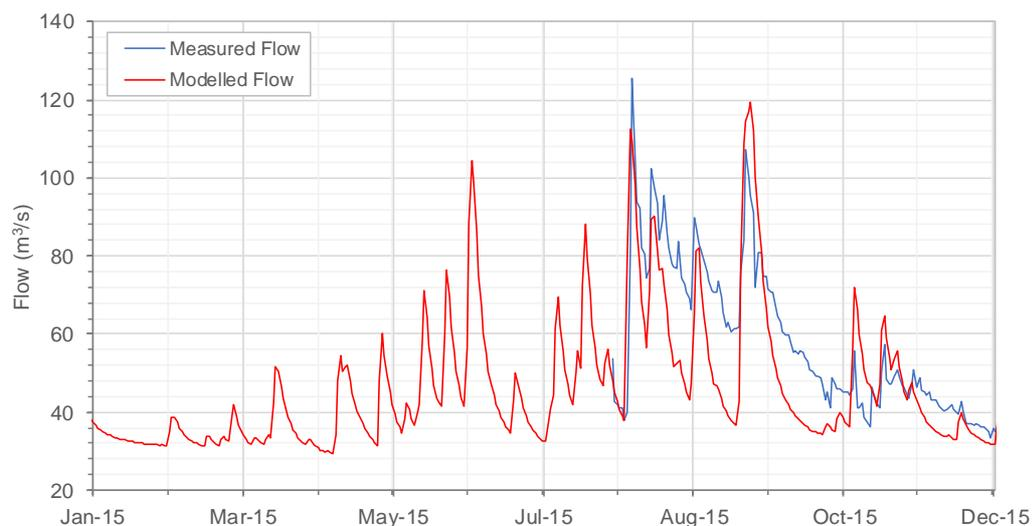


Figure 64. Hydrograph of the modelled and measured flow of the Rangitāiki River at Waiohou Bridge.

Table 53. Summary of measured versus model flow statistics for the Rangitāiki River at Waiohou Bridge.

Statistic	Measured Flow	Modelled Flow
Min	25.8	26.2
MALF	29.6	24.7
Median	25.8	26.2
Mean	52.3	40.8
Max	25.8	26.2
95%ile	91.8	67.4
99%ile	136.3	88.5

Based on visual observation of the measured and modelled flow hydrographs, the model was shown to successfully predict the magnitude and timing of peak flow events, however, predicted a quicker recession of the falling limb. Due to the limited period of available measured flow data at this location, a level of uncertainty exists in confidence of the model to predict flows. However, it is noted, the model does predict reasonable match to the limited available data, particularly the peak and low flows.

Table 54. Calibrated SMWBM parameters for catchments draining to Rangitāiki River at Waiohou Bridge.

SC ID	ST (mm)	ZMAX (mm/hr)	FT (mm/d)	K _v (m/s)	D (m)
SC #027	551	10	11.0	5.88E-06	35
SC #028	595	10	11.7	5.99E-06	23
SC #030	576	10	10.0	3.45E-06	18
SC #031	726	10	9.0	1.29E-06	82
SC #051	193	10	2.0	2.13E-07	226

Bay of Plenty Regional Council
Kaituna-Pongakawa-Waitahanui & Rangitāiki Catchment Models



SC ID	ST (mm)	ZMAX (mm/hr)	FT (mm/d)	K _v (m/s)	D (m)
SC #060	429	8	5.0	9.00E-07	35
SC #061	706	9	5.0	9.90E-07	73
SC #062	591	7	5.0	9.00E-07	54
SC #063	676	10	5.0	1.13E-06	56
SC #064	708	10	5.0	9.00E-07	40
SC #065	645	10	5.0	1.09E-06	68
SC #066	665	9	4.0	9.00E-07	44
SC #067	649	10	5.0	1.10E-06	82
SC #068	649	10	5.0	1.10E-06	101
SC #069	695	10	0.5	1.32E-06	79
SC #070	743	10	0.4	9.55E-07	67
SC #074	203	10	0.9	4.34E-07	241
SC #075	717	10	1.0	7.49E-06	40
SC #076	633	10	3.2	6.78E-06	40
SC #077	204	10	2.0	4.29E-07	172
SC #078	416	9	4.0	7.49E-06	35
SC #079	192	10	1.0	2.65E-07	203
SC #080	190	10	0.5	2.80E-07	159
SC #082	195	10	1.0	3.55E-07	140
SC #083	743	10	4.0	7.46E-06	25
SC #085	294	10	2.5	5.06E-07	183
SC #086	719	10	2.9	3.31E-06	37
SC #087	209	10	1.0	2.24E-07	190
SC #088	711	9	3.5	1.58E-06	77
SC #092	698	9	6.0	9.66E-07	34
SC #093	730	9	1.0	9.55E-07	72
SC #094	743	10	5.0	9.20E-07	63
SC #095	743	10	5.0	9.01E-07	100
SC #096	743	10	5.0	9.17E-07	77
SC #097	736	10	9.0	1.01E-06	90
SC #099	248	10	3.2	2.71E-07	191
SC #100	505	10	3.1	5.14E-07	111

The calibrated model parameter values assigned (**Table 55**) are reflective of the following catchment characteristics:

- **ST** – soil moisture storage values vary across the catchment from low values around 200 mm in the east to high values around 740 mm in the west. The low ST values are reflective of moderately shallow soils associated with hard rock parent geology, whereas the higher values reflect porous pumice-based soils and alluviums.
- **ZMAX** – infiltration rates are moderately high ranging from 7 to 10 mm/hr.
- **FT** – there is significant variation in sub-soil drainage rates across the catchment from 0.5 to 12 mm/day. In general, sub-soil drainage rates are low in the east and increase towards the porous pumice country in the west.
- **K_v** – similarly vertical hydraulic conductivity values vary significantly across the catchment from east to west from approximately 2×10^{-7} m/s to 7.5×10^{-6} m/s in the east, which is correlated to the geology.
- **D** – depth to groundwater is quite deep over the vast majority of this catchment (>40 m), with a range of approximately 20 to >200 m.

6.2.7 Rangitāiki River at Te Teko

The Te Teko gauge captures all sub-catchments between the Waiohou Bridge and this location, including the Matahina dam. The flow calibration for the Rangitāiki River at Te Teko gauge is shown in the hydrograph and FDC presented in **Figure 65** and **Figure 66**, respectively, while **Table 55** provides comparative statistics between the measured and modelled flow and **Table 56** summarises the calibrated SMWBM model parameters.

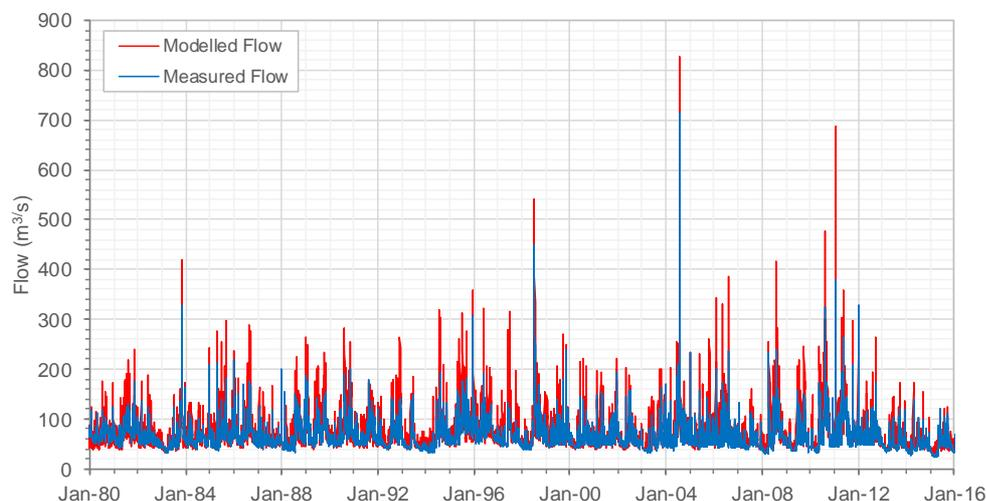


Figure 65. Hydrograph of the modelled and measured flow of the Rangitāiki River at Te Teko.

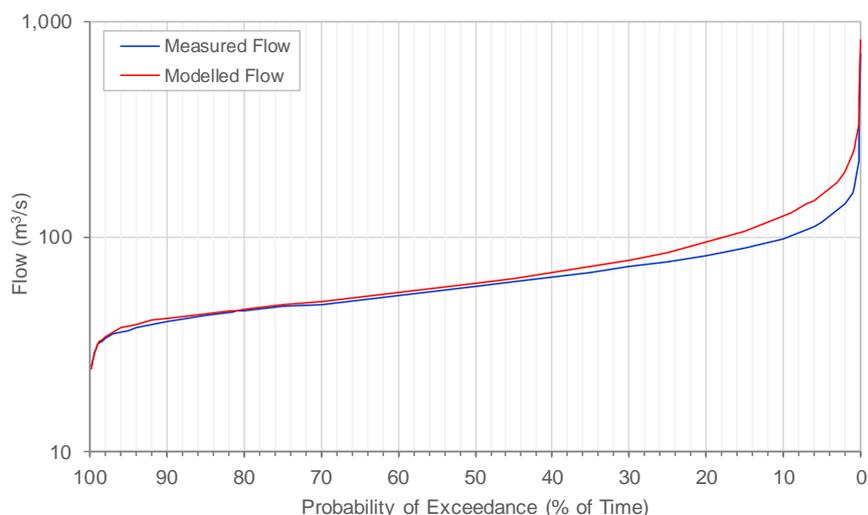


Figure 66. FDC of the modelled and measured flow of the Rangitāiki River at Te Teko.

Table 55. Summary of measured versus model flow statistics for Rangitāiki River at Te Teko.

Statistic	Measured Flow	Modelled Flow
Min	23.4	24.9
MALF	39.3	37.5
Median	58.8	61.1
Mean	65.8	74.7
Max	714.7	829.6
95%ile	117.4	157.1
99%ile	159.8	245.7
NSE (-)	0.41	
PBIAS (%)	-14.18	

The accuracy of the model calibration at Rangitāiki River at Te Teko gauge is summarised as follows:

- **PEC** – based on the PEC outlined in **Table 24**, the model’s ability to predict flow at this monitoring location is considered Satisfactory with NSE of 0.41.
- **PBIAS** – based on the PEC outlined in **Table 25**, the model’s ability to predict flow at this monitoring location is considered Satisfactory with PBIAS of -14.18, with some tendency to over predict flow at this location.
- **FDC** – the FDC indicates a good match for low to medium flows, but the model is currently over predicting higher flows. This is likely to improve by implementing the recommendation mentioned for the Pokairoa River and could also be applied to SC#60 to SC#69 in the western highlands of the Waihua River catchment.

Based visual observation of the hydrograph the model successfully simulates the general timing of both baseflow and high flow events, however tends to over-predict the magnitude of the high flow events. Overall, flow model performance at this site is considered satisfactory.

Table 56. Calibrated SMWBM parameters for catchments draining to Rangitāiki River at Te Teko.

SC ID	ST (mm)	ZMAX (mm/hr)	FT (mm/d)	K _v (m/s)	D (m)
SC #033	727	9.1	1.6	1.14E-06	60
SC #035	679	8.2	1.9	2.20E-06	64
SC #037	587	6.1	3.2	5.88E-06	12
SC #098	743	9.9	7.2	9.00E-07	111
SC #112	743	9.3	1.1	8.82E-07	57
SC #113	743	9.3	1.4	1.62E-06	83
SC #114	743	9.3	1.5	2.14E-06	54
SC #115	743	9.2	0.9	1.40E-06	60
SC #117	739	6.6	0.9	4.84E-06	3
SC #102	743	9.3	7.7	7.62E-07	119
SC #104	663	9.1	1.6	1.25E-06	116

The calibrated model parameter values assigned (**Table 57**) are reflective of the following catchment characteristics:

- **ST** – soil moisture storage values are fairly consistent in these catchments varying from approximately 600 to 750 mm. This is reflective of the porous light alluvial soils.
- **ZMAX** – infiltration rates are moderately high ranging from approximately 6.5 to 10 mm/hr.
- **FT** – there is significant variation in sub-soil drainage rates across the catchment from approximately 1 to 8 mm/day. In general, sub-soil drainage rates are low in the east and increase towards the porous pumice country in the west.
- **K_v** – vertical hydraulic conductivity values are moderate and vary from approximately 8×10^{-7} m/s to 6×10^{-6} m/s.
- **D** – depth to groundwater ranges from shallow (<5 m) in the lowlands to deep in the higher elevation sub-catchments (SC#102 and 104).

6.2.8 Rangitāiki Catchment Calibration Summary

6.2.8.1 Discharge Characteristics

Table 57 provides a collated summary of key flow regime statistics from the calibration to the gauged sites. The data is provided for comparison between different parts of the model domain. It should be noted, while these are the same statistics as presented in **Section 4**, the values presented in **Table 57** were calculated based on the modelled flow outputs, and therefore may differ slightly to those presented in **Section 4**, which were calculated from available measured flow data.

Table 57. Rangitāiki – Calibrated model catchment discharge characteristics.

Calibration Sites	Area (km ²)	Mean Flow (m ³ /s)	Specific Q (m ³ /s/km ²)	Q Coefficient (% MAP)
Rangitāiki at SH5	101	3.3	0.032	72%
Rangitāiki at Murupara	1,148	20.1	0.017	40%
Whirinaki at Galatea	507	14.7	0.029	67%
Pokairoa at Railway Culvert	118	3.2	0.027	55%
Rangitāiki at Waiohou Bridge	2,689	72.2	0.027	60%
Waihua at Gorge	46	1.6	0.034	69%
Rangitāiki at Te Teko	2,846	73.9	0.026	57%

The range in catchment specific discharge from **Table 57** is from 0.017 m³/s/km² in the Rangitāiki at Murupara catchment to 0.034 m³/s/km² in the Waihua at Gorge catchment, with typical values around 0.027 m³/s/km².

6.2.8.2 Water Balance Summary

Table 58 summarises the partitioning of rainfall within each catchment or catchment water balance. It is evident that percolation to groundwater is the largest component of the catchment water balance, ranging from 38% to 72% of MAP. This is reflective of the highly permeable soils and sub-soil geological profile within the WMA.

Soil evaporation is typically the second largest component ranging from 11% to 21% of the water balance. The exception to this would be the Raparapahoe catchment where surface runoff accounts for 30% of the water balance, which is a function of the generally steeper catchment and slightly lower permeability soils.

Table 58. Rangitāiki WMA calibrated model water balance summary (% of MAP).

Catchment	Interception Loss	Pondage Evaporation	Soil Evaporation	Percolation to Groundwater	Surface Runoff
Rangitāiki at SH5	18%	0%	10%	67%	5%
Rangitāiki at Murupara	19%	0%	25%	32%	23%
Whirinaki at Galatea	16%	0%	14%	19%	51%
Pokairoa at Railway Culvert	16%	1%	29%	34%	21%
Rangitāiki at Waiohou Bridge	12%	0%	15%	22%	51%
Waihua at Gorge	16%	0%	25%	33%	26%
Rangitāiki at Te Teko	15%	0%	26%	32%	26%

6.3 Parameter Application to Ungauged Catchments

To determine the model parameters for the ungauged catchments, relationships were established between the catchment physical characteristics and calibrated SMWBM parameters for the gauged catchments. These relationships characterise the physical characteristics of the sub-catchments and were used to assign SMWBM parameter values to the ungauged catchments.

Due to the different geological and topographical features between the Kaituna and Rangitāiki sub-catchments, the range of parameter values assigned to sub-catchments between the two catchments varied. Therefore, separate relationships were derived for the Kaituna and Rangitāiki catchments. Within the Kaituna WMA a relationship was derived for each gauged catchment, and therefore the parameters applied for the ungauged catchments were based on proximity to the closest established relationship.

Relationships were established for the six SMWBM parameters described in

Table 59 by fitting curves to the gauged catchment parameters and corresponding physical property. An iterative process was employed to determine the type of relationship for each parameter which produced the best calibration results. The curves fitted to the data are intended to highlight the general trend relationship between catchment properties and SMWBM parameters, and therefore is not appropriate to assign statistical measures or correlation coefficients (such as r^2 values) to these relationships. These relationships are discussed in turn in the following sections.

The remaining SMWBM parameters were assigned constant values across all sub-catchments and are outlined in **Section 6.3.7**.

Table 59. Summary of the relationships developed between key catchment characteristics and SMWBM parameters.

SMWBM Parameter	Catchment Characteristic	Description
ST (maximum soil moisture content)	Soil Depth (m)	ST defines the size of the maximum soil moisture capacity. In a simplistic sense, ST increases as the potential rooting depth (PRD) increases. Typically, ST is defined as follows: $ST = \text{Soil Depth} \times \text{Profile Average Porosity}$ However, in modelling, other factors (including model structural limitations) may mean that this relationship is only used as a guide. For example, in areas where significant depth to groundwater occurs, such as on the Kaiangaroa Plateau, and where the active depth range that moisture is drawn from during canopy evapotranspiration exceeds the soil depth (due to deep penetrating tree roots or stringers). In cases like these, the ST value may exceed the value estimated by this relationship.
ZMAX (maximum infiltration rate)	Soil permeability (mm/hr)	ZMAX defines the maximum infiltration rate of the soil. ZMAX regulates the volume of water entering the soil moisture store and hence the partitioning of rainfall into surface runoff or infiltration. ZMAX increases with higher soil permeability.
FT (sub-soil drainage rate from soil moisture storage at full capacity)	Geology permeability (mm/d)	FT defines the maximum rate of percolation through the soil zone. FT is the primary control on the quantum of water percolating from the soil moisture store to the underlying aquifer system, and FT increases as parent geology permeability increases.
DIV (surface ponding coefficient)	Sub-catchment slope (°)	DIV is the proportion of excess rainfall that ponds (and subsequently infiltrates the soil) versus becoming surface runoff. A value of 1 means all 100% of excess rainfall ponds versus a value of 0 means all the excess rainfall is routed into surface runoff or quick flow. DIV increases as catchment slope decreases.

<p>TL (Surface routing coefficient)</p>	<p>Sub-catchment area (km²)</p>	<p>TL is the coefficient for the surface routing coefficient and controls the attenuation of surface water runoff. As catchment area increases the attenuation of surface water runoff increases, which reduces peak flow but extends recession limbs from storm events.</p>
<p>Kv (saturated vertical hydraulic conductivity)</p>	<p>Estimated rock vertical hydraulic conductivity (m/s)</p>	<p>Saturated vertical hydraulic conductivity (Kv) defines the ability of the earth material to transmit water in a vertical direction, both upwards or downwards. In the zone above the groundwater table (vadose zone) the vertical hydraulic conductivity is typically reduced. The model automatically calculates the unsaturated hydraulic conductivity based on Kv and the degree of wetness in the overlying soil zone. Kv was mapped to each SC based on the QMap rock types and Kv values estimated from typically publicised values.</p>

6.3.1 ST and Soil Depth

The relationships between the SMap plant rooting depth and ST parameter for each gauged catchment in the Kaituna and Rangitāiki WMAs are shown in **Figure 67** and **Figure 68** respectively.

The two figures below show that for both WMAs the ST parameter increases with increasing plant rooting depth. Multiple relationships were developed for the Kaituna sub-catchments, while a single relationship was determined to be representative of all the Rangitāiki sub-catchments.

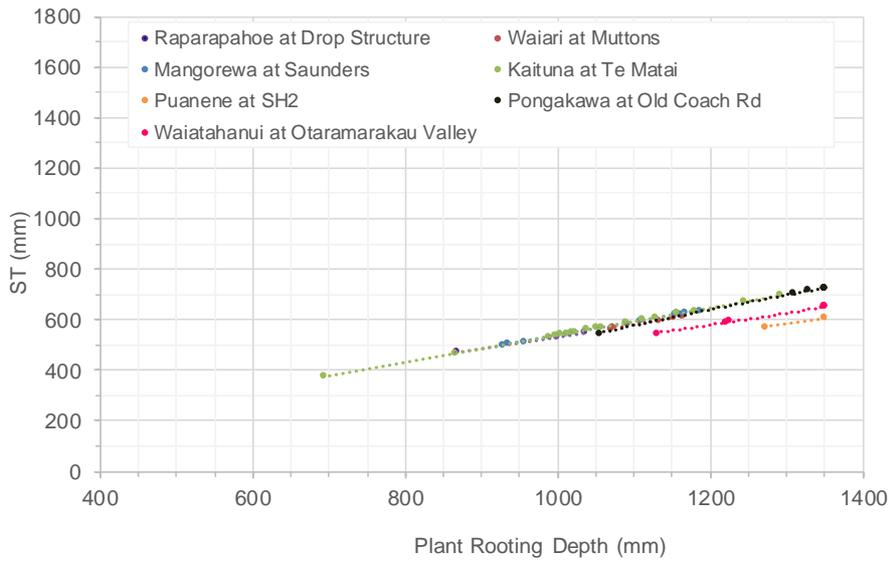


Figure 67. Kaituna relationship between maximum soil water content (ST) and potential rooting depth.

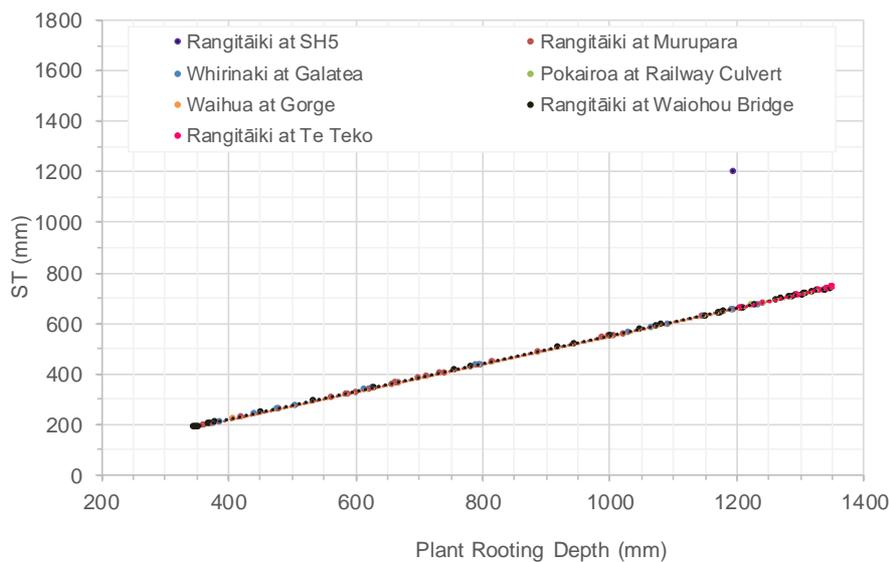


Figure 68. Rangitāiki relationship between maximum soil water content (ST) and plant rooting depth.

6.3.2 ZMAX and Soil Permeability

The relationship between the SMap soil permeability class and the ZMAX parameter for each gauged catchment in the Kaituna and Rangitāiki WMAs are shown in **Figure 69** and **Figure 70** respectively.

Individual relationships were established for each gauged location within the Kaituna and Rangitāiki WMAs. The differing relationships between sub-catchments reflect the combination of different catchment characteristics (e.g. topography). All sub-catchments display the same trend of increasing ZMAX values with increasing soil permeability.

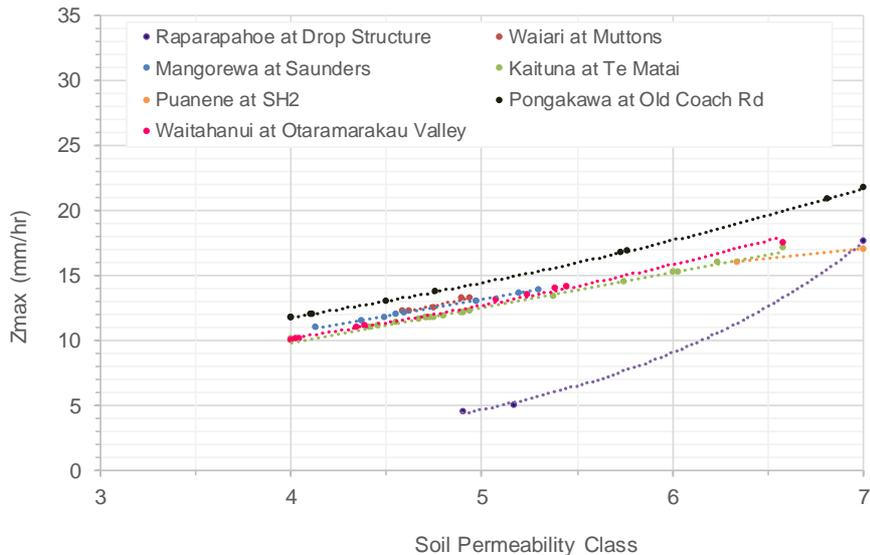


Figure 69. Kaituna relationship between maximum infiltration rate (ZMAX) and soil permeability class.

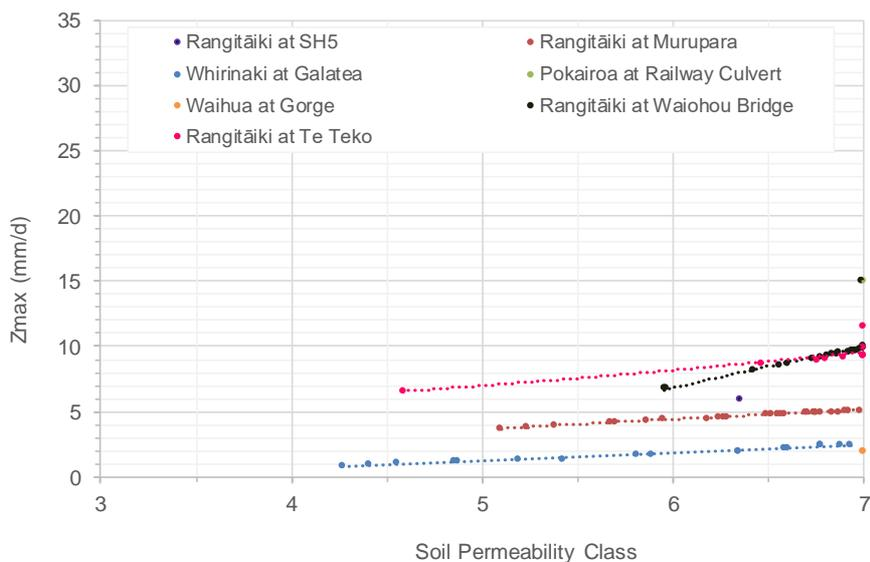


Figure 70. Rangitāiki relationship between maximum infiltration rate (ZMAX) and soil permeability class.

6.3.3 FT and Rock Permeability

Relationships were developed between the GNS Science QMap derived rock permeability and the FT parameter for each gauged catchment in the Kaituna and Rangitāiki WMAs, and are shown in **Figure 71** and **Figure 72** respectively.

Multiple relationships were found in the Kaituna Catchment, with larger FT values corresponding to Pongakawa River at Old Coach Road, and lower FT values seen in the other catchments in the WMA. For example, Paraiti (Mangorewa) at Saunders which has less sub-surface drainage as the larger soil moisture capacity of the catchment allows for more water to be ‘held’.

Multiple relationships were also found for the Rangitāiki Catchment. The scatter of data around the trendline for Rangitāiki at Waiohou Bridge catchment reflects the large range of different physical characteristics within the catchment being combined, for example the western sub-catchments are typically rolling hills, while the eastern sub-catchments are steep.

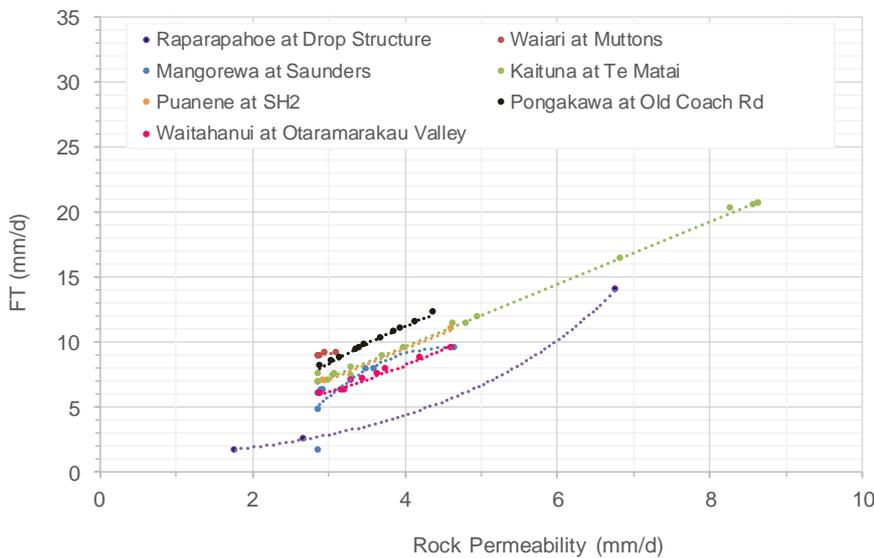


Figure 71. Kaituna relationship between sub-soil drainage rate (FT) and rock permeability.

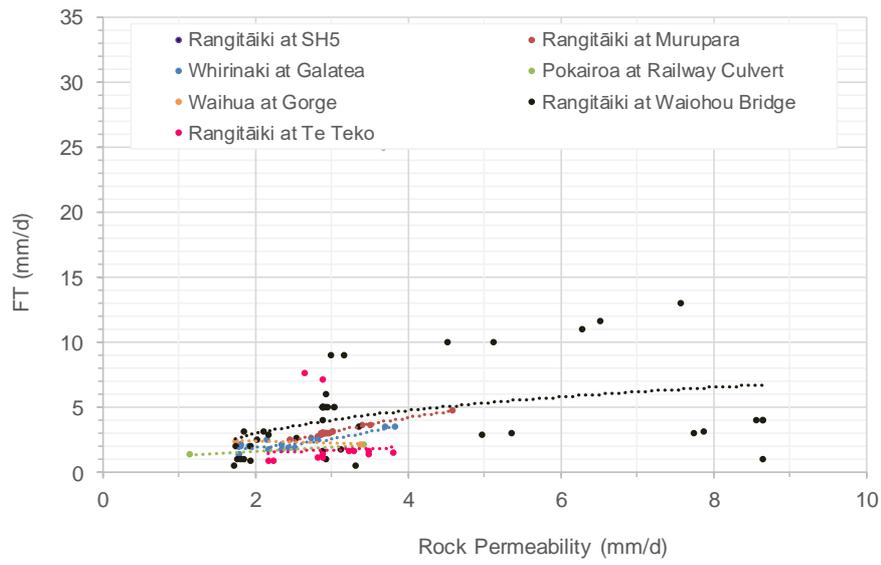


Figure 72. Rangitāiki relationship between sub-soil drainage rate (FT) and rock permeability.

6.3.4 DIV and Catchment Average Slope

The DIV parameter was related to the mean slope of the sub-catchments on the basis that steeper sloped catchments will produce less surface ponding than low sloped or flat catchments. The relationships derived are shown in **Figure 73** and **Figure 74** for the Kaituna and Rangitāiki catchments respectively.

The relationships in the Kaituna and Rangitāiki WMAs all show similar trends of decreasing DIV values with increasing slope, until approximately 16 degrees. Sub-catchments with an average slope of 16 degrees or greater all have a DIV value of 0, reflecting that the catchments are too steep for surface water ponding to occur.

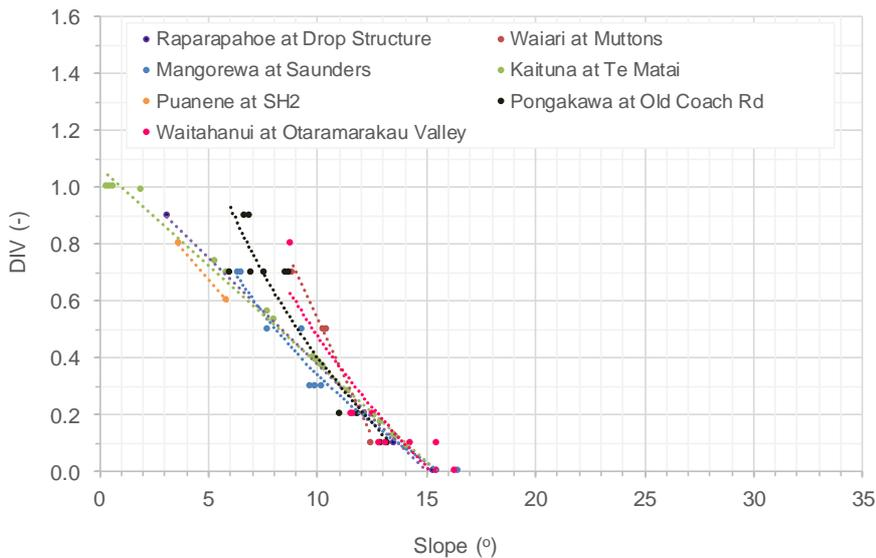


Figure 73. Kaituna relationship between surface water ponding (DIV) and catchment slope.

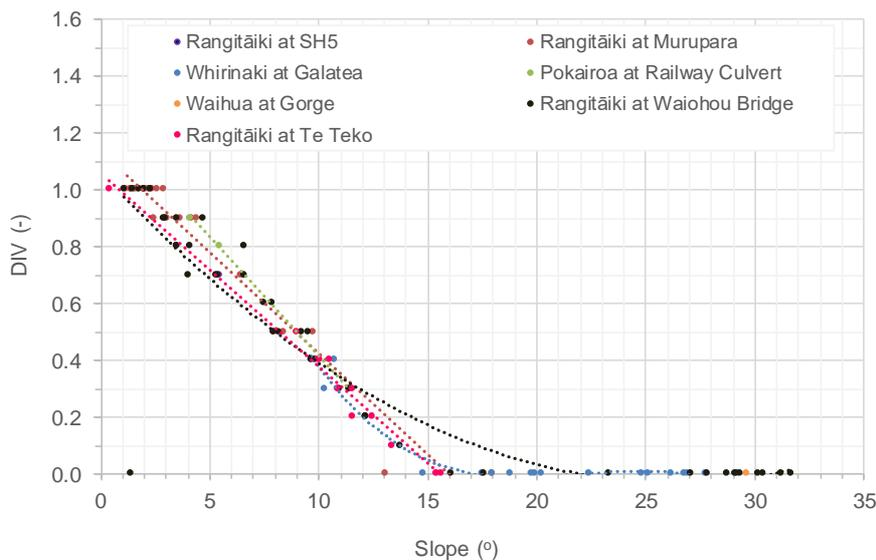


Figure 74. Rangitāiki relationship between surface water ponding (DIV) and catchment slope.

6.3.5 TL and Catchment Area

Catchment area was used to derive the relationships for surface water runoff lag (TL). In larger sub-catchments it is expected TL will be larger than smaller sub-catchments, due to the time taken for surface water runoff to reach the stream and river networks and vice versa.

Individual relationships were derived for each gauged catchment in the Kaituna and Rangitāiki WMAs and are shown in **Figure 75** and **Figure 76** respectively.

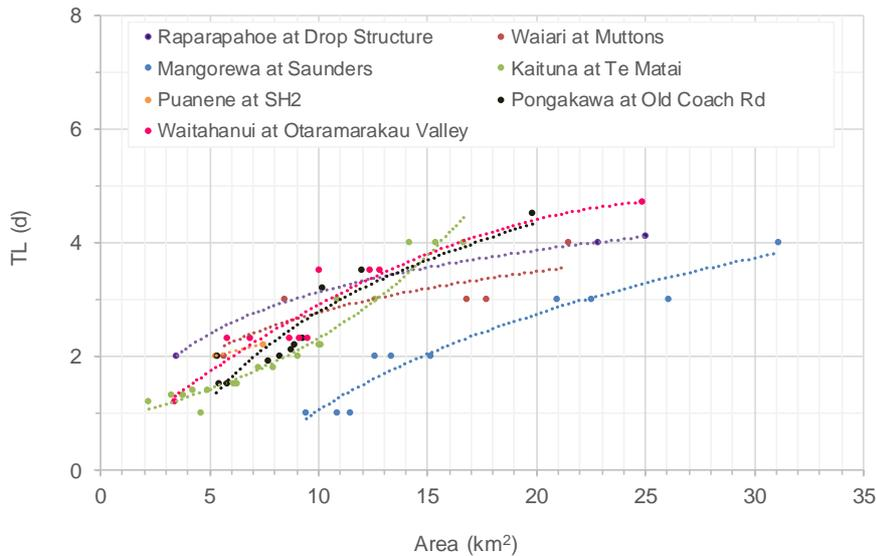


Figure 75. Kaituna relationship between surface routing coefficient (TL) and catchment area.

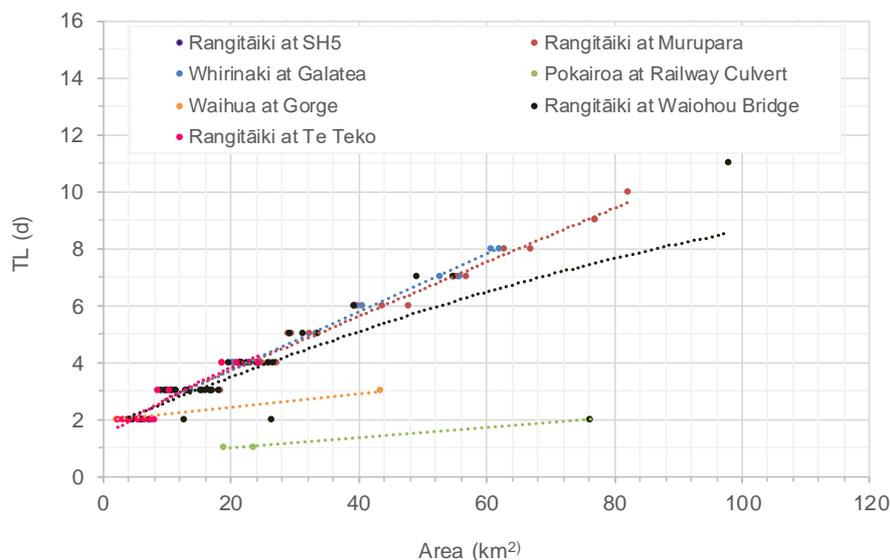


Figure 76. Rangitāiki relationship between surface routing coefficient (TL) and catchment area.

6.3.6 Kv and Vertical Hydraulic Conductivity

The relationships derived between estimated parent rock horizontal hydraulic conductivity (K_h) and vertical hydraulic conductivity (K_v) for each gauged catchment in the Kaituna and Rangitāiki WMAs are shown in **Figure 77** and **Figure 78**, respectively. As described in **Section 3.3**, there are a range of geological materials encountered in the Kaituna and Rangitāiki WMAs. Each geological material type was assigned an estimated vertical hydraulic conductivity based on the materials saturated horizontal conductivity as outlined in **Table 60**.

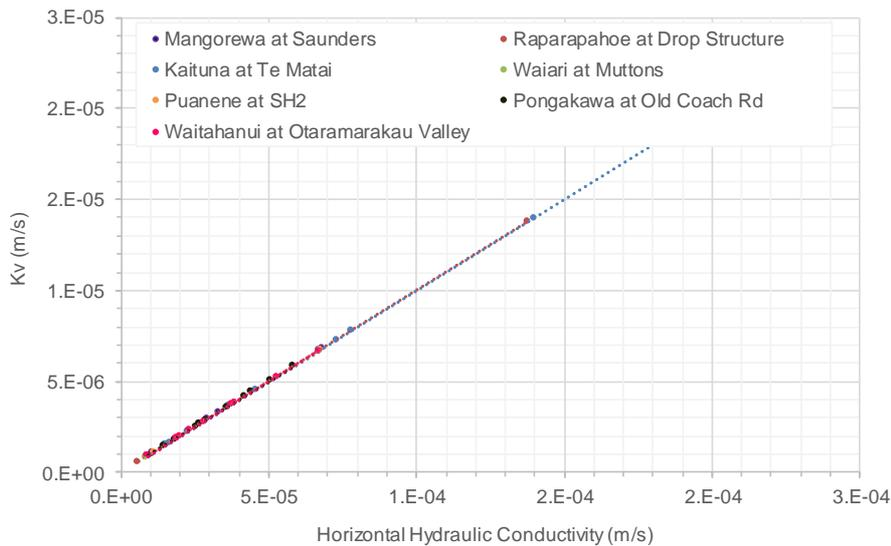


Figure 77. Kaituna relationship between vadose zone travel time (k_v) and hydraulic conductivity.

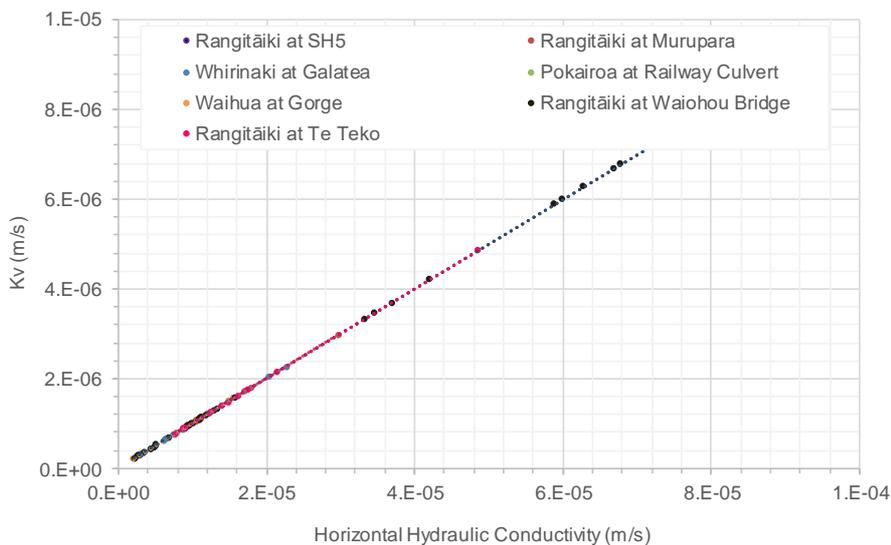


Figure 78. Rangitāiki relationship between vadose zone travel time (k_v) and hydraulic conductivity.

Table 60. Summary of indicative rock saturated horizontal (Kh) and vertical (Kv) hydraulic conductivity estimates.

Geological Material Type	Kh (m/s)	Kv (m/s)
Mudstone	1.00E-07	1.00E-08
Tephra	1.00E-07	1.00E-08
Andesite	1.00E-06	1.00E-07
Ignimbrite	9.00E-06	9.00E-07
Peat	5.00E-06	5.00E-07
Breccia	1.00E-06	1.00E-07
Sandstone	2.00E-06	2.00E-07
Sand	5.00E-05	5.00E-06
Pumice	4.00E-05	4.00E-06
Rhyolite	5.00E-06	5.00E-07
Broken formation	5.00E-05	5.00E-06
Gravel (Kaituna)	2.00E-04	2.00E-05
Gravel (Rangitāiki)	7.50E-05	7.50E-06

6.3.7 Remaining Parameters

The remaining SMWBM parameters were set at constant values across all sub-catchments, with the exception of POW, AI and $V_{z_{por}}$ where minor adjustments were required in a number of sub-catchments to achieve the appropriate calibration. The final range of values applied is shown in **Table 61**.

Table 61. Summary of minor SMWBM parameter values implemented in ungauged catchments.

Parameter	Value	
ZMIN	Minimum infiltration rate (mm/hr)	0
SL	Soil moisture content where drainage ceases (mm)	0
POW	Power of the soil moisture percolation equation (-)	1-2
R	Evaporation and soil moisture relationship	0
AI	Impervious portion of catchment connected to drainage (prop)	0.00 -0.09
GL	Groundwater lag time (days)	1
S_{por}	Soil porosity (prop)	0.45
$V_{z_{por}}$	Rock porosity (prop)	0.05-0.45

6.4 Flow Model Assumptions

A number of assumptions were required during the flow model development where insufficient data were available or where simplifications were required in order to streamline model development. A detailed summary of the key assumptions made during development of the flow model, their significance, and potential work to verify or reduce the significance of the assumptions is provided in **Table 62**.

Table 62. Summary of assumptions related to the flow model development.

ID#	Current Assumption		Significance of Assumption	Potential Further Work to Reduce Significance of Assumption
	Title	Description		
1.	Relationship between catchment physical characteristics and SMWBM parameters	The SOURCE catchments have various relationships and parameters applied to the individual calibration locations as each catchment displays different slopes, geology, land use cover, and soil type. The process averages physical characteristics at a smaller scale over the larger area of the relevant sub-catchments.	Due to averaging, discrete features are not modelled explicitly.	No - for the following reasons: <ul style="list-style-type: none"> • Small landforms are encapsulated in the averaging; • Small area changes will not impact on water results given the overall scale of the model domain; and • Changes would represent a major re-discretisation of the model.
2.	Flow from the Rotorua Lake catchments is not explicitly modelled.	The measured outflow from Lake Rotoiti (Kaituna at Taheke gauge) was assigned as an inflow node.	The effects of changes in catchment characteristics (e.g. land use or stocking density) upstream of the Kaituna at Taheke gauge at the outflow from Lake Rotoiti are not included in the model scenarios.	N/A
3.	Flow loss in the Paraiti (Mangorewa) River at Saunders	Preliminary flow simulation results displayed an over prediction by approximately 15-20%. Due to the catchment characteristics it was assumed that: <ul style="list-style-type: none"> • A portion of the drainage system in this area is reporting to the adjoining Lake Rotorua catchment rather than the Saunders gauge catchment itself (18.75 km²). • A significant baseflow component (2.5 m³/s) is lost from the catchment to a deep aquifer and is not reporting to the gauge. 	In order to achieve calibration, loss nodes were required in individual catchments, with loss amounts assigned relative to the catchments specific discharge. The ground water losses were then re-accounted for in downstream sub-catchments as groundwater gains.	Survey and hydrogeological investigations could be undertaken to confirm these assumptions.
4.	Flow loss in the Puanene River upstream of SH2	Preliminary flow simulation results were consistently over predicting by approximately 20-25%. Hydrological analysis on measured flow confirmed that catchment discharge was significantly under reported at the gauge (as detailed in Section 4.3 and 6.1.8). It was assumed that surface water seepage to groundwater occurs due to the change in slope and geology as the river emerges from the hills onto the coastal plain. This loss to groundwater is assumed to discharge as sub-surface coastal discharge.	In order to achieve calibration, loss nodes were required in individual catchments. It is uncertain if this loss occurs in practice, and where the discharge to groundwater re-emerges prior to the coast or whether is discharges directly to the seafloor.	A review of the groundwater-surface water interaction data as part of the Jacobs groundwater model may assist in answering these questions and confirming the current assumptions.
5.	Flow loss in the headwater catchments of SC#63, SC#65 to SC#70, SC#79, SC#80 and Pongakawa River.	In a similar mechanism to assumptions 3 and 4, it is assumed there is a loss of surface water to groundwater in the headwaters of these catchments. This was identified via recordings in spot gauge GN198111 located in SC#71 and GN178816 located in SC#73. The basis for the	Not significant as internal reconfiguration of water flow. Nevertheless, an important insight into the catchment water balance.	A review of the groundwater-surface water interaction data as part of the Jacobs groundwater model may assist in answering these questions and confirming the current assumptions.

ID#	Current Assumption		Significance of Assumption	Potential Further Work to Reduce Significance of Assumption
	Title	Description		
		assumption is the change in soil type from highly drainable pumice and lapilli, to slightly heavier pumice soils. Similar to the characteristics of Puanene at SH2 the flow is lost to the alluvial aquifer and the spot gauge data within the river downstream of these sites support this assumption. The modelled discharge is assumed to be lost to deeper groundwater which is discharged as a coastal loss.		
6.	Flow within the Waitahanui River at Otamarakau Valley Road	The preliminary calibration of Waitahanui River at Otamarakau Valley Rd resulted in consistent under prediction. Analysis of rainfall and the gauged flow data revealed there was less rain falling in the catchment compared to that which was being measured at the gauge. It was therefore assumed that Lake Rotoehu had sub-surface discharge contributing to the Waitahanui catchment. A groundwater gain node was added to account for this process.	An important insight into the catchment water balance.	Undertake an assessment of groundwater-surface water interactions for this catchment.
7.	Flow within the Rangitāiki River at Murupara	Preliminary simulations of the Rangitāiki at Murupara catchment consistently over predicted discharge (as discussed in Section 4 and 6.2.2). This suggests that the gauge is not measuring all the flow in the catchment, with a proportion of the catchment discharge likely partitioned to groundwater. To represent this groundwater discharge, a head dependent surface water-groundwater loss relationship was developed and adjusted as part of the calibration process.	An important insight into the catchment water balance.	Undertake an assessment of groundwater-surface water interactions for this catchment.
8.	Lake Matahina	Measured outflow (release) data was available for Lake Matahina and applied as a fixed variable in the model. However, due to the absence of measured lake level data and the fact that SOURCE simulates inflow from upstream catchments, the calculated model variable was set to lake level rather than flow.	This assumption is considered appropriate and not likely to affect model results.	
9.	Aniwhenua Dam	As measured outflow data for Aniwhenua was not available, the dam was simulated as a level pool storage.	This assumption is not considered to have a significant effect on project outcomes. The key aspect is accurate simulation of flow downstream and water quality.	N/A
10.	Efficient use of irrigation water	The modelled actual use irrigation data assumes water permit holders irrigate small amounts of irrigation water frequently as follows: <ul style="list-style-type: none"> • Kiwifruit: 10 mm of water is applied whenever the soil moisture falls below 50% of plant available water. 	This assumption is of minor significance as the marginal difference in water volume used if this assumption is incorrect is likely to be minimal.	

ID#	Current Assumption		Significance of Assumption	Potential Further Work to Reduce Significance of Assumption
	Title	Description		
		<ul style="list-style-type: none"> Pasture: 3.5 to 4.5 mm of water are applied whenever the soil moisture falls below 50% of plant available water. 		
11.	Actual use irrigation data has an application efficiency of 80%	It was assumed that irrigators abstract 20% more water than required to maintain soil moisture at appropriate levels due to system losses.	This assumption is of moderate significance as the volume of water extracted for irrigation use will impact the accurate simulation of flow.	None recommended – this is current industry standard.
12.	Consent/water permit holders irrigate only 80% of the consented irrigated area	It was assumed consent/water permit holders irrigate only 80% of consented irrigated area. However, this may vary over time and with changes in land use.	Important to recognise.	N/A
13.	Maximum irrigation rate	A daily cap on water use is applied based on annual consented volume and average number of irrigation days.	This assumption is of low significance as it is based on current consented volumes.	N/A
14.	Non-Municipal Demands: Industrial, Domestic, Commercial	Non-municipal consents were configured based on consented limits. The annual maximum abstraction volume was disaggregated into a daily rate over the full consented period.	This assumption is considered appropriate and not likely to affect model results.	N/A
15.	Municipal Takes	Metered use data were utilised. Where data gaps occurred, the consented annual volume was disaggregated to a daily value.	This assumption is considered appropriate and not likely to affect model results.	N/A
16.	Wastewater Facility Takes and Discharges	The Te Puke WWTP, Fonterra Factory, and the AFFCO Factory consents were configured using the same method as for as the municipal supply consents or using the supplied consent metered data where available.	This assumption is considered appropriate and not likely to affect model results.	N/A

7. Constituent Model Development

Following the development of the flow models (detailed in **Section 6**), the constituent models were configured in SOURCE. Constituents are defined as the materials that are generated, transported and transformed within a catchment and affect water quality. The constituent models simulate the generation, transport and transformation of the constituents. Assessment of the following constituents was requested by BOPRC:

- Total nitrogen (TN);
- Total phosphorus (TP);
- Total suspended solids (TSS); and
- Escherichia coli (*E. coli*).

Due to the differing generation mechanisms, transformations, and transport pathways from catchment to the stream network for each constituent, individual constituent models were developed for each of the four constituents as follows:

- TN generation was simulated using a combination of the Agricultural Production Systems sIMulator (APSIM) model and generated based on catchment characteristics (**Section 7.2**).
- TP was generated based on catchment characteristics and runoff (**Section 7.2**).
- TSS was simulated using the Dynamic SedNET model (**Section 7.4**).
- *E. coli* was generated based on catchment characteristics and runoff (**Section 7.5**).

As mentioned above, constituent model parameters were linked to physical characteristics. Different combinations of physical characteristics (e.g. vegetation cover, slope, erodibility etc.) were used depending on the model parameter of interest. Each physical characteristic was assigned a weighting based on the expected influence it was considered to have on a given model parameter. For example, stocking rate was considered to have a higher weighting on *E. coli* generation concentrations than average catchment slope. The physical characteristic and weightings assigned were used to develop constituent generation indices. The physical characteristics and weighting assigned were adjusted as part of the calibration process. These generation indices are further described in each of the constituent sections below.

The technique described above of assigning model parameters based on catchment physical characteristics follows a similar approach to that used by GNS in Westerhoff, Tschirmer, & White (2017).

Development and calibration of the constituent models followed a similar process to the development of the flow models whereby an iterative approach was employed of systematically adjusting individual model parameters and comparing calibration simulation results against available measured data. A schematic overview of the constituent model development process is shown in **Figure 79**, noting that the decay function is not applied to every constituent.

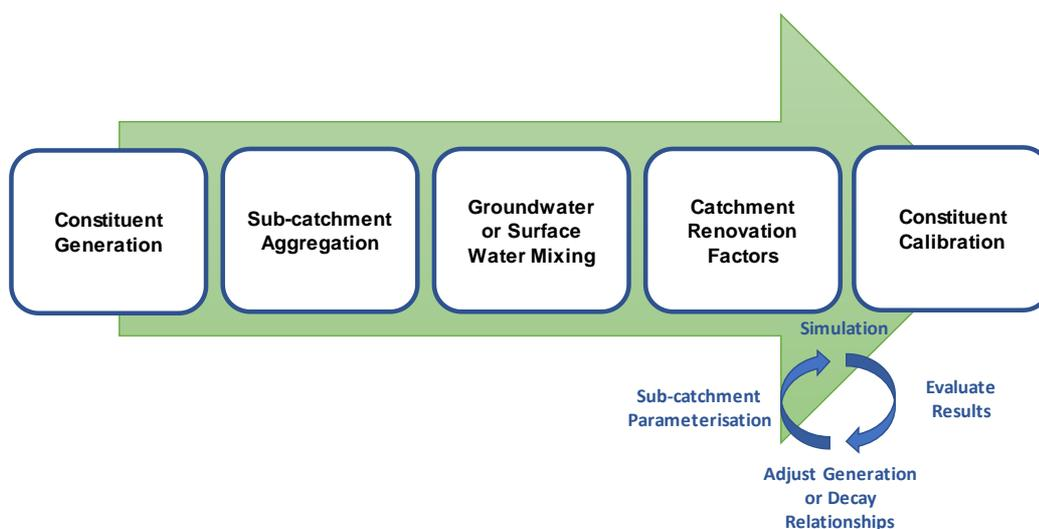


Figure 79. Constituent model development process.

During the constituent calibration process, simulated constituent concentrations were compared against measured constituent data provided by BOPRC. The constituent monitoring sites utilised for calibration are detailed in **Appendix B**. Model performance was assessed using the performance measures outlined in **Section 5.4** and through boxplot comparison figures.

The constituent calibration focussed primarily on the period January 2011 to June 2016, with an aim of ensuring the models were representative of present-day conditions for which land use has been ground-truthed. If dynamic land use layers are developed, then calibration could focus on longer periods. It should be noted, the constituent models are calibrated in terms of the concentration and load produced in the catchment upstream of the monitoring locations, but not for the individual sections of land use within the catchment. Therefore, there may be some slight over and under predictions from different land uses, which when averaged over all land uses within a catchment produce the calibrated concentration and load.

The performance of each constituent model was classified based on the model performance criteria outlined in **Table 25**. *E. coli* were classified following the criteria for sediment on the basis that *E. coli* follow a similar transportation pathway as sediments.

An overview of the configuration of the constituent models in SOURCE is provided below in **Section 7.1**. The development of the individual constituent models is detailed in **Sections 7.2 to 7.5**, and the assumptions associated with the development of each of the constituent models is then provided in **Section 7.6**.

7.1 SOURCE Constituent Configuration

SOURCE includes a variety of options to generate and transport constituents through the model. Constituent generation models simulate the concentrations of constituents produced, and when combined with flows simulated by the SMWBM (flow model) simulate the resulting load delivered to the sub-catchment drainage network.

Constituents can be generated at a node, a link, or at the catchment model level as follows:

- **Node generation** - Generating a constituent at a node allows the user to define a concentration or load using a fixed value, a daily time series of values, or an equation (referred to as a 'function' in SOURCE). The configuration of this process varies slightly depending on the type of node.

- **Model generation** - The generation of constituents at the catchment model level, allows the user to define a generation model and a filter model per each functional unit in each sub-catchment.

For the Kaituna WMA constituents were generated at the catchment model level, at inflow nodes and at storage nodes. In the Rangitāiki WMA, constituents were generated at the catchment model level and at storage nodes.

Table 63 outlines the constituent generation models applied at the catchment level, and **Table 64** outlines the constituent generation method used at the inflow and storage nodes.

Table 63. The different catchment level constituent generation models in SOURCE included in the Kaituna and Rangitāiki SOURCE models.

Generation Model ¹⁵	Description	Utilised in this project
EMC / DWC	The event mean concentration (EMC) / dry weather concentration (DWC) model applies two fixed values to an area. During events (high flow) the EMC value will be applied and during dry weather (non-event times) the DWC concentration or load is applied.	For the generation of <i>E. coli</i> (section 7.5)
Observed concentration	This model allows the user to define a known concentration or load to the quick flow and slow flow components of a functional unit. The known concentration can be applied as a fixed value, time series or using an equation.	TN, TP, TSS, <i>E. coli</i> .

Where measured constituent concentration and flow data were available (Lake Rotoiti and Lake Rotoehu), a combination of fixed value and dynamic time series were used to represent constituent contributions from the upstream catchments as further detailed in **Table 64**.

Table 64. The different constituent generation models applied to inflow and storage nodes in the Kaituna and Rangitāiki SOURCE models.

Node	Constituent	Constituent generation method applied	Rationale
Inflow – Lake Rotoiti	TN	<u>Observed concentration</u> : time series (seasonal averages and timeframes based on measured data)	Lake Rotoiti enters the Kaituna WMA as surface flow. Long term constituent monitoring data are available at this gauge, allowing for an accurate representation of the constituent's inflow and seasonal cycle to the catchment.
	TSS	<u>Observed concentration</u> : time series (seasonal averages based on measured data)	
	TP	<u>Observed concentration</u> : Fluctuating dynamic time series (seasonal averages and timeframes based on measured data)	
	<i>E. Coli</i>	<u>Observed concentration</u> : time series (seasonal averages based on measured data)	
Storage – Lake Rotoehu	TN	<u>Observed concentration</u> : Fixed value (the average of measured TN data from LAWA)	Lake Rotoehu enters the Kaituna WMA as groundwater.

¹⁵ Plugins can also be added to increase the suite of available generation models, for example the dynamic SedNET plugin used to simulate total suspended solid – further described in **Section 7.2**.

Node	Constituent	Constituent generation method applied	Rationale
	TSS	<u>Observed concentration:</u> Fixed value (the average of the measured TSS data from Lake Rotoiti)	There are long term constituent monitoring data within the lake based on LAWA data. This was applied as a constant inflow to the Kaituna WMA given the relatively stable concentrations in the lake.
	TP	<u>Observed concentration:</u> Fixed value ((the average of measured TN data from LAWA)	
	<i>E. Coli</i>	<u>Nil Constituents:</u> There were no measured data for this location and calibrations were easily achieved downstream without an <i>E. coli</i> concentration attached to the lake.	
Inflows in the following sub-catchments; <ul style="list-style-type: none"> • Kaituna SC#96 • Kaituna SC#23 • Rangitāiki SC#31 	TN	<p><u>Observed concentration:</u> Fixed value, based on common groundwater nitrogen concentrations from models in nearby areas (i.e. the Wairakei models).</p> <p>No other constituents were generated at these inflows as they reflect groundwater returning to the river and it is assumed TSS, TP and <i>E. coli</i> do not return to the surface water as they are denitrified or caught in the deeper groundwater aquifers.</p>	The spring inflows contain constituents that are represented as constant inflows. This is due to the extensive residence time in the deeper aquifer and therefore these spring flows show less variability in constituent concentration compared to flows affected by surficial influences.
Storage – Lake Aniwanuiwa and Storage – Lake Matahina	TSS	<u>Observed Concentration:</u> Time series (of the sediment concentration that enters the lake).	The dams located within the Rangitāiki catchment were configured so that the outflow would have an accurate calibration to the measured data.
	<i>E. Coli</i>	<u>Storage Decay Model:</u> Configured as a fixed decay rate to represent the natural die-off of <i>E. coli</i> organisms.	
	TP	<u>Initial Concentration:</u> A starting fixed value which determined the constituent mass in the link at the start of the model simulation.	
	TN	<u>Initial Concentration:</u> A starting fixed value which determined the constituent mass in the link at the start of the model simulation.	

7.2 Total Nitrogen

Total Nitrogen (TN) is the sum of all organic and inorganic forms of nitrogen that are found in a water sample (i.e., nitrate-nitrogen (NO₃-N), nitrite-nitrogen (NO₂-N), ammoniacal-nitrogen (NH₄-N) and organic nitrogen such as amino acids or plant tissue). TN typically makes its way into waterways through groundwater seepage from diffuse sources such as agricultural land use or from discrete sources such as septic tank discharges to ground, and direct inputs to waters from sewerage treatment plants and factories. Intermittent increases in TN may also occur following rainfall events where N in a variety of forms (e.g. urine patches, fertiliser and faecal material) can accumulate in the soil profile during prolonged dry periods and are transported in overland flow in response to rainfall events.

The baseflow (slow flow) component of TN included in this study included the sub-soil drainage and leaching, and subsequent groundwater transport including vertical percolation to groundwater and horizontal saturated groundwater flow, as illustrated in **Figure 80**. The sub-soil leaching component was simulated using the Agricultural Production Systems Simulator (APSIM) model, while groundwater flow component, which relates to the timing of and reduction in TN, was simulated using the SMWBM within SOURCE.

APSIM simulated TN leaching on a land use basis using the rainfall, soil depth and the groundwater processes to simulate the full TN baseflow pathway. An overview of the APSIM model and generation of the baseflow component of TN are provided in **Sections 7.2.1 to 7.2.5**.

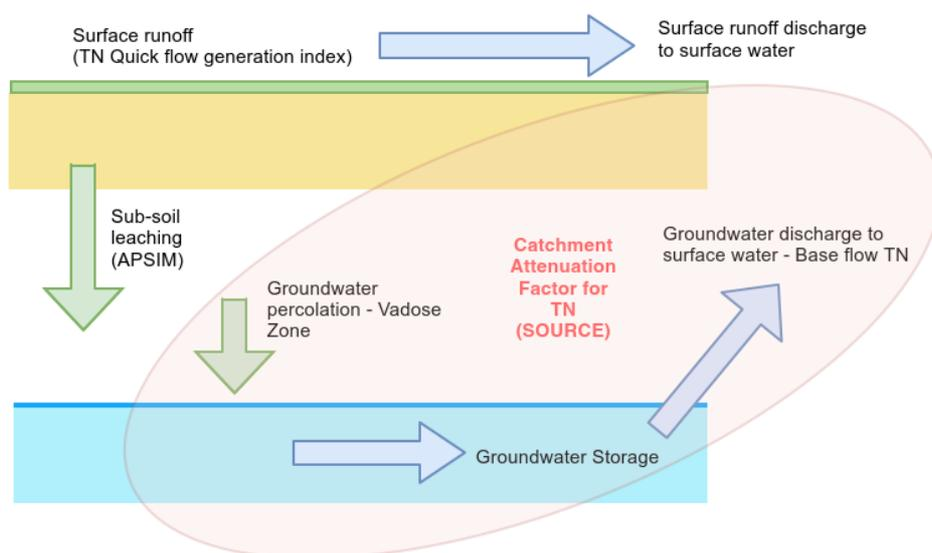


Figure 80. Summary of the process for TN reaching waterways considered in the SOURCE Modelling project.

It should be noted, APSIM does not address variations in farm management between sub-catchments, provides an indication of N losses based on land use rather than management practices (such as stock management practices).

The generation of the surface runoff component of TN was simulated through the development of a TN generation index which characterised each sub-catchment based on slope, stocking rate and vegetation cover. Generation of the overland flow component of TN is outlined in **Section 7.2.6**.

7.2.1 APSIM Overview

APSIM is an internationally recognised tool developed by the Agricultural Production System Research Unit in Australia for the simulation of a range of plant, animal, soil, climate and land management interactions. The APSIM modelling framework consists of the following components:

- A set of biophysical modules that simulate biological and physical processes in farming systems;
- A set of management modules that allow the user to specify the intended management rules that characterise the scenario being simulated; and
- A simulation engine that drives the simulation process and facilitates communication between the independent modules.

APSIM was utilised in this project to simulate nitrogen leaching from a range of different land uses. APSIM is a process-based model that is able to operate on a fine spatial scale and simulate processes on a daily timestep. Whereas, the commonly used alternative, OVERSEER, simulates relatively large areas, with drainage and leaching calculations only occurring on a monthly timestep (Eco Logical, 2017).

APSIM models were initially developed by Ecological Australia as part of the larger project catchment water quantity and quality modelling for the Kaituna and Rangitāiki River systems and is detailed in the report “*APSIM Modelling of Farm System Nutrient Dynamics*” by Eco Logical (2017). This report also provides a more in-depth contrast and comparison of APSIM and OVERSEER and their relative merits to this project in addition to those described above.

WWLA was commissioned to undertake a review of the drainage volumes simulated in the APSIM model developed for the Kaituna and Rangitāiki river systems to ensure the drainage volumes simulated by APSIM and the SMWBM (used to simulate flows within SOURCE) produced similar temporal rates and annual volumes of drainage.

The following sections outline the review, drainage volume comparisons, improvements made to the Eco Logical developed APSIM model (referred to as the Original APSIM model), and implications of these on model simulations.

Full details on the development and benchmarking of APSIM models is provided in the WWLA (2020b) *Kaituna and Rangitāiki APSIM Models* report.

7.2.2 Original APSIM models

Individual APSIM models were developed for each combination of the five different soil types and ten land use types outlined in **Table 65**, and 38 climate stations for the region.

Table 65. APSIM model types.

Soil type	Land use type
Taupo Matahina	Dairy (background)
Oropi	Dairy (urine low)
Paengaroa	Dairy (urine high)
Kaingaroa	Sheep & beef (background)
Urewera	Sheep & beef (urine)
	Kiwifruit
	Forest
	Maize
	Vegetables
	Lifestyle

7.2.3 Drainage comparison between APSIM and SMWBM_Vz

The hydrological model SWIM (Soil Water Infiltration and Movement) was incorporated in the APSIM models to simulate the movement of water and solute (nutrients) within the soil zone. Although the hydrological model within APSIM simulates a number of the same processes as the SMWBM_Vz (e.g. infiltration), they are simulated using different methods and techniques. Therefore, it was important to confirm the sub-soil drainage predicted by the two models were similar before applying the load of TN leached from the soil as predicted by APSIM to the baseflow (slow flow) component of the flow regime as predicted by the SMWBM_Vz in SOURCE.

Simulation in the SMWBM_Vz occurs at a catchment scale, while APSIM simulations occur on a paddock scale. To allow for an initial comparison, specific APSIM models were selected that were representative of the bulk of a land use and compared to its equivalent SMWBM_Vz catchment.

The dairy, sheep & beef (background and urine) and forest models were selected from the APSIM models and compared against the SMWBM sub-catchments as listed in **Table 66**.

Table 66. APSIM and SMWBM models selected.

WMAs	APSIM				SMWBM
	Land use	Soil	Met station	Land use percentage	Catchment No.
Kaituna	Dairy	Oropi	28396	49%	8
		Paengaroa	30005	76%	100
		Taupo-Matahina	27389	77%	116
	Forest	Oropi	30464	62%	1
		Paengaroa	27389	77%	105
		Taupo Matahina	31076	56%	107
	Sheep & Beef	Oropi	27882	59%	40
		Paengaroa	28415	53%	65
		Taupo Matahina	27389	37%	118
Rangitāiki	Dairy	Kaingaroa	28955	40%	5
		Taupo Matahina	29006	75%	109
		Urewera	28461	25%	44
	Forest	Kaingaroa	30510	89%	13
		Taupo Matahina	28435	75%	73
		Urewera	27410	94%	17
	Sheep & Beef	Kaingaroa	28954	42%	1
		Taupo Matahina	29006	29%	114
		Urewera	28461	8%	42

The results of the Taupo-Matahina dairy soil comparison are presented below, noting that the results for every other soil group and met-station provide similar relative responses. **Figure 81** presents a comparison of the daily drainage rates between the three APSIM models and the SMWBM for the same soil type, rainfall and area.

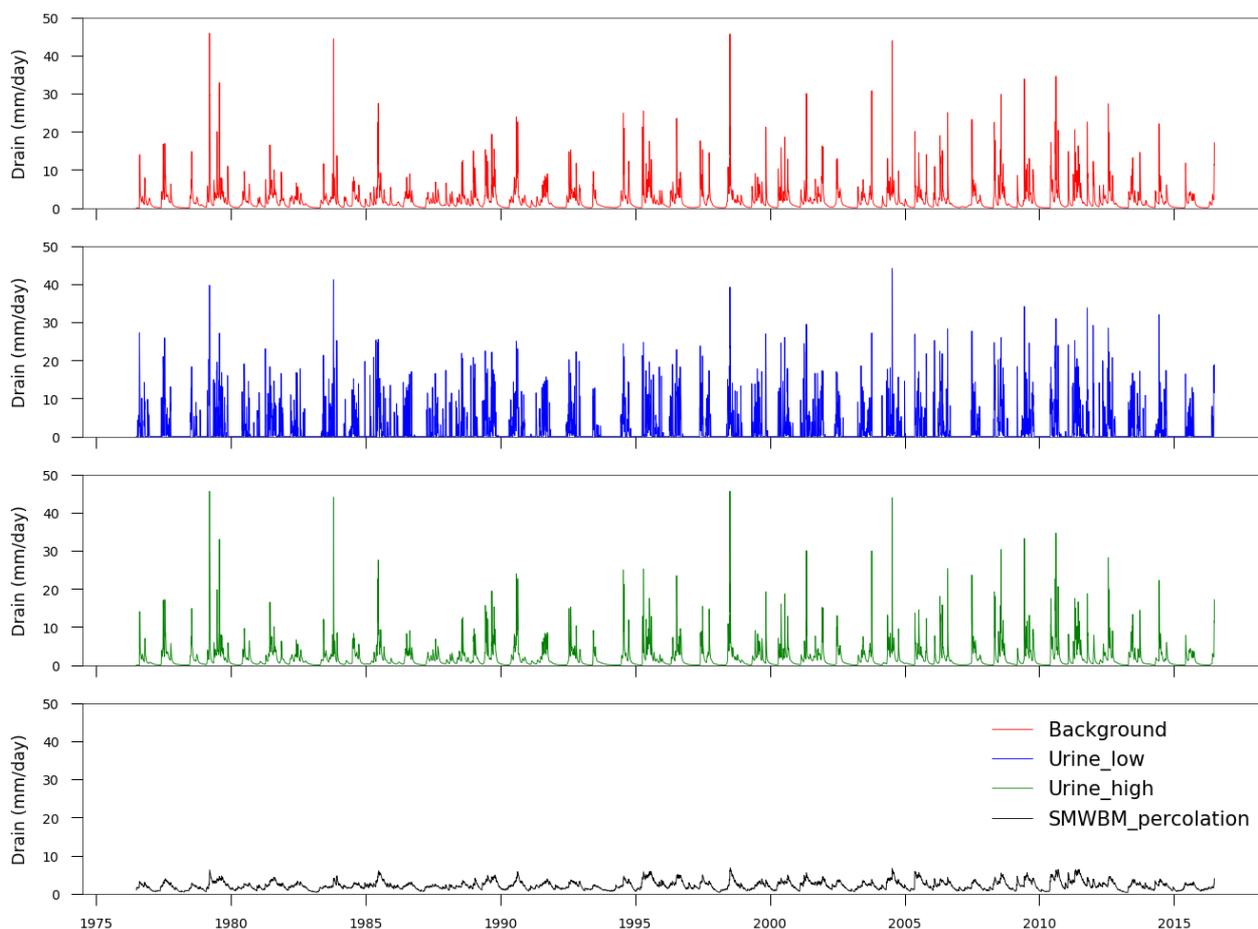


Figure 81. Drainage comparison for Kaituna Taupo Matahina dairy.

In general, the simulated drainage rates from APSIM have significantly higher temporal variability with extremely high drainage volumes occurring during rainfall events and then rapid recession to zero during dry periods. In comparison, drainage from the SMWBM is more attenuated, being maintained throughout the whole simulation period, albeit with fluctuations at lower peak daily rates than for the APSIM model.

The summary statistics provided in **Table 67** present a comparison of statistics between APSIM and the SMWBM model. In particular, the minimum values demonstrate the soil profile cessation of drainage in APSIM and the much larger standard deviation values for the APSIM models highlights the extreme fluctuation in drainage. The maximum values predicted by APSIM are also much higher than realistically occur based on our experience.

Table 67. Comparative summary drainage (mm/day) statistics for the Kaituna, Taupo Matahina dairy APSIM and SMWBMs.

Model	Min	Max	Mean	Std. Dev.
APSIM background	0	45.84	2.14	3.04
APSIM urine low	0	44.06	2.10	4.49
APSIM urine high	0	45.65	1.95	2.99
SMWBM	0.3	6.75	2.19	1.12

Note: Mean annual rainfall was 1,416 mm

7.2.4 Model Improvements

The SMWBM models were calibrated against flow gauge observations, and therefore, the APSIM model parameters were adjusted so that the model produced similar drainage rates to the SMWBM to provide consistency between the two models (the flow model - SOURCE, and the TN model – APSIM). This also ensured TN leaching followed the same SMWBM pathways through the groundwater sector. The relevant soil hydraulic information derived from the calibrated SMWBM models (e.g. infiltration rate, and sub-soil drainage rate) were used to guide the re-parameterisation of the selected APSIM models.

The APSIM models were initially improved through re-classification and parameterisation of the soil characteristics. Soil in the coastal Bay of Plenty region is primarily derived from the pumaceous rhyolitic tephra, which are of moderate to high permeability and hence have high infiltration and sub-soil drainage characteristics in general. SMap suggests that the soil depths across the region vary between approximately 400mm – 1400 mm. Therefore, given that the hydraulic characteristics are relatively uniform and high (the average soil permeability in the Kaituna WMA is 5.2 mm/day, while within the Rangitāiki WMA it is 6.5 mm/day), the key variation in soil characteristics is soil depth, and therefore, the APSIM soil models were re-classified based on soil depth distribution in the region.

Five soil depth categories were identified based on the catchment soil depth values used in the SMWBM model, shown in **Table 68**. Percolation results from the selected SMWBM models were used to re-parameterise the dairy land use APSIM models. These updated soil parameters were then applied to the other land use models (e.g. forest) of the same soil type.

Table 68. Soil depth categories.

Soil depth APSIM model (mm)	Soil Type	No. of Kaituna catchments	No. of Rangitāiki catchments
0 - 500	Urewera Soil: A well - drained sandy loam soil	9	16
500 - 700	Kaingaroa Soil: A well - drained sandy loam soil	6	15
700 -1000	Paengaroa Soil: A well - drained sandy loam soil	19	18
1000 - 1200	Oropi Soil: A well - drained sandy loam over loam soil	38	21
1200 - 1400	Taupo/ Matahina Soil: A well - drained sandy loam soil	47	47
Total	n/a	119	117

The five soil depths were then matched with corresponding soil types from the FSL. These soil types did not cover the whole catchment (**Figure 82**) so the soil types were extrapolated using soil depth as a guide so that each sub-catchment was assigned one soil type and therefore one soil depth as shown in **Figure 83**. The implication of this is that each sub-catchment is represented by a single soil type in the APSIM models.

Figure 82. Distribution of the Soil Types from the Fundamental Soils Layer for APSIM. (Refer A3 attachment at rear).

Figure 83. Extrapolated Soil Types for each sub – catchment for APSIM. (Refer A3 attachment at rear).

In addition, the APSIM models were updated to use the NIWA VCSN rainfall data, rather than the met station data used in the original APSIM models. This ensured consistency in input data between the two models.

A comparison of the re-parametrised APSIM drainage rates and SMWBM percolation rates for a representative site for each of the soil depth models is presented **Table 69**. The re-parameterised APSIM model was shown to predict drainage rates much closer to those from the SMWBM than the original APSIM model.

Table 69. Comparison statistics between the current APSIM drainage and SMWBM percolation.

Soil depth APSIM model	Water budget component	APSIM drainage		SMWBM percolation	
		(mm/day)	(%MAP)	(mm/day)	(%MAP*)
0-500	Rain	3.85		3.85	
	Runoff	0.35	9.1	0.34	8.8
	Drainage	1.66	43.1	1.64	42.6
	Loss	1.84	47.8	1.84	47.8
500-700	Rain	3.70		3.70	
	Runoff	0.53	14.3	0.57	15.5
	Drainage	1.36	36.8	1.34	36.3
	Loss	1.80	48.6	1.81	49.0
700-1000	Rain	3.91		3.91	
	Runoff	0.12	3.0	0.09	2.3
	Drainage	2.41	61.5	2.42	61.9
	Loss	1.37	34.9	1.39	35.5
1000-1200	Rain	6.41		6.41	
	Runoff	0.46	7.2	0.46	7.1
	Drainage	4.17	65.1	4.16	64.8
	Loss	1.75	27.3	1.79	28
1200-1400	Rain	4.57		4.57	
	Runoff	0.24	5.2	0.22	4.9
	Drainage	2.70	59.1	2.70	59.0
	Loss	1.60	35.0	1.63	35.7

*Mean annual precipitation

7.2.5 TN simulation

APSIM produces a daily times-series of TN mass per hectare (kg/ha/day) for each combination of soil depth, climate and land use (575 combinations in Kaituna and 341 in Rangitāiki). To apply these values to SOURCE an aggregation process was used to combine the predicted TN loads for each land use in each sub-catchment, i.e. accounting for all land uses across the soil types and climate regime in each sub-catchment.

The TN load for each sub-catchment was calculated as an area weighted average of the multiple land use types within a sub-catchment, producing a daily mass representative of the entire sub-catchment.

Three APSIM sub-models were used to represent the dairy land use – dairy background, urine low, and urine high. These were combined to produce a single representation of the dairy land use, using the following weighting: 75% background, 5% low urine and 20% high urine. The weightings applied to combine the three dairy sub-models to produce an overall representation of dairy land use was agreed with the BOPRC and reflects that dairy land use does not typically consist of entirely dairy, but may also include some sheep and beef (dairy background).

After the individual land uses were aggregated to provide an area weighted average TN value for the sub-catchment, the daily mass was converted into a daily concentration using the vadose zone process described below.

7.2.5.1 Vadose Zone Process

APSIM simulates the leaching of TN to the bottom of the soil zone or sub-soil drainage, which then travels through the vadose zone before reaching groundwater. As the TN mass travels through the vadose zone the mass is attenuated (the signal is smoothed, and total mass is conserved) before reaching the groundwater store, as shown in **Figure 84**.

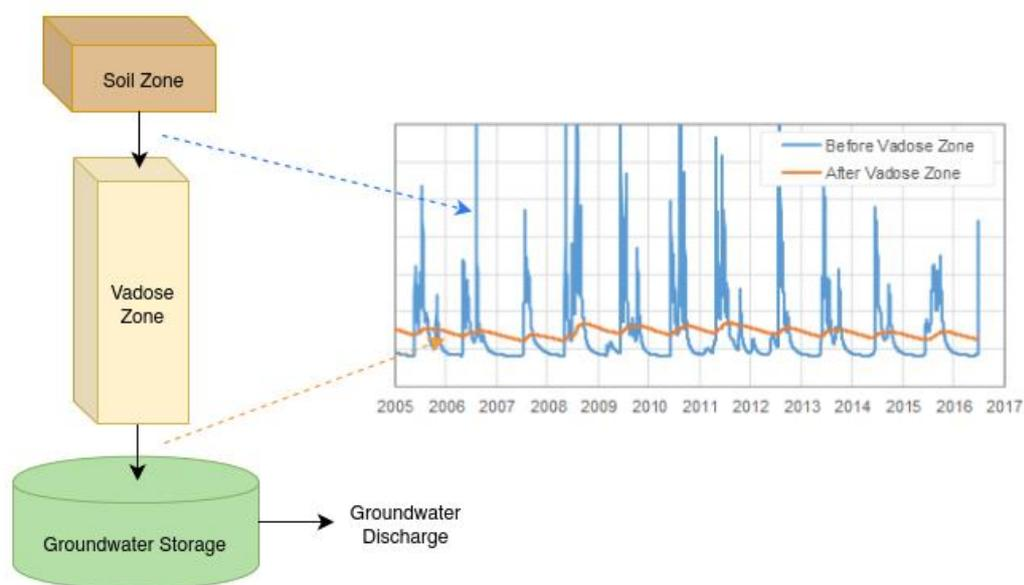


Figure 84. Transformation of TN mass in the vadose zone.

The Muskingum routing procedure was used for the vadose zone process (Williamson, 2017) to simulate the change in response (attenuation) of the sub-soil drainage hydrograph as water moves through vadose zone (reservoir), as given by **Equation 4**. This process is important as it affects the temporal pattern of TN delivery to the groundwater, as shown in **Figure 84**.

Equation 4. Muskingum routing equation.

$$O_2 = C_1 * (I_1 - O_1) + C_2 * (I_2 - I_1) + O_1$$

Where:

$$C_1 = 1/(T + 0.5)$$

$$C_2 = 0.5 * C_1$$

O₁ is the output (previous day)

O₂ is the output (current day)

I₁ = input (previous day)

I₂ = input (current day)

T = cumulative average vertical travel time

The analysis was undertaken as a pre-processing step (prior to SOURCE) using an R code, that utilised APSIM output as the input (I₂), and the cumulative average vertical travel time (T) calculated in the Vadose Zone

Module of the SMWBM for each sub-catchment in SOURCE. The output from the vadose zone processing for TN was an attenuated time series of leaching load (mg/m²/day) per sub-catchment.

7.2.5.2 Groundwater Mixing

The daily variable TN mass load is converted to a discharge concentration via a process that uses the simulated groundwater store (GWS¹⁶) for mixing and tracking of groundwater concentration, and the simulated groundwater discharge to surface from the SMWBM. This process ensures that the delivery of TN load to the surface waters is consistent with the simulated groundwater discharges in the SOURCE model.

The R code described in **Section 7.2.5.1** performs mass balance calculations from concentration in the GWS, using the calculated mass attached to the water storage and discharge volumes simulated in the SMWBM, in accordance with **Equation 5**.

Equation 5. Ground water storage mass balance equation	$\text{GWS mass (current day)} = \text{GWS mass (previous day)} + \text{mass input load (current day)} - \text{mass output load (previous day)}$
---	--

Concentration in the GWS is calculated from the mass of constituent and volume of water residing in the store, as shown in **Equation 6**. The initial mass in the GWS is assigned at the start of the simulation through an optimisation process, whereby the calculated concentration on day one is equal to the average of the calculated concentrations over the entire simulation period.

Equation 6. Groundwater Store concentration.

$$\text{GWS concentration } \left(\frac{\text{mg}}{\text{L}}\right) = \frac{\text{GWS mass (mg/m}^2\text{)}}{\text{GWS volume (L/m}^2\text{)}}$$

7.2.5.3 Catchment Attenuation Factor

Mass losses of TN in a catchment are known to occur in the groundwater system and riparian margin due to a combination of factors such as biogeochemical transformations (e.g. denitrification, volatilisation etc.). Mass loss also occurs via instream processes including various biological growth-related uptakes e.g. bacteria, riparian plants and submerged macrophytes. The uptake of nitrogen by biological processes is a physical process however the biogeochemical and biological process are not explicitly accounted for in the modelling process utilised for this study. Therefore, to represent these processes a scaling factor (referred to as the “Catchment Attenuation Factor” (CAF)), was developed to capture the cumulative effect of biogeochemical processes on instream TN concentrations.

In earlier version of this report, and in initial discussions with BOPRC we referred to the representation of biogeochemical transformations of TN as a catchment reduction or catchment renovation factor. These terms represent the same processes as the CAF. However, we now refer to this as the CAF, for consistency across regional councils based on the recently published Parliamentary Commissioner for the Environment (2018) report.

While the method of applying a spatially varying CAF does represent a simplification of the full biogeochemical transformations which occur in nature, it is a technique which has been widely used in similar water quality modelling assessments throughout New Zealand (e.g. PCE, 2018, NIWA, 2016, WWLA, 2017 & 2018). An

¹⁶ GWS is an arbitrary volume or depth (in mm) that increases or decreases in a relative sense depending on whether groundwater recharge (PERC) exceeds groundwater discharge to surface water (GWQT) and vice versa.

alternative, and more sophisticated approach, that could be investigated in the future, once the Kaituna and Rangitāiki WMA groundwater models are complete, is the use of a groundwater flow and transport model, that can simulate first order decay (attenuation) within different geological layers of a groundwater model.

Initial model simulations without a CAF showed TN was over simulated at the majority of available instream TN monitoring locations.

The following steps were developed into a python code to quantify an appropriate CAF for each sub-catchment. Application of the code was intended to adjust modelled TN mass to reflect natural attenuation of TN for each sub-catchment. The following points detail the procedure used to reach an appropriate calibration for each monitoring site:

1. Using evaporation (L/m²/day) as an indicator of ambient climatic conditions, the modelled TN mass (exported from SOURCE) at the monitoring site was evaluated based on the daily evaporation for the day.
2. These values were directly compared to the measured TN concentrations recorded (at the site).
3. Using only days where there was a measured TN concentration recorded, TN constituent mass was calculated for measured and modelled data.
4. The total measured mass and total modelled mass were compared, and the difference calculated. The difference is then converted to a percentage, equating to the percentage reduction (mass reduction) required overall for modelled TN to match measured TN.
5. The resulting reduction factors were then correlated to the daily evaporation to generate a potential reduction factor correlation equation. **Figure 85** shows an example of the correlation equation developed.
6. The correlation was then used to calculate the average attenuation factor, and adjust the APSIM calculated TN concentration for each sub-catchment to reflect estimated mass loss in relation to climatic conditions.

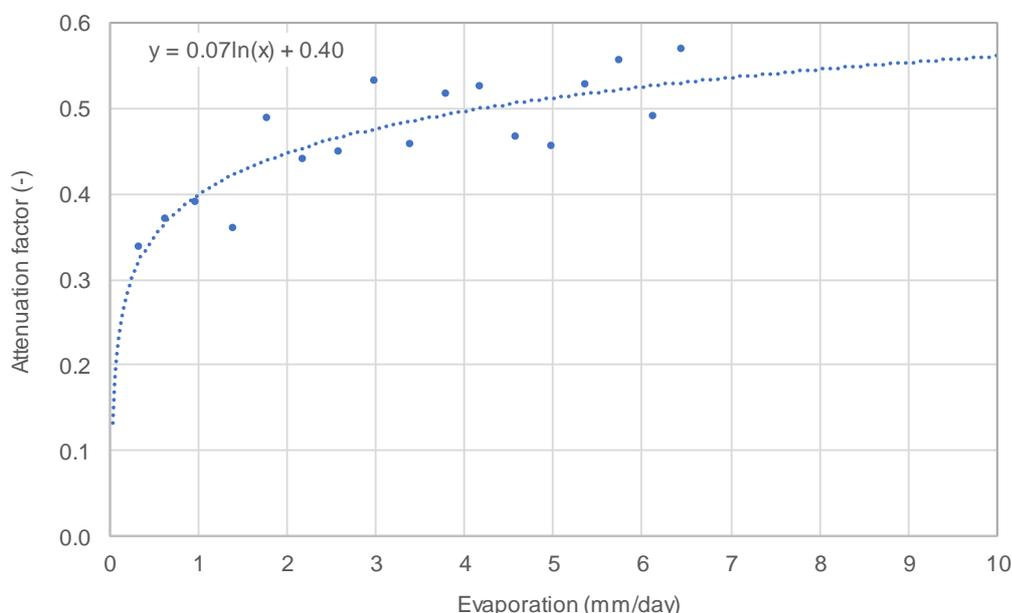


Figure 85. Example Catchment Attenuation Factor (CAF) evaporation correlation relationship.

The revised time series of TN per sub-catchment were then imported and re-run through the SOURCE model and compared to the measured data. Reiterations and adjustments of the CAF were made until the highest level of calibration possible was achieved.

7.2.6 TN Quick Flow Concentrations

Quick flow via overland flow also provides a pathway for the transport of TN to surface waterways. TN quick flow operates on parcels of land which have poorly drained or sloping soils or in response to significant rainfall events. Quick flow is an intermittent process (as opposed to baseflow which is continuous) which can cause temporarily large increases in TN loads when the pathway operates. For example, N in a variety of forms can accumulate in the soil profile during summer (e.g. urine patches, fertiliser, faecal material), particularly in pasture, which is then transported to surface water in response to autumn rains.

To quantify the TN generated through the quick flow pathway a TN generation index was developed. The index was based on the premise that during significant rainfall events there would be a supply of TN from the wash-off of surface deposits of TN (e.g. dung and urine patches and un-degraded fertiliser pellets) to the stream network.

The TN generation index was based on the following factors which were considered the key controls affecting the supply of TN directly to surface waters via quick flow:

- **Slope** – It is assumed that runoff generated in catchments with steeper slopes will transport TN more readily due to the erosivity across the surface compared to flat land. Catchments with steeper slopes were parameterised to have more QF generation, however the premise the slopes will deliver more TN to waterways is still warranted due to the assumption that these slopes will be more unstable compared to flat lands).
- **Vegetation cover** – It is assumed that catchment vegetation cover will influence the load of TN transported to the river and stream network. Increased vegetation density will likely produce a buffer, and act to limit the quick flow transport of TN to the river and stream network.
- **Stocking Rate** – Represent the diffuse source of TN from fertiliser application and dung and urine patches. It is assumed higher stocking rates correlate to higher fertiliser application and therefore, more TN available to be mobilised (Drewry, *et al.*, 2006 & MfE, 2017). Higher stocking rates were applied to catchments in lowlands compared to the eastern and western parts of the Kaituna WMA and highlands in the Rangitāiki WMA, as shown in **Figure 86** and **Figure 87**.

Each land-use within a sub-catchment was classified based on average slope and the values presented in **Table 70** and **Table 71** for vegetation cover and stocking rates respectively. An area weighted average was calculated for each sub-catchment.

Table 70. Classification values for vegetation cover (dimensionless)

Vegetation Type	Vegetation Cover Value	Note
Forest	0.005	
Dairy	0.01	
Urban, Road, Rail & Unknown	1	<i>Relatively Impermeable</i>
Scrub	0.005	
Wetlands	0.01	

Table 71. Classification values for stocking rates (stock units).

Stock Type	Location	Stocking Rate (SU/ha) ¹⁷
Dairy	Lowland	20.8
Dairy	Highland	16.25
Sheep and Beef	All	10
Lifestyle Blocks	All	0.2
All others	All	0

Figure 86. Kaituna lowland, western and eastern area. (Refer A3 attachment at rear).

Figure 87. Rangitāiki lowland, highland and middle area. (Refer A3 attachment at rear).

The largest influence on TN generation in quick flow is likely to be the land use within the sub-catchment. It was assumed that dairy, and sheep and beef land uses will generate more TN compared to other land uses due to the addition of fertiliser applied to increase the productivity of the pasture. Therefore, stocking rate was assigned a higher weighting than slope and vegetation cover.

The TN generation index was then calculated as the weighted sum of the three catchment properties for each sub-catchment. A weighting factor of four, one and eight were assigned to the area weighted catchment average slope, vegetation cover and stocking rate respectively.

A relationship was developed between the attenuated surface runoff for the catchment and the TN index so the proportion of TN quick flow was scaled to the amount of surface flow in the catchment. This relationship is displayed in **Figure 88** and **Figure 89**, for the Kaituna and Rangitāiki WMAs respectively.

¹⁷ One dairy cow was assumed equivalent to 6.5 stock units. A stocking rate of 3.2 cows per ha and 2.5 cows per hectare was assumed for lowland and highland areas, respectively.

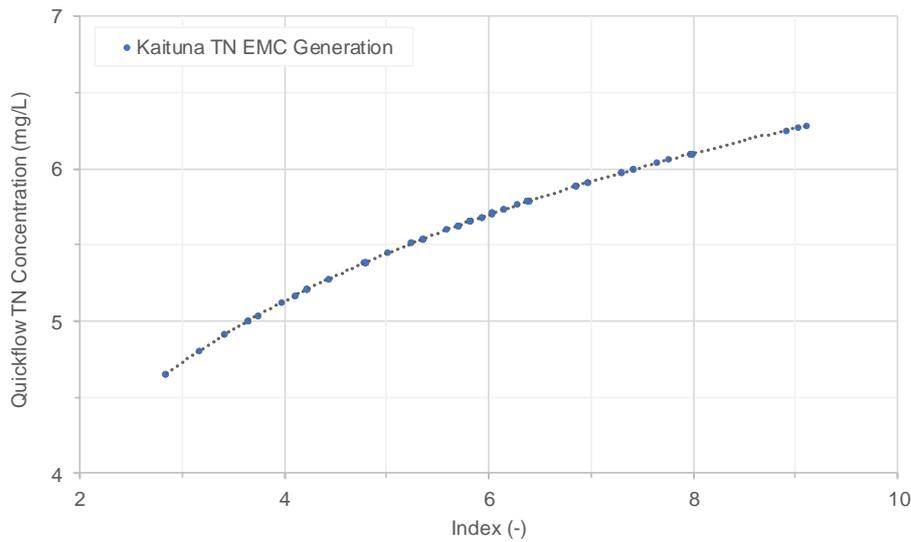


Figure 88. Kaituna TN Index Generation Relationship.

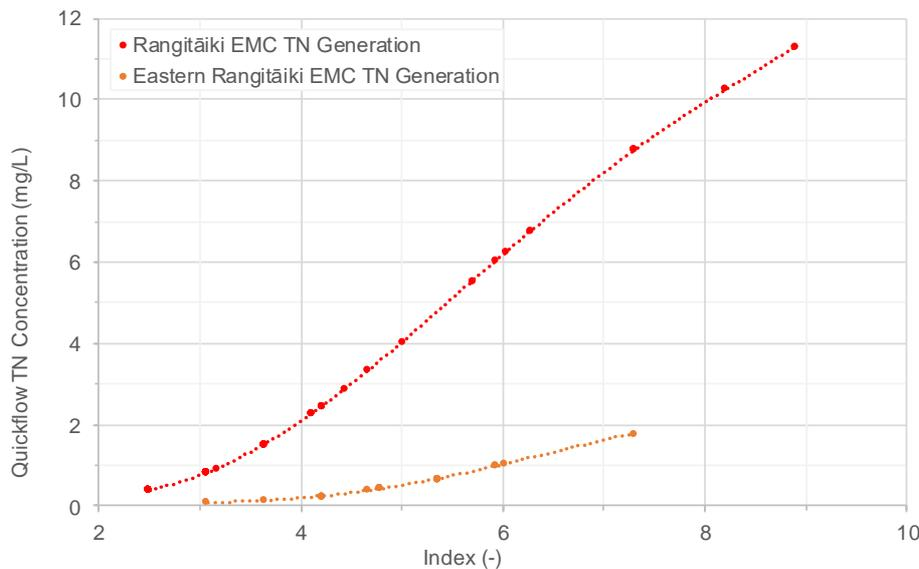


Figure 89. Rangitāiki TN Index Generation Relationship.

7.2.7 TN Inflows

To characterise the TN inflow loads from Lake Rotoehu and Lake Rotoiti into the downstream catchments the measured TN data supplied by BOPRC was analysed (**Appendix C**). As described previously in **Section 6.4**, flow contributions from Lake Rotoehu are thought to enter the catchment downstream through groundwater inflow, and constituent concentrations remain stable around an average concentration. Therefore, the mean TN concentration from the measured data was applied as a constant concentration.

Lake Rotoiti enters the downstream catchment through surface inflow, and therefore TN concentrations display more variability than those from Lake Rotoehu. The measured TN data for Lake Rotoiti showed three distinct

time periods where observations seemed to differ: 1990-1999, 2000-2010, 2011-2016. For each of the three periods, the data was monthly averaged and applied as a time series of monthly averages in SOURCE.

In the Kaituna catchment, the proportional loss nodes which remove water from the stream network and partition it to the deeper groundwater system resurface as recharge downstream before the gauge at Te Matai. It was assumed that not all the TN lost in these locations is returning to the surface waters and therefore a fixed inflow concentration of 0.2 mg/L was applied to the inflow nodes that represent the resurfacing of deeper groundwater. This assumption was based on spring inflow data for the WMA provided by BOPRC.

7.2.8 TN Calibration Results

The key parameter adjusted during calibration of TN was the CAF, which represented the biochemical up take of nitrogen as it is transported through the catchment along multiple pathways.

TN calibration results for the primary monitoring sites are detailed in **Section 7.2.8.1** and **7.2.8.2** for the Kaituna and Rangitāiki WMAs respectively. The calibration results are presented in-text as comparison time series plots, summary statistics, and statistical performance measures for six representative primary calibration sites in the Kaituna and Rangitāiki WMAs (three in each WMA). A boxplot comparison of measured and modelled TN concentrations, PBIAS classifications and general comments for all primary calibration sites are also presented.

Time series comparison plots and summary statistics for all primary and secondary monitoring sites are presented in **Appendix F**.

7.2.8.1 Kaituna

The CAF applied to each of the monitored sites in the Kaituna WMA in order to provide the best calibration to the measured TN data is shown in **Figure 90**.

Figure 90. Kaituna Catchment Attenuation Factor applied. (Refer A3 attachment at rear).

7.2.8.1.1 Kaituna at Te Matai (SCID26)

A time series comparison plot of the measured and modelled TN for the Kaituna River at the Te Matai gauge is shown in **Figure 91** and the summary statistics presented in **Table 72**. The model was shown to predict the magnitude and temporal variability seen in the measured data. The model accurately simulates the general pattern of higher TN concentrations during winter, and lower TN concentrations during summer. TN concentrations between the minimum and 95th percentile were well predicted.

The model performance at this site is considered Very Good based on the monthly PBIAS value of 7.1%.

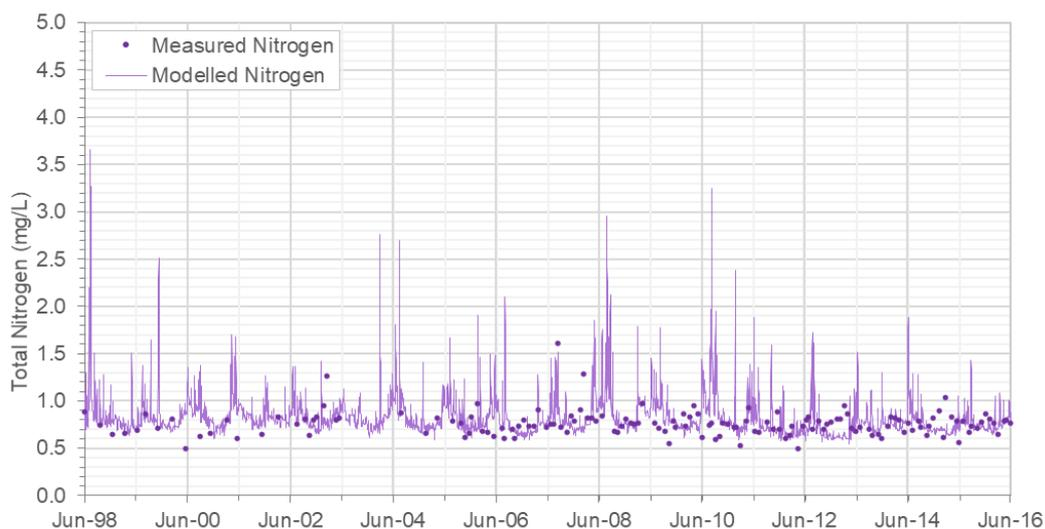


Figure 91. Constituent Hydrograph Comparing Measured and Modelled TN data for the Kaituna at Te Matai gauge.

Table 72. Summary of measured and modelled TN concentration (mg/L) statistics for the Kaituna at Te Matai gauge (Jan 2011–Jun 2016).

	Modelled Data	Measured Data
Statistic	All data	All data
Count	2008	70
Mean	0.8	0.7
Standard Deviation	0.2	0.1
Minimum	0.5	0.5
5th Percentile	0.6	0.6
25th Percentile	0.7	0.7
50th Percentile	0.7	0.7
75th Percentile	0.8	0.8
95th Percentile	1.1	0.9
Maximum	2.4	1.0

7.2.8.1.2 Pongakawa at Old Coach Rd (SCID96)

A time series comparison plot of the measured and modelled TN for the Pongakawa River at the Old Coach Rd gauge is shown in **Figure 91** and the summary statistics presented in **Table 73**. TN concentrations were well predicted throughout the listed percentile concentrations.

The model performance at this site is considered Very Good based on the monthly PBIAS value of 7.0%.

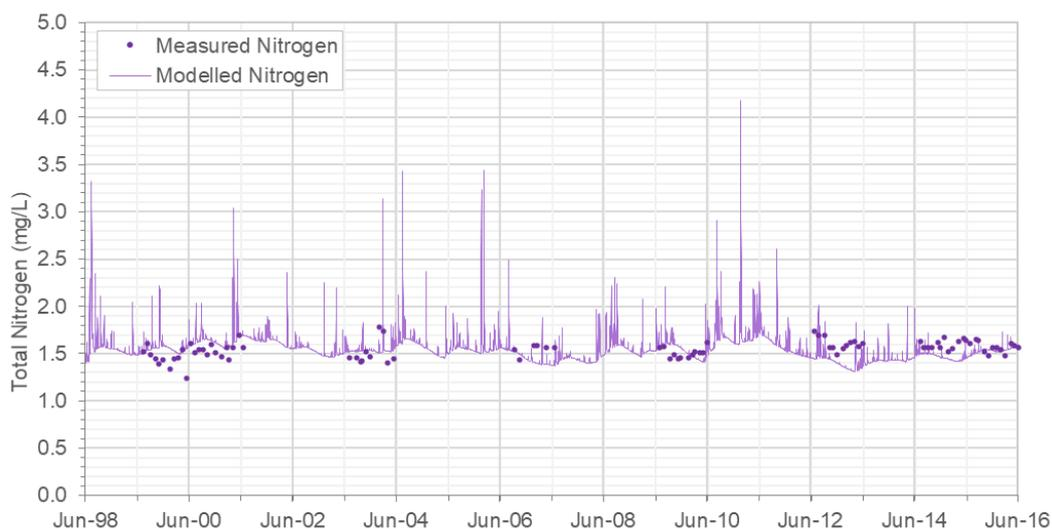


Figure 92. Constituent Hydrograph Comparing Measured and Modelled TN data for the Pongakawa at Old Coach Rd gauge.

Table 73. Summary of measured and modelled TN concentration (mg/L) statistics for the Pongakawa at Old Coach Rd gauge (Jan 2011–Jun 2016).

	Modelled Data	Measured Data
Statistic	All data	All data
Count	2008	36
Mean	1.5	1.6
Standard Deviation	0.2	0.1
Minimum	1.3	1.5
5th Percentile	1.4	1.5
25th Percentile	1.4	1.6
50th Percentile	1.5	1.6
75th Percentile	1.6	1.6
95th Percentile	1.7	1.7
Maximum	4.2	1.7

7.2.8.1.3 Waitahanui River (SCID114)

A time series comparison plot of the measured and modelled TN for the Waitahanui River at the secondary site located in SCID114 is shown in **Figure 93** and the summary statistics presented in **Table 74**. In general, the magnitude and temporal variations in TN concentrations were well predicted, especially during the last two years of the calibration period. The model simulated similar percentile concentrations to those observed in the measured data.

The model performance at this site is considered Very Good based on the monthly PBIAS value of -5.0%.

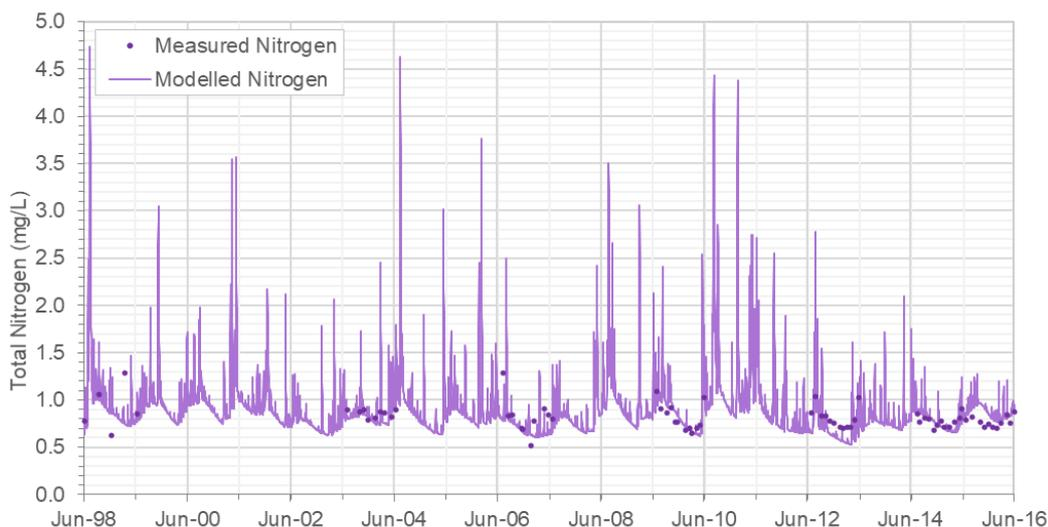


Figure 93. Constituent Hydrograph Comparing Measured and Modelled TN data for the SCID114 site.

Table 74. Summary of measured and modelled TN concentration (mg/L) statistics for the SCID114 site (Jan 2011–Jun 2016).

	Modelled Data	Measured Data
Statistic	All data	All data
Count	2008	35
Mean	0.9	0.8
Standard Deviation	0.3	0.1
Minimum	0.5	0.7
5th Percentile	0.6	0.7
25th Percentile	0.7	0.7
50th Percentile	0.8	0.8
75th Percentile	0.8	0.8
95th Percentile	1.4	0.9
Maximum	4.4	1.0

7.2.8.1.4 Overall Kaituna Performance

The boxplots presented in **Figure 110** and model performance statistics presented in **Table 75** provide a comparison of measured and modelled TN for all primary calibration sites. The model successfully predicts the spatial variation in TN concentrations observed between the western (SCID22 to SCID57) and eastern (SCID96 to SCID98) sub-catchments in the Kaituna WMA.

Monthly PBIAS values range from -22% to 11% which corresponds to a model performance from Satisfactory to Very Good. The RMSE values range from 0.1 mg/l to 0.3 mg/l.

Overall, the model is considered an appropriate tool for the prediction of the magnitude and spatial variation in TN concentrations across the Kaituna WMA.

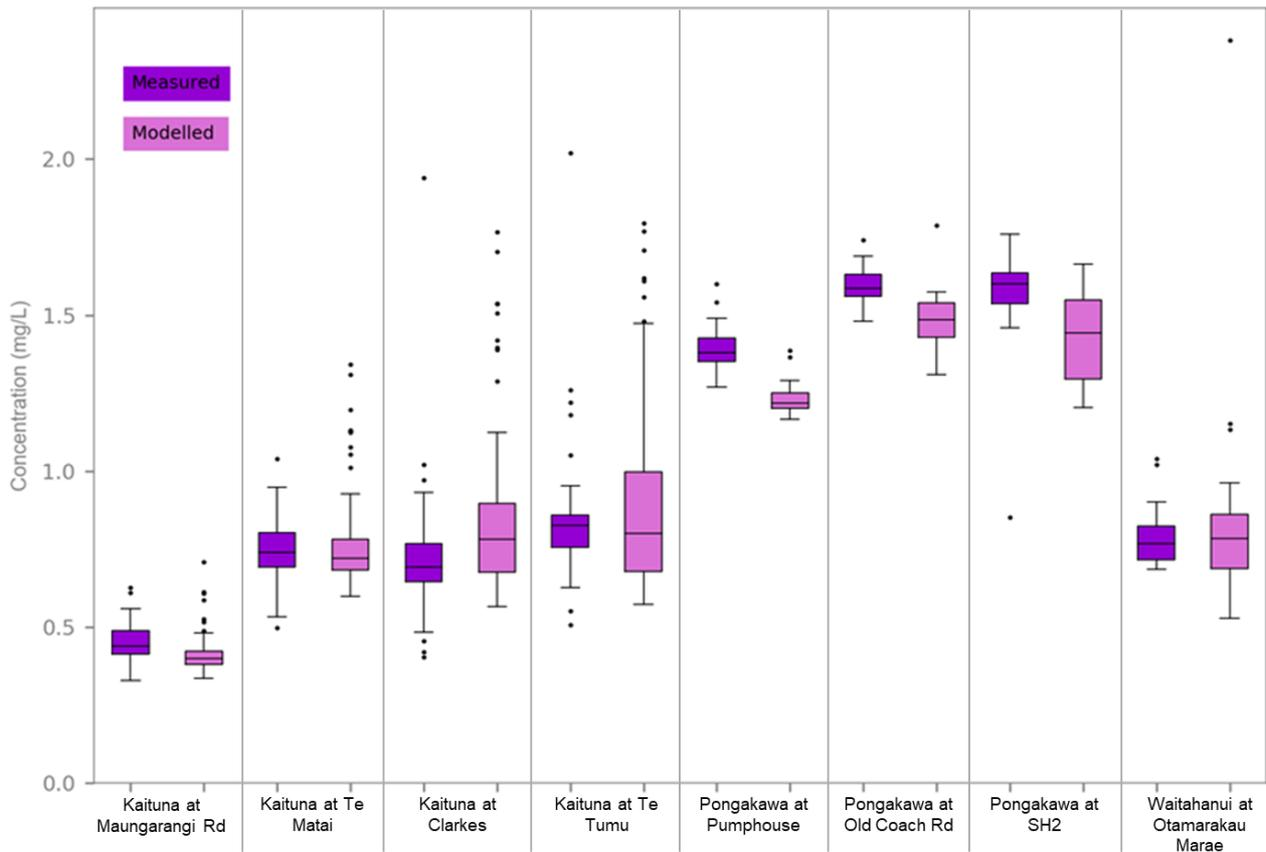


Figure 94. Box plot comparison of measured and modelled TN concentration for all primary calibration sites in the Kaituna WMA.

Table 75. Summary of TN model performance at primary calibration sites in the Kaituna WMA.

Location	Observed Data Points	Model Accuracy (PBIAS)		RMSE	CAF (Avg. % reduction on Baseflow)	General Comments
		Value (%)	Class			
Kaituna at Maungarangi Rd (SC22)	63	7.1	Very Good	0.1	N/A	In general, the model slightly under predicted TN concentrations and the range in concentrations compared to the measured data.
Kaituna at Te Matai (SCID26)	64	-3.7	Very Good	0.2	0.1%	The model predicted good agreement with the observed TN concentrations at this location.
Kaituna at Clarkes (SC53)	62	-22	Satisfactory	0.3	80%	The model predicted good agreement with the observed TN concentrations at this location.
Kaituna at Te Tumu (SC57)	75	-7.9	Very Good	0.3	0.1%	The model over predicted TN concentrations at the 50 th and 75 th percentile and maximum concentration in comparison to the measured data.
Pongakawa at Pumphouse (SC96 Forest)	33	11	Good	0.2	N/A	The model slightly under predicted TN concentration at this location, however, the range (variability) in concentrations is similar to that seen in the measured data.
Pongakawa at Old Coach Rd (SC96)	36	7.0	Very Good	0.2	5%	The model slightly under predicted TN concentration at this location, however, the range (variability) in concentrations is similar to that seen in the measured data.
Pongakawa at SH2 (SC98)	36	8.4	Very Good	0.3	79%	The model predicted good agreement with the observed TN concentrations at this location.
Waitahanui at Otamarakau (SC114)	35	-5.0	Very Good	0.3	60%	The model predicted good agreement with the observed TN concentrations at this location.

7.2.8.2 Rangitāiki

The CAF applied to each of the monitored sites in the Rangitāiki WMA in order to provide the best calibration to the measured TN data is shown in **Figure 95**.

Figure 95. Rangitāiki Catchment Attenuation Factor applied. (Refer A3 attachment at rear).

7.2.8.2.1 Rangitāiki at Murupara (SCID26)

A time series comparison plot of the measured and modelled TN for the Rangitāiki River at the Murupara gauge is shown in **Figure 96** and the summary statistics presented in **Table 76**. The model was shown to simulate a similar magnitude of TN concentrations, however, tended to under predict during the first half of the calibration period (2011 - 2013), and over predict during the latter half of the calibration period (2013 – 2016). The model predicted a similar percentile distribution of concentrations as seen in the measured data.

Change in land use in the upper catchment during the late 90's (conversion of some dry stock to dairy) may have resulted in a rapid increase in observed TN concentrations during the 2000's. As the SOURCE model is based on a constant land use within the catchment, this change was not reflected in the modelled TN concentrations. Future refinements of the model could include the addition of a time varying land use map, and a numeric groundwater model, which would allow the simulation of dynamic land use change.

Irrespective of this, the model performance at this site is considered Very Good according to the monthly PBIAS value of 3.8%.

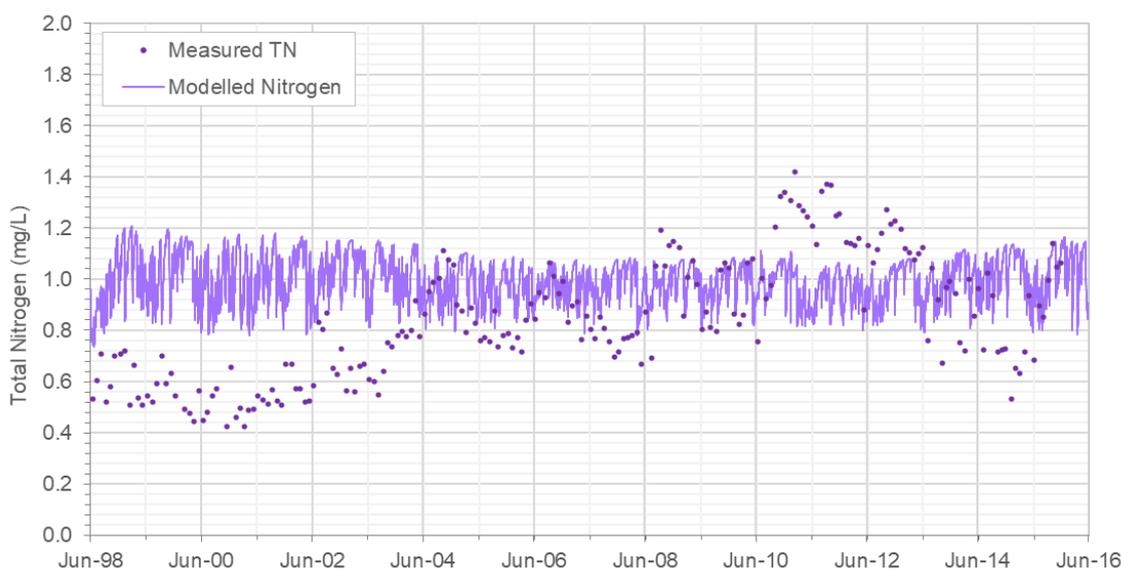


Figure 96. Constituent Hydrograph Comparing Measured and Modelled TN data for the Rangitāiki at Murupara gauge.

Table 76. Summary of measured and modelled TN concentration (mg/L) statistics for the Rangitāiki at Murupara gauge (Jan 2011–Jun 2016).

	Modelled Data	Measured Data
Statistic	All data	All data
Count	1980	60
Mean	1.0	1.0
Standard Deviation	0.1	0.2
Minimum	0.8	0.5
5th Percentile	0.8	0.7
25th Percentile	0.9	0.9
50th Percentile	1.0	1.1
75th Percentile	1.1	1.2
95th Percentile	1.1	1.3
Maximum	1.3	1.4

7.2.8.2.2 Whirinaki at Galatea (SCID47)

A time series comparison plot of the measured and modelled TN for the Whirinaki River at Galatea gauge is shown in **Figure 97** and the summary statistics presented in **Table 77**. The model was shown to successfully predict the magnitude and temporal variation in TN concentrations seen in the observed data, with higher TN concentration occurring during winter compared to summer. The model also accurately predicted the percentile concentrations observed in the measured data shown in **Table 77**.

The model performance at this site is considered Good based on the monthly PBIAS value of 17%.

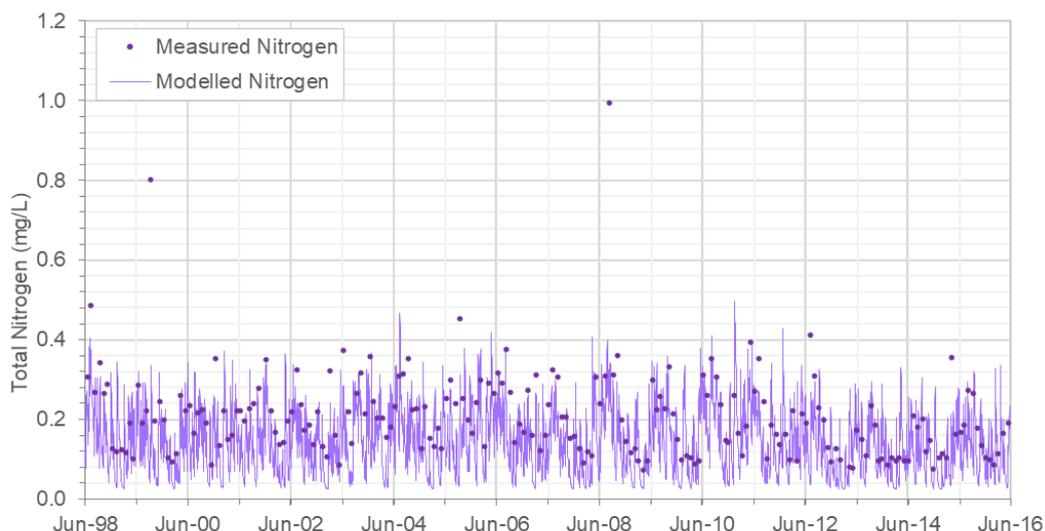


Figure 97. Constituent Hydrograph Comparing Measured and Modelled TN data for the Whirinaki at Galatea gauge.

Table 77. Summary of measured and modelled TN concentration (mg/L) statistics for the Whirinaki at Galatea gauge (Jan 2011–Jun 2016).

	Modelled Data	Measured Data
Statistic	All data	All data
Count	1980	52
Mean	0.13	0.2
Standard Deviation	0.08	0.1
Minimum	0.02	0.1
5th Percentile	0.03	0.1
25th Percentile	0.07	0.1
50th Percentile	0.12	0.1
75th Percentile	0.19	0.2
95th Percentile	0.28	0.4
Maximum	0.54	0.4

7.2.8.2.3 Rangitāiki River at Matahina (SCID34)

A time series comparison plot of the measured and modelled TN for the Rangitāiki River at the secondary site located in SCID34 (downstream of Lake Matahina) is shown in **Figure 98**, and the summary statistics presented in **Table 78**. Only sparse measured data were available at this location, and in general the model was shown to over-predict concentrations in comparison to the available measured data.

The model performance at this site is considered Satisfactory based on the monthly PBIAS value of -25%.

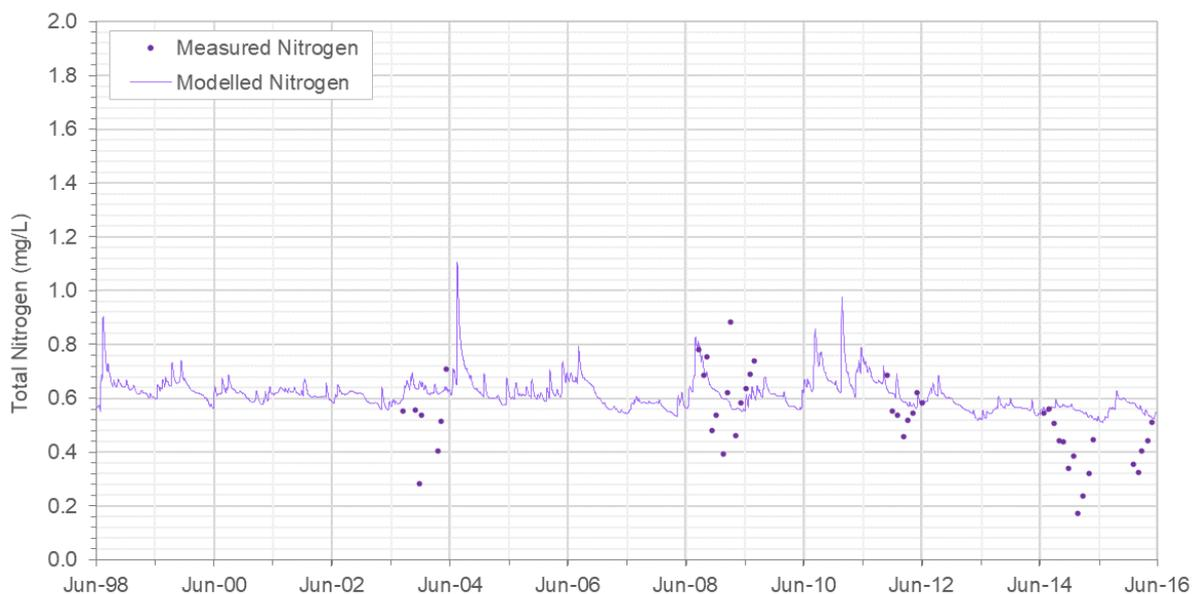


Figure 98. Constituent Hydrograph Comparing Measured and Modelled TN data for the SCID34 site.

Table 78. Summary of measured and modelled TN concentration (mg/L) statistics for the SCID34 site (Jan 2011–Jun 2016).

	Modelled Data	Measured Data
Statistic	All data	All data
Count	1980	25
Mean	0.6	0.5
Standard Deviation	0.1	0.1
Minimum	0.5	0.2
5th Percentile	0.5	0.3
25th Percentile	0.6	0.4
50th Percentile	0.6	0.5
75th Percentile	0.6	0.5
95th Percentile	0.7	0.6
Maximum	1.0	0.7

7.2.8.2.4 Overall Rangitāiki Performance

The boxplots presented in **Figure 99** and model performance statistics presented in **Table 79** provide a comparison of measured and modelled TN for all primary calibration sites. The model successfully predicts the spatial variation in TN concentrations observed across the WMA, with higher concentrations successfully predicted at the Rangitāiki at SH5 and Murupara monitoring locations, and the lowest concentrations at the Whirinaki at Galatea monitoring location in comparison to the other sites.

Monthly PBIAS values range from 3.8% to -25% which corresponds to model performance from Very Good to Satisfactory.

Overall, the model is considered an effective tool for the prediction of the magnitude and spatial variation in TN concentrations across the Rangitāiki WMA.

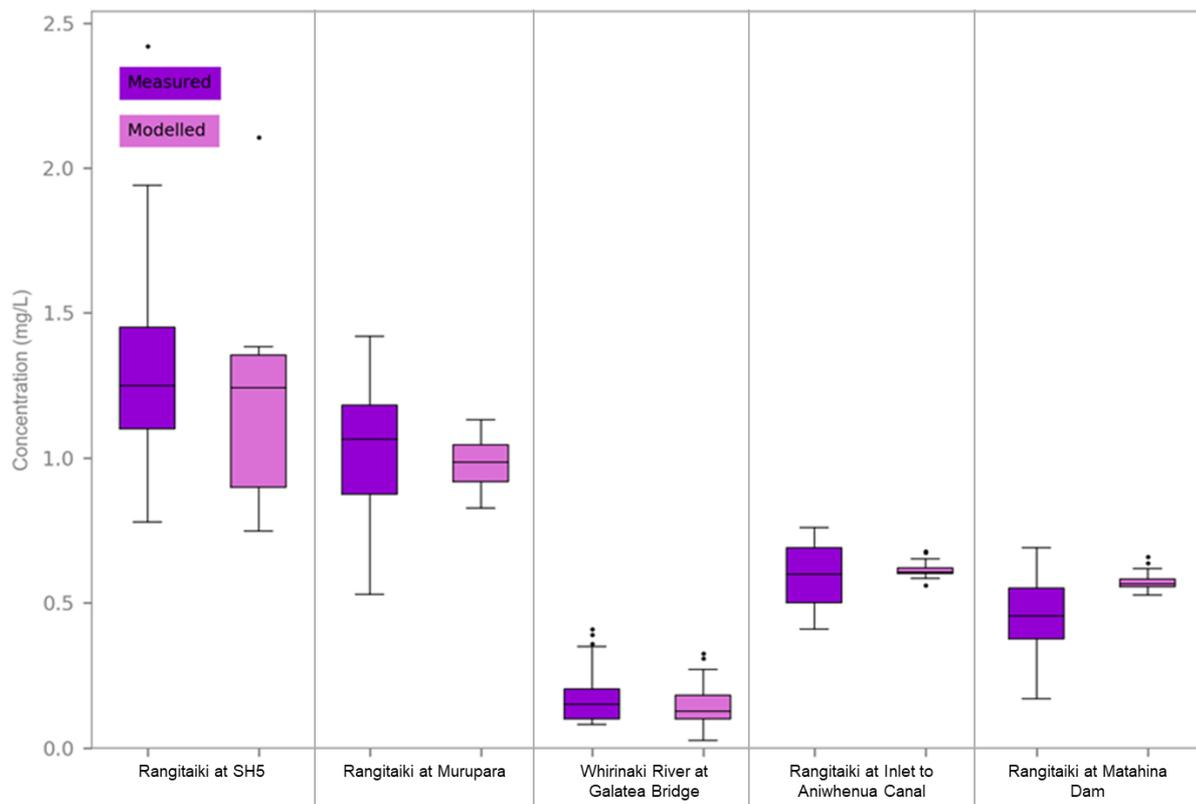


Figure 99. Box plot comparison of measured and modelled N concentration for all primary calibration sites in the Rangitāiki WMA.

Table 79. Summary of TN model performance at primary calibration sites in the Rangitāiki WMA.

Location	Observed Data Points	Model Accuracy (PBIAS)		RMSE	CAF (Ave % reduction on BF)	General Comments
		Value (%)	Class			
Rangitāiki at SH5 (SC1)	29	12	Very Good	0.4	N/A	The model generally over simulates TN in comparison to the measured data. The median concentration of the modelled data is greater than the 75th percentile of the measured data. However, the model successfully predicted this location as having the higher TN concentrations in comparison to the other monitoring sites.
Rangitāiki at Murupara (SC26)	60	3.8	Very Good	0.3	35%	The model predicts similar concentrations to those seen in the measured data. However, the variability (range) of concentrations predicted by the model is smaller than observed in the measured data.
Whirinaki at Galatea Bridge (SC47)	52	17	Good	0.1	98%	The model accurately predicts TN concentrations at this location, with very similar median, 25 th and 75 th percentile and maximum concentrations predicted compared to the measured data.
Rangitāiki at Inlet to Aniwhenua Canal (SC30)	21	-3.0	Very Good	0.1	75%	The model predicts similar median concentrations to those seen in the measured data. However, the variability (range) of concentrations predicted by the model is smaller than observed in the measured data. Therefore, while on average concentrations are well predicted, observed concentrations may be slightly higher or lower than predicted at times.
Rangitāiki at Matahina Dam (SC34)	24	-25	Satisfactory	0.2	75%	The model predicts similar concentrations to those seen in the measured data. However, the variability (range) of concentrations predicted by the model is smaller than observed in the measured data.

7.3 Total Phosphorus

Total phosphorus occurs in waterways in two fractions; organic phosphorus, and inorganic phosphate (PO₄). Both fractions can be present in particulate and dissolved forms. Organic phosphate consists of phosphate molecules associated with carbon-based molecules (i.e. in plant or animal tissue) and inorganic phosphate is all phosphate molecules that are not associated with carbon-based molecules (i.e. dissolved mineral).

When assessing water quality two forms of phosphorus are commonly tested; dissolved reactive phosphorus (DRP), and total phosphorus (TP). The DRP is an indicator of the phosphorus readily available for biological uptake, whereas TP is effectively the sum of dissolved and particulate Phosphorus.

In most sub-catchments which are dominated by agriculture the diffuse sources of phosphorus dominate the input into rivers (Davis and Koop 2001; Heathwaite 2003; McDowell et al. 2004, Drewry et al, 2006). Phosphorus present in water ways in New Zealand is typically derived from surficial runoff (e.g. of soil, fertiliser) and from the weathering of parent geological materials. The combination of sources of phosphorus, its release, and the delivery to waterways control the amount of phosphorus found within the waterways (Drewry, et al, 2006).

Initially dSedNET (further described in **Section 7.4.1**) was investigated as a potential method of simulating the generation of TP. The premise of this method was that phosphorous readily binds to clay colloids and is typically mobilised and deposited in-stream with sediment. As modelling proceeded it was discovered that there was only a very weak relationship between measured TP and TSS concentrations (potentially an artefact of the observed data frequency). Therefore, an acceptable calibration could not be achieved.

The second method trialled was to relate TP to the flow generated in each sub-catchment. The premise for this method was that surface water runoff would mobilise TP and transport it into in the streams network. An analysis of the flow data and the observed TP concentrations also highlighted an acceptable relationship between these two variables. While this method achieved better results than the first, the relationship established fails to acknowledge that land use and catchment management play a significant role in governing TP generation. Therefore, the method below was developed to relate TP concentrations to catchment characteristics and land use.

7.3.1 Generation of TP Components

Three TP generation and transportation pathways were identified for the Kaituna and Rangitāiki WMAs through discussion and workshops with BOPRC. These are schematically shown in **Figure 100**, and summarised as follows:

- **Surface Load** – Represents the quick flow of fine sediment and particulate P under normal wet weather conditions and is dependent on land uses within each sub-catchment (e.g. agricultural and horticultural land uses). This represents the anthropogenic derived load of TP (e.g. from fertiliser applications).
- **Event Surface Load** – An additional supply of TP delivered via surface processes during storm events, where additional parent soil material is mobilised during increased runoff, providing an additional source of naturally occurring TP in the river.
- **Natural Load** – Represents the natural background levels of TP found leaching from the parent soil (under standard climatic conditions), which moves through the sub-soil system and is then delivered instream. The natural load also included spring inflows.

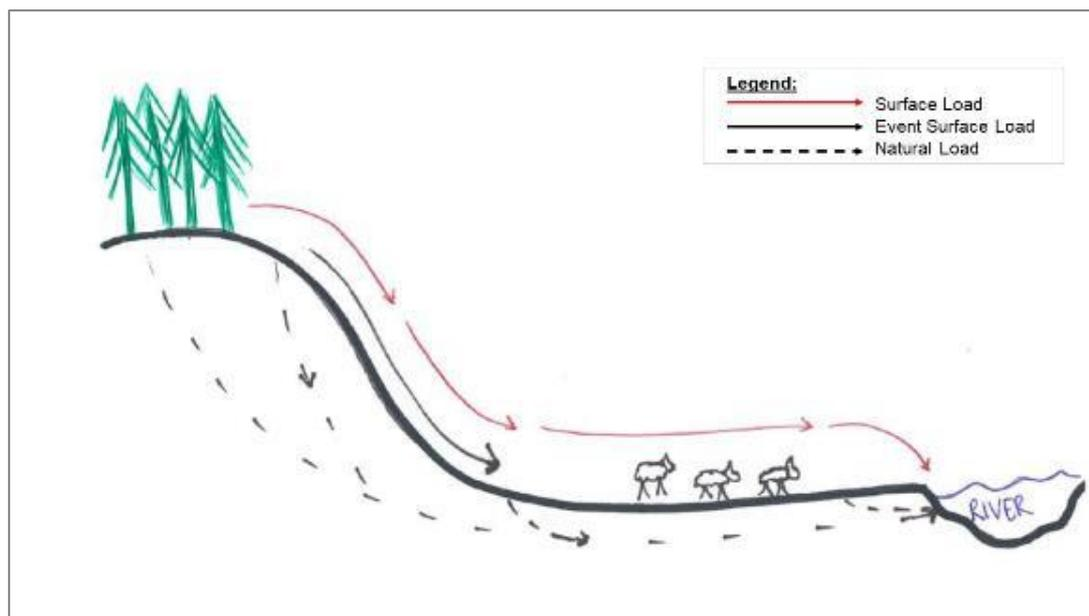


Figure 100. Schematic showing the three components incorporated in the TP constituent model.

Each of the components and their modelled generation methods are detailed in the sub-sections below.

7.3.1.1 Surface Load

The Surface Load component of TP was simulated by calculating the aggregated daily mass of TP generated by each land use within a catchment and assigning the TP mass to the quick flow using the SMWBM outputs of un-attenuated (instantaneous) runoff and surface runoff.

The mass of TP was calculated by applying a ratio of 0.08:1 (TP:TN) to the mass of TN leaching to the soil as predicted by APSIM (described in **Section 7.2**) for each catchment. This ratio was calculated based on previous OVERSEER modelling undertaken for Hawke's Bay Regional Council (WWLA, 2018).

Unattenuated surface runoff output from the SMWBM was utilised as a shape-factor to increase the TP mass delivered during wetter periods and decrease the TP mass when there is little to no rainfall (dry conditions), while conserving the overall mass produced from the generation method described above. Surface runoff from the SMWBM was then used to constrain the delivery of TP to the stream network to only periods when simulated surface runoff was occurring. No concentration was assigned to the base flow component of the flow regime.

A schematic overview of the Surface Load TP generation is provided in **Figure 101**.

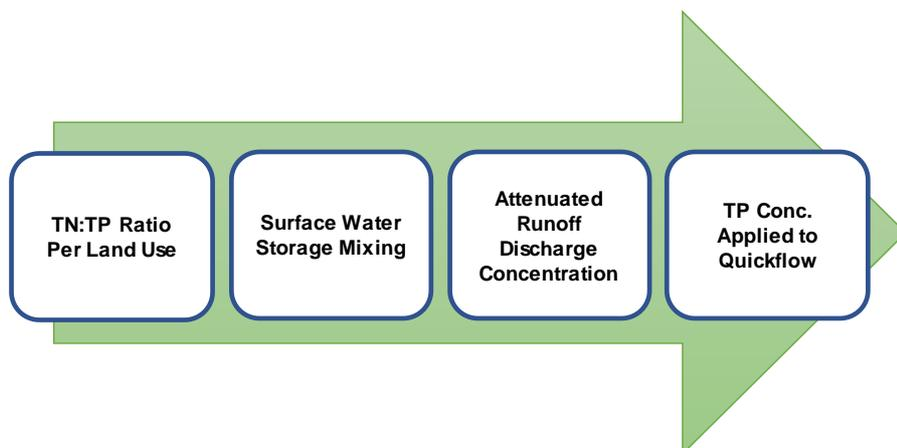


Figure 101. Schematic view of surface load TP generation from land use.

The Surface Load TP component was implemented as a time series pre-processed outside of SOURCE and applied as an observed quick flow (surface water) concentration.

7.3.1.2 Event Surface Load

Phosphorus is delivered via surface processes during storm events, where parent soil material is mobilised during increased runoff, providing an additional source of naturally occurring TP in the river (Drewry, *et al*, 2006). This was incorporated into the SOURCE model as the Event Surface Load.

The Event Surface Load component was calculated through the development of a TP potential risk index map, which characterised the potential for mobilisation of natural TP from the parent soil during storm events. The TP potential risk index map is referred to as the “PLSC” layer and was calculated as the product of the following catchment characteristic values:

- The natural TP load (calculated from the BOPRC supplied acid soluble phosphorus content GIS layer) (P);
- Mean catchment slope length (L);
- Mean catchment slope gradient (S); and
- Vegetation cover (C).

The PLSC index layer map is shown in **Figure 102** and **Figure 103** for the Kaituna and Rangitāiki WMAs respectively. The high PLSC values in the east of the Kaituna WMA at Pongakawa are due to spring TP inflows at these locations.

Figure 102. Kaituna PLSC Risk Map (Refer A3 attachment at rear).

Figure 103. Rangitāiki PLSC Risk Map (Refer A3 attachment at rear).

Through an iterative calibration process a relationship was developed between the PLSC index and TP concentration for the quick flow component of the flow regime. High PLSC index values corresponded to catchments with high potential for mobilisation of TP from the parent soils during storm events and vice versa.

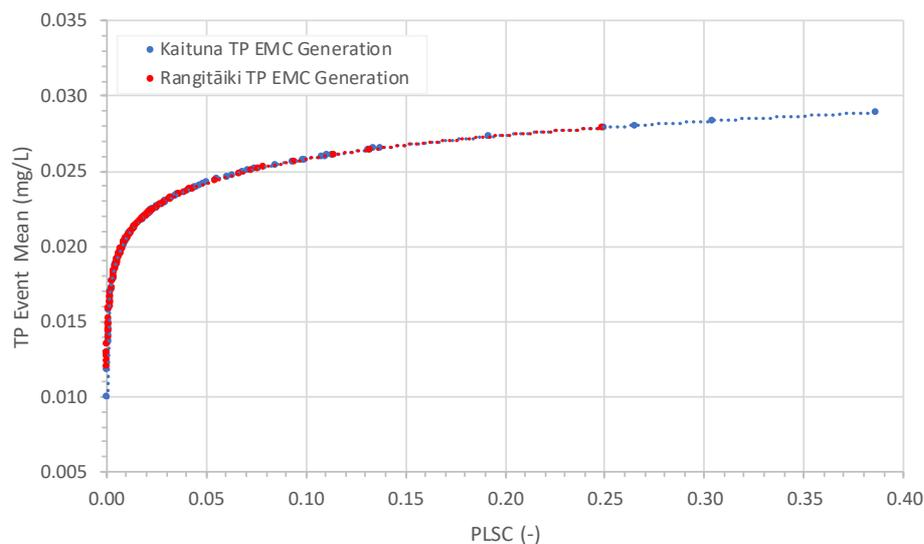


Figure 104 Relationship between PLSC index and TP concentration

The event surface load TP component was implemented in source as a time series pre-processed outside of SOURCE and applied as an observed quick flow (surface water) concentration.

7.3.1.3 Natural Load

Phosphorus is commonly found in low concentrations naturally in soils across New Zealand (Thomas *et al*, 2001; McDowell, 2012). The natural leaching of phosphorus from soils was incorporated into the SOURCE models as the Natural Load component.

The natural load component of TP was calculated by multiplying the underlying soil's acid soluble phosphorus content (as given in GIS layer of acid soluble phosphorus content of different soil types supplied by BOPRC) by the average SMWBM sub-soil percolation for each sub-catchment to produce a TP leaching concentration.

The natural TP load component was implemented in source as a fixed dry weather concentration attached to the base flow component of the flow regime for each sub-catchment.

7.3.1.3.1 Spring Inflow Load

During the TP calibration process several catchments were identified where TP concentrations were continually under-predicted. After reviewing and confirming the input parameters for the three TP components detailed above, it was concluded that an additional unaccounted source of TP was influencing these catchments. This additional component of TP was attributed to the spring inflows described in **Section 3.6**.

To replicate the TP contributions from the spring inflows an Acid Soluble Phosphate (ASP) weighted average was applied to the Kaituna WMA and to the catchments inflowing to the Rangitāiki at Murupara Gauge. The ASP weighted average assigned higher TP spring inflow concentrations to sub-catchments with high ASP values, and lower concentrations to sub-catchments with lower ASP values.

The spring inflow load was modelled as part of the natural load. The inclusion of TP contributions from springs improved the calibration of the Kaituna and Murupara catchments.

Figure 105 and **Figure 106** display the acid soluble phosphorus for each sub-catchment in the Kaituna and Rangitāiki WMA combined with the additional phosphorus inflow from the spring data.

Figure 105. Acid Soluble Phosphorus combined with spring inflow for the Kaituna WMA. (Refer A3 attachment at rear).

Figure 106. Acid Soluble Phosphorus combined with spring inflow for the Rangitāiki WMA. (Refer A3 attachment at rear).

7.3.2 TP Calibration Results

Calibration results for the primary monitoring sites are detailed in **Section 7.3.2.1** and **Section 7.3.2.2** for the Kaituna and Rangitāiki WMAs respectively. The calibration results are presented as comparison time series plots, summary statistics, and statistical performance measures for six primary sites that are considered representative of the Kaituna and Rangitāiki WMAs (three in each WMA). Boxplot comparisons of measured and modelled TP concentrations, PBIAS classifications and general comments for all primary calibration sites are also presented.

Time series comparison plots and summary statistics for all primary and secondary monitoring sites are presented in **Appendix F**.

7.3.2.1 Kaituna

7.3.2.1.1 Kaituna at Te Matai (SCID26)

A time series comparison plot of measured and modelled TP for the Kaituna River at the Te Matai gauge is shown in **Figure 104** and the summary statistics presented in **Table 80**. Although the quantity of measured data is sparse in comparison to the modelled TP data, the model was shown to successfully predict the magnitude and temporal variability of the available measured data. The model accurately simulates TP between the minimum, 5thth and 95th percentile, but over predicted the maximum measured TP concentration.

The model performance at this site is considered Very Good based on the monthly PBIAS value of 4.4%.

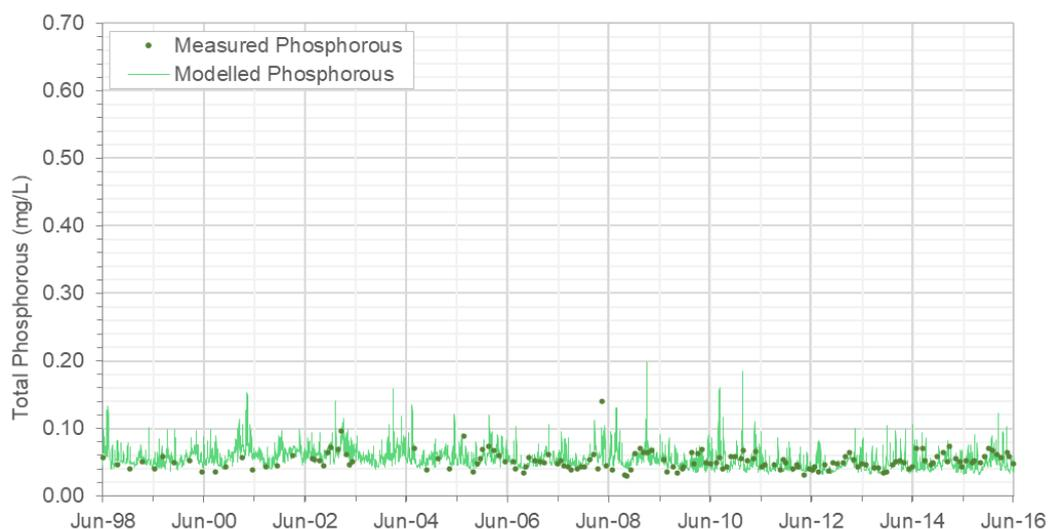


Figure 107. Constituent Hydrograph Comparing Measured and Modelled TP data for the Kaituna at Te Matai gauge.

Table 80. Summary of measured and modelled TP concentration (mg/L) statistics for the Kaituna at Te Matai gauge (Jan 2011–Jun 2016).

	Modelled Data	Measured Data
Statistic	All data	All data
Count	2008	64
Mean	0.05	0.05
Standard Deviation	0.02	0.01
Minimum	0.03	0.03
5th Percentile	0.03	0.04
25th Percentile	0.04	0.04
50th Percentile	0.04	0.05
75th Percentile	0.05	0.06
95th Percentile	0.07	0.07
Maximum	0.18	0.07

7.3.2.1.2 Pongakawa at Old Coach Rd (SCID96)

A time series comparison plot of measured and modelled TP for the Pongakawa River at the Old Coach Rd gauge is shown in **Figure 108**, and summary statistics comparison and statistics is reported in **Table 81**.

The model accurately simulates the minimum measured concentration, and slightly under predicts the larger percentile values measured, with the exception of the maximum. However, it should be noted the summary statistics do not provide a direct like for like comparison, as there is approximately two years of no measured data at this location during the January 2011 to June 2016 assessment period. Despite this, there is still a good agreement between the observed and measured percentile concentrations.

The model performance at this site is considered Very Good according to the monthly PBIAS value of -1.3%.

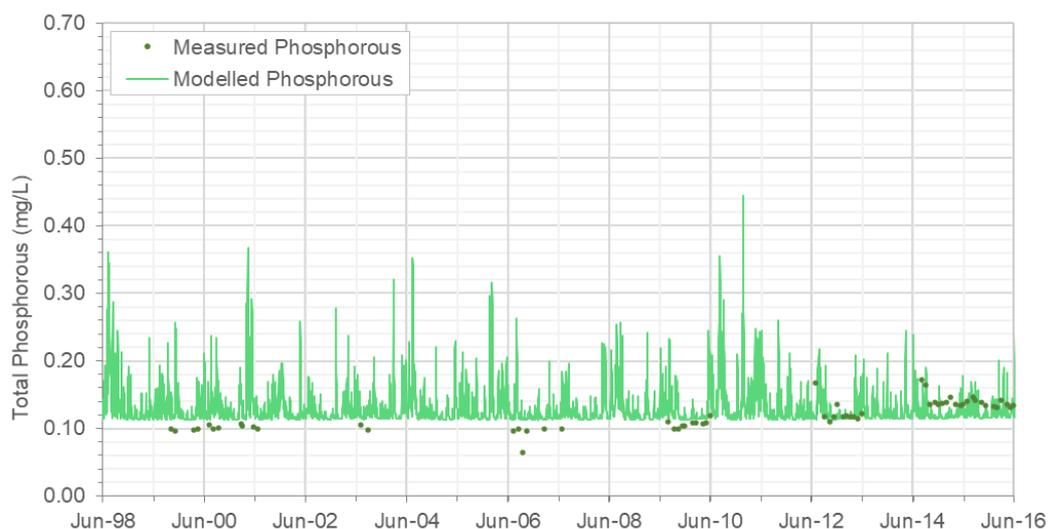


Figure 108. Constituent Hydrograph Comparing Measured and Modelled TP data for the Pongakawa at Old Coach Rd.

Table 81. Summary of measured and modelled TP concentration (mg/L) statistics for the Pongakawa at Old Coach Rd (Jan 2011–Jun 2016).

	Modelled Data	Measured Data
Statistic	All data	All data
Count	2008	38
Mean	0.13	0.15
Standard Deviation	0.03	0.05
Minimum	0.11	0.11
5th Percentile	0.11	0.12
25th Percentile	0.12	0.13
50th Percentile	0.12	0.14
75th Percentile	0.13	0.15
95th Percentile	0.18	0.20
Maximum	0.44	0.35

7.3.2.1.3 Waitahanui River (SCID114)

A time series comparison plot of the measured and modelled TP concentrations for the Waitahanui River at the secondary site located in SCID114 is shown in **Figure 109**, and summary statistics outlined in **Table 82**.

The model slightly under predicts TP concentrations in each of the presented summary statistics, with the exception of the maximum concentration. However, it should be noted the summary statistics do not provide a direct like for like comparison, as there is approximately two years of no measured data at this location during the January 2011 to June 2016 assessment period. Despite this, there is still a close agreement between the observed and measured percentile concentrations.

The model performance at this site is Good based on the monthly PBIAS value of 18%.

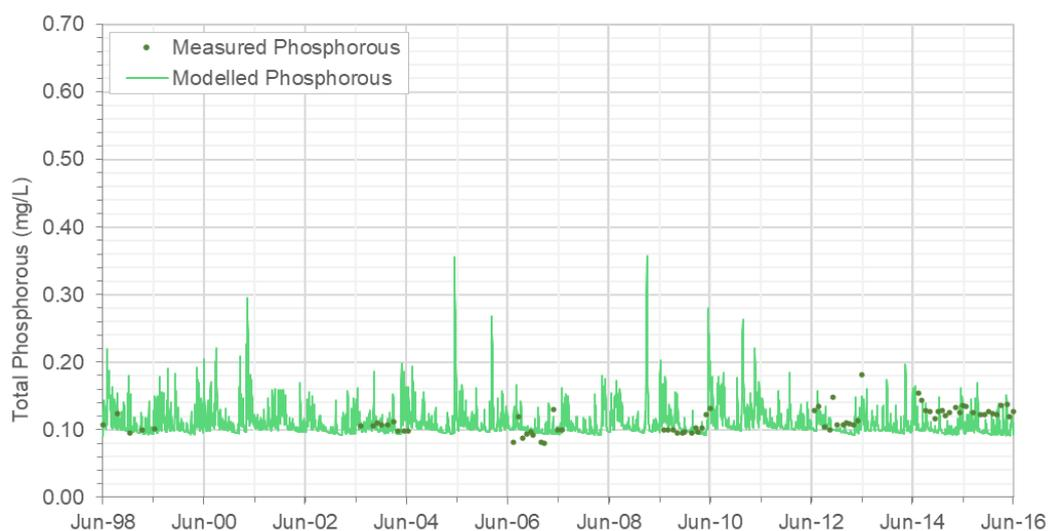


Figure 109. Constituent Hydrograph Comparing Measured and Modelled TP data for the SCID114 site.

Table 82. Summary of measured and modelled TP concentration (mg/L) statistics for the SCID114 site. Gauge (Jan 2011–Jun 2016).

	Modelled Data	Measured Data
Statistic	All data	All data
Count	2008	35
Mean	0.11	0.13
Standard Deviation	0.02	0.02
Minimum	0.09	0.10
5th Percentile	0.09	0.11
25th Percentile	0.10	0.12
50th Percentile	0.10	0.13
75th Percentile	0.11	0.13
95th Percentile	0.14	0.15
Maximum	0.26	0.18

7.3.2.1.4 Overall Kaituna TP Model Performance

The boxplots presented in **Figure 110** and model performance statistics presented in **Table 83** provide a comparison of measured and modelled TP for all primary calibration sites. The model successfully predicts the difference in TP concentrations observed between the Kaituna River, and the Pongakawa and Waitahanui Rivers.

Overall, the model is considered an appropriate tool for the prediction of the magnitude and spatial variation in TP concentrations across the Kaituna WMA.

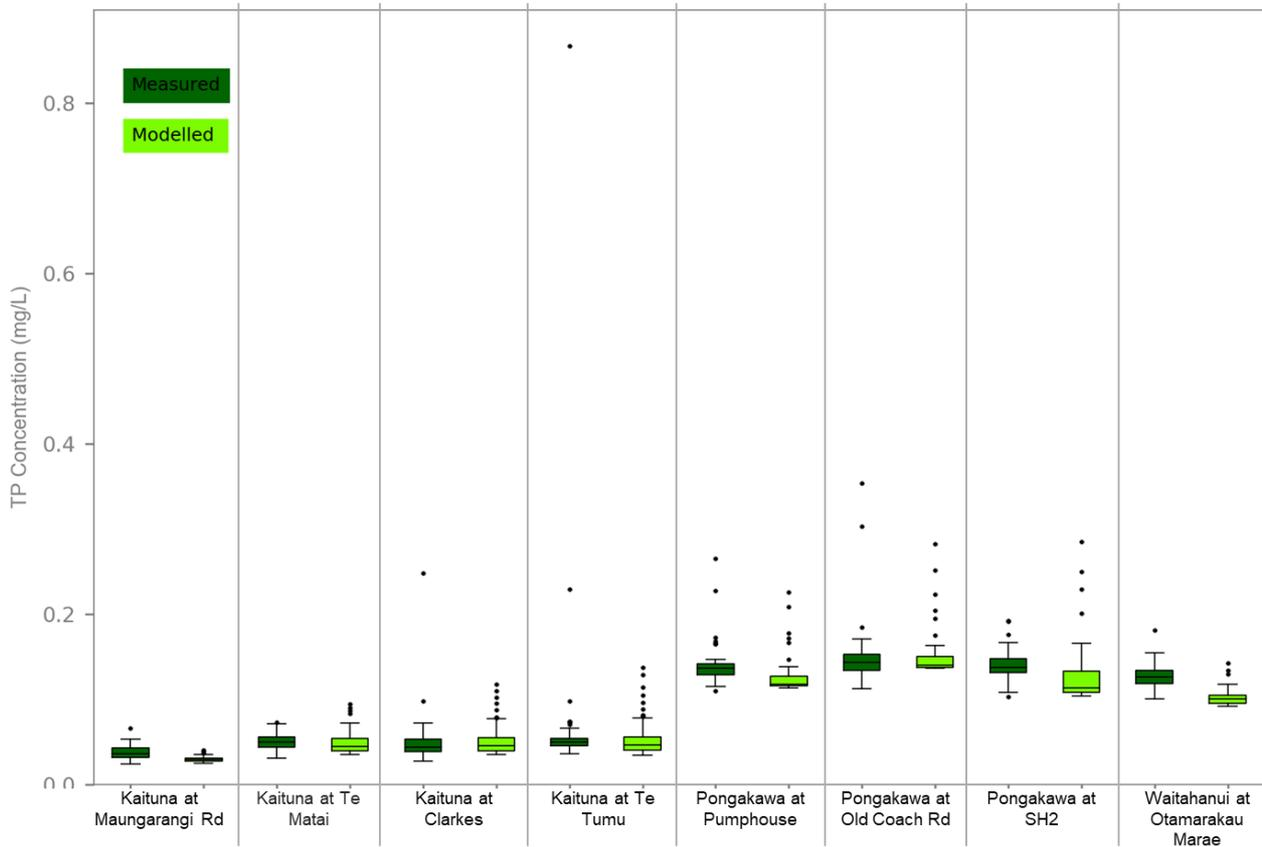


Figure 110. Box plot comparison of measured and modelled TP concentration for all primary calibration sites in the Kaituna WMA.

Table 83. Summary of TP model performance at primary calibration sites in the Kaituna WMA (Jan 2011–Jun 2016).

Location	Observed Data Points	Model Accuracy (PBIAS)		RMSE	General Comments
		Value (%)	Class		
Kaituna at Maungarangi Rd (SC22)	63	21	Satisfactory	0.011	The model is under predicting TP in comparison to the measured data. The boxplot shows the modelled data is quite constrained. The maximum and the 75 th percentile of the measured data is considerably higher than the modelled. The overall range in the measured concentrations is greater than the modelled.
Kaituna at Te Matai (SCID26)	64	4.4	Very Good	0.014	The model simulates a similar range in TP concentration compared to the measured data at the interquartile 25%ile. The median and 75%ile is being under simulated by the model when compared to the measured.
Kaituna at Clarkes (SC53)	62	-3.8	Very Good	0.028	The model simulates a similar range in TP concentration compared to the measured data. The 25 th to 75 th percentile concentrations are similar to the measured data.
Kaituna at Te Tumu (SC57)	74	15	Good	0.087	The model is under predicting TP in comparison to the measured data. The boxplot shows the measured data is quite constrained. The minimum and the 25 th percentile of the measured data is considerably higher than the modelled. The overall range in the measured concentrations is greater than the modelled.
Pongakawa at Pumphouse (SC96 Forest)	36	8.3	Very Good	0.024	The model under simulates the range in TP concentration compared to the measured data. The 25 th to 75 th percentile modelled concentrations are lower than the measured data.
Pongakawa at Old Coach Rd (SC96)	38	-1.3	Very Good	0.029	The model under simulates the range in TP concentration compared to the measured data. The 25 th to 75 th percentile modelled concentrations are lower than the measured and a considerable number of outliers are identified in the upper ranges of the measured and modelled data.
Pongakawa at SH2 (SC98)	36	6.2	Very Good	0.049	The model under simulates the range in TP concentration compared to the measured data. The 25 th to 75 th percentile modelled concentrations are lower than the measured and a considerable number of outliers are identified in the upper ranges of the modelled data.
Waitahanui at Otamarakau (SC114)	35	18	Good	0.028	The model under simulates the range in TP concentration compared to the measured data. The 25 th to 75 th percentile modelled concentrations are lower than the measured data.

7.3.2.2 Rangitāiki

7.3.2.2.1 Rangitāiki at Murupara (SCID26)

A time series comparison plot of measured and modelled TP concentrations is shown in **Figure 111**, and a comparison of summary statistics is presented in **Table 84** for the Rangitāiki at Murupara gauge.

The model is shown to accurately simulate the minimum and low TP concentrations and temporal variability, however over predicts higher concentrations, from the 75th percentile and higher concentrations.

The model performance at this site is considered Not Satisfactory based on the monthly PBIAS value of -47%.

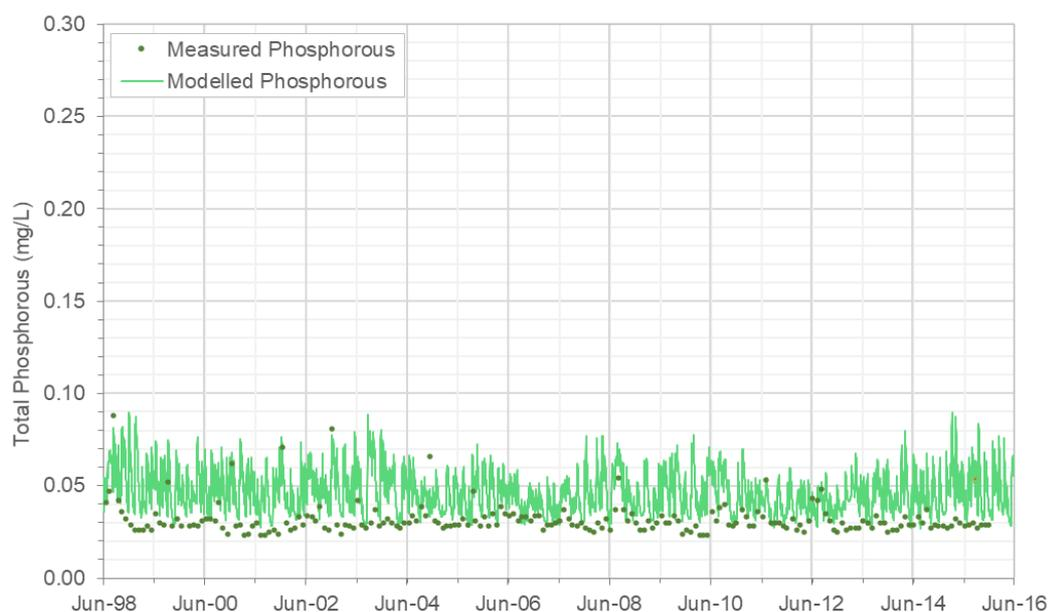


Figure 111. Constituent Hydrograph Comparing Measured and Modelled TP data for the Rangitāiki at Murupara gauge.

Table 84. Summary of measured and modelled TP concentration (mg/L) statistics for the Rangitāiki at Murupara gauge (Jan 2011–Jun 2016).

	Modelled Data	Measured Data
Statistic	All data	All data
Count	1980	60
Mean	0.04	0.03
Standard Deviation	0.01	0.01
Minimum	0.03	0.03
5th Percentile	0.03	0.03
25th Percentile	0.04	0.03
50th Percentile	0.04	0.03
75th Percentile	0.05	0.03
95th Percentile	0.07	0.04
Maximum	0.09	0.05

7.3.2.2 Whirinaki at Galatea (SCID47)

A time series comparison plot of measured and modelled TP concentrations is shown in **Figure 112**, and a comparison of summary statistics are presented in **Table 85** for the Whirinaki at Galatea gauge.

The model accurately simulates concentrations between the minimum and 75th percentile, however under predicts the less frequent peak event TP concentrations as indicated by the 95th and maximum concentrations. This suggests baseflow (slow flow) contributions are accurately simulated, but the quick flow component is under predicted during peak periods.

The model performance at this site is considered Very Good based on the monthly PBIAS value of 12%.

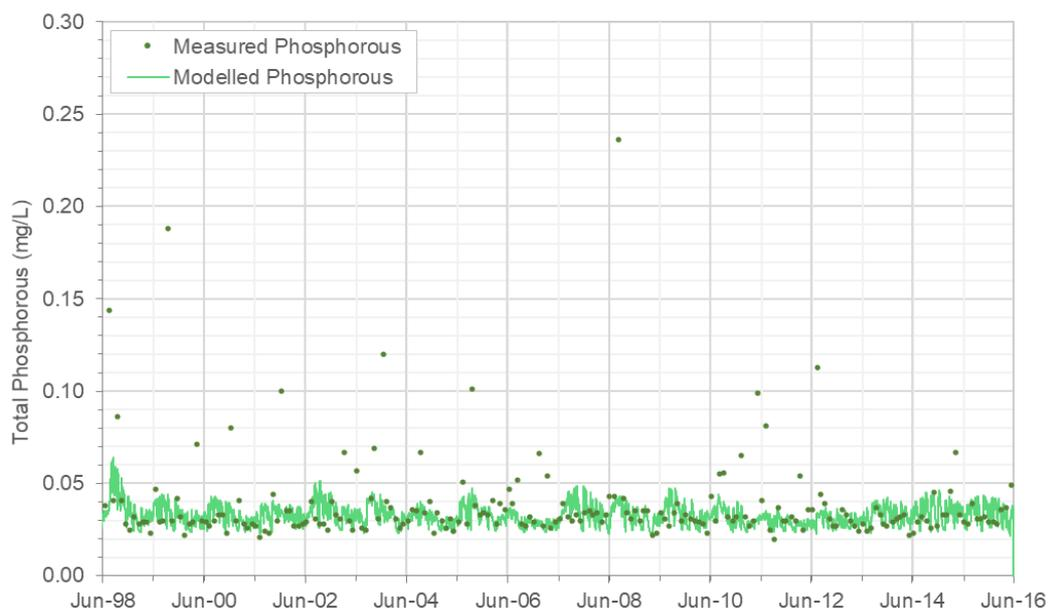


Figure 112. Constituent Hydrograph Comparing Measured and Modelled TP data for the Whirinaki at Galatea gauge.

Table 85. Summary of measured and modelled TP concentration (mg/L) statistics for the Whirinaki at Galatea gauge (Jan 2011–Jun 2016).

	Modelled Data	Measured Data
Statistic	All data	All data
Count	1980	59
Mean	0.03	0.04
Standard Deviation	0.01	0.02
Minimum	0.02	0.02
5th Percentile	0.02	0.02
25th Percentile	0.03	0.03
50th Percentile	0.03	0.03
75th Percentile	0.04	0.04
95th Percentile	0.04	0.07
Maximum	0.05	0.11

7.3.2.2.3 Rangitāiki River at Matahina (SCID34)

A time series comparison plot of measured and modelled TP concentrations is shown in **Figure 113**, and a comparison of summary statistics are presented in **Table 86** for the secondary site located in SCID34 (downstream of Lake Matahina).

Only sparse measured data are available at this monitoring location. The model under predicted TP concentrations throughout the January 2011 to June 2016 calibration period which is also reflected in the summary statistics comparison.

The model accuracy at this site is considered Not Satisfactory based to the monthly PBIAS value of 39%.

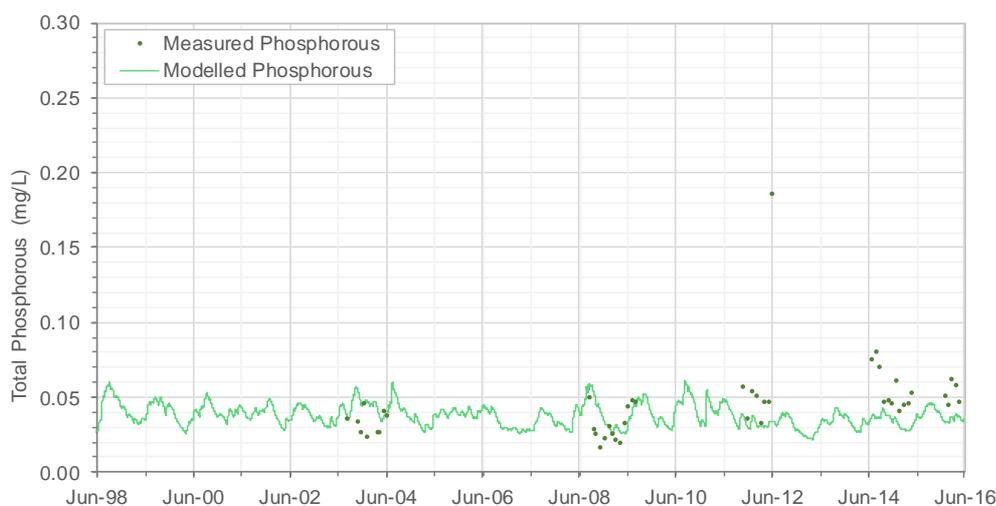


Figure 113. Constituent Hydrograph Comparing Measured and Modelled TP data for the SCID34 site.

Table 86. Summary of measured and modelled TP concentration (mg/L) statistics for the SCID34 site (Jan 2011–Jun 2016).

	Modelled Data	Measured Data
Statistic	All data	All data
Count	1980	25
Mean	0.04	0.06
Standard Deviation	0.01	0.03
Minimum	0.02	0.03
5th Percentile	0.03	0.04
25th Percentile	0.03	0.05
50th Percentile	0.04	0.05
75th Percentile	0.04	0.06
95th Percentile	0.05	0.08
Maximum	0.06	0.19

7.3.2.2.4 Overall Rangitāiki TP Model Performance

The boxplots presented in **Figure 114** provide a comparison of measured and modelled TP concentrations at all primary calibration sites in the Rangitāiki WMA during the period January 2011 to June 2016.

A summary of the model performance statistics for the primary calibration sites in the Rangitāiki WMA is presented in **Table 87**. The monthly PBIAS values range from 12% to +/-47%, which corresponds to model performance classifications of Very Good to Not Satisfactory.

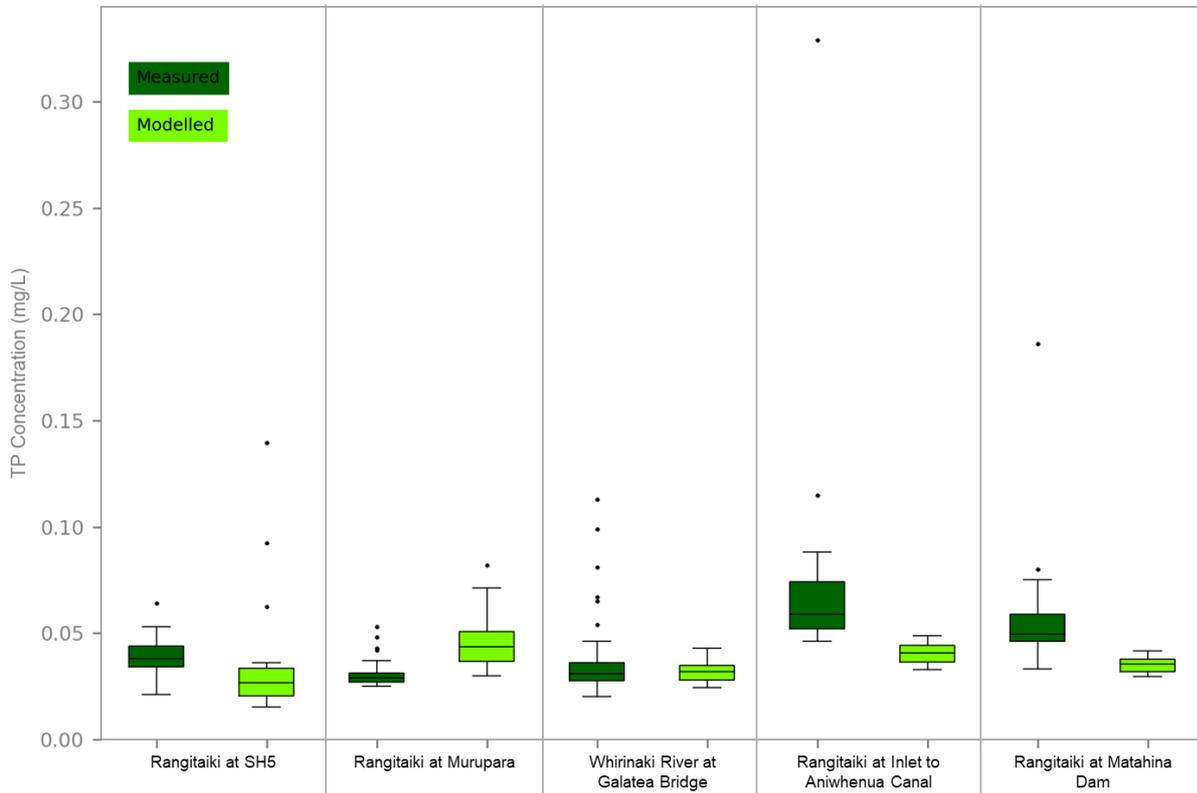


Figure 114. Box plot comparison of measured and modelled TP concentration for all primary calibration sites in the Rangitāiki WMA.

Table 87. Summary of TP model performance at primary calibration sites in the Rangitāiki WMA.

Location	Observed Data Points	Model Accuracy (PBIAS)		RMSE	General Comments
		Value (%)	Class		
Rangitāiki at SH5 (SC1)	29	16	Good	0.027	The range of modelled TP values is greater than the measured data at this location, with the interquartile range of the measured data sitting between the median and 75th percentile of the modelled data.
Rangitāiki at Murupara (SC26)	60	-47	Not Satisfactory	0.017	The range of modelled TP concentrations is much larger than observed in the measured data which shows little variability. However, the measured and modelled concentrations in general are of similar magnitude.
Whirinaki at Galatea Bridge (SC47)	59	12	Very Good	0.017	The model under predicted TP concentrations in comparison to the measured data. The modelled concentrations showed significantly less variability than seen in the measured data, however, the median concentrations are similar.
Rangitāiki at Inlet to Aniwhenua Canal (SC30)	20	47	Not Satisfactory	0.068	The model under predicted TP concentrations in comparison to the measured data. The boxplot shows the variability in modelled data was significantly less than observed in the measured data. The modelled minimum, 25 th , 50 th and 75 th percentile concentrations were all less than the measured data.
Rangitāiki at Matahina Dam (SC34)	24	39	Not Satisfactory	0.036	The model under predicted TP concentrations in comparison to the measured data. The minimum and the 25th percentile of the measured data are considerably higher than the modelled. The overall range in the measured concentrations was greater than the modelled.

Although model performance at the Rangitāiki at Inlet to Aniwhenua Canal and at Matahina Dam primary calibration sites was considered Not Satisfactory based solely on the PBIAS classification, visual observation of the time series comparison plots (**Figure F-105** and **F-107**, respectively) qualitatively suggests good model performance.

At the Inlet to Aniwhenua Canal site (**Figure F-105**), the model simulated close match to available observed data between 1998 to 2012. However, in June 2014 to June 2015 five samples were collected that were higher than all samples collected previously, one of which was approximately four times higher than the previous maximum. Therefore, while the model was representative of the long-term historic conditions, the 2014-2015 data strongly influenced the PBIAS classification.

At the Matahina Dam site (**Figure F-107**), the model simulated good agreement to the available observed data prior to 2011, however, tended to under-predict TP concentrations in the following years. This suggests there may have been a change in the up-stream catchment (e.g. land use) that is not entirely reflected in the model.

7.4 Total Suspended Solids

Total suspended solids (TSS) refers to the material in a stream network that is held in suspension due to the turbulence and velocity of the water. Total suspended solids typically include fine particles such as clay and silt, and organic matter, and under high flows occasionally sand and coarse material. Sediment generation and the delivery of sediment to the stream network can be caused by natural erosion process and through a range of anthropogenic processes associated with land use, land management practices, and land disturbance. The temporal and spatial scale of suspended sediment generation varies greatly due to many contributing factors, such as; geomorphology, slope, land use type and rainfall intensity (Basher, 2013).

Although the process of sediment being delivered to waterways is a natural process, sedimentation rates are now an order of magnitude higher than prior to human activities (NIWA, 2014). This is especially true for the anthropogenic process of deforestation, and the subsequent development of agricultural land use and urban development. New Zealand has some of the highest erosion rates globally (Hicks *et al.*, 1996), and therefore increasing emphasis has been placed on the management and control of erosion processes and the resulting TSS concentration in stream networks over recent years.

Total suspended solids in streams and rivers can significantly degrade the ecological health by reducing light infiltration, suffocating sediment sensitive flora and fauna, and causing significant build up and sediment deposition in low velocity areas. In addition, other constituents such as total phosphorus often bind to TSS, and enter river and stream networks during erosion processes, and therefore also impact stream health.

The following sub-sections outline the development, calibration and simulation of TSS in the Kaituna and Rangitāiki WMA's using the Dynamic SedNET model plugin with SOURCE.

7.4.1 TSS Generation Using Dynamic SedNET

Dynamic SedNET (dSedNET) is a SOURCE plugin, designed to generate and deposit sediment through the hydrological network on a daily time scale. It is applied as a constituent generation model and simulates sediment generation and delivery processes from surficial hillslope and gully erosion separately. Dynamic SedNET works by generating mean annual hillslope erosion loads, using the Modified Universal Soil Loss Equation (MUSLE). The loads are then disaggregated internally to produce daily sediment concentrations using the rainfall and runoff component of SOURCE (the SMWBM).

While dSedNET is primarily a sediment generation model, it has been calibrated against measured total suspended solids data throughout the Kaituna and Rangitāiki WMAs. Therefore, dSedNET was applied to provide a representation of all total suspended solids, rather than only the suspended sediment component.

Although dSedNET can be configured to produce both hillslope and gully erosion, for this project only hillslope erosion processes were generated due to:

- The heavy data and computational requirements of simulating gully erosion;
- The assumption that hillslope processes are likely responsible for the majority of the sediment generated and deposited in both the Kaituna and Rangitāiki WMAs. Catchments with steeper slopes $>28^\circ$ are more susceptible to landslides however they can occur on slopes down to 15° , and the debris from these landslides frequently extend onto gentler slopes (Dymond, 2014., Basher, 2013); and
- The assumption that gully erosion can be implicitly included in the calibration outputs for hillslope processes by calibrating to measured instream TSS.

While the assumption was made that hillslope processes are likely responsible for the majority of sediment generated, it is acknowledged that this is not always true. For example, Hughes and Hoyle (2014) used sediment radionuclide concentrations to determine the contributions of river bank and hillslope sources of sediment in the Kopurererua Stream (which drains into the Tauranga Harbour). It was estimated over 90%

of sediment deposited at the mouth was generated from river bank sources. However, as noted in Hughes (2015), this study was unable to differentiate river bank sources from other sub-surface source such as mass wasting and urban development, and therefore may have over-estimated the importance of river bank sources, although still likely to provide a large contribution.

However, given river bank erosion was implicitly included in our assessment through calibration to measured instream TSS concentration data, the assumption of only modelling hillslope processes is considered appropriate.

The hillslope component of dSedNET was configured using the daily rainfall time series and the ten parameters outlined in **Table 88**. The input parameters were calculated externally and imported into the dSedNET plugin within SOURCE.

Table 88. dSedNET Parameters.

Parameter	Unit	Description
Mean annual rainfall	mm	The mean annual rainfall for each functional unit in each sub-catchment for the period of 1976 – 2016.
Mean summer rainfall	mm	The average summer rainfall for each functional unit in each sub-catchment for the period of 1976 – 2016.
R Factor Rainfall Threshold	mm	The threshold of minimum rainfall required before rainfall erosion will occur.
Alpha	Dimensionless	Alpha defines latitude and Beta and Eta are factors that define the erosivity nature of rainfall from the Earth's latitude. The values are not considered sensitive and default values were applied.
Beta	Dimensionless	
Eta	Dimensionless	
DWC	mg/L	The dry weather concentration of sediment (i.e. the base flow concentration present when no sediment is being generated or deposited in a catchment).
KLSC	Dimensionless	A factor that represents the soil erodibility, the slope length, the slope gradient and the vegetation cover of the sub-catchment.
HSDR	Ratio	The Hill Slope Delivery Ratio (HSDR) determines the percentage of sediment that arrives at the stream after generation.
Off Set	Days	The lag in time it takes sediment generated to be deposited into the stream network.

The dSedNET parameters were defined for every sub-catchment. A weighted average was applied to each land use type in the sub-catchment, based on percentage of area covered, to determine the average catchment KLSC value. The DWC, R factor and HSDR all used components of the KLSC value to produce separate relationships (**Section 7.4.2**). The mean annual rainfall and mean summer rainfall parameters were calculated using the NIWA VCSN data. The offset parameter was set to 180 to ensure high loads were simulated in winter. The remaining parameters (Alpha, Beta and Eta) were set to their default values.

The KLSC parameter was calculated using the method outlined in Cetin *et al.* (2016), Wilkinson *et al.* (2014), and Dymond *et al.* (2014). The equation applied to calculate KLSC is shown in **Equation 7**, while **Table 89** describes each component and shows its method of calculation.

Equation 7. The KLSC factor of the modified universal soil loss equation.

$$KLSC = K * LS * C$$

Table 89. Data requirements, methods and assumptions used to calculate the KLSC value.

Variable	Data required	Method
K – Soil erodibility	SMap soil texture geospatial layer and SMap particle size geospatial layer.	<p>Different soil textures were identified within both WMAs and assigned a K factor based on previous values utilised by Dymond <i>et al.</i> (2014);</p> <ul style="list-style-type: none"> • Sand = 0.05 • Silt = 0.35 • Clay = 0.20 • Loam = 0.25 <p>Previous studies have also applied a uniform value of 0.25 to all areas, this was trialled and deemed unsatisfactory for this project on the basis the uniform 0.25 value did not simulate the level of variability in TSS concentration that was observed in the available measured data.</p>
LS – Slope length and gradient factor	Raster files of the slope gradient and slope length (generated from the LINZ 15m DEM).	<p>The LS factor was calculated using the following equation:</p> $LS = \left(\frac{\lambda}{22.13} \right)^m$ <p>Where: λ is the slope length (m); and m is the S (slope gradient) factor.</p> <p>The S factor is calculated using the following equations:</p> $S = 10.8 \sin\theta + 0.03 \quad \text{where slope gradient} \leq 9\%$ $S = 16.8 \sin\theta - 0.05 \quad \text{where slope gradient} > 9\%$ <p>In previous studies (e.g. Cetin <i>et al.</i>, 2016) successful prediction of TSS has been achieved using a constant λ variable. This approach was applied, and a fixed value of 50 m was determined to be the most appropriate value for this project as it resulted in a similar range of LS values compared to other New Zealand examples.</p>
C – Vegetation Cover	Land use spatial layer provided by the BOPRC	<p>The C factor is applied to each land use based on vegetation cover. Using previous New Zealand examples (i.e. Dymond <i>et al.</i> 2014) the following C Factor values were applied;</p> <ul style="list-style-type: none"> • Bare ground, roads, rail and urban areas = 1.0 • Pasture and developed land = 0.01 • Forest and dense scrub = 0.005 <p>For plantation forest land use a C value of 0.23 was applied to represent the area weighted average value of typical plantation forest tree age composition (A number of sensitivity tests were undertaken on the impact of Vegetation Cover values assigned to each age class, and the final model values as agreed with BOPRC provided in Table 90.</p>

Information on typical plantation forest tree age class composition, along with representative aerial photograph examples for Timberlands forests in the Rangitāiki, were provided by Colin Maunder of Timberlands Limited. A number of sensitivity tests were undertaken on the impact of Vegetation Cover values assigned to each age class, and the final model values as agreed with BOPRC provided in **Table 90.**

Table 90. Plantation forest tree age class composition and assigned Vegetation Cover (C) values.

Tree Age Class (Years)	Area Cover (%)	Vegetation Cover (C)
0-2	7%	1
3-4	8%	0.75
5-10	19%	0.5
11-20	30%	0.01
20+	36%	0.005

Figure 115 and **Figure 116** present the spatial distribution of KLSC values assigned to the SOURCE sub-catchments in the Kaituna and Rangitāiki WMAs respectively. KLSC values range from 0.00 – 0.42 for the Kaituna WMA, and 0.00 – 0.66 for the Rangitāiki WMA. These values are consistent with values used in the application of SedNET in previous New Zealand Studies (Cetin *et al.*, 2016). The highest KLSC values typically occur where slopes are steep, and C values are high (e.g. for plantation forest).

Figure 115. KLSC value with the sub-catchments of the Kaituna WMA. (Refer A3 attachment at rear).

Figure 116. KLSC value with the sub-catchments of the Rangitāiki WMA. (Refer A3 attachment at rear).

7.4.2 dSedNET Parameterisation

Initial dSedNET model parameters were defined based on an understanding of land use and catchment characteristics. An iterative calibration procedure was then employed whereby key dSedNET model parameters were systematically adjusted to obtain the best fit between simulated and available measured TSS concentrations. The key model parameters adjusted were:

- R factor (rainfall threshold);
- DWC (dry weather concentration); and
- HSDR (hill slope delivery ratio).

The relationships developed to determine DWC from KLSC were determined based on the relationship required to match instream DWC at available gauged sites. The HSDR (which controls the ratio of sediment delivered instream) is known to vary significantly, and was considered the key calibration parameter.

After calibration was completed for sites with measured TSS data, relationships were established between catchment characteristics and the calibration parameters to inform what values to assign to unmonitored catchments, similar to the process undertaken for flow calibration and the SMWBM parameters described in in **Section 6.3**.

As TSS concentrations are typically not measured during peak storm events (e.g. flash flood events), event TSS concentrations were over-simulated to provide a conservative assessment in the absence of frequent and long-term measured data during storm events.

Peak flow sampling of TSS concentrations during two rainfall events are presented in Park (2010), with three samples collected on the 30th of June 2007 and two samples on the 17th of August 2007, at selected locations in the Kaituna catchment. However, these samples represent the concentration at an instantaneous point in time of the rainfall events, while dSedNET predicts average daily concentrations. Therefore, while the rainfall event sampling TSS concentrations presented in Park (2010) provide a useful upper limit of concentrations on those days, they were unable to be directly used for model calibration.

7.4.2.1 Rainfall Threshold (R)

The rainfall threshold value was determined based on vegetation cover (C factor) for each land use. It was assumed that areas of well established, dense vegetation (low C Factor) would require a higher rainfall threshold, under the premise there would be increased soil stability and canopy interception. In areas with high C factors it was assumed a lower rainfall threshold was required as the surface is more readily exposed to rainfall events and often has loose or poorly developed soils (i.e. pastures or bare ground). The above assumption is shown in **(Figure 117)**, with higher rainfall thresholds for a number of sub-catchments in the Rangitāiki WMA, which are predominately categorised by forest vegetation.

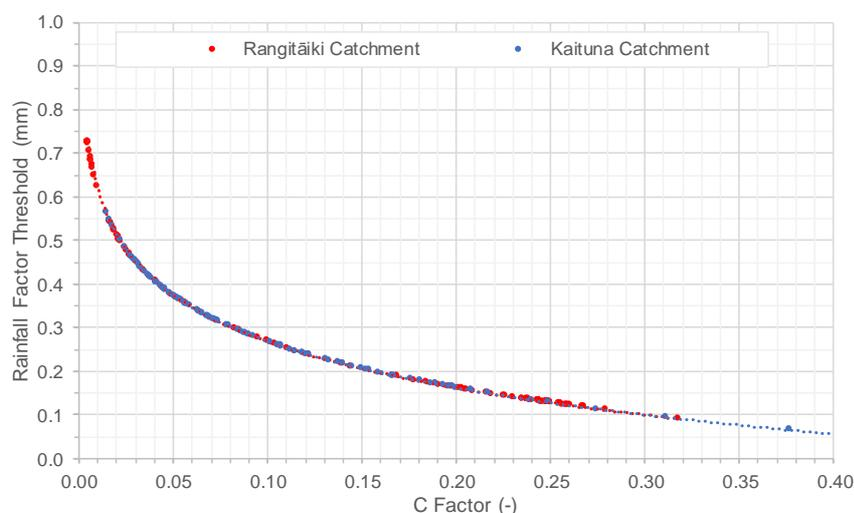


Figure 117. The relationships established between canopy (C) Factor and rainfall (R) Factor.

7.4.2.2 Dry Weather Concentration (DWC)

The DWC parameter controls the concentration of TSS instream during dry weather conditions, in the absence of rainfall or hillslope erosion events. Low base line concentrations of TSS in a stream or river is typically a function of low erodibility, low land disturbance and gentle or low gradients. To represent this, a relationship was developed between the KLSC Factor and the average DWC concentration required to mimic measured low flow concentrations of TSS at the available monitored locations.

Individual relationships were established between the KLSC and DWC parameters for the Kaituna and Rangitāiki WMAs and are shown in **Figure 119** and **Figure 120**. Individual relationships were required as the available measured data displayed a high degree of variability between the two WMAs.

The spatial extent of the various relationships applied in the Kaituna WMA are displayed in **Figure 118**.

Figure 118. Spatial extent of the four KLSC and DWC relationships developed for the Kaituna WMA. (See A3 attachment at rear).

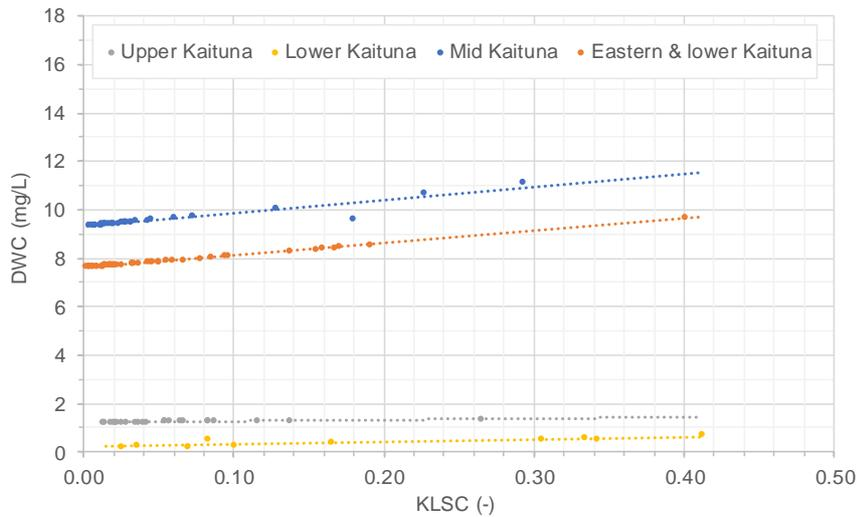


Figure 119. Relationship between KLSC and DWC assigned to the Kaituna WMA.

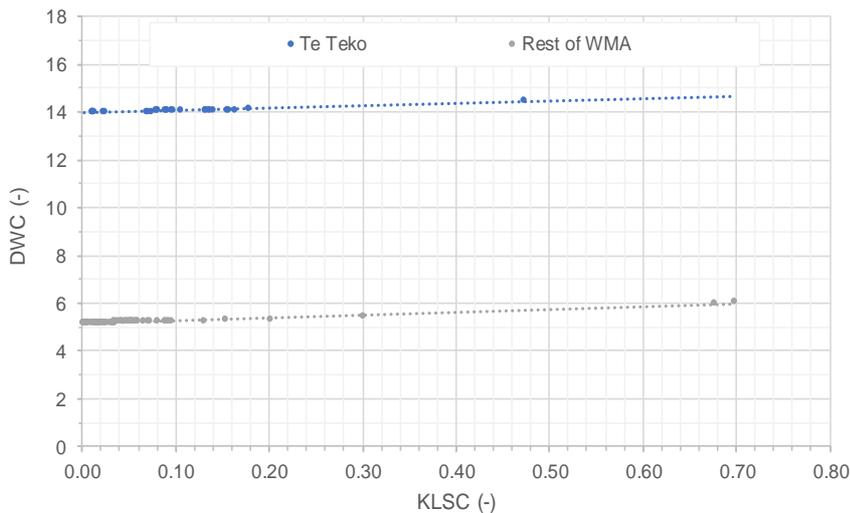


Figure 120. Relationship between KLSC and DWC assigned to the Rangitāiki WMA.

7.4.2.3 Hill Slope Delivery Ratio (HSDR)

The HSDR parameter was the most sensitive calibration parameter and strongly influenced the concentration of TSS delivered instream. To determine appropriate HSDR values for each sub-catchment, relationships were explored against a range of catchment physical properties, including:

- Slope (including the LS factor);
- Soil erodibility;
- Vegetation cover and density;
- Level of land development; and
- Parameters controlling surface runoff off within the SMWBM.

Average catchment slope was found to provide the best relationship with HSDR. The assumption was that catchments with a steeper average slope have the greatest influence on HSDR and the amount of TSS delivered to the river and stream network. These relationships are displayed in **Figure 121** and **Figure 122**.

In both the Kaituna and Rangitāiki WMAs multiple relationships were required to calibrate the HSDR at each gauge, as shown **Figure 121** and **Figure 122**. This is reflective of the differing physical attributes (primarily soil type, geology and land use) of the gauged TSS reaches. Ungauged catchments were assigned the relationship of the closest calibrated reach.

In general, the HSDR relationships show that as slope in a sub-catchment increases so does the rate of sediment delivery. However, the rate of delivery varies significantly between catchments. For example, in the Rangitāiki WMA the Whirinaki at Galatea catchment has a larger HSDR which corresponds to a steeper slope while Rangitāiki at Murupara has a smaller HSDR corresponding to its lower slope.

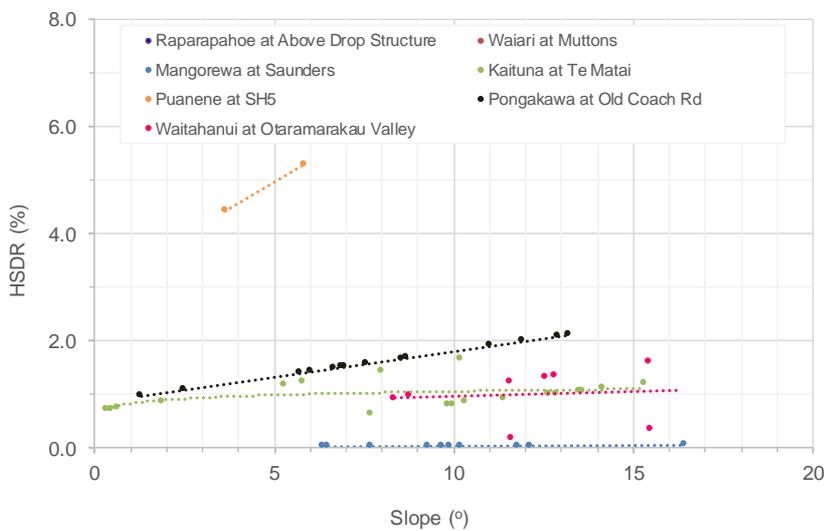


Figure 121. The relationships established between the slope and the HSDR value assigned to the Kaituna WMA.

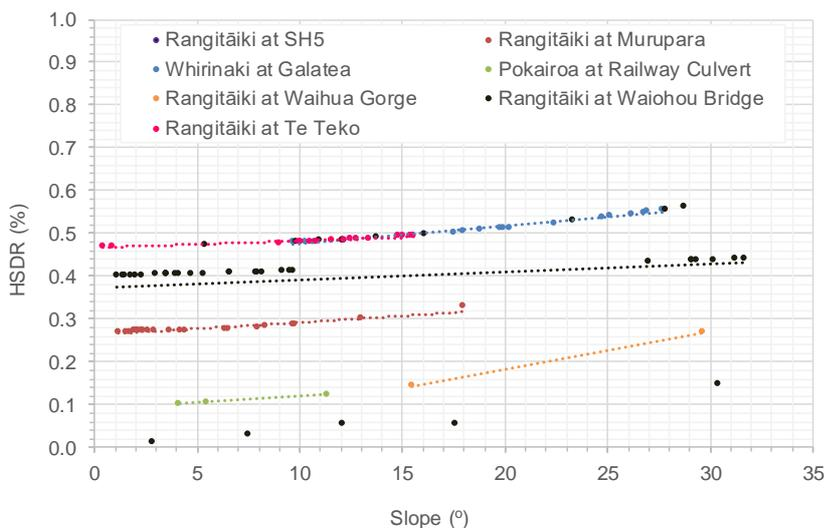


Figure 122. The relationships established between the slope and the HSDR value assigned in the Rangitāiki WMA.

A literature review was undertaken to compare the HSDR values determined for this project against similar catchments in New Zealand. However, while SedNET has been commonly applied across New Zealand, it was found the more recently developed dSedNET model has not been. Due to differing temporal resolutions of the models (annual vs. daily), model parameters could not be directly compared.

The HSDR's defined for the Kaituna WMA are of similar magnitude to values applied for the Burdekin catchment in Queensland (Wilkinson, *et al.*, 2014), where an average HSDR of 18% was applied, and for southern Australia (Freebairn, *et al.*, 2015), where 5% was determined as appropriate.

However, while the HSDR values assigned for the Rangitāiki WMA are lower than applied in the Kaituna and the two Australian studies mentioned above, the developers of dSedNET state they do not advocate a particular algorithm to determine HSDR, as delivery of sediment is limited by the transport capacity of runoff, and generally decreases with increasing particle size, soil infiltration capacity, and runoff transit time (Wilkinson *et al.*, 2014). Therefore, it is recommended HSDR is estimated based on available data, as was undertaken for both the Kaituna and Rangitāiki (**Section 7.4.2.3**).

7.4.2.4 Lake Contributions and Losses

To achieve satisfactory calibration, TSS concentrations were assigned to both lake inflows in the Kaituna Model. Lake Rotoiti was assigned a seasonal average concentration calculated from observed data. Lake Rotoehu was assigned a constant TSS input concentration based on analysis of the LAWA Lake Rotoehu observed data. The assignment of TSS concentration to groundwater from Lake Rotoehu was an exception to the assumption that constituent mass is removed from the model once passed to groundwater. This exception was required to achieve downstream calibration.

Deposition of suspended solids occurs within Lake Aniwanuiwa and Lake Matahina in the Rangitāiki catchment. An iterative calibration process was used to determine the proportional loss (deposition within the lakes) of TSS from the river and stream networks. A proportional loss of 50% and 65% off TSS in Lake Aniwanuiwa and Lake Matahina respectively was found to produce the highest level of calibration at the downstream TSS monitoring locations. Although the proportional loss of TSS through deposition is lower in Lake Aniwanuiwa than Lake Matahina, the total mass of deposition is greater in Lake Aniwanuiwa due to the larger load of TSS from the upstream Rangitāiki at Murupara and Whirinaki at Galatea catchments.

7.4.2.5 Summary of Calibrated dSedNET Model Parameters

A summary of the calibrated model parameter ranges applied in dSedNET for the Kaituna and Rangitāiki WMAs is provided in **Table 91**.

Table 91. Summary of the calibrated model parameter ranges applied in dSedNET.

Parameter	Kaituna	Rangitāiki
Mean annual rainfall (mm)	813 – 2366	1800 – 1225
Mean summer rainfall (mm)	178 – 492	396 – 259
R Factor Rainfall Threshold (mm)	0.9 – 7.9	0.6 – 7.9
Alpha (-)	1.7	1.7
Beta (-)	0.21	0.21
Eta (-)	0.38	0.38
DWC (mg/L)	0.2 – 2.1	0.3 – 2.7
KLSC (-)	0.0008 -0.0244	0.0003 – 0.5020
HSDR (%)	0.1 – 24.04	0.03 – 17.02
Off Set (days)	180	180

A summary of TSS calibration results are provided below in **Section 7.4.3**, and the full TSS calibration results for each TSS monitoring location are provided in **Appendix F**.

7.4.3 TSS Calibration Results

TSS calibration results for the primary calibration sites are detailed in **Sections 7.4.3.1** and **7.4.3.2** for the Kaituna and Rangitāiki WMAs respectively. The calibration results are presented in-text as comparison time series plots, summary statistics, and statistical performance measures for three representative primary calibration sites in the Kaituna and Rangitāiki WMAs. A boxplot comparison of measured and modelled TSS concentrations, PBIAS classifications and general comments for all primary calibration sites is also presented.

Summary statistics, time series comparison plots and probability plots which show the likely magnitude of TSS overestimation are provided in **Appendix F** for all primary and secondary calibration sites.

Additional secondary calibration was also undertaken at six sites in the Rangitāiki WMA, against monitoring data provided by Timberlands Ltd. In general, the model showed reasonable agreement to the limited additional monitoring data (ninety-eight data points, across six sites between 2005 - 2019). However, these data were useful secondary checks due to the fact they are located within forestry blocks. As this data is confidential, it has not been published or included in this report, and thus was only used as an internal secondary check during model development.

It should be noted, peak TSS concentrations are likely overestimated due to the absence of available measured data to accurately calibrate too during peak event periods. This provides a conservative analysis in that the simulated loads are greater than measured.

7.4.3.1 Kaituna

7.4.3.1.1 Kaituna at Te Matai (SCID26)

A time series comparison plot of measured and modelled TSS concentrations for the Kaituna River at the Te Matai gauge is shown in **Figure 122** and a comparison of summary statistics is presented in **Table 92**.

In general, the model over predicts TSS concentrations with the exception of the 25th and 50th percentile concentrations. This over prediction in the upper percentiles is consistent with the conservative approach to over-representing peak event concentrations and the absence of measured data during these periods.

The model performance at this site is Very Good based on the monthly PBIAS value of -1.8%.

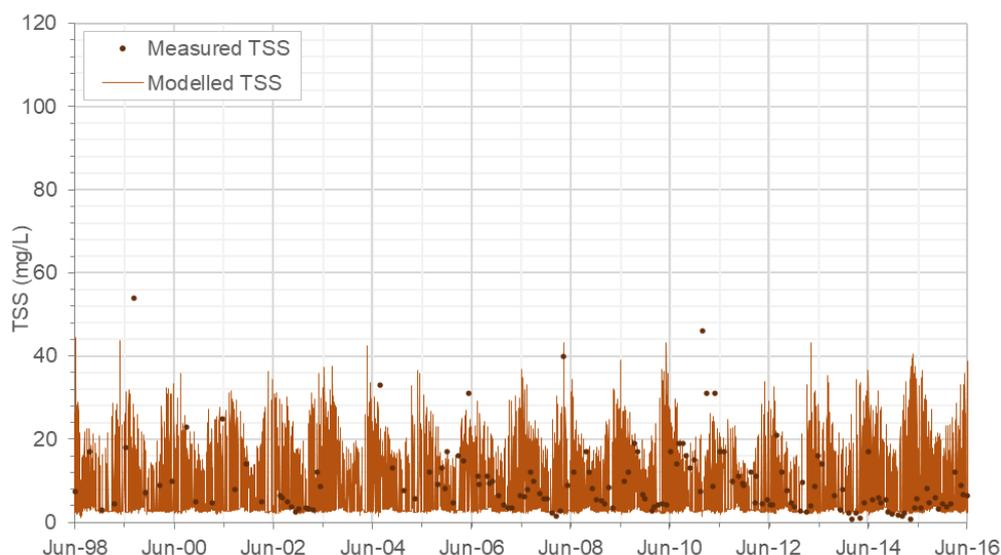


Figure 123. Time series comparison of measured and modelled TSS data for the Kaituna at Te Matai gauge.

Table 92. Summary of measured and modelled TSS concentration (mg/L) statistics for the Kaituna at Te Matai gauge (Jan 2011–Jun 2016).

	Modelled Data	Measured Data
Statistic	All data	All data
Count	2008	63
Mean	8.3	8.1
Standard Deviation	8.3	7.9
Minimum	1.5	0.7
5th Percentile	2.3	1.4
25th Percentile	2.6	3.7
50th Percentile	3.0	5.5
75th Percentile	13.9	9.5
95th Percentile	25.1	20.6
Maximum	43.3	46.0

7.4.3.1.2 Pongakawa at Old Coach Rd (SCID96)

A time series comparison plot of measured and modelled TSS concentrations for the Pongakawa River at the Old Coach Road gauge is shown in **Figure 124** and a comparison of summary statistics is presented in **Table 93**.

The model is shown to over predict TSS concentrations at all percentile concentrations, with the exception of the 50th percentile concentration. The over prediction of the minimum and 5th percentile concentrations suggest that generation of TSS during dry weather conditions is slightly over-predicted. The over prediction in the upper percentiles is due to the absence of measured data during the peak event periods when TSS concentrations are highest.

The model accuracy at this site is considered Very Good based on the monthly PBIAS value of -9.6%.

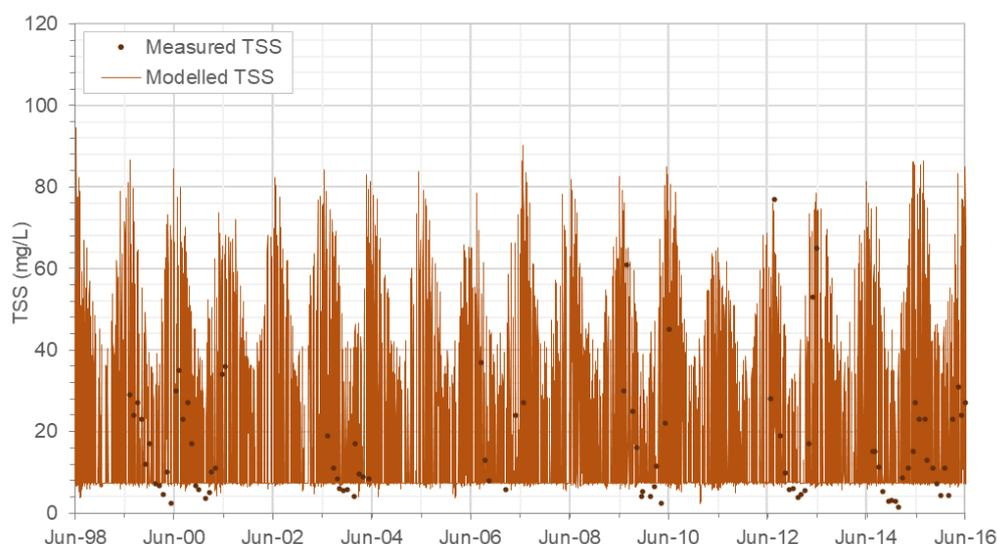


Figure 124. Constituent Hydrograph Comparing Measured and Modelled TSS data for the Pongakawa at Old Coach Rd gauge.

Table 93. Summary of measured and modelled TSS concentration (mg/L) statistics for the Pongakawa at Old Coach Rd gauge (Jan 2011–Jun 2016).

	Modelled Data	Measured Data
Statistic	All data	All data
Count	2008	36
Mean	19.7	17.1
Standard Deviation	19.2	17.1
Minimum	2.2	1.4
5th Percentile	6.9	2.9
25th Percentile	7.4	5.5
50th Percentile	7.4	11.1
75th Percentile	32.3	23.0
95th Percentile	60.4	56.0
Maximum	96	77.0

7.4.3.1.3 Waitahanui River (SCID114)

A comparison time series plot of measured and modelled TSS concentrations for the Waitahanui River at the site located in SCID114 is shown in **Figure 125** and a comparison of the summary statistics are presented in **Table 94**.

In general, the model was shown to over predict TSS concentrations. Similar to the Te Matai and Old Coach Road sites, the over prediction in the upper percentiles is likely due to the absence of measured data during the peak event periods when TSS concentrations are highest.

The model accuracy at this site is Not Satisfactory according to the monthly PBIAS value of -26%. However, visual observation of the time series comparison plot below, and probability plot (**Appendix F, Figure F-77**), demonstrate that the model produces reasonable agreement to average TSS concentrations. Therefore, the model is considered to provide a reasonable representation of average TSS concentrations, but model performance should be acknowledged when interrogating model results over shorter time scales (e.g. daily concentrations).

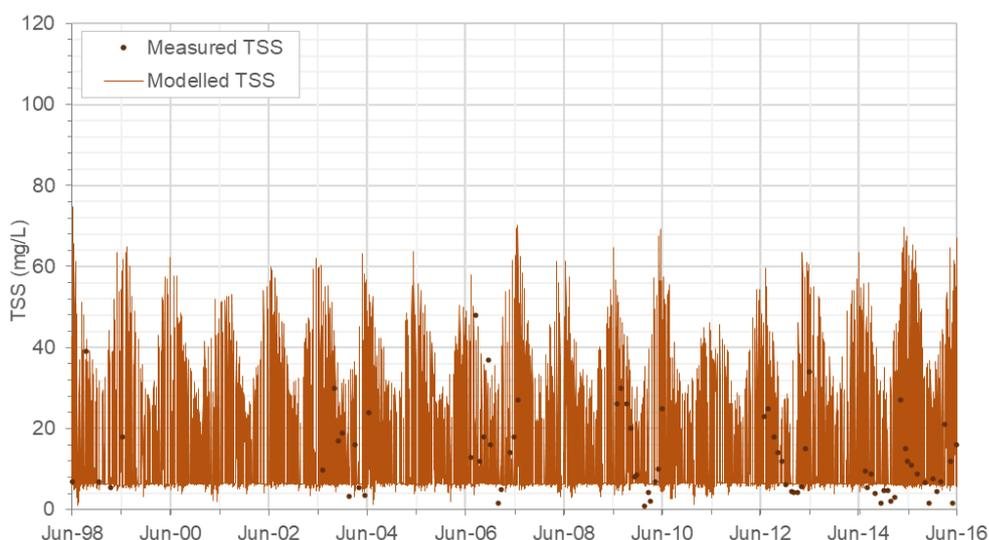


Figure 125. Constituent Hydrograph Comparing Measured and Modelled TSS data for the SCID114 site.

Table 94. Summary of measured and modelled TSS concentration (mg/L) statistics for the SCID114 site (Jan 2011–Jun 2016).

	Modelled Data	Measured Data
Statistic	All data	All data
Count	2008	35
Mean	15.5	10.3
Standard Deviation	14.6	8.0
Minimum	1.2	1.6
5th Percentile	5.5	1.7
25th Percentile	6.1	4.5
50th Percentile	6.4	7.6
75th Percentile	25.2	14.5
95th Percentile	46.2	25.6
Maximum	69.7	34.0

7.4.3.1.4 Overall Kaituna Performance

The boxplots presented in **Figure 126** provide a comparison of measured and modelled TSS concentrations for all primary calibration sites in the Kaituna WMA during the period January 2011 to June 2016.

In general, the model closely predicts the 25th percentile and median concentrations, but over predicts at the higher percentiles and maximum concentrations in comparison to the available measured data. This is consistent with the aim of conservatively over predicting the higher concentrations due to the absence of measured data during these periods. The model also successfully predicts the wider range and higher median and 75th percentile TSS concentrations observed at Pongakawa at Old Coach Road and SH2 in comparison to the remaining calibration sites.

The monthly PBIAS values range from -110% to -1.8% which corresponds to model performance classifications of Not Satisfactory to Very Good. However, it should be noted that both the PBIAS and RMSE performance statistics are strongly influenced by the conservative approach of over prediction due to the absence of measured TSS concentration data during peak event periods.

A summary of model performance at Te for all primary calibration sites is provided in **Table 95**.

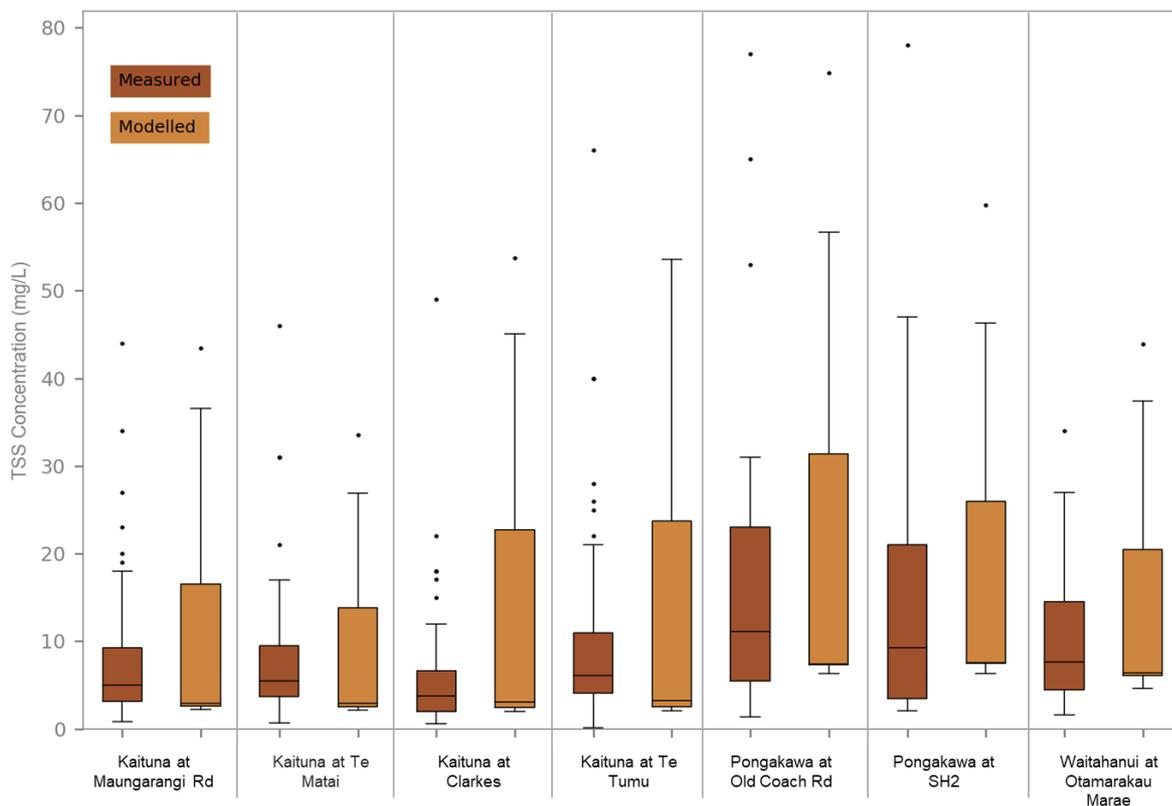


Figure 126. Box plot comparison of measured and modelled TSS concentration for all primary calibration sites in the Kaituna WMA.

Table 95. Summary of TSS model performance at the primary calibration sites in the Kaituna WMA.

Location	Observed Data Points	Model Accuracy (PBIAS)		RMSE	General Comments
		Value (%)	Class		
Kaituna at Maungarangi Rd (SC22)	62	-20	Satisfactory	13.2	The range in TSS concentrations modelled was greater than observed at the 25 th and 75 th percentiles, however, the modelled and measured median TSS concentrations were similar. Both data sets have multiple outliers identified, representing infrequent larger events.
Kaituna at Te Matai (SCID26)	63	-1.8	Very Good	11.0	The range in TSS concentrations modelled was greater than observed at the 75 th percentile and maximum concentration, however, the modelled and measured 25 th percentile and median TSS concentrations were similar.
Kaituna at Clarkes (SC53)	61	-110	Not Satisfactory	17.2	The range in TSS concentrations modelled was greater than observed at the 25 th and 75 th percentiles, however, the modelled and measured median TSS concentrations are similar. Both data sets have multiple outliers identified, representing infrequent large events.
Kaituna at Te Tumu (SC57)	77	-39	Not Satisfactory	23.2	Modelled TSS concentrations were over predicted at the 75 th percentile and maximum concentration. However, the modelled 25 th percentile and median concentration are similar to those observed in the measured data.
Pongakawa at Pumphouse (SC96 Forest)	36	-9.6	Very Good	23.2	The modelled TSS concentrations were over predicted at the 25 th and 75 th percentile and maximum concentrations, while the median concentration was slightly under predicted in comparison to the measured data.
Pongakawa at Old Coach Rd (SC96)	35	-7	Very Good	20.6	The modelled TSS concentrations were over predicted at the 25 th and 75 th percentile and maximum concentrations, while the median concentration was slightly under predicted in comparison to the measured data.
Pongakawa at SH2 (SC98)	35	-26	Not Satisfactory	14.2	The modelled TSS concentration was over predicted at the 25 th percentile, while good agreement was predicted at the median and 75 th percentile concentrations.

While a number of primary calibration sites are considered Not Satisfactory based on the PBIAS classification, visual observation of the time series plot and comparison of summary statistics qualitatively suggests the model is capable of predicting the general magnitude, range, and average TSS concentrations.

Overall, the model provides a suitable tool for the prediction of the general magnitude and spatial variation of TSS concentrations across the Kaituna WMA. The model performance is considered appropriate for undertaking land use change and mitigation scenarios at a regional scale when considering results over longer time-periods (e.g. annual average concentrations). However, given the temporal variability in observed and modelled TSS concentrations, caution is advised when interpreting model results at a finer (e.g. daily) timescale for this constituent.

7.4.3.2 Rangitāiki

7.4.3.2.1 Rangitāiki at Murupara (SCID26)

A time series comparison plot of the measured and modelled TSS concentrations for Rangitāiki at Murupara is shown in **Figure 127**, and a comparison of summary statistics is presented in **Table 96**.

In general, the model is shown to over predict TSS concentrations throughout the calibration period. The model closely predicts the minimum to 50th percentile concentrations, however, like the Kaituna WMA sites, the over prediction in the upper percentiles is due to the absence of measured data during the peak event periods when TSS concentrations are highest.

The model performance at this site is Not Satisfactory based on the monthly PBIAS value of -59%.

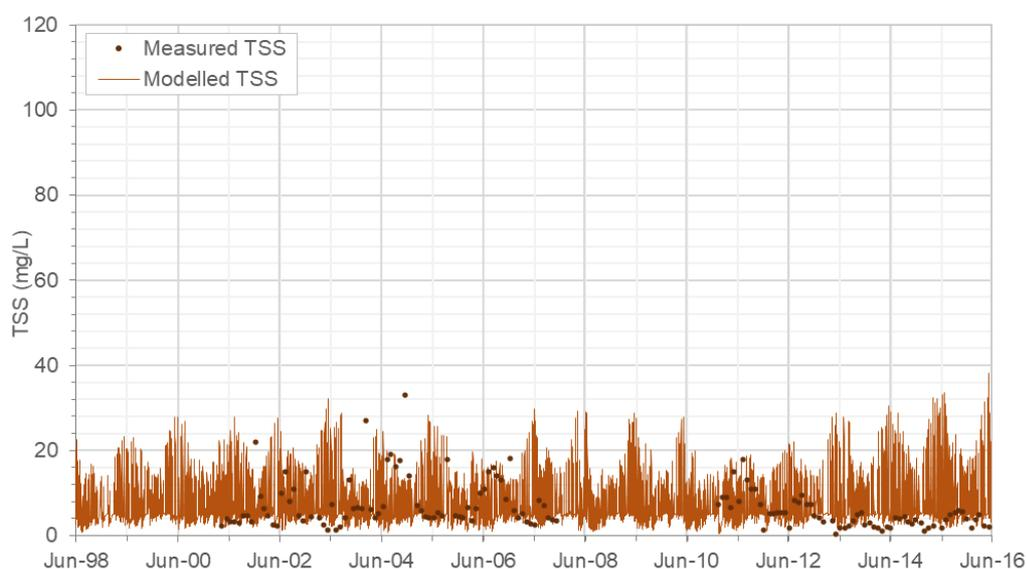


Figure 127. Constituent Hydrograph Comparing Measured and Modelled TSS data for the Rangitāiki at Murupara gauge.

Table 96. Summary of measured and modelled TSS concentration (mg/L) statistics for the Rangitāiki at Murupara gauge (Jan 2011–Jun 2016).

	Modelled Data	Measured Data
Statistic	All data	All data
Count	1980	64
Mean	7.8	5.0
Standard Deviation	6.2	3.4
Minimum	0.5	0.4
5th Percentile	2.5	1.4
25th Percentile	4.0	2.2
50th Percentile	5.0	4.3
75th Percentile	10.7	6.0
95th Percentile	21.3	11.0
Maximum	38.1	18.0

7.4.3.2.2 Whirinaki at Galatea (SCID47)

A time series comparison plot of measured and modelled TSS concentrations is shown in **Figure 128**, and a comparison of summary statistics is presented in **Table 97** for the Whirinaki River at Galatea gauge.

The model accurately predicts concentrations between the minimum and 50th percentile of measured concentrations, however, over predicts the higher percentile concentrations.

The model performance at this site is considered Not Satisfactory based on the monthly PBIAS value of -134%.

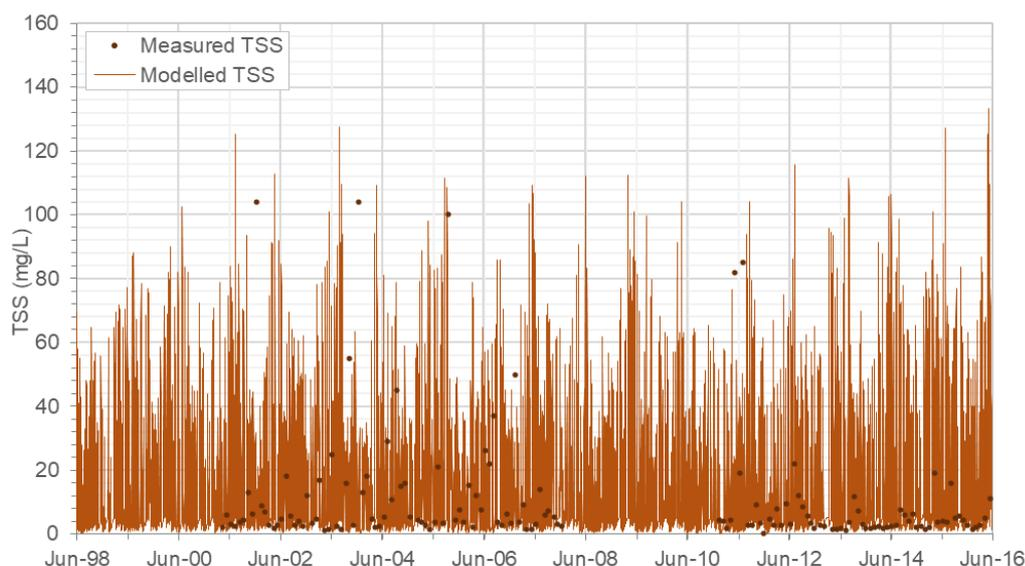


Figure 128. Constituent Hydrograph Comparing Measured and Modelled TSS data for the Whirinaki at Galatea gauge.

Table 97. Summary of measured and modelled TSS concentration (mg/L) statistics for the Whirinaki at Galatea gauge (Jan 2011–Jun 2016).

	Modelled Data	Measured Data
Statistic	All data	All data
Count	1980	65
Mean	15.9	7.4
Standard Deviation	21.8	14.4
Minimum	0.2	0.3
5th Percentile	1.0	1.5
25th Percentile	2.3	2.2
50th Percentile	4.2	3.4
75th Percentile	24.0	6.2
95th Percentile	63.8	19.0
Maximum	133.5	85.0

7.4.3.2.3 Rangitāiki River at Matahina (SCID34)

A time series comparison plot and summary statistics of the measured and modelled TSS for the Rangitāiki River at the secondary site located in SCID34 (downstream of Lake Matahina) are shown in **Figure 129** and **Table 98** respectively.

Similar to the previous calibration locations, predicted TSS concentrations at SCID34 closely match at the minimum to 50th percentile concentrations, but are over predicted at the higher percentile concentrations. The model also accurately predicts the general temporal pattern displayed in the sparse observed data, with higher TSS concentrations occurring in summer in comparison to winter.

The model performance at this site is considered Not Satisfactory based on the monthly PBIAS value of -50%.

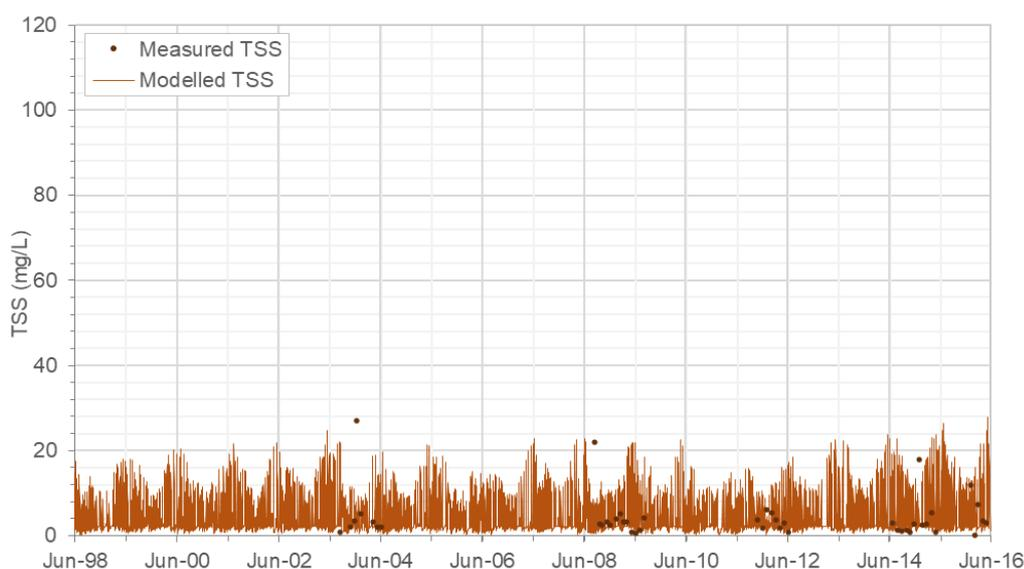


Figure 129. Constituent Hydrograph Comparing Measured and Modelled TSS data for the SCID34 site.

Table 98. Summary of measured and modelled TSS concentration (mg/L) statistics for the SCID34 site (Jan 2011–Jun 2016).

	Modelled Data	Measured Data
Statistic	All data	All data
Count	1980	23
Mean	4.8	3.8
Standard Deviation	5.0	4.0
Minimum	0.1	0.8
5th Percentile	0.9	0.8
25th Percentile	1.6	1.6
50th Percentile	2.1	2.9
75th Percentile	7.2	4.6
95th Percentile	15.9	11.5
Maximum	27.8	18.0

7.4.3.2.4 Overall Rangitāiki Performance

The boxplots presented in **Figure 130** provides an overview of measured and modelled TSS in various streams and rivers within the Rangitāiki Catchment for the period 2011-2016.

PBIAS values range from -141% to 6.2% which corresponds to model performance classifications of Not satisfactory to Very Good (**Table 99**). The RMSE produced have values ranging from 6.1 to 30.5 mg/L. However, it should be noted both the PBIAS and RMSE performance statistics are strongly influenced by the conservative approach of over prediction, due to the absence of measured TSS concentration data during peak event periods.

Comments on the model's performance in predicting TSS concentrations at available monitoring locations in the Rangitāiki catchment are provided in **Table 99**.

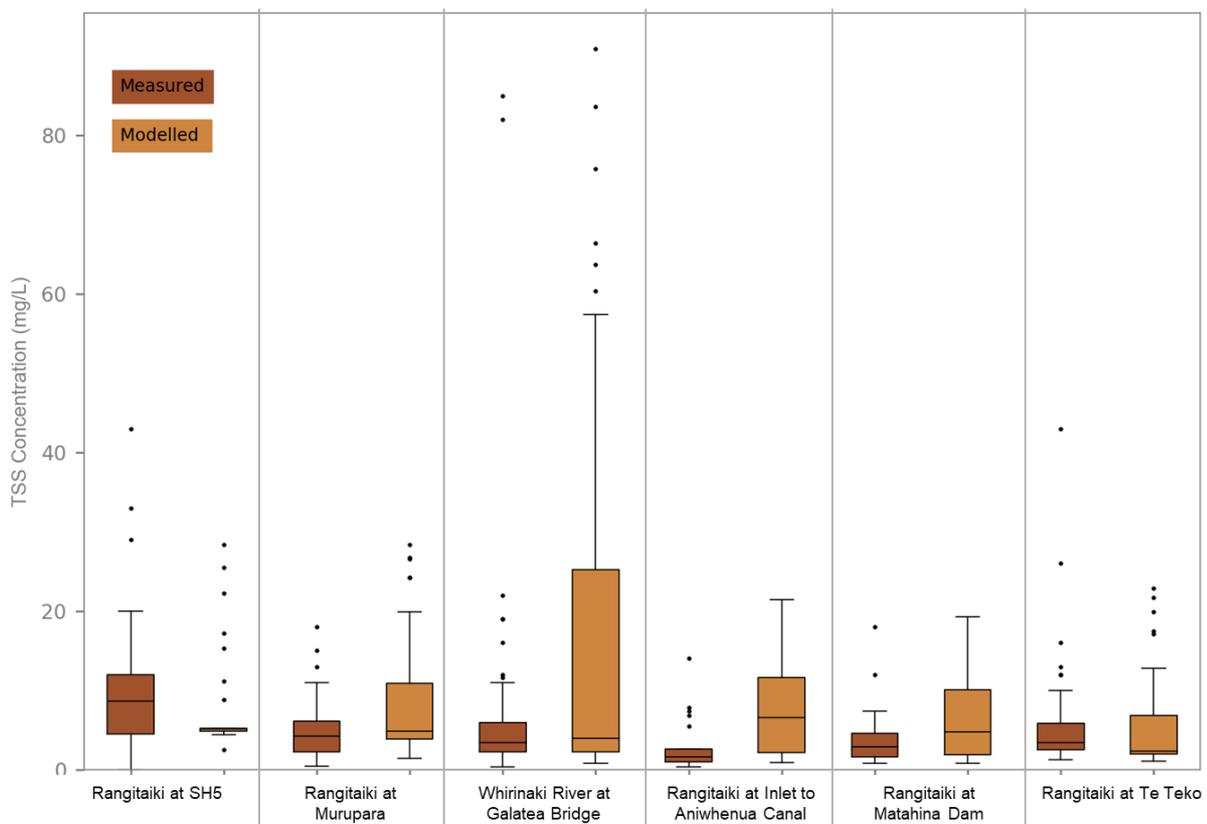


Figure 130. Box Plots Comparing Measured and Modelled TSS data for all Main Sites in Rangitāiki Catchment.

Table 99. Summary of TSS model performance at the primary calibration sites in the Rangitāiki WMA.

Location	Observed Data Points	Model Accuracy (PBIAS)		RMSE	General Comments
		Value (%)	Class		
Rangitāiki at SH5 (SC1)	29	24	Not Satisfactory	13.1	The modelled TSS concentrations were under predicted, with the modelled 75 th percentile concentration similar to the 25 th percentile observed in the measured data.
Rangitāiki at Murupara (SC26)	63	-59	Not Satisfactory	8.9	The magnitude and range of modelled concentrations is similar to those observed in the measured data.
Whirinaki at Galatea Bridge (SC47)	64	-134	Not Satisfactory	30.5	The range in TSS concentrations were over predicted in comparison to the measured data. The 75 th percentile concentration of the modelled TSS concentrations was larger than the maximum measured concentration (excluding a number of outlier samples).
Rangitāiki at Inlet to Aniwhenua Canal (SC30)	21	-141	Not Satisfactory	7.7	Modelled and observed median TSS concentrations are similar, however, the range in modelled concentrations is larger than seen in the measured data.
Rangitāiki at Matahina Dam (SC34)	23	-50	Not Satisfactory	6.1	Modelled and observed median TSS concentrations are similar, however, the range in modelled concentrations is larger than seen in the measured data.
Rangitāiki at Te Teko (SC37)	62	6	Very Good	8.7	Modelled and observed median TSS concentrations are similar, however, the range in modelled concentrations is smaller than seen in the measured data.

While five of the primary calibration sites are considered Not Satisfactory based on the PBIAS classification, visual observation of the time series plot and comparison of summary statistics (e.g. median concentrations) qualitatively suggests the model is capable of simulating the general magnitude, range, and average TSS concentration.

Overall, the model provides a suitable tool for the prediction of the general magnitude and spatial variation of TSS concentrations across the Rangitāiki WMA. The model performance is considered appropriate for undertaking land use change and mitigation scenarios at a regional scale when considering average concentrations over longer time-periods (e.g. annual average concentrations) and the relative difference (i.e. percentage change) between scenarios. However, given the temporal variability in observed and modelled TSS concentrations, caution is advised when interpreting model results at a finer (e.g. daily) timescale.

7.5 Escherichia Coli

Escherichia coli (*E. coli*) is a group of bacteria commonly found in the intestines of warm-blooded animals (including humans), which in freshwater environments are often used to indicate the presence of harmful pathogens (such as *Campylobacter*) from animal and human faeces. Therefore, *E. coli* concentrations in a freshwater body provide a measure of its potential risk to public health.

Sources of faecal contamination in rivers are diverse and range from point source wastewater discharges from municipal and industry treatment works to diffuse sources such as the run-off of faecal matter deposited by wild and feral animals. In New Zealand grazing livestock are a key source of contamination of faecal material through direct deposition into rivers and streams where access is not restricted, and through transport in overland and subsurface flow (Collins & Rutherford, 2004).

E. coli can persist for varying periods of time in open environments. *E. coli* can survive in soil, manure and water (Van *et al.*, 2011., Kudva *et al.*, 1998; Jiang *et al.*, 2002; Vital *et al.*, 2008). *E. coli* can also migrate between these zones, for instance *E. coli* can leach from the surface through the soil zone to sub surface flow (Mankin *et al.*, 2007). However, fluctuating environmental conditions typically impair their growth (Van *et al.*, 2011).

E. coli are more likely to survive and grow in environments which have a stable temperature compared to fluctuating environments (Van *et al.*, 2011). Within the headwaters of the Kaituna and Rangitāiki the fluctuating nature of water and temperature is likely to cause larger *E. coli* die-off.

E. coli die-off is more pronounced during times of temperature increase (causing more stress due to energy use) compared to decreases in temperature (Semenov *et al.*, 2007). Although the coastal areas in the BOP region can have higher temperatures, the constant input of bacteria from diffuse sources (rural and urban areas) cause a continual presence of *E. coli* in the river and stream networks.

The following sub-sections describe the method used to develop the *E. coli* generation model and presents the results of the *E. coli* constituent calibration against available measured data.

7.5.1 *E. coli* Generation

To predict the generation of *E. coli* from each sub-catchment, an *E. coli* generation index was developed. The *E. coli* generation index was formed on the basis that *E. coli* are predominantly transported by overland flow (the quick flow component), in addition to smaller contributions through sub-surface flow pathways. The index characterised *E. coli* generation to the stream network based on the following catchment characteristics:

- **Stocking Rate** – Increased concentrations of *E. coli* generation are well correlated to increased stocking rates and vice versa (Collins and Rutherford, 2004) – catchment stocking rates are shown in **Figure 86** and **Figure 87**.
- **Slope** – Sub-catchments with steeper slopes will transport bacteria across the surface more readily compared to flat lands where runoff may pond.
- **Vegetation cover** – It is assumed that flow and *E. coli* tend to become entrapped on the landward side of riparian areas, therefore reducing concentrations with increases in the degree of vegetation density.

The *E. coli* generation index was calculated as a weighted sum based on the above catchment characteristics. The largest weighting was assigned to the catchment stocking rate as this is the source of *E. coli* generation, and lower weightings assigned to the catchment slope and vegetation cover which influence the transportation.

Individual relationships were then developed relating the Dry Weather Concentration (DWC) and Event Mean Concentration (EMC) to the *E. coli* generation index. The relationships were developed using an iterative calibration procedure where the DWC and EMC were systematically adjusted, with the aim of over prediction of in-stream *E. coli* concentrations compared to available measured data, as the simulated concentrations

would be reduced once the process of *E. coli* decay (die-off) are included in the model (as described in **Section 7.5.1.1**). These relationships are shown in **Figure 131** through **Figure 134**.

The higher *E. coli* concentrations for a given index value applied to the Kaituna catchment in comparison to the Rangitāiki catchment is due to the difference in measured *E. coli* concentrations between the two WMAs. An analysis was undertaken on the primary measured Kaituna and Rangitāiki sites for the period 1st January 2011 to 30 June 2016 and it was found the Kaituna sites have a median and 95th concentration of 60 CFU/100 ml and 940 CFU/100 ml respectively, compared to the Rangitāiki praimry sites which have a median and 95th percentile measured concentration of 22 CFU/100 ml and 372 CFU/100 ml respectively.

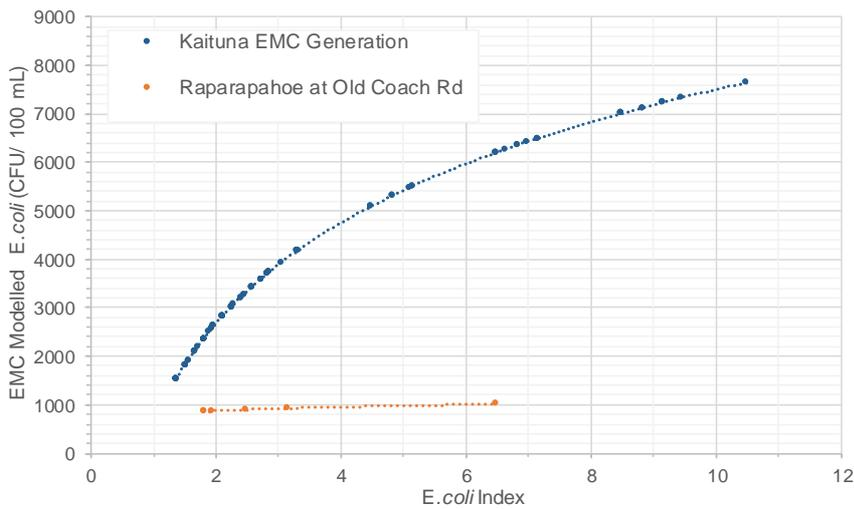


Figure 131. Kaituna EMC *E. coli* generation relationship.

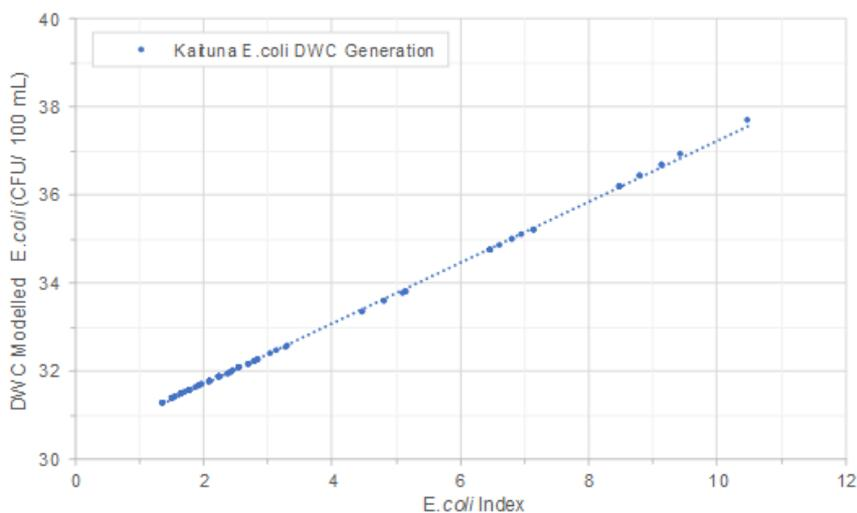


Figure 132. Kaituna DWC *E. coli* generation relationship.

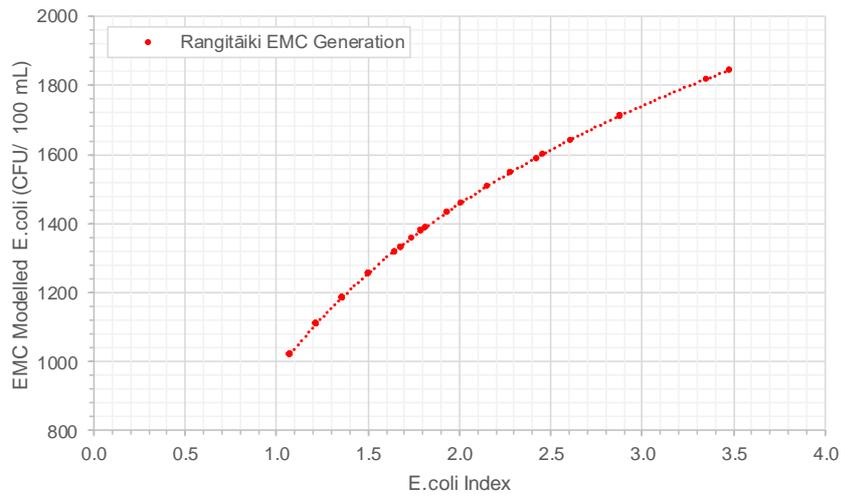


Figure 133. Rangitāiki EMC *E. coli* generation relationship.

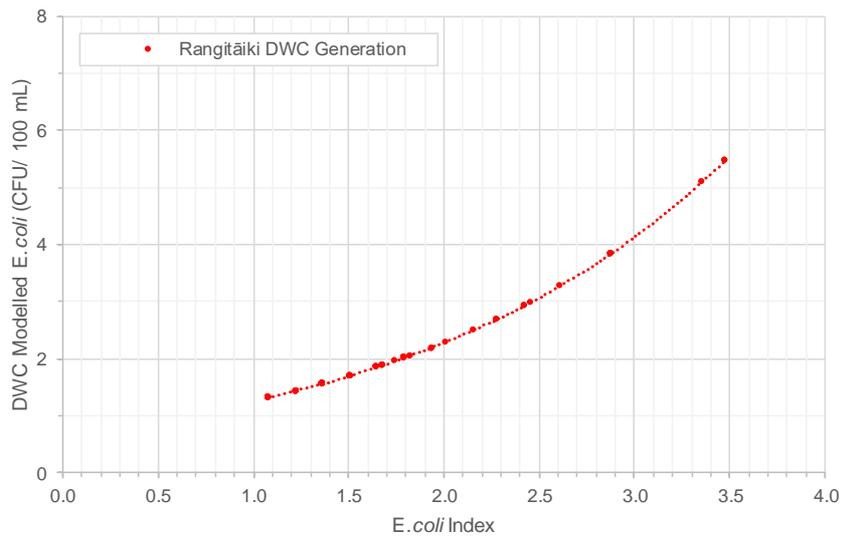


Figure 134. Rangitāiki DWC *E. coli* generation relationship

7.5.1.1 E. coli Decay

A first order decay function (1st Order Kinetic k-C* filter) was applied in the models to represent the natural die-off of *E. coli* as they are transported through the catchment and river network. The function applied describing *E. coli* decay is given in **Equation 8**, and parameterisation of the function is described below.

Equation 8. *E. coli* decay function.

$$\frac{C_{out} - C^*}{C_{in} - C^*} = e^{-\frac{k}{q}}$$

Where:

C* is the background concentration (mg/L)

C_{in} is the input concentration (mg/L)

C_{out} is the output concentration (mg/L)

k is the decay rate constant

q is the hydraulic loading (flow rate per surface area) of the treatment area.

C* is the event background concentration, which was applied at all times during higher flow. This is the same as the C*-slow flow which is the background concentration assigned to baseflow and is applied when flows are largely confined to a low flow channel.

The event background and slow flow concentrations were assigned based on pooled measured *E. coli* data from headwater sub-catchments (SC42, 51 & 75) in the Rangitāiki WMA with 100% native forest cover. The event background (quick flow) concentration was defined as the concentrations two standard deviations below the mean, and the slow flow concentration as the 5th percentile concentration of the pooled measured *E. coli* data. These were assumed to be representative of the natural *E. coli* concentrations found within catchments without the influence of anthropogenic processes and land use change.

The K and the K-slow flow represent the decay rate constants applied to the quick flow and slow flow components (EMC and DWC) respectively. The quick flow and slow flow decay rate constants control the rate of exponential decay of concentrations towards background values (C* and C*-slow flow). *E. coli* die-off is strongly influenced by temperature and therefore, catchment elevation was used as a proxy for temperature to determine the decay constants for each catchment. Higher elevation catchments were assigned larger decay rate constants than low elevation catchments and vice versa.

The treatment area specified for hydraulic loading (q) was the catchment area, on the basis that the decay occurs as *E. coli* are transported through the catchment. Therefore, *E. coli* transported through larger catchments were subject to increased decay compared with smaller catchments.

The most reliable measured *E. coli* monitoring sites are located upstream in the catchments, as monitoring sites downstream on the Kaituna and Rangitāiki plains may be influenced by tidal inflows. Therefore, to provide a conservative assessment and account for additional sources of *E. coli* in the plains which could not be explicitly included in the model (management of dairy shed wastes including discharge to land, waste treatment ponds and leaky sewage pipes) the low elevation catchments were assigned a higher weighting and no decay was applied.

The relationships describing *E. coli* decay as a function of catchment elevation are shown in **Figure 135** and **Figure 136** for the Kaituna and Rangitāiki WMAs respectively. Both the Kaituna and Rangitāiki WMAs show the relationship of increased decay occurring in catchments at a higher elevation, however, the rate of increase in decay with elevation changes between catchments.

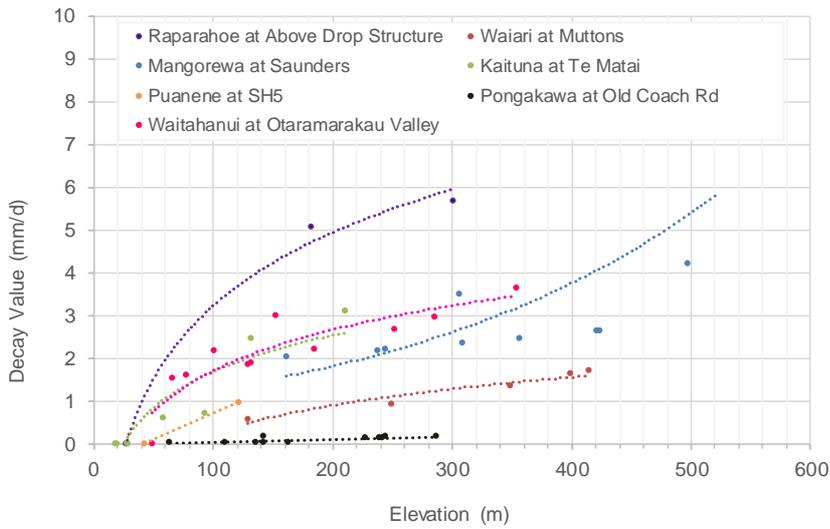


Figure 135. Kaituna decay model relationship with catchment elevation.

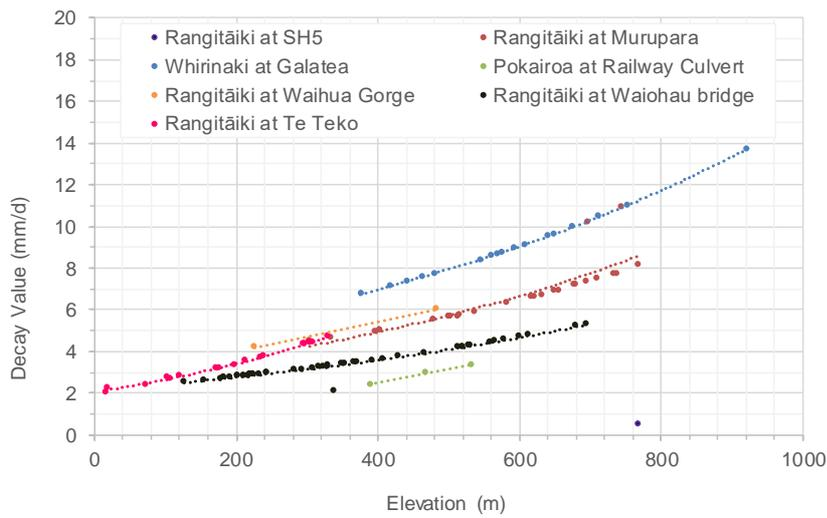


Figure 136. Rangitāiki decay model relationship with catchment elevation.

The assumptions associated with the generation of the *E. coli* constituent are summarised in **Table 100**.

Table 100: Assumptions associated with *E. coli* constituent generation.

Assumption	Explanation
Vegetation cover, Slope and Stocking rates control the generation of <i>E. coli</i> within the catchment.	Areas with low vegetation cover, high slope and stocking rates produce increased <i>E. coli</i> generation and vice versa.
Background <i>E. coli</i> concentrations are equal to concentrations found in existing natural state environments.	This was found by analysing the measured <i>E. coli</i> in those catchments in the Kaituna and Rangitāiki WMAs which are 100% native forest and using the second standard deviation from the mean as the quick flow background and the 5%ile as the baseflow background.
Decay model surface area occurs over the entire catchment.	The surface area for the quick flow and baseflow hydraulic loading treatment area was equal to the catchment area. Within SOURCE flow is generated within the whole sub-catchment so the decay model is applied to the whole surface area and not just reserved for the main instream area.
Areal decay rate is a function of temperature, and therefore also elevation.	<i>E. coli</i> die-off is strongly influenced by temperature and sunlight (Collins & Rutherford, 2004). The areal decay rate constant was defined based on a relationship using catchment elevation as a proxy for a range of environmental conditions such as temperature, clarity and solar radiation, which are known to influence <i>E. coli</i> decay rates. The decay applied was the same for both the quick flow and slow flow components as temperature likely affect both processes similarly.

7.5.2 *E. coli* Calibration Results

The *E. coli* calibration results for the primary calibration sites are detailed in **Section 7.5.2.1** and **Section 7.5.2.2** for the Kaituna and Rangitāiki WMAs respectively. The calibration results are presented in-text as comparison time series plots, summary statistics, and statistical performance measures for three representative primary calibration sites in the Kaituna and Rangitāiki WMAs. A boxplot comparison of measured and modelled *E. coli* concentrations, PBIAS classifications and general comments for all primary calibration sites are also presented.

Time series comparison plots and summary statistics for all primary and secondary monitoring sites are presented in **Appendix F**.

7.5.2.1 Kaituna

7.5.2.1.1 Kaituna at Te Matai (SCID26)

A time series comparison plot and comparison summary statistics of measured and modelled *E. coli* concentrations for the Kaituna River at the Te Matai gauge are shown in **Figure 137** and **Table 101** respectively.

The model closely simulated the minimum observed *E. coli* concentration, however under simulated at all higher percentile concentrations with the exception of the maximum concentration which was over predicted.

The model performance at this site is considered Not Satisfactory based on the monthly PBIAS value of 63%.

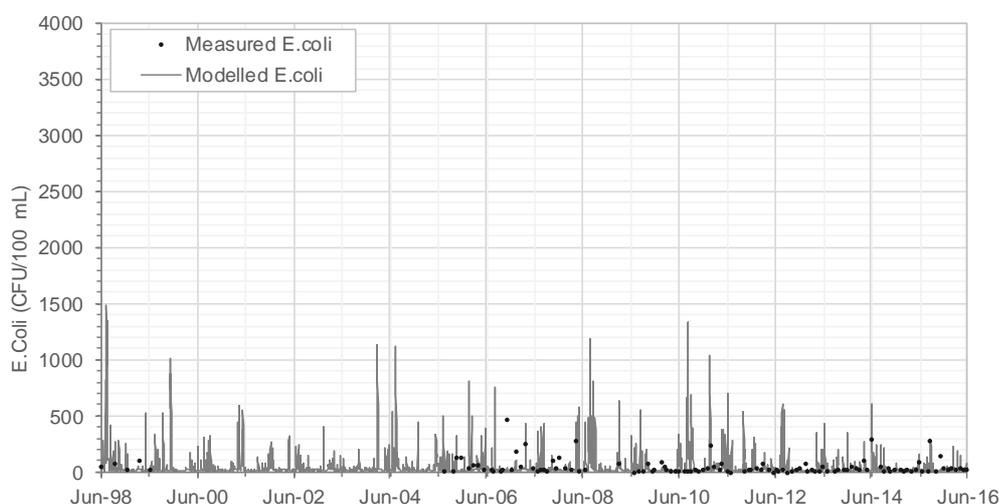


Figure 137. Constituent Hydrograph Comparing Measured and Modelled *E. coli* concentrations for the Kaituna at Te Matai gauge.

Table 101. Summary of measured and modelled *E. coli* concentration (CFU/100 ml) statistics for the Kaituna at Te Matai gauge (Jan 2011–Jun 2016).

	Modelled Data	Measured Data
Statistic	All data	All data
Count	2,008	63
Mean	37	77
Standard Deviation	74	125
Minimum	7	4
5th Percentile	9	14
25th Percentile	12	24
50th Percentile	14	44
75th Percentile	23	61
95th Percentile	168	276
Maximum	1,031	870

7.5.2.1.2 Pongakawa at Old Coach Rd (SCID96)

A time series comparison plot and comparison summary statistics of measured and modelled *E. coli* concentrations for the Pongakawa River at the Old Coach Road gauge are shown in **Figure 138** and **Table 102** respectively.

The model slightly over predicted the minimum and 5th percentile *E. coli* concentration, but under predicted concentrations at all higher percentiles at the Old Coach Road monitoring site. The model did however predict the temporal variation in concentrations, with lower concentrations successfully predicted in January to May 2013 and October to November 2015 and increased concentrations in July to August 2015 and January to May 2016.

The model performance at this site is considered Not Satisfactory based on the monthly PBIAS value of 72%.

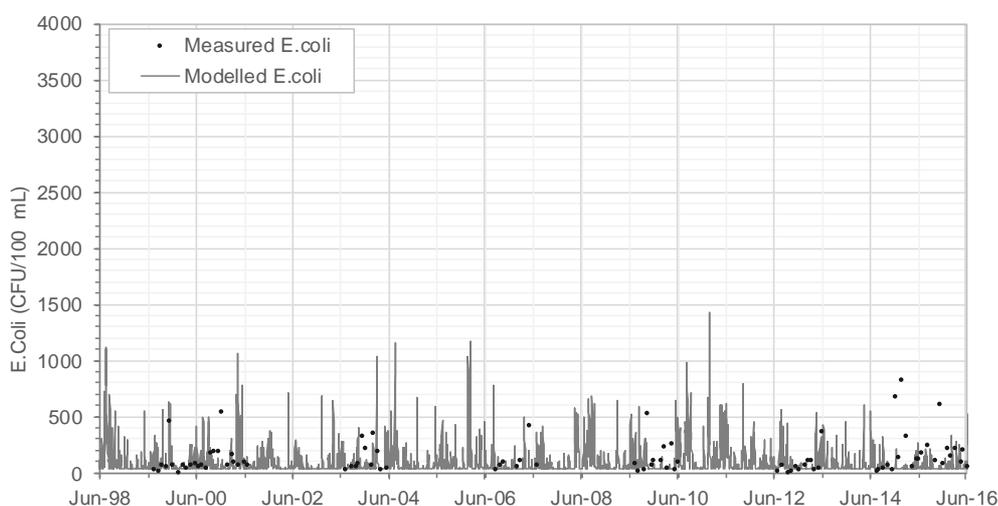


Figure 138. Constituent Hydrograph Comparing Measured and Modelled *E. coli* concentrations for the Pongakawa at Old Coach Rd gauge.

Table 102. Summary of measured and modelled *E. coli* concentration (CFU/100 ml) statistics for the Pongakawa at Old Coach Rd gauge (Jan 2011–Jun 2016).

	Modelled Data	Measured Data
Statistic	All data	All data
Count	2,008	36
Mean	81	273
Standard Deviation	111	683
Minimum	29	9
5th Percentile	29	22
25th Percentile	30	54
50th Percentile	36	105
75th Percentile	77	213
95th Percentile	290	718
Maximum	1,430	4,100

7.5.2.1.3 Waitahanui River (SCID114)

A time series comparison plot and comparison summary statistics of measured and modelled *E. coli* concentrations for the Waitahanui River at the secondary site located in SCID114 are shown in **Figure 139** and **Table 103** respectively.

The model under predicted *E. coli* concentrations within the lower and upper ranges (excluding the maximum modelled concentration).

The model performance at this site is considered to be Not Satisfactory based on the monthly PBIAS value of 72%.

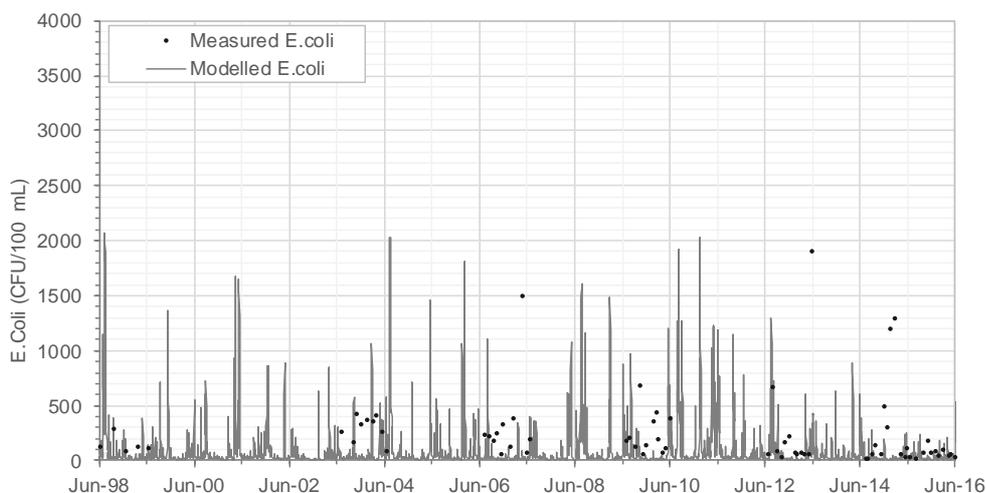


Figure 139. Constituent Hydrograph Comparing Measured and Modelled *E. coli* concentrations for the SCID114 site.

Table 103. Summary of measured and modelled *E. coli* concentration (CFU/100 ml) statistics for the SCID114 site (Jan 2011–Jun 2016).

	Modelled Data	Measured Data
Statistic	All data	All data
Count	2,008	35
Mean	78	230
Standard Deviation	172	417
Minimum	9	15
5th Percentile	11	23
25th Percentile	15	52
50th Percentile	24	70
75th Percentile	52	155
95th Percentile	357	1,230
Maximum	2,035	1,900

7.5.2.1.4 Overall Kaituna Performance

The boxplots presented in **Figure 140** provide a comparison of measured and modelled *E. coli* concentrations for all monitoring locations with greater than 30 measured data points in Kaituna WMA during the period January 2011 to June 2016.

Comments on the model's performance at each of the monitoring sites are given in **Table 104**. The PBIAS values range from 42% to 80% which corresponds to a model performance of Not satisfactory. The RMSE values range from 55 to 426 CFU/100 ml.

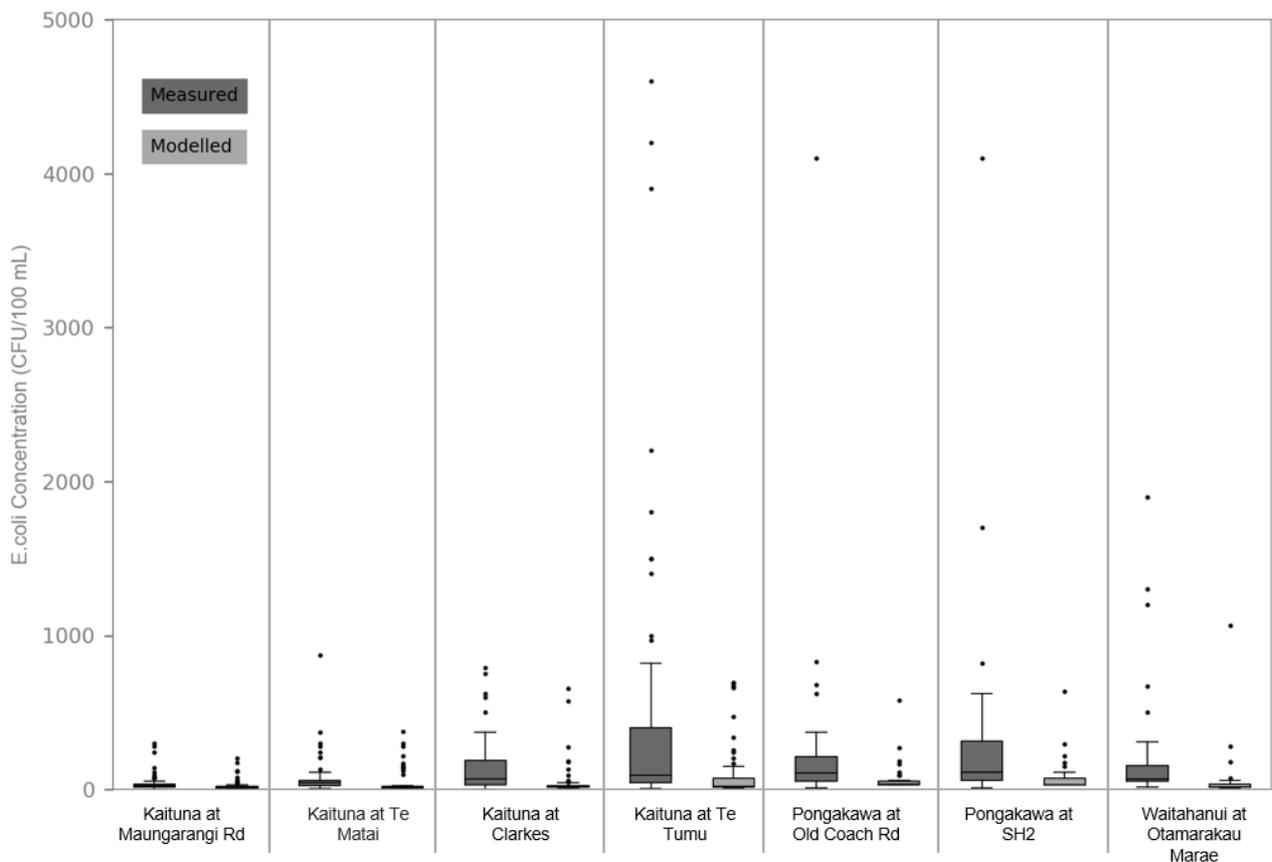


Figure 140. Box Plots Comparing Measured and Modelled *E. coli* data for all Main Sites in the Kaituna Catchment.

Figure 141. Kaituna NOF bands based on the 95%ile. (Refer A3 attachment at rear).

Table 104. Summary of *E. coli* model performance at the primary calibration sites in the Kaituna WMA.

Location	Observed Data Points	Model Accuracy (PBIAS)		RMSE	General Comments
		Value (%)	Class		
Kaituna at Maungarangi Rd (SC22)	62	42	Not Satisfactory	55	The model under predicted <i>E. coli</i> concentrations compared to the measured data. The modelled median, 25 th , and 75 th percentile concentrations predicted were lower in comparison to the measured data.
Kaituna at Te Matai (SCID26)	63	43	Not Satisfactory	118	The model under predicted the median and range in <i>E. coli</i> concentrations compared to the measured data. The interquartile range of the modelled <i>E. coli</i> concentrations was smaller than observed in the measured data.
Kaituna at Clarkes (SC53)	61	70	Not Satisfactory	208	The model under predicted the range in <i>E. coli</i> concentrations compared to the measured data. The interquartile range of the modelled <i>E. coli</i> concentrations was smaller than observed in the measured data.
Kaituna at Te Tumu (SC57)	69	80	Not Satisfactory	426	The model under predicted the median and range in <i>E. coli</i> concentration compared to the measured data. The interquartile range of the modelled <i>E. coli</i> concentrations was smaller than observed in the measured data.
Pongakawa at Pumphouse (SC96 Forest)	36	72	Not Satisfactory	417	The model under predicted the median and range in <i>E. coli</i> concentrations compared to the measured data. The interquartile range of the modelled <i>E. coli</i> concentrations was smaller than observed in the measured data.
Pongakawa at Old Coach Rd (SC96)	56	66	Not Satisfactory	263	The model under predicted the median and range in <i>E. coli</i> concentrations compared to the measured data. The interquartile range of the modelled <i>E. coli</i> concentrations was smaller than observed in the measured data.
Pongakawa at SH2 (SC98)	35	72	Not Satisfactory	425	The model under predicted the median and range in <i>E. coli</i> concentrations compared to the measured data. The interquartile range of the modelled <i>E. coli</i> concentrations was smaller than the measured data.

The inherent large natural variability in *E. coli* concentrations (which commonly span multiple orders of magnitude) in addition to the limited available observed data often proved troubling during model calibration, and single or few large values significantly influence the PBIAS classifications.

The simulated performance for *E. coli* is generally Not Satisfactory based on PBIAS classification, and poor to sufficient based on visual observation of the time series plots. However, acknowledging the inherent difficulty in measuring a statistically robust observed *E. coli* dataset and its impact on model performance measures, and as the generation of *E. coli* (and TN, TP, & TSS) concentrations were linked to physical catchment characteristics, the model is considered suitable for undertaking relative change assessments resulting from land use change or mitigation-based scenarios at a catchment scale.

7.5.2.2 Rangitāiki

7.5.2.2.1 Rangitāiki at Murupara (SCID26)

A time series comparison plot and comparison summary statistics of measured and modelled *E. coli* concentrations for the Rangitāiki at Murupara monitoring site are shown in **Figure 142** and **Table 105** respectively.

The model accurately predicted the minimum *E. coli* concentration, but over predicted at each of the higher percentiles, with the exception of the maximum concentration.

The model performance at this site is considered Not Satisfactory based to the monthly PBIAS value of 47%.

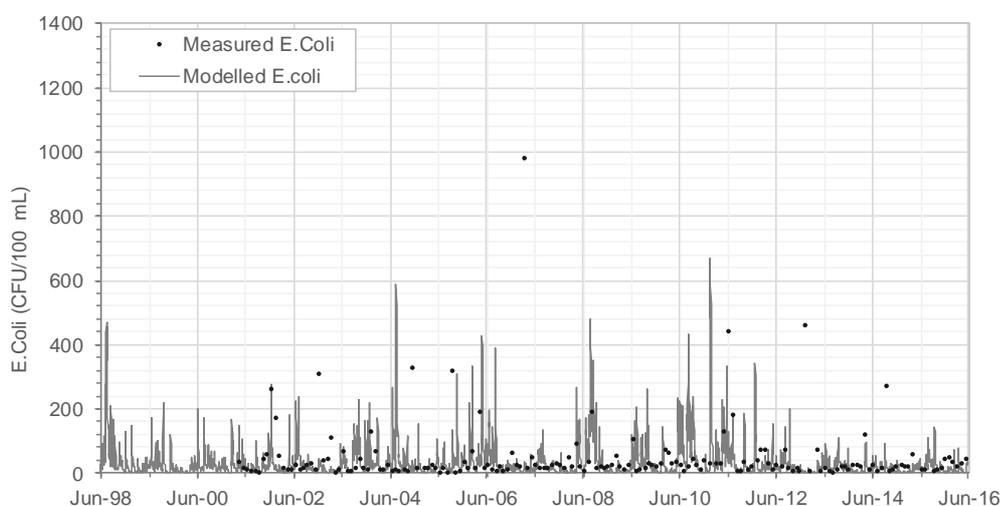


Figure 142. Constituent Hydrograph Comparing Measured and Modelled *E. coli* data for the Rangitāiki at Murupara gauge.

Table 105. Summary of measured and modelled *E. coli* concentration (CFU/100 ml) statistics for the Rangitāiki at Murupara gauge (Jan 2011–Jun 2016).

	Modelled Data	Measured Data
Statistic	All data	All data
Count	1,980	68
Mean	25	45
Standard Deviation	49	83
Minimum	1	1
5th Percentile	2	5
25th Percentile	5	11
50th Percentile	14	21
75th Percentile	26	36
95th Percentile	85	163
Maximum	668	460

7.5.2.2.2 Whirinaki at Galatea (SCID47)

A time series comparison plot and comparison summary statistics of measured and modelled *E. coli* concentrations for Whirinaki at Galatea are shown in **Figure 142** and **Table 105** respectively.

Based on the summary statistics the model closely predicts the full distribution of percentile concentrations observed in the measured data.

The model performance at this site is considered Not Satisfactory based on the monthly PBIAS value of 35%.

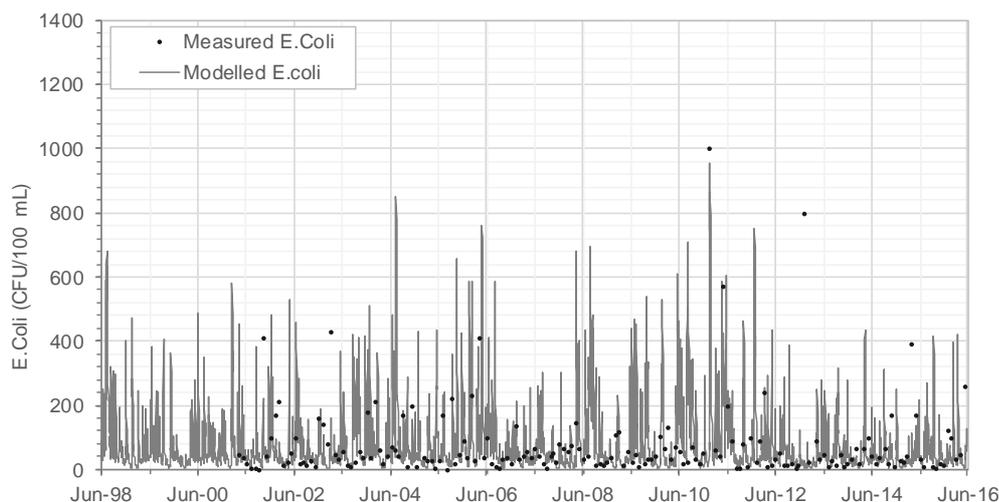


Figure 143. Constituent Hydrograph Comparing Measured and Modelled *E. coli* data for the Whirinaki at Galatea gauge.

Table 106. Summary of measured and modelled *E. coli* concentration (CFU/100 ml) statistics for the Whirinaki at Galatea gauge (Jan 2011–Jun 2016).

	Modelled Data	Measured Data
Statistic	All data	All data
Count	1,980	63
Mean	66	91
Standard Deviation	99	177
Minimum	1	4
5th Percentile	7	4
25th Percentile	20	15
50th Percentile	34	33
75th Percentile	65	84
95th Percentile	246	377
Maximum	954	1,000

7.5.2.2.3 Rangitāiki River at Matahina (SCID34)

A time series comparison plot and comparison summary statistics of measured and modelled *E. coli* at the secondary site located in SCID34 (downstream of Lake Matahina) is shown in **Figure 144** and **Table 107** respectively.

The model closely predicts the full distribution of observed percentile concentrations, with the exception of the maximum observed concentration which was under predicted.

The model performance at this site is considered Satisfactory based on the monthly PBIAS value of 29%.

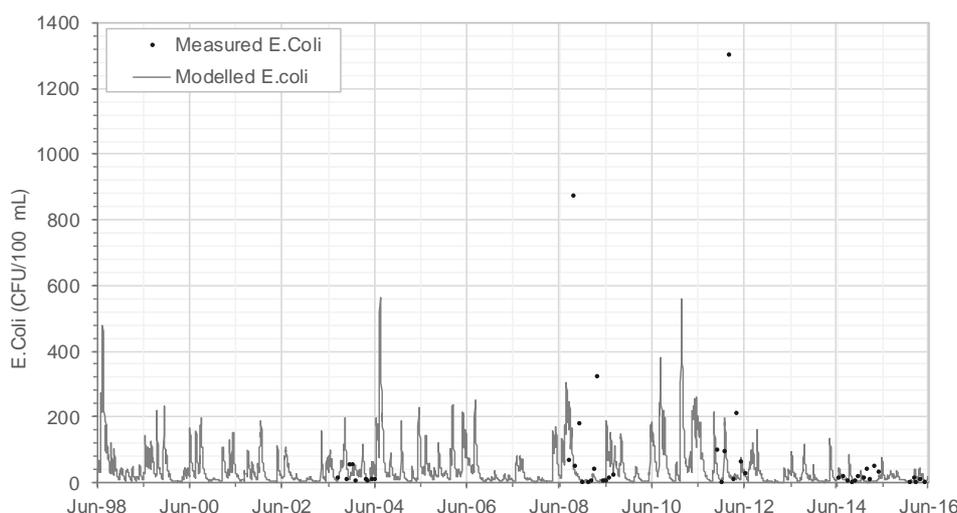


Figure 144. Constituent Hydrograph Comparing Measured and Modelled *E. coli* data for SCID34.

Table 107. Summary of measured and modelled *E. coli* concentration (CFU/100 ml) statistics for the SCID34 site (Jan 2011–Jun 2016).

	Modelled Data	Measured Data
Statistic	All data	All data
Count	1,980	25
Mean	33	81
Standard Deviation	57	258
Minimum	1	0
5th Percentile	2	0
25th Percentile	6	3
50th Percentile	13	15
75th Percentile	33	41
95th Percentile	158	188
Maximum	560	1,300

7.5.2.2.4 Overall Rangitāiki Performance

The boxplots presented in **Figure 145** provide an overview of measured and modelled *E. coli* concentrations for all primary calibration sites in the Rangitāiki WMA during the period January 2011 to June 2016.

The PBIAS values range from 29% to 86% which correspond to model performance classification of Satisfactory to Not Satisfactory. The RMSE values ranged from 89.6 to 277.6. Comments on the model's ability to predict *E. coli* concentrations in the Rangitāiki WMAs are provided in **Table 108**.

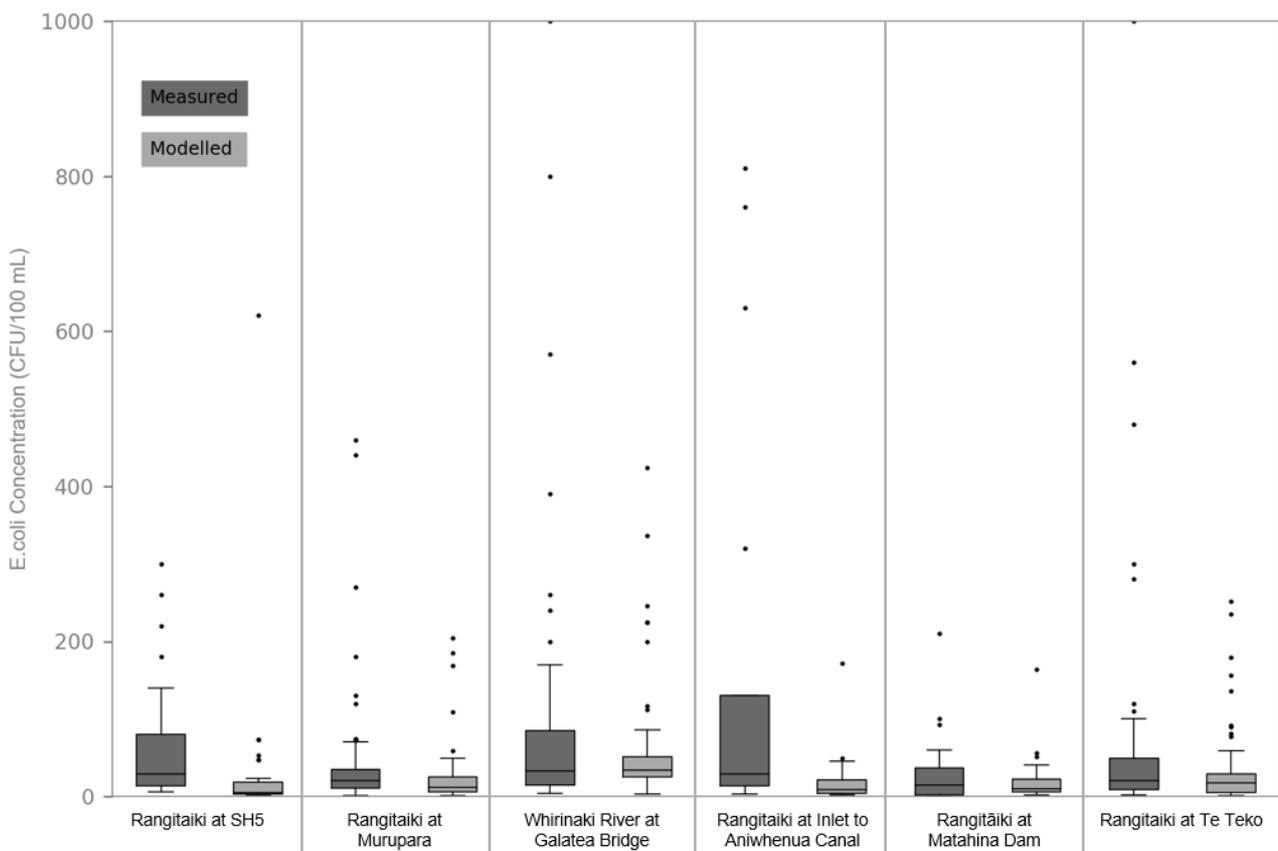


Figure 145. Box Plots Comparing Measured and Modelled *E. coli* data for all Main Sites in Rangitāiki Catchment.

Figure 146. Rangitāiki NOF bands based on the 95%ile. (Refer A3 attachment at rear).

Table 108. Summary of *E. coli* model performance at the primary calibration sites in the Rangitāiki WMA.

Location	Observed Data Points	Model Accuracy (PBIAS)		RMSE	General Comments
		Value (%)	Class		
Rangitāiki at SH5 (SC1)	29	43	Not Satisfactory	102.7	The model under predicted the range in <i>E. coli</i> concentrations compared to the measured data. The modelled <i>E. coli</i> concentrations are less than the measured data at the 25 th , 50 th and 75 th percentile concentrations.
Rangitāiki at Murupara (SC26)	61	47	Not Satisfactory	89.6	The model predicted a similar range in <i>E. coli</i> concentrations compared to the measured data, however the modelled median concentration was lower, and closer to the 25 th percentile of the measured data.
Whirinaki at Galatea Bridge (SC47)	62	35	Not Satisfactory	177.5	The model under predicted the range in <i>E. coli</i> concentrations compared to the measured data. The modelled <i>E. coli</i> concentrations are less than the measured data at the 25 th , 50 th and 75 th percentile concentrations.
Rangitāiki at Inlet to Aniwhenua Canal (SC30)	21	86	Not Satisfactory	277.6	The model predicted a median <i>E. coli</i> concentration similar to the 25 th percentile concentration of the measured data, and a significantly smaller range of concentrations, with the maximum modelled concentration less than the 75 th percentile concentration of the measured data.
Rangitāiki at Matahina Dam (SC34)	23	29	Satisfactory	46.9	The model predicted a similar range in <i>E. coli</i> concentrations compared to the measured data. The 25 th percentile and median concentration are similar to the measured data, while the 75 th percentile and maximum concentration were slightly under predicted.
Rangitāiki at Te Teko (SC1)	61	50	Not Satisfactory	150.8	The model predicted a similar range in <i>E. coli</i> concentrations compared to the measured data. The 25 th percentile and median concentration are similar to the measured data, while the 75 th percentile and maximum concentration were slightly under predicted.

The simulated performance for *E. coli* is generally Not Satisfactory to Satisfactory based on PBIAS classification and visual observation of the time series plots. As noted for the Kaituna WMA *E. coli* calibration, the generation of *E. coli* concentrations were linked to physical catchment characteristics. Therefore, the model is considered suitable for undertaking relative change assessments resulting from land use change or mitigation-based scenarios at a catchment scale. However, caution is advised if considering absolute concentrations at a daily timescale.

7.6 Constituent Model Assumptions

A summary of the key assumptions relevant to development of the constituent model is provided in **Table 109**.

Table 109. Summary of assumptions related to the water quality model development.

ID#	Current Assumption		Implication of Assumption	Potential Further Work to Reduce Significance of Assumption
	Title	Description		
1.	TN loss in the Kaituna and Rangitāiki WMAs.	Loss nodes remove flow as well as any constituent mass attached to that flow. It is assumed that TN discharges to groundwater from rivers are subject to a significant degree of nitrogen reduction within the groundwater system. The concentration of the return groundwater has been set at 0.2 mg/L.	In the absence of this assumption, TN concentration in lowland rivers where gains from groundwater are simulated, typically exceed the measured concentrations in the river.	Ultimately, interaction with the groundwater modelling team and coupling the SOURCE model with output data from MODFLOW MT3D would remove the assumption.
2.	Constant TN input concentration of 0.37 mg/L assumed from Lake Rotoehu into the Waitahanui River.	To simulate the initial concentration in the Waitahanui River at Otamarakau Valley Rd, a constant concentration of 0.37 mg/L was assumed at this gauge. The assumption is based on limited available measured TN data provided by BOPRC.	Sets a constant base mass load of TN in the Waitahanui River.	Collection of additional monitoring data would enable improved representation of any temporal changes in concentration.
3.	APSIM Drainage.	Using the SMWBM drainage information we were able to produce a realistic TN time series.	The SMWBM models were calibrated against flow gauge observations. Therefore, the simulated percolation from the SMWBM was used to provide consistency between the two models	N/A
4.	APSIM Soil characteristics.	Using soil depth rather than the soil characteristics to characterise the soil properties.	The hydraulic characteristics are relatively uniform and high (the average soil permeability in the Kaituna WMA is 5.2 while within the Rangitāiki WMA it is 6.5). The key variation in soil characteristics was soil depth, and therefore APSIM was classified based on soil depth distribution in the region.	N/A
5.	APSIM Solute Transport through the Groundwater System.	The size of the groundwater storage had a significant control on how oscillatory the response was. The approach used calculated the aquifer thickness based on the catchment average ground surface elevation, estimated depth to groundwater, and an arbitrary datum of mean sea level. 10% of the estimated aquifer thickness was defined as the initial groundwater storage.	This effectively provides a buffer and results in a smoother transition following drought.	Integration of a numerical groundwater model (e.g. MODFLOW MT3DMS).
6.	APSIM Forestry.	APSIM does not simulate the mixture of trees with different ages on land. The simulation is based on the tree planted at a point in time and is driven by the tree growth module. The	It does not fully simulate the forestry cycle.	N/A

ID#	Current Assumption		Implication of Assumption	Potential Further Work to Reduce Significance of Assumption
	Title	Description		
		simulated time series will have more TN leaching right after planting due to establishment and start levelling off with time. In practice, fertiliser is only applied to young trees, but in the model, this was continued with a proportional dose to reflect that there is always a percentage of small trees.		
7.	APSIM sheep and beef component.	Within Sheep and Beef Sheep and Beef Background = 80% (68% is sheep and beef, 12% is sheep and beef urine) Sheep and beef dairy support = 20% dairy background.	This assumes that 20% of the sheep and beef component of the APSIM module is highly intensified.	APSIM modules need to be adjusted to take into consideration different management practices.
8.	APSIM Dairy component.	Within the dairy model, Dairy support = 20% Dairy background = 80% (Within dairy background, 60% is background, 4% high urine, and 16% low urine).	This assumes that 20% of the dairy component of the APSIM module has a low intensity area (dairy support).	APSIM modules need to be adjusted to take into consideration different management practices.
9.	Classification of lowland area within the Kaituna.	Lowland areas within the Kaituna were determined to be sub-catchments which have an elevation less than 50m and a slope less than 5.	This is significant for the dairy stocking units which we place for each sub-catchment. Lowland areas have a higher stocking unit compared to the highland areas.	Survey stock counts across the WMA to allow for increased accuracy in stocking unit classification.
10.	Classification of lowland area within the Rangitāiki.	Lowland areas within the Rangitāiki catchment were defined as the galatea plains and coastal Rangitāiki.	This is significant for the dairy stocking units which we place for each sub-catchment. Lowland areas have a higher stocking unit compared to the highland areas.	Survey stock counts across the WMA to allow for increased accuracy in stocking unit classification.
11	Slope length is constantly 50 m	To calibrate the TSS a fixed slope length of 50 m was used in the calculation process. The application of a constant value across all catchments was based on previous NZ studies where dSedNET had successfully been applied.	This assumption generates comparable KLSC values to other New Zealand studies that have used SedNet to simulate TSS concentrations.	Further work could be carried out to calculate the actual slope length of each catchment, but the method is timely and may have minimal impact on the simulated results which are reflective of TSS generated in other New Zealand catchments.
12	K – soil erodibility factor.	The K soil erodibility factor was based on previously reported values (primarily by LandCare Research Dymond et al. 2014).	This assumption generates K factors reflective of other primary sediment generation studies carried out in New Zealand (i.e. Waikato, Northland and Hawkes Bay).	N/A
13.	C – Vegetation cover Factor.	The C Factor values were determined from previous New Zealand studies (primarily by LandCare Research	The assumption generates comparable C and subsequently KLSC factors for	N/A

ID#	Current Assumption		Implication of Assumption	Potential Further Work to Reduce Significance of Assumption
	Title	Description		
		Dymond et al. 2014), for all land uses with the exception of plantation forest (described below).	the generation of sediment similar assessments completed in NZ.	
14.	Plantation Forest.	<p>The Vegetation Cover Factor (C) for Plantation forest TSS generation was modelled separately to account for the felling cycle. The age of trees within a plot/ ha was provided to us by Timberlands Ltd & BOPRC, and defined as:</p> <ul style="list-style-type: none"> • 0-2 years 7% (Vegetation Cover of 1) • 3-4 years 8% (Vegetation Cover 0.75) • 5-10 years 19% (Vegetation Cover of 0.5) • 11- 20 years 36% (Vegetation Cover of 0.01) • >20 years 30% (Vegetation Cover of 0.005) <p>Note, the higher the vegetation density cover value, the lower the amount of actual vegetation coverage (i.e. it is inversely proportional).</p>	A weighted average was applied to the vegetation density and the percentage of plantation forest growth, producing a value of 0.23. This value is quite large compared to other vegetation types. This larger value results in higher TSS generation within catchments with plantation forest land uses.	<p>Sensitivity testing of alternative vegetation cover values, particularly for age classes between 0-10 years demonstrated high model sensitivity.</p> <p>Ongoing high-resolution (i.e. daily) TSS monitoring within forestry blocks, and event-based monitoring during harvesting would be required for further model calibration. In addition, a temporally varying land use map (including the temporal and spatial variation of plantation forest tree age classes) would improve TSS calibration.</p>
15.	Gully slope erosion.	The dSedNet model can generate sediment based on gully erosion processes, however this was not included in this assessment.	The generation of gully erosion could have a large influence on the generated sediment load. However, it is uncertain and gully erosion was implicitly included through calibration to instream TSS data. Previous New Zealand studies using the dSedNET model consistently do not utilise this component of the tool and believe the hill slope processes accurately reflect majority of the sediment generated.	Gully processes could be simulated in dSedNET. However, this process is computationally intensive and time consuming and would require significant additional time to implement and calibrate.
16.	TSS input for Kaituna River.	To simulate the initial background concentration in the Kaituna River at Taheke, a seasonal time series was developed. This was based off an analysis on the measured data in the Rotoiti Lake provided by BOPRC.	Sets a constant base mass load of TSS in the Kaituna River.	N/A
17.	TSS input for Waitahanui River.	To simulate the initial concentration in the Waitahanui River at Otamarakau Valley Rd, a constant concentration of 0.3 mg/L was assumed at this gauge based on analysis of data from LAWA.	Sets a constant base concentration of TSS in the Waitahanui River.	N/A

ID#	Current Assumption		Implication of Assumption	Potential Further Work to Reduce Significance of Assumption
	Title	Description		
		This location was an exception to the assumption that constituent mass was lost to groundwater.		
18.	<i>E. coli</i> generation relationship.	The values used to generate <i>E. coli</i> were based off an index for each catchment which takes into consideration the vegetation cover, stocking rates and slope degree. The larger the index the larger the amount of <i>E. coli</i> found within the catchment	Simulates a singular relationship for the quick flow and slow flow generation of <i>E. coli</i> .	Introduce more components into the index to improve representation of <i>E. coli</i> generation.
19.	<i>E. coli</i> decay relationship.	To replicate the die-off of <i>E. coli</i> a 1 st order decay model was employed. A relationship between Elevation and <i>E. coli</i> decay was derived. Elevation was used as a proxy for temperature as it is assumed areas which have cooler climates (higher elevations) will have larger die off compared to areas with warmer climates (lower elevations). This is because organisms need warmth to live longer, therefore, less decay/ die off for areas which have the capacity to sustain <i>E. coli</i> .	Areas with warmer climates have lower decay rates, making these areas a greater risk to contamination.	Use average or seasonal temperature to determine the decay rate, rather than using elevation as a proxy.
20.	<i>E. coli</i> in lowlands.	The decay function in the lowland areas for both Kaituna and Rangitāiki were turned off. Also, a larger weighting was placed on the Kaituna lowland areas to increase the amount of <i>E. coli</i> generated in these areas. This was done to replicate the characteristically high <i>E. coli</i> found in the lowland areas which is a function of the slow-moving drains and constant input from land uses which generate higher <i>E. coli</i> loads.	The lowland areas in the Kaituna comprised of areas less than 50m and having a slope less than 5. In the Rangitāiki this comprised of coastal catchments (the sub-catchments below the Te Teko gauge).	N/A
21.	Constant <i>E. coli</i> input concentration assumed for Kaituna River from Lake Rotoiti.	The constant input concentration was assumed based on measured data within Lake Rotoiti.	No temporal variability in <i>E. coli</i> concentrations from Lake Rotoiti.	More extensive data collection would allow a seasonal or temporally varying concentration to be applied, rather than the constant value used.
22.	<i>E. coli</i> contributions from Lake Rotoehu.	There is no <i>E. coli</i> contribution from Lake Rotoehu as the water entering the Waitahanui river is groundwater. As this constituent passes into the groundwater system they are removed via die-off.	No <i>E. coli</i> enter the river network via groundwater.	N/A
23.	<i>E. coli</i> die-off for Lake Matahina and Lake Aniwanui.	To account for <i>E. coli</i> die-off in Lake Aniwanui and Lake Matahina the storage node was configured with a	The decay rate was the calibration parameter found to	N/A

ID#	Current Assumption		Implication of Assumption	Potential Further Work to Reduce Significance of Assumption
	Title	Description		
		first order half-life decay rate of 1.7 hours.	produce a good match downstream.	
24.	Constant TP input to the Waitahanui catchment from Lake Rotoehu.	There is no input of TP to the Waitahanui River as the water entering from the lake is governed by groundwater.	As water from Lake Rotoehu seep into the Waitahanui catchment the TP is filtered by the aquifer matrix.	N/A
25.	<i>E. coli</i> , TSS, and TP loss through groundwater.	<i>E. coli</i> , TSS, and TP are permanently removed from the SOURCE model on the assumption that once these constituents pass into the groundwater system they are removed via die-off (<i>E. coli</i>) and filtration by the aquifer matrix.	<i>E. coli</i> , TSS and TP mass are removed from the system.	Analysis of TSS and TP concentrations in the local groundwater systems.
26.	TP inflow from Lake Rotoiti.	A time series of TP concentrations was applied to represent TP inflow from Lake Rotoiti. Based on analysis of measured data it was found that there were three prominent periods where significant changes in TP concentrations occurred at the Lake Rotoiti outlet.	A constant concentration was applied for each of the three periods.	Additional monitoring data would allow concentrations to more accurately specified.
27.	TN inflow from Lake Rotoiti.	A time series of TN concentrations was applied to represent TN inflow from Lake Rotoiti. Based on analysis of measured data it was found that there were three prominent periods where significant changes in TN concentrations occurred at the Lake Rotoiti outlet.	A constant concentration was applied for each of the three periods.	Additional monitoring data would allow concentrations to more accurately specified.
28.	Initial TN concentration in Lake Aniwanuiwa of 0.696 mg/L.	This starting condition is based on the median modelled inflow before the dam and measured information believed to be taken from within the lake.	Sets the initial concentration in the lake.	Confirmation of where the measured data was collected from.
29.	Initial TN concentration in Lake Matahina of 0.45 mg/L.	This starting condition is based on the median modelled inflow before the dam and measured information believed to be taken from within the lake.	Sets the initial concentration in the lake.	Confirmation of where the measured data was collected from.
30.	Initial TP concentration in Lake Aniwanuiwa of 0.04 mg/L.	This starting condition is based on the median modelled inflow before the dam and measured information believed to be taken from within the lake.	Sets the initial concentration in the lake.	Confirmation of where the measured data was collected from.
31.	Initial TP concentration in Lake Matahina of 0.04 mg/L.	This starting condition is based on the median modelled inflow before the dam and measured information believed to be taken from within the lake.	Sets the initial concentration in the lake.	Confirmation of where the measured data were collected from.
32.	TP surface flow Generation.	A ratio of 0.08:1 TP:TN was assumed to determine surface load of TP. The PLSC relationship was also combined with this to generate additional TP during times of high storm events and	A constant ratio of TP to TN was applied to represent the surface load of TP.	Measurement and analysis of the TP:TN ratio in the Kaituna and Rangitāiki catchments.

ID#	Current Assumption		Implication of Assumption	Potential Further Work to Reduce Significance of Assumption
	Title	Description		
		flash floods. This was based off the same principles of KLSC for TSS.		
33.	TP Baseflow generation.	The background TP load is assumed to be a constant TP baseflow for each catchment based off the acid soluble phosphorus content found in each soil type.	The background (natural) TP load represented in the model is a constant rate through time.	N/A
34.	TN surface flow generation.	Quick flow TN generation represents the process of a TN being mobilised by the surface water component of a catchment. A TN generation relationship was developed based on slope, vegetation cover and stocking rate, with the largest weighting applied to stocking rate (Increased TN is produced in areas which have higher stocking rates as these areas have higher nutrient loading. For example, through the application fertiliser). The TN is mobilised based on the slope factor of the catchment, and the vegetation cover influences the amount of TN delivered to the river or stream network.	The generation of the quick flow component of TN is controlled by stocking rate, slope and vegetation cover.	Develop an index which considers rates of fertiliser application in addition to stocking rates.
35.	TP Inflow to Waitahanui and Pongakawa Rivers.	Springs in the headwater of the Waitahanui and Pongakawa Rivers provide an additional input of dissolved P these catchments.	A constant inflow load of TP was assigned to these springs based on groundwater water quality data provided by BOPRC.	N/A

7.6.1 Point Source Contributions

The average daily discharge, mean concentration and annual average load (where applicable) for the three point source discharges included in the SOURCE models are summarised in **Table 110**. Constituent data were not applied to the Fonterra or Te Puke WWTW, and therefore only the average daily discharge is presented.

Table 110. Point source contributions.

Parameter	Statistic	Point Source		
		AFFCO	Fonterra	Te Puke
Flow	Average daily discharge (m ³ /day)	2,332	173	1,296
TN	Mean concentration (mg/L)	2.51	-	-
	Average annual load (kg/year)	3,980	-	-
TP	Mean concentration (mg/L)	12	-	-
	Average annual load (kg/year)	6,090	-	-
TSS	Mean concentration (mg/L)	49	-	-
	Average annual load (kg/year)	21,000	-	-
<i>E. coli</i>	Mean concentration (CFU/100 ml)	475	-	-
	Average annual load (CFUx10 ⁹)	847	-	-

7.7 Seasonal Variation of Constituents

The generation and transport of water quality constituents is largely controlled by rainfall, and therefore follows a similar seasonal pattern, with higher instream constituent loads occurring during winter in comparison to summer. A summary of the proportional contribution of the of the seasonal load to total annual load (spring / summer, and autumn / winter) is presented in **Table 111**.

Table 111. Average seasonal variation in discrete constituent load (2011-2015).

WMA	FMU	Spring / Summer Load (%)				Autumn / Winter Load (%)			
		TN	TP	TSS	<i>E. coli</i>	TN	TP	TSS	<i>E. coli</i>
Kaituna-Pongakawa-Waitahanui	Waitahanui	42	43	35	38	58	57	65	62
	Waiari Water Supply	40	40	32	39	60	60	68	61
	Pongakawa-Waihi Lowland	33	37	31	38	67	63	69	62
	Pongakawa-Waihi Middle and Upper	42	41	34	40	58	59	66	60
	Kaituna Middle and Upper	40	41	34	36	60	59	66	64
	Kaituna Lowland	27	36	26	36	73	64	74	64
Rangitāiki	Rangitāiki Natural	42	40	34	47	58	60	66	53
	Middle and Upper Rangitāiki	45	44	37	45	55	56	63	55
	Lower Rangitāiki	35	36	35	46	65	64	65	54

8. Summary and Conclusions

A catchment wide hydrological model was developed using the Soil Moisture Water Balance Model (SMWBM) and the SOURCE modelling framework to simulate the water quantity and quality in the Kaituna and Rangitāiki catchments. Flow models were developed to simulate the quantity of water, and these were combined with constituent generation models to simulate water quality.

The flow models were simulated using the NIWA VCSN gridded climate dataset to capture the spatial variability in climatic conditions across the region and calibrated against eight primary flow gauging locations in the Kaituna WMA, and seven in the Rangitāiki WMA. The model was configured with water takes and discharges, and included interactions from the underlying groundwater system, sub-surface spring inflows and lakes.

Overall, the flow models in the both the Kaituna and Rangitāiki WMAs were well calibrated against available gauge data. Model performance evaluation criteria were calculated for the primary gauge locations and ranged from Not Satisfactory to Very Good in the Kaituna WMA and Not Satisfactory to Good in the Rangitāiki WMA based on the Nash-Sutcliffe Efficiency Coefficient (NSE). Model performance based on the Percentage Bias (PBIAS) model performance evaluation criteria ranged from Good to Very Good in the Kaituna WMA and Not Satisfactory to Very Good in the Rangitāiki WMA.

Constituent generation models were developed using a combination of third-party modelling tools, SOURCE plugins, and derived catchment specific constituent generation relationships, and are summarised as follows:

- Total Nitrogen (TN) – Generated using the Agricultural Production Systems Simulator (APSIM), and a TN generation index relating slope, vegetation cover and stocking rate to instream TN concentrations.
- Total Phosphorus (TP) – Generated using a TN:TP ratio for the surface load, a TP generation index relating the natural TP load, catchment slope length and gradient, and vegetation cover to instream TP concentrations for the event surface load, the natural load calculated from the Acid Soluble Phosphate content of soils GIS layer, and estimates of spring inflow loads.
- Total Suspended Solids (TSS) – Generated using the dSedNET SOURCE plugin.
- *E. coli* – Generated based on a generation index relating stocking rate, catchment slope, and vegetation cover to instream *E. coli* concentrations, with a first order decay function applied.

The constituent generation models were calibrated against eight primary monitoring sites in the Kaituna WMA, six in the Rangitāiki WMA, and against a range of additional secondary monitoring locations where limited data was available. Model performance, based on the PBIAS, criteria across all primary monitoring sites was considered Satisfactory (2 primary sites) to Very Good (10 primary sites) for TN, Not Satisfactory (3) to Very Good (6) for TP, Not Satisfactory (8) to Very Good (1) for TSS, and Not Satisfactory (12) to Satisfactory (1) for *E. coli*.

The performance of the model to predict flow, TN, TP and TSS concentrations at most monitoring locations was satisfactory or better in terms of statistics and / or visual representation. However, the performance in terms of *E. coli* concentrations was generally Not Satisfactory and caution should be used in interpreting output for this constituent when considering absolute concentrations. As the generation of *E. coli* (and TN, TP, & TSS) concentrations were linked to physical catchment characteristics, the model is considered suitable and appropriate for undertaking relative change (i.e. percentage change) analysis resulting from land use change or mitigation-based scenarios at the catchment scale.

Overall, the model is considered an effective tool that can be used to aid in the planning and management of water allocation and water quality assessments at the catchment scale, through potential land use change and mitigation scenario simulations. The current model is considered suitable and appropriate for the analysis of relative change assessments for land use change and mitigation scenarios across the Kaituna and Rangitāiki WMAs, for flow and all four constituents (TN, TP, TSS and *E. coli*). Analysis of finer scale effects such as discharges at an individual property level cannot be undertaken with this model.

The model was used to assess four land use change scenarios representing the Current State (Scenario 1), a Reference State (Scenario 2) that reflected the natural land use prior to anthropogenic modification, and two future development states (Scenarios 3 & 4) which represented differing level of proposed development, primarily increases in dairy, kiwifruit and orchards, and plantation forest. In addition, a suite of mitigation measures (known as the M1 Mitigation package), were assessed. The development, results, and analysis of these scenarios are detailed in WWLA (2020c) *Kaituna and Rangitāiki SOURCE Modelling – Scenarios Report*.

9. Recommendations

Flow Model Calibration

The following recommendations are made to further improve the flow calibrations within the timeframe of this project (i.e. the plan change process):

- Apply a loss node within the Pokairoa at Railway Culvert gauge to simulate the physical process of flow being lost to deeper groundwater.
- Interrogation of the Jacob's MODFLOW model or hydrogeological survey/investigations to confirm and/or rule out surface flow losses to deeper aquifers for the following catchments:
 - Paraiti (Mangorewa) River at Saunders;
 - Puanene River upstream of SH2;
 - Headwater catchments of SCID63, SCID65 to 70, SCID79, SCID80 and Pongakawa River; and
 - Rangitāiki River at Murupara.
- Interrogation of the Jacob's MODFLOW model or hydrogeological survey/investigations to confirm and/or rule out surface flow gains from sub-surface discharges for the Waitahanui River at Otamarakau Valley Road.
- Verify the depth to groundwater estimates assumed in this project against that predicted by the Jacob's MODFLOW model.
- Consider integration of the SOURCE and MODFLOW models to ensure water balance closure between both projects.

Constituent Model Calibration

The following recommendations are made to further improve constituent calibrations or reduce model uncertainty within the timeframe of this project:

- Increased monitoring of TSS concentrations over the duration of a number of rainfall events at the primary monitoring sites, and subsequent recalibration of the event TSS calibration.
- Investigate the potential for using seasonal temperature as a direct control on *E. coli* decay rate rather than using catchment elevation as a proxy for average temperature.

Future Recommendations

The following recommendations are provided for future applications beyond the timeframe of this project (i.e. the plan change process):

- Increase the number of monitoring sites in the main reaches of the Kaituna and Rangitāiki WMA for both flow and water quality in order to provide additional calibration points.
- Investigate potential model sensitivity to the explicit inclusion of gully erosion processes in dSedNET.
- Couple (link) the groundwater model developed by Jacobs to the SOURCE models developed for this project, to enable:
 - Simulation of groundwater flow and baseflow TN concentrations; and
 - N attenuation to be explicitly modelled, with spatially varying attenuation (decay) rates to be applied.
- Development of historic land use maps to enable simulation of and calibration to dynamic land use maps.

10. References

- Aqualinc, (2015) *Assessing unconsented or permitted water use in the Bay of Plenty Region*. Aqualinc Consultants report prepared for Bay of Plenty Regional Council.
- BOPRC (2010) *Soils of the Bay of Plenty Volume 1*. Western Bay of Plenty. Environment Bay of Plenty Environmental Publication 2010/11-1.
- Basher, L. R. (2013). *Erosion processes and their control in New Zealand*. Ecosystem services in New Zealand—conditions and trends, 2013, 363-374.
- Cetin, L.T., Freebairn, A., Easton, S., Sands, M., and Pedruco, P (2016) *Application of daily SedNet for modelling catchment-scale sediment generation and transport: New Zealand case study*. HWRS 2016.
- Collins, R. and Rutherford, K., (2004) *Modelling bacterial water quality in streams draining pastoral land*. Water Research, 38(3), pp.700-712.
- Davis, J.R. and Koop, K. (2001). *Current understanding of the eutrophication process in Australia*. In Regional Management of Water Resources: Proceedings of an International Symposium (Symposium S2) Held During the Sixth Scientific Assembly of the International Association of Hydrological Sciences (IAHS) at Maastricht, The Netherlands, from 18 to 27 July 2001 International Assn of Hydrological Sciences. No. 268, pp. 89.
- Donald, R., (1997) *Rotorua Lakes Summary Report (Environmental Report No. 97/21)*. Environment Bay of Plenty.
- Drewry, J.J., Newham, L.T.H., Greene, R.S.B., Jakeman, A.J. and Croke, B.F.W., (2006) *A review of nitrogen and phosphorus export to waterways: context for catchment modelling*. Marine and Freshwater Research, 57(8), pp.757-774.
- Dymond, J., Herzig, A., Ausseil, A. G., & Roygard, J. (2014) *Using SedNetNZ to assess the impact of the Sustainable Land Use Initiative in the Manawatu-Wanganui region on river sediment loads*. Horizons Regional Council.
- Eco Logical (2017) *APSIM Modelling of Farm System Nutrient Dynamics*.
- eWater SOURCE (2012) *Source User Guide*, eWater Cooperative Research Centre, Canberra, Australia.
- Freebairn, A., Fleming, N., van der Lindern, L., He, Y., Cuddy, SM., Cox, J., Bridgart, R. (2015) *Extending the water quality modelling capability within eWater SOURCE – developing the dSedNET plugin*. Goyder Institute for Water Research Technical Report Series No. 15/42.
- Heathwaite, A. L. (2003). *Making process-based knowledge useable at the operational level: a framework for modelling diffuse pollution from agricultural land*. Environmental Modelling & Software, 18(8-9), 753-760.
- Hicks DM, Hill J, Shankar U (1996). *Variation of suspended sediment yields around New Zealand: the relative importance of rainfall and geology*. IAHS Publication 236: 149–156.
- Hughes and Hoyle (2014) *The importance of bank erosion as a source of suspended sediment within the Kopurererua Catchment*. Report prepared for Bay of Plenty Regional Council
- Hughes (2015) *Waikato River Suspended Sediment: Loads, sources and sink. Information to inform economic modelling for the Healthy Rivers Wai Ora Project*.
- NIWA (June 2016). *Sediment Attributes Stage 1. Project Number: MFE16502*. Prepared for Ministry for the Environment

Jiang, X., Morgan, J., & Doyle, M. P. (2002). *Fate of Escherichia coli O157: H7 in manure-amended soil*. Applied and environmental microbiology, 68(5), pp 2605-2609.

Krause, P., Boyle, D. P., & Bäse, F., (2005) *Comparison of different efficiency criteria for hydrological model assessment*. Advances in geosciences, Vol. 5: 89-97.

Kudva, I. T., Blanch, K., & Hovde, C. J. (1998). *Analysis of Escherichia coli O157: H7 survival in ovine or bovine manure and manure slurry*. Applied and environmental microbiology, 64(9), pp 3166-3174.

Larned, S.T., Scarsbrook, M.R., Snelder, T.H., Norton, N.J. and Biggs, B.J., 2004. *Water quality in low-elevation streams and rivers of New Zealand: Recent state and trends in contrasting land-cover classes*. New Zealand journal of marine and freshwater research, 38(2), pp.347-366.

Mankin KR, Wang L, Hutchinson SL, Marchin GL. (2007) *Escherichia coli sorption to sand and silt loam soil*. Transactions of the ASABE, 50, pp 1159–1165.

McCuen, R. H., Knight, Z., & Cutter, A. G., 2006. *Evaluation of the Nash–Sutcliffe efficiency index*. *Journal of Hydrologic Engineering*, Vol. 11(6), 597-602.

McDowell, R. W., & Sharpley, A. N. (2004). *Variation of phosphorus leached from Pennsylvanian soils amended with manures, composts or inorganic fertilizer*. Agriculture, ecosystems & environment, 102(1), pp 17-27.

McDowell, R. W. (2012). *Challenges and opportunities to decrease phosphorus losses from land to water*. Advanced Nutrient Management: Gains from the Past-Goals for the Future. (Eds LD Currie and C L Christensen). <http://firc.massey.ac.nz/publications.html>. Occasional Report, (25).

McIntosh, J., (2010) *The effect of discharging treated sewage effluent from Lakes Rotoiti, Rotoehu and Rotoma to the Waitahanui catchment*. Lochmoigh Ltd.

Ministry of Agriculture and Forestry. (August 2011). *Waikato / Bay of Plenty intensive sheep and beef*. ISBN 978-0-478-38493-2, Taken from www.maf.govt.nz. (Stocking rates)

Ministry for Primary Industries (October 2012). *Waikato / Bay of Plenty intensive sheep and beef*. ISBN 978-0-478-40406-7, Taken from www.mpi.govt.nz (Stocking rates)

Moriasi, D. N., Arnold, J. G., Van Liew, M. W., Bingner, R. L., Harmel, R. D., & Veith, T. L., (2007) *Model evaluation guidelines for systematic quantification of accuracy in watershed simulations*. *American Society of Agricultural and Biological Engineers*. Vol. 50(3), 885-900.

Moriasi, D.N., M.W. Gitau, N. Pai, P. Daggupati., (2015) *Hydrological and Water Quality Models: Performance Measures and Evaluation Criteria*. American Society of Agricultural and Biological Engineers. Vol. 58(6): 1763-1785.

Parliamentary Commissioner for the Environment (2018) *Overseer and regulatory oversight: Models, uncertainty and cleaning up our waterways*. <https://www.pce.parliament.nz/publications/overseer-and-regulatory-oversight-models-uncertainty-and-cleaning-up-our-waterways>

Sands, M., Nation, T, Baker., Sturgeon, C., (2017) *Values and Current Allocation of Responsibility for Contaminant Discharges*. Prepared for Horticulture New Zealand.

Said, A., Stevens, D. K., & Sehlke, G. (2003). *The relationship of land-use to total nitrogen/phosphorus in streams*. Utah State University, Logan, UT.

Semenov, A. V., Van Bruggen, A. H., Van Overbeek, L., Termorshuizen, A. J., & Semenov, A. M. (2007). Influence of temperature fluctuations on Escherichia coli O157: H7 and Salmonella enterica serovar Typhimurium in cow manure. *FEMS microbiology ecology*, 60(3), 419-428.

Thomas, M. B., Spurway, M. I., & Adams, J. A. (2001). *Availability of phosphorus to nursery plants*. In The International Plant Propagators' Society Combined Proceedings (Vol. 50, No. 2000, pp. 49-54).

Van Elsas, J.D., Semenov, A.V., Costa, R. and Trevors, J.T., (2011) *Survival of Escherichia coli in the environment: fundamental and public health aspects*. The ISME journal, 5(2), p.173.

Westerhoff, R.S., Tschirter, C., White, P.A. (2017) *Development of hydrogeological information to evaluate national-scale hydrological parameters*. Lower Hutt (NZ): GNS Science. 21 p. (GNS Science report; 2017/23).

White, P.A., Della Pasqua, F., Meilhac, C., (2009) *Groundwater resource investigations of the Paengaroa-Matata area stage 1 - conceptual geological and hydrogeological models and preliminary allocation assessment* (GNS Science Consultancy Report No. 2008/134). Prepared by GNS for Bay of Plenty Regional Council.

Wilkinson, S. N., Dougall, C., Kinsey-Henderson, A. E., Searle, R. D., Ellis, R. J., & Bartley, R. (2014). *Development of a time-stepping sediment budget model for assessing land use impacts in large river basins*. Science of the Total Environment, 468, 1210-1224.

Williamson, J. (2017) *Development of Vadose Zone Functionality for Regional Scale Catchment Modelling in eWater SOURCE*. Conference paper presented at the New Zealand Hydrological Society Conference. 2017.

Williamson Water Advisory (WWLA) (2017) *Actual Irrigation Water Use Modelling*. Report prepared for Bay of Plenty Regional Council.

Williamson Water Advisory (WWLA) (2020b) *Kaituna-Pongakawa-Waitahanui and Rangitāiki APSIM Modelling Report*. Report prepared for Bay of Plenty Regional Council.

Williamson Water Advisory (WWLA) (2020c) *Kaituna-Pongakawa-Waitahanui and Rangitāiki SOURCE Modelling – Scenarios Report*. Report prepared for Bay of Plenty Regional Council.